



**UNIVERSITY
OF TRENTO - Italy**

International Ph.D. Program in Biomolecular Sciences

32nd Cycle

**Tackling Prion Replication and Toxicity by
Targeting the Cellular Prion Protein with
Different Pharmacological Strategies**

Silvia Biggi

Dulbecco Telethon Laboratory of Prions and Amyloids

Department of Cellular, Computational and Integrative Biology (CIBIO)

University of Trento

Academic Year 2018 – 2019

Tutor Prof. Emiliano Biasini

Advisor Dr. Tania Massignan

*To Dodo, the first scientist I met,
who taught me to be curious and patient,
and to Lina, who taught me to be stubborn.*

CONTENTS

ABSTRACT	6
LIST OF ABBREVIATIONS	7
CHAPTER 1. INTRODUCTION	11
1.1 Prion Diseases: A Brief Overview	11
1.2 The Cellular Prion Protein	12
1.3 Trafficking of PrP ^C	15
1.4 The Function of PrP ^C	20
1.4.1 Knock-out models	21
1.4.2 Metal Ions Homeostasis	22
1.4.3 Stress-protection	22
1.4.4 Synaptic Functions	23
1.4.5 Cellular Differentiation	24
1.4.6 Myelin Maintenance	25
1.5 PrP Paralogs	25
1.6 The Prion Hypothesis	26
1.7 Structure and Conversion of PrP ^{Sc}	30
1.8 The Cellular Site of Conversion	32
1.9 The Concept of Prion Strains	34
1.10 Species Barrier Phenomenon	35
1.11 Mechanisms of Prion Toxicity	38
1.11.1 PrP ^C -Mediated Toxicity	38
1.11.2 Autophagy and Unfolded Protein Response	41
1.11.3 Synaptic Alterations	43
1.12 PrP ^C as a Receptor for Misfolded Protein Isoforms	46
1.13 Human Prion Diseases	48
1.13.1 Creutzfeldt-Jakob Disease	49
1.13.2 Sporadic CJD	50
1.13.3 Familial CJD	52
1.13.4 Variant CJD	53
1.13.5 Iatrogenic CJD	54
1.13.6 Kuru	55
1.13.7 Fatal Familial Insomnia	56
1.13.8 Gerstmann-Straussler-Scheinker Syndrome	57
1.14 Animal Prion Diseases	58
1.14.1 Scrapie	58
1.14.2 Bovine Spongiform Encephalopathy	58
1.14.3 Chronic Wasting Disease of Cervids	59
1.14.4 Transmissible Mink Encephalopathy	60

1.14.5 Exotic Ungulate Spongiform Encephalopathy	61
1.14.6 Feline Spongiform Encephalopathy	61
1.15 Experimental Models of Prion Diseases (animal, <i>ex vivo</i> , cellular, cell-free)	62
1.15.1 Animal Models of Prion Diseases	62
1.15.2 <i>Ex Vivo</i> Models of Prion Diseases	65
1.15.3 <i>In Vitro</i> Models of Prion Diseases	66
1.15.4 Cell-free Assays	67
1.16 Diagnosis of Prion Diseases	69
1.17 Therapies for Prion Diseases	70
1.17.1 Therapeutic Agents Targeting Prion Propagation	70
1.17.2 Therapeutic Agents Targeting PrP ^C	72
1.18 Clinical Trials	76
CHAPTER 2. AIMS AND OBJECTIVES	79
2.1 PART I. Re-localizing PrP ^C	79
2.2 PART II. Targeting PrP ^C toxicity	80
CHAPTER 3. MATERIALS AND METHODS	81
3.1 Institutional Ethical Approval	81
3.2 Organic synthesis schemes	81
3.3 Plasmids	82
3.4 Cell Cultures	82
3.5 Treatments	83
3.6 HCS Screening	83
3.7 HCS Dose-Response Assays	84
3.8 Cell Imaging	84
3.9 DBCA Screening	85
3.10 DBCA	85
3.11 Prion-Infected Cells	86
3.12 PK Digestion	86
3.13 Western Blots	87
3.14 Immunocytochemistry	87
3.15 Dynamic Mass Redistribution	88
3.16 Patch Clamp	89
3.17 Primary Neuronal Cultures	89
3.18 Preparation of A β Oligomers	89
3.19 Detection of A β Toxicity in Primary Neurons	90
3.20 Prion Toxicity in Brain Slices	91
3.21 <i>In Silico</i> Analyses	92
3.22 Statistical Analyses	93

CHAPTER 4. RESULTS PART I	94
4.1 Specific Aims and Rationale	94
4.2 Experimental Layout	94
4.3 Definition of the Z prime	97
4.4 Identification of PrP ^C -re-Localizing Compounds	98
4.5 Validation of the Hits	99
4.6 Dose-Response Assays	100
4.7 Elimination of False Positives	103
4.8 Specificity of the Internalization	105
4.9 Evaluation of PrPC Binding	107
4.10 Effect on PrPC Synthesis	109
4.11 Secondary Assays to Assess Efficacy	111
4.12 HM Inhibits Prion Propagation in Cell Cultures	111
4.13 HM Inhibits Prion Toxicity in Cell Cultures	115
4.14 Overview of the Hits	117
4.15 HM Doesn't Alter the Membrane Dynamic of an Endogenous Protein	118
4.16 In Silico Pharmacokinetic Profiling of HM	120
4.17 HM's Effect Could be Mimicked by a CK2 Inhibitor	121
4.18 Discussion	123
CHAPTER 5. RESULTS PART II	129
5.1 Specific Aims and Rationale	129
5.2 Experimental Workflow	129
5.3 Characterization of LD24	132
5.4 Five LD24 Derivatives Show Improved Rescuing Activity	134
5.5 Three LD24 Derivatives Showed an Improved IC50	135
5.6 SM231 Does not Act by Directly Binding to PrP ^C	136
5.7 SM231 Does not Alter PrP ^C Expression	137
5.8 SM231 Does not Change PrP-EGFP Localization	138
5.9 SM231 Fails to Suppress Prion Replication in Cells	140
5.10 SM231 Suppresses the Channel Activity of Mutant PrP	141
5.11 SM231 Inhibits the PrP-Dependent Synaptotoxicity of A β Oligomers	143
5.12 A Derivative of SM231 Shows Improved Rescuing Activity in DBCA	146
5.13 SM884 Inhibits Acute Prion Toxicity in Brain Slices	148
5.14 Discussion	150
CHAPTER 6. CONCLUSIONS	154
ACKNOWLEDGEMENTS	156
BIBLIOGRAPHY	157
APPENDIX	195

ABSTRACT

The great majority of therapeutic strategies tested so far for prion diseases, fatal transmissible neurodegenerative disorders, tackled PrP^{Sc}, the infectious isoform of the cellular prion protein (PrP^C), with largely unsuccessful results. Conversely, targeting PrP^C is a poorly explored strategy. In this thesis, I exploited the concepts of altering PrP^C cell surface localization and tackling PrP^C-mediated cytotoxicity to design two different screening paradigms and study the effect of novel anti-prion compounds.

We recently shed light on the mode of action of chlorpromazine, an anti-psychotic drug known to inhibit prion replication and toxicity by inducing the re-localization of PrP^C from the plasma membrane. Unfortunately, chlorpromazine possesses pharmacokinetic properties unsuitable for chronic use *in vivo*, namely low specificity and high toxicity. In the first part of my thesis, I employed cells expressing EGFP-PrP to carry out a semi-automated high content screening (HCS) of a chemical library directed at identifying non-cytotoxic molecules capable of specifically re-localizing PrP^C from the plasma membrane as well as inhibiting prion replication and toxicity in cell cultures. I found four candidate hits inducing a significant reduction in cell surface PrP^C, one of which also inhibited prion propagation and toxicity in cell cultures in a strain-independent fashion.

In a previous publication, an artificial mutant of PrP^C (Δ CR), sensitizing cells to several cationic antibiotics as Zeocin, was used to screen a library of compounds rescuing Zeocin-induced cytotoxicity. However, the main hit of the screening, named LD24, had low efficiency and high toxicity. In the second part of my thesis, I coupled cycles of chemical rearrangement and screening steps using Δ CR cells, to test a small library of derivatives of LD24 and validated the selected compounds with a panel of cellular assays. I found that one molecule, SM231 and its derivative SM884, counteracted PrP^C-mediated toxicity in cellular and *ex vivo* models of prion disease and Alzheimer's disease.

Collectively, these studies define new screening methods and novel anti-prion compounds supporting the notion that removing PrP^C from the cell surface and blocking its cytotoxicity could represent viable therapeutic strategies for prion diseases and other neurodegenerative conditions.

LIST OF ABBREVIATIONS

4R β S: Four-rung β -solenoid model

4PL: 4 parameter logistic

AD: Alzheimer's Disease

ADME: Absorption, distribution, metabolism, elimination

AMPARe: α -amino-3-hydroxy-5-methyl-4-isoxazolepropionic acid receptors

APP: Amyloid precursor protein

ASOs: Antisense oligonucleotides

BBB: Blood brain barrier

BFA: Brefeldin

BSE: Bovine spongiform encephalopathy

BV: Bank vole

CD: Circular dichroism spectroscopy

CGL: Cerebellar granule layer

CJD: Creutzfeldt-Jakob disease

CK2: Casein kinase II

CLDs: Caveolae-like domains

CNS: Central nervous system

COCS: Cultured organotypic cerebellar slices

CPZ: Chlorpromazine

CR: Congo Red

CryoEM: Cryo-electron microscopy

CSF: Cerebral spinal fluid

CTR+: Positive control

CWD: Chronic Wasting Disease

DBCA: Drug Based Cellular Assay

DIV12: 12 days *in vitro*

DMR: Dynamic mass redistribution

DMSO: Dimethyl sulfoxide

Dpl: Downstream prion protein-like gene Doppel

DS: Dextran sulphate

EC50: Half maximal effective concentration

EEG: Electroencephalography

ER: Endoplasmic Reticulum

EUE: Exotic Ungulate Spongiform Encephalopathy

FAT: Fast axonal transport

FBS: Fetal bovine serum

FFI: Fatal familial insomnia

FSE: Feline Spongiform Encephalopathy

FTIR: Fourier-transform infrared spectroscopy,

GABAR: γ -aminobutyric acid receptor

GAGs: Glycosaminoglycans

GPI: Glycosylphosphatidylinositol

GPR126: G-protein coupled receptor 126

GSS: Gerstmann–Straussler–Scheinker disease

HCS: High content screening

HFS: High frequency stimulation

HGH: Human Growth Hormone

HM: Hematein

HRO: Harmalol Hydrochloride

IC: Intracerebral

IC50: Half maximal inhibitory concentration

ICV: Intra-cerebro-ventricular injection

IDOX: 40-iodo-40-deoxy-doxorubicin

I-O: input-output curve

KO: Knock-out

LD24: Dibenzo [3,4][c,e]thiazine 5,5-dioxide

LD50: Half-maximal lethal dose

LTP: long-term potentiation

MAPK: Mitogen-activated protein kinase

MBM: Meat and bone meal

MEA: Multi electrode array

mEPSCs: Miniature excitatory postsynaptic currents

moRK: Rabbit kidney epithelial (RK) cells expressing murine PrP^C

MTT: 3-(4,5-dimethylthiazol-2-yl)-2,5-diphenyltetrazolium bromide

MVBs: Multivesicular bodies

MW: Molecular weight

N2a: Mouse neuroblastoma cell line

NBH: Normal brain homogenate

NCAM: Neural cell adhesion molecule

NEAA: Non-essential amino acids

NMDARs: N-methyl-D-aspartate receptors

NMR: Nuclear Magnetic Resonance

NP: Natural products

NSCs: Neural Stem Cells

PAINS: pan-assay interference compounds

PD: Parkinson's disease

PERK: Protein kinase R (PKR)-like

PFA: Paraformaldehyde

PGs: Proteoglycans

PIPLC: Phosphoinositide phospholipase C

PIRIBS: Parallel in-register intermolecular beta-sheet model

PK: Proteinase K

PKA: cAMP-dependent protein kinase 1

PLC: Phospholipase C

PMCA: Protein misfolding cyclic amplification

PNS: Peripheral nervous system

PPS: Pentosan polysulphate

PrP-FEHTA: FRET-based high throughput assay

PSD-95: Post-synaptic density protein 95

PTP: Post-tetanic potentiation

QNC: Quinacrine

RML: Rocky Mountains laboratory prion strain

ROS: Reactive Oxygen Species
RRP: Readily releasable pool
RT-QuIC: Real-time quaking-induced conversion
SAR: Structure-activity relationship
SM: Small molecule
SPR: Surface plasmon resonance
ST11: Stress-inducible protein 1
S/I: % Surface/Internal EGFP-PrP^C
TAC: Tacrolimus
Tg: Transgenic
ThT: Thioflavin-T
TME: Transmissible mink encephalopathy
TSE: Transmissible Spongiform Encephalopathies
UPR: Unfolded Protein Response
UTR: Untranslated region
VGCCs: Voltage-gated calcium channels
VGLUT1: Vesicular glutamate transporter 1
VHC: Vehicle
WT: Wild-type
Z': Z prime
 Δ CR: Artificial mutant of PrP, deleted within the central region (residues 105-125)

CHAPTER 1. INTRODUCTION

1.1 Prion Diseases: A Brief Overview

Prion diseases, also known as Transmissible Spongiform Encephalopathies (TSE), are a class of fatal rare neurodegenerative conditions occurring both in humans and in animals. The main peculiarity of prion diseases is that they can manifest as infectious, genetic or sporadic disorders (Prusiner et al., 1998). Human prion diseases include Creutzfeldt-Jakob disease (CJD) in its sporadic, genetic or infectious variants, Gerstmann–Straussler–Scheinker disease (GSS), fatal familial insomnia (FFI) and kuru (Gambetti et al., 2003a). The animal forms include scrapie of sheep and goats, bovine spongiform encephalopathy (BSE) or mad cow disease, transmissible mink encephalopathy (TME), feline spongiform encephalopathy (FSE), exotic ungulate spongiform encephalopathy (EUE), chronic wasting disease of cervids (CWD) and spongiform encephalopathy of primates (Imran and Mahmood, 2011). From a neurological standpoint, prion diseases are characterized by a variety of clinical manifestations, ranging from rapidly developing dementia, gait, ataxia, to confusion and hallucinations (Ironside et al., 2017). Brains of affected individuals generally display some common alterations at histopathological evaluation. The most prominent is a diffuse vacuolation, which affects the gray matter, also defined as spongiosis. This is generally coupled to neural loss and astrogliosis in absence of neuroinflammation. Lastly, the deposition of amyloid aggregates is generally observed at a variable extent (Iwasaki et al., 2017). For many decades, the nature of the TSE agent has been a mystery, until Stanley Prusiner, who had been later awarded with a Nobel prize, made a seminal discovery. According to the prion hypothesis, the etiological agent of TSEs was indeed a “proteinaceous infectious particle”, thus named prion, able to promote the spreading of the disease with a virus-like mechanism, in absence of nucleic acids (Prusiner et al., 1982). It is now widely accepted that prion diseases are caused by the misfolding of the cellular prion protein (PrP^{C}) into its pathological “scrapie” isoform (called PrP^{Sc}) (Prusiner, 1991). PrP^{C} is a glycosylphosphatidylinositol (GPI)-anchored glycoprotein, typically expressed in the outer leaflet of the plasma membrane of many different cell types, particularly enriched in neurons and glial cells. PrP^{C} is structurally organized in two domains, a flexible, unstructured N-terminus and a globular C-terminus encompassing three α -helices and two short β -sheets (Turk et al., 1988). Once converted into PrP^{Sc} , the protein acquires a β -sheet-rich

conformation, which is protease-resistant, highly insoluble and likely organized as an amyloid based on a 4-rung β -solenoid architecture (Spagnolli et al., 2019). Importantly, PrP^{Sc} is able to bind native PrP^C isoforms and promote their conversion into PrP^{Sc}, unleashing a misfolding cascade which drives the spreading of the disease) (Prusiner, 1991). Infectious forms of TSEs are caused by the horizontal transmission of biological material containing PrP^{Sc}, while in the genetic ones pathological mutations in the PrP^C gene (*PRNP*) make the protein more prone to misfold (Gambetti et al., 2003a). It is still not clear, however, what causes the sporadic forms, which are thought to be determined by rare, stochastic misfolding events of PrP^C. Despite the unceasing effort, no effective therapeutic options exist to treat prion diseases. A great deal of evidence, however, indicates that targeting directly PrP^{Sc} could not be a viable strategy. In fact, all the anti-PrP^{Sc} compounds identified so far in prion-infected cells either showed poor effects in preclinical *in vivo* studies or failed to translate into patients effectively (Barreca et al., 2018). Moreover, it has been extensively proven that PrP^C is not just a passive substrate for prion conversion, but also a key-mediator of PrP^{Sc} toxicity (Mallucci et al., 2003). For this reason, more recent efforts have tried to directly target PrP^C, in order to block PrP^{Sc} replication but also to inhibit any downstream, PrP^C-mediated toxicity.

1.2 The Cellular Prion Protein

In 1985 Oesch and colleagues firstly cloned *Prnp*, the gene encoding for rodent PrP, starting from a scrapie-infected hamster brain cDNA library and probing it with oligonucleotides corresponding to the N terminus of PrP (Oesch et al., 1985). Southern blotting with PrP cDNA revealed a single gene expressed both in scrapie-infected and uninfected animals, not just in the CNS, but also in several visceral organs (Kretzschmar et al., 1986), (Oesch et al., 1985). In the same period, murine PrP specific cDNA has also been cloned starting from normal and infected mouse brain (Chesebro et al., 1985).

Human genome analysis then revealed that *PRNP*, the human homologue of the gene, is localized in the short arm of chromosome 20 (Liao et al., 1986), (Robakis et al., 1986, Sparkes et al., 1986). The promoter region has no TATA box but contains an alternative sequence found for several housekeeping genes (Basler et al., 1986). *PRNP* coding sequence is uninterrupted and encodes a protein of 240 amino acids, while the 5' untranslated region (UTR) contains an intron of 10 kb (Oesch et al., 1985).

The first spectroscopic findings showed that the secondary structure of PrP^C is largely enriched by α -helices (43%) while virtually devoid of β -sheets (Pan et al., 1993). Further analyses, conducted by multidimensional heteronuclear Nuclear Magnetic Resonance (NMR) (Donne et al., 1997), revealed that recombinant Syrian hamster PrP of residues 125–231 is composed by three helices and possibly two short β -strands, while residues 29–124 appear as highly flexible (Fig. 1b). Similar results were obtained in a report describing a preliminary analysis of the NMR spectrum of MoPrP(23–231) (Riek et al., 1997). Thus it appears that the C-terminal of PrP^C, encompassing residues 125–228, has a well-structured core domain (James et al., 1997) while a hydrophobic cluster encompasses the central domain (residues 113–128) and separates the unstructured, highly flexible N-terminal domain (Liu et al., 1999). Noteworthy, through a crystallography-based analysis of HuPrP, complexed with a nanobody that inhibits prion propagation, the presence of a third β -strand located in the unstructured N-terminal has been proposed (Abskharon et al., 2014).

PrP^C is a GPI anchored sialoglycoprotein physiologically expressed in the outer leaflet of the plasma membrane. The protein is structurally divided into a globular C-terminal (125–228), containing two glycosylation sites and an intramolecular disulfide bond, linking Cys 179 and 214, a central hydrophobic domain and an unstructured N-terminal (23–124), containing an highly conserved octapeptide repeat region (51–91), which has been associated with copper binding (Viles et al., 1999) and a polybasic region (23–31) (Fig. 1a) (Turk et al., 1988). As predicted by the analysis of the cDNA sequence, the cleavage of an N-terminal signal peptide of 22 amino acids and a C-terminal signal peptide of 23 residues renders the mature polypeptide chain a final product of 208 amino acids (Hope et al., 1986), (Stahl et al., 1987). The aminoterminal signal peptide (1–22) contains the signal sequence for the Endoplasmic Reticulum (ER); once translocated to the ER the 23 C-terminal residues receive a GPI anchor, allowing its membrane localization (Hay et al., 1987, Hope et al., 1986), (Stahl et al., 1987). Enzymatic treatment of cells showed that PrP^C is released in the culture medium upon treatment with Trypsin or phosphoinositide phospholipase C (PIPLC), confirming that PrP^C is anchored to the cell surface by a phosphatidylinositol-containing glycolipid (Caughey et al., 1989), (Stahl et al., 1987).

During the transit in the ER PrP^C also receives a double glycosylation. Glycan chains are further rearranged after the subsequent passage through the Golgi. Initial cloning of PrP cDNA established two potential sites for Asn-linked N-glycosylation (Oesch et al., 1985) on amino acids 181–183 (Asn-Ile-Thr) and 197–199 (Asn-Phe-Thr) (Haraguchi et al., 1989),

(Stahl et al., 1993). These predictions were then confirmed after chemical or enzymatic deglycosylation with PNGase F and endoglycosidase H of both the PrP^{Sc} and PrP^C isoforms (Bolton et al., 1985) and also by inhibiting the addition of sugars during synthesis using tunicamycin (Caughey et al., 1989), (Haraguchi et al., 1989), (Taraboulos et al., 1990). The analysis of glycan chains revealed a set of at least 52 different bi-, tri- and tetra-antennary glycans, composed of different relative proportions of individual saccharides (Stimson et al., 1999). Despite the numerous efforts, the functional relevance of the glycosylation of PrP^C has not been clarified yet. PrP^C mutants on the glycosylation sites, resulting in unglycosylated PrP, showed a different behavior, ranging from a correct membrane localization (Korth et al., 2000) to an impairment in the delivery to the cell surface (Puig et al., 2011), (Salamat et al., 2011), depending on the cellular model used. Moreover, it seems that altered glycosylation promotes the conversion to PrP^{Sc} (Winklhofer et al., 2003), (Yi et al., 2018) and affects the disease spreading (Cancellotti et al., 2010).

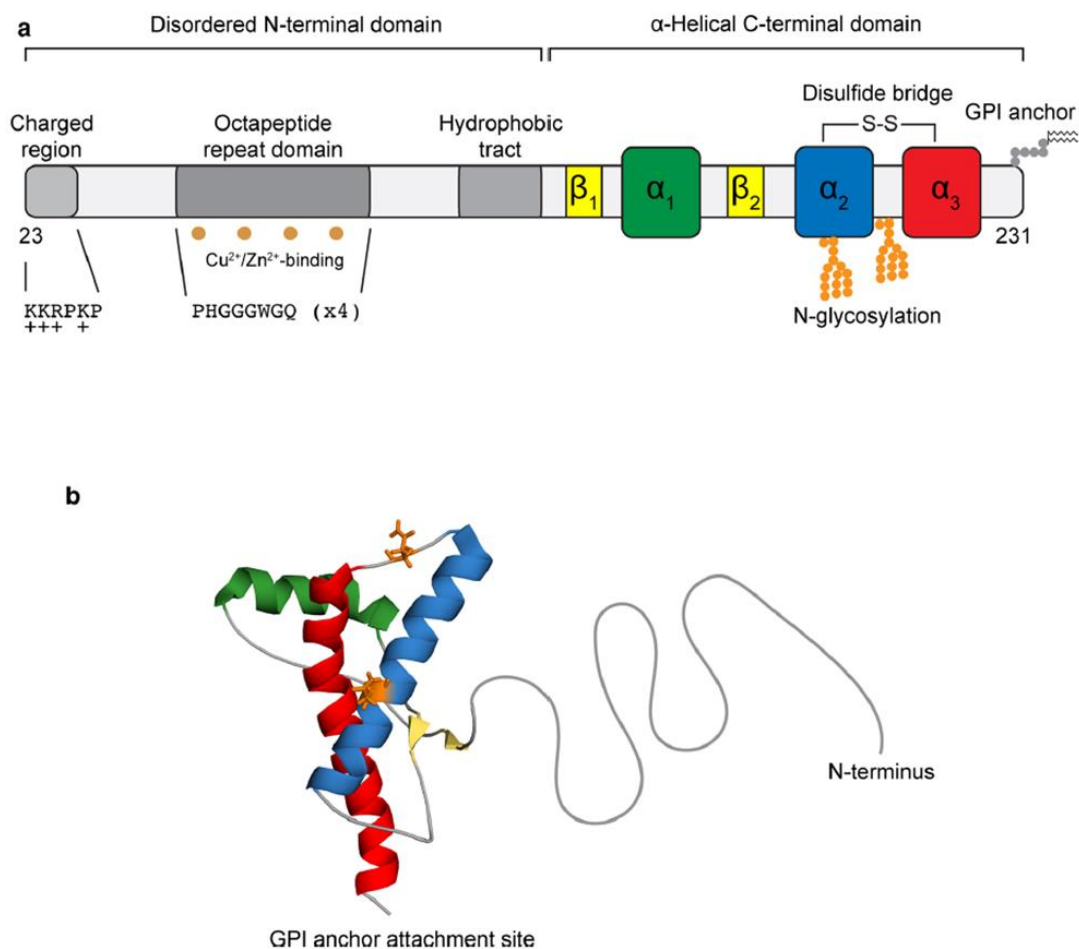


Figure 1: Domains and Structure of Human PrP^C. (a) The structure of PrP^C can be divided into two distinct domains: an N-terminal disordered domain and a C-terminal α -helical domain. The N-terminal includes a positively charged region at the N-terminus, implicated in the endocytosis of PrP^C, a series of four octapeptide repeats that allow PrP^C to bind divalent metal cations such as Cu²⁺ and Zn²⁺, and a hydrophobic tract. The C-terminal domain consists of three α -helices and two short β -strands. In the C-terminal up to two N-glycans are added within the α -helical domain, a single disulfide bridge links helices 2 and 3, and a GPI anchor at the C-terminus attaches PrP^C to the outer surface of the plasma membrane. (b) Three-dimensional (3D) structure of recombinant human PrP^C (PDB #1HJM) residues 121–230 at pH 7.0 as determined by NMR spectroscopy and rendered using PyMOL. N-glycosylated residues are indicated in orange and the intrinsically disordered N-terminal domain, which is not present in the NMR structure, is shown as a theoretical representation (Readapted from (Watts et al., 2018)).

It has been reported that a minimal fraction of precursor molecules fail to translocate into the ER lumen after the synthesis, being retained in the cytoplasm. Interestingly, it has been postulated that ER stress upregulates the levels of this immature, non-translocated PrP^C (Orsi et al., 2006). Another form, known as CtmPrP, partially enters the ER as the hydrophobic region acts as a transmembrane domain, leaving the C-terminal region within the ER lumen and the N-terminal region in the cytoplasm. Reports suggest that CtmPrP is retained either in the ER or in the Golgi apparatus before the eventual degradation by the proteasome (Stewart et al., 2001), (Stewart and Harris, 2005). Another transmembrane form of PrP^C, named NtmPrP, is produced when the molecule inserts into the ER membrane in the opposite orientation to CtmPrP (Chakrabarti and Hegde, 2009). However, these forms appear more related to disease than physiological PrP^C function.

1.3 Trafficking of PrP^C

Earlier studies established that PrP^C synthesis begins with the translocation in the ER, followed by the modification of the N-linked carbohydrates in the Golgi and the delivery to the plasma membrane by the secretory pathway within 60 min (Fig. 2) (Caughey et al., 1989). Once on the cell surface, PrP^C has a half-life of 3 to 6 hours (Borchelt et al., 1990), (Caughey et al., 1989), (Caughey, 1991).

A neat confirmation of the transit in the ER and Golgi compartments has been obtained by treating cells with Brefeldin (BFA), a toxin that impairs the delivery of proteins from the ER to the Golgi. BFA blocks the synthesis of PrP^{Sc}, as the inhibition of PrP^C maturation and membrane delivery blocks the conversion (Borchelt et al., 1992), (Taraboulos et al., 1992).

The close involvement of the membrane compartments in the pathological process has been highlighted already in the '70s, when with cellular fractions purification, prion activity was found to be closely associated with the plasma membrane (Millson et al., 1971). Then, with the discovery of PrP^C, both PrP^{Sc} and PrP^C were found only in membrane fractions after subcellular fractionation of infected hamster brains (Meyer et al., 1986). In 1987 Stahl and colleagues showed that both PrP^C and PrP^{Sc} contain a phosphatidylinositol glycolipid anchor (Stahl et al., 1987) containing a sialic acid, making it uncommon among mammalian GPIs (Stahl et al., 1992). Treatments of cells with trypsin and PIPLC indicated that the mature PrP species were expressed on the cell surface (Borchelt et al., 1990), (Caughey et al., 1989), (Harris et al., 1993) and dampened the conversion rate (Caughey, 1991), suggesting that the conversion involves membrane-bound GPI-linked PrP. Similarly, cells expressing anchorless PrP exposed to 22L prions are resistant to chronic infection (McNally et al., 2009). However, other reports indicate that anchorless PrP can be converted into PrP^{Sc} (Kocisko et al., 1994). In mouse models carrying PrP^C form deleted of the GPI anchor on a PrP null background there is an alteration in the diffuse and punctate pattern of PrP^{Sc} found in the brain and a reduction in the infectivity. More interestingly, once infected, these anchorless PrP mice showed a complete lack, or a significant delay of clinical signs, suggesting that PrP mislocalization might impair the delivery of neurotoxic signals (Chesebro et al., 2005), (Chesebro et al., 2010). Also, in another work from Stohr and colleagues, the overexpression of a GPI-depleted PrP (PrP, ΔGPI) induced a late-onset, neurologic dysfunction with prion aggregates deposition together, interestingly, the co-expression of wild-type (WT) PrP, induced a marked acceleration of disease onset (Stohr et al., 2011).

As the other GPI-anchored proteins PrP^C resides in lipid rafts, membrane domains highly enriched in cholesterol and sphingolipids (Brown and Waneck, 1992) which can be purified in Triton insoluble fractions (Taraboulos et al., 1995). Interestingly, when infected cells are depleted of cholesterol using lovastatin, the generation of PrP^{Sc} molecules is reduced (Taraboulos et al., 1995), suggesting that exposure at the plasma membrane is not sufficient for prion conversion, and PrP^C has to be expressed in the rafts microenvironment. Accordingly, fusing PrP to a transmembrane domain blocks conversion to PrP^{Sc} (Taraboulos et al., 1995).

In another report from the same period, it has been observed that PrP^C continuously cycles between the cell surface and the acidic endocytic compartment, with a transit time of ~60 minutes (Shyng et al., 1993). In 1994 Shyng and colleagues observed that in mouse

neuroblastoma (N2a) cells PrP is concentrated within clathrin-coated pits fraction (Shyng et al., 1994) and is internalized through this pathway as also results from further studies highlighting that PrP co-precipitates with clathrin (Sarnataro et al., 2009). However, targets of clathrin-mediated endocytosis need to have an intracellular domain in order to be recognized by the endocytic machinery (Ferreira and Boucrot, 2018). Thus it has been hypothesized that the N-terminal of PrP, likely the N-terminal polybasic region, binds either directly or indirectly to the extracellular domain of a transmembrane protein that contains a coated-pit internalization signal and is endocytosed (Shyng et al., 1995) after moving to detergent-soluble region of the plasma membrane (Taylor et al., 2005), which is permissive for clathrin-mediated endocytosis. However, this model has been later contested, since the cellular model used is devoid of the other main endocytosis mechanism, the caveolin-mediated one (Shyng et al., 1994). Furthermore, caveolin-mediated endocytosis has been associated with a variety of GPI-anchored proteins (Taylor and Hooper, 2006), and it consequently appears as a more likely mechanism. On this account, opposing reports state that PrP^C is clustered and endocytosed in caveolae or caveolae-like domains (CLDs), possibly through a direct binding of PrP^C to caveolin-1 through the octarepeat region (Marella et al., 2002), (Peters et al., 2003), (Vey et al., 1996).

Although the mechanism of internalization is still debated (Fig. 2), it is widely accepted that PrP is endocytosed through a dynamin-dependent pathway, since the expression of mutants of dynamin or the treatment with dynamin inhibitors, result in an inhibition of PrP endocytosis or a marked increase in un-fissed membrane-bound vesicles containing PrP (Kang et al., 2009, Caetano et al., 2008), (Magalhaes et al., 2002), (Sarnataro et al., 2009).

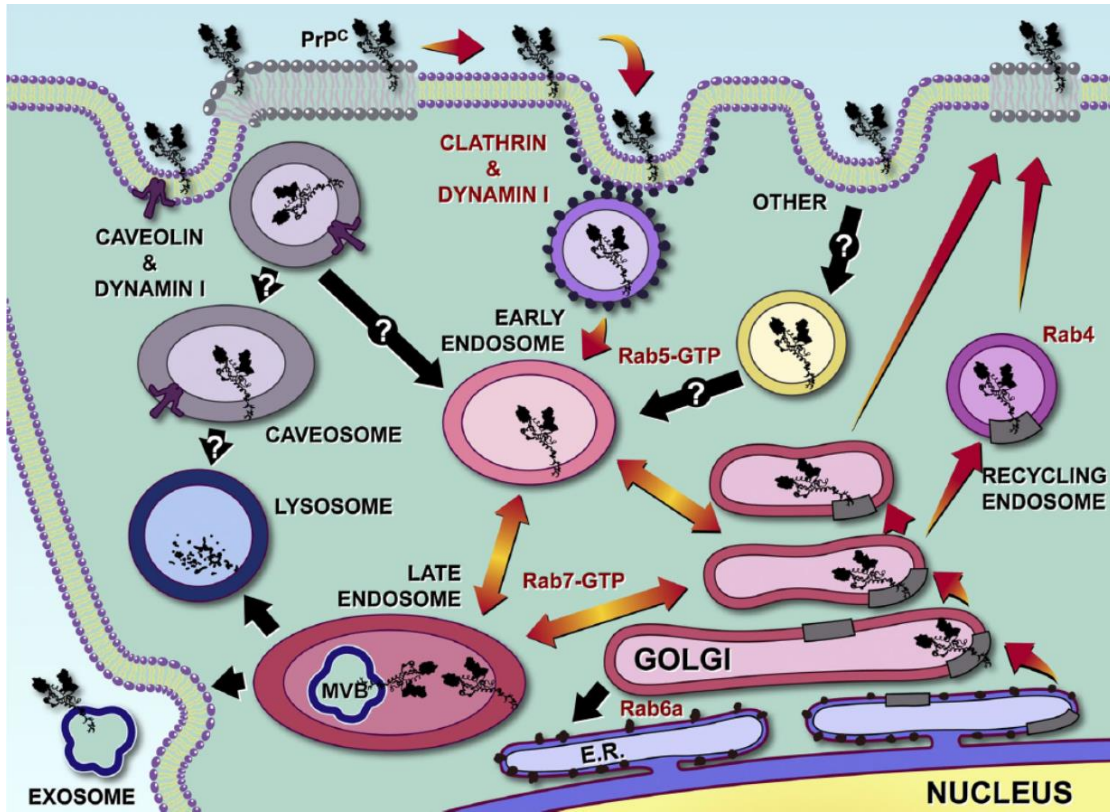


Figure 2: Subcellular Trafficking of PrP^C. Figure represents the intracellular compartments and routes involved in the synthesis and internalization of PrP^C, arrows indicate trafficking direction. The most likely pathways based on current experimental evidence are shown by red arrows. (Taken from (Linden et al., 2008).

During the transit in the endocytic compartment a small fraction of protein is proteolytically cleaved in the N-terminal, while the C-terminal cycles back to the cells surface, where it stably accumulates for up to 24 hours (Shyng et al., 1993). Over the decades different possible cleavage processes for PrP have been observed; the most prominent is the α -cleavage, but two other types of processing, named β -cleavage and shedding, can also occur (Fig. 3).

α -cleavage: In 1993 Harris and colleagues observed the presence of an N-terminal fragment of PrP released in the medium of cultured cells (Harris et al., 1993), suggesting the presence of a cleavage site in the central domain. This cleavage, which was termed α -cleavage (Mange et al., 2004), (Taraboulos et al., 1995), leads to a resulting C-terminal product called C1, mostly associated with the membrane fraction on the cell surface (Chen et al., 1995,

(Harris et al., 1993), while the corresponding N-terminal fragment (termed N1) is coherently detected in culture medium and cerebral spinal fluid (CSF) (Harris et al., 1993, Shyng et al., 1993), (Vincent et al., 2000).

The proteolytic α -cleavage of PrP^C in the brain is blocked by inhibitors of metalloproteases, although there are still conflicting reports on the proteases responsible for the process (Vincent et al., 2001). It is widely accepted however that ADAM10, ADAM17, and ADAM8 are the main proteases involved in α -cleavage, even though it is still uncertain whether one of them is prevalent (Liang and Kong, 2012). α -cleavage can be considered as a protective mechanism against prion propagation (Lewis et al., 2009). The cleavage site in-fact encompasses the neurotoxic domain, thereby destroying the part of PrP^C that is necessary for the conversion to PrP^{Sc} (Chen et al., 1995). Additionally, it removes the polybasic region within the N-terminus, which has been shown to be crucial for the initial interaction between PrP^C and PrP^{Sc} (Turnbaugh et al., 2012). This hypothesis is also supported by other data proposing the C1 fragment as a dominant negative inhibitor of the conversion process (Westergard et al., 2011) and showing that the released N1 fragment has a neuroprotective effect *in vitro* and *in vivo* (Guillot-Sestier et al., 2009).

β -cleavage: A less frequent type of cleavage was found in the brains of patients with CJD (Chen et al., 1995), (Jimenez-Huete et al., 1998) and in experimental models and cells (Caughey, 1991). In this second type of processing, termed β -cleavage, PrP^C is cleaved by the end of the octapeptide repeat, in a region around amino acid position 90, generating a C2 and an N2 fragment. The proteases involved in β -cleavage and the biological significance of this event are still unclear (Owen et al., 2007), (Yadavalli et al., 2004), although it seems to be part of the cellular physiological response against oxidative stress (Mange et al., 2004), (McMahon et al., 2001), (Watt et al., 2005), while the increase in C2 and an N2 fragment levels recorded during the infection probably reflects the failure of cellular proteases to degrade PrP^{Sc} (Altmeppen et al., 2012), (Dron et al., 2010).

Shedding: An additional proteolytic cleavage of PrP^C, named shedding, takes place in close proximity to its GPI anchor and releases almost full-length prion protein from the cell (Borchelt et al., 1993). Shed PrP^C has been found in the media of cell cultures (Borchelt et al., 1993, Harris et al., 1993) and in human cerebrospinal fluid (Tagliavini et al., 1992), suggesting that this cleavage *per se* might have a physiological role, and it is not just a consequence of the pathological process. The Glatzel group subsequently confirmed that ADAM10 is the primary sheddase for PrP^C, and the event occurs between Gly228 and

Arg229 (Altmeppen et al., 2011). Despite the lack of information on the physiological role of shedding, it has been speculated that it might have a protective effect during prion infection, by reducing cell surface levels of PrP^C, and thus the substrate for prion conversion and the mediator of neurotoxicity (Altmeppen et al., 2012). However, the misfolding of already shed PrP^C would produce anchorless PrP^{Sc} and favor the spreading process (Chesebro et al., 2005), (Kocisko et al., 1994), (Rogers et al., 1993), (Taylor et al., 2009).

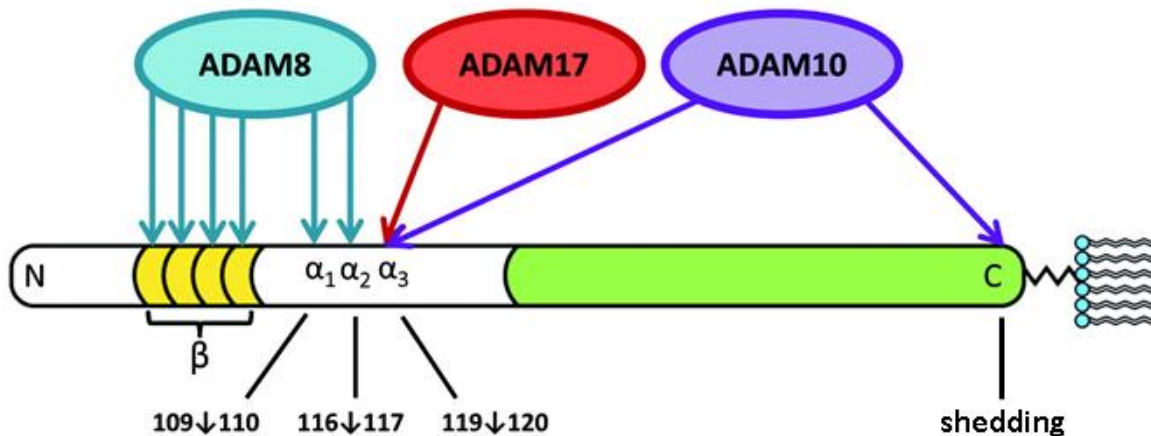


Figure 3: Proteolytic Cleavage of PrP^C. N-terminal (white) and C-terminal (green) domains are shown, with octarepeats (gold). ADAM8, ADAM10, and ADAM17 produce α -cleavage at distinct sites, noted as α_1 , α_2 , and α_3 . ADAM10 also acts as a sheddase by cleaving near the C-terminus to release the protein from the membrane. Also shown are the sites in the octarepeat domain where ADAM8 produces β -cleavage. (Readapted from McDonald and Millhauser, 2014).

1.4 The Function of PrP^C

PrP^C is prevalently expressed in the central nervous system (CNS) even though *PRNP* transcripts can also be found in many other tissue/cell types at lower levels (Ramasamy et al., 2003). At the protein level, PrP^C expression in the brain reaches a peak in early life during development, and decreases in adulthood (Ade-Biassette et al., 2006), (Sales et al., 2002). In the CNS PrP^C is expressed not only in neurons but also in astrocytes (Hartmann et al., 2013), (Lima et al., 2007), oligodendrocytes (Bribian et al., 2012, Moser et al., 1995), and microglia (Ade-Biassette et al., 2006), while outside the CNS, PrP^C has been traced in immune cells, as T-lymphocytes, natural killer cells and mast cells (Durig et al., 2000),

(Haddon et al., 2009), in the heart, pancreas, intestine, spleen, liver, and kidneys (Peralta and Eyestone, 2009).

1.4.1 Knock-out models

To gain a better comprehension of the physiological role of PrP^C, several PrP^C-knockout (KO) mice lines have been generated over the decades. The first ones, referred to as Zurich I (Bueler et al., 1992) and Npu (Manson et al., 1994), were created in the early 1990s by gene targeting methods. Initial analyses revealed no striking phenotype (Bueler et al., 1992), (Manson et al., 1994).

Few years later other KO lines, known as Rcm0 (Moore et al., 1995), Ngsk (Sakaguchi et al., 1996), Rikn (Yokoyama et al., 2001), and Zurich II (Rossi et al., 2001) were produced. Surprisingly, all lines developed a late-onset ataxia caused by the death of Purkinje neurons in the cerebellum (Moore et al., 1995), (Rossi et al., 2001), (Sakaguchi et al., 1996), (Yokoyama et al., 2001), which has afterwards been imputed to the ectopic expression of Doppel (Dpl) under the control of the *PRNP* regulatory sequences (Moore et al., 1995). In 2016 a new mouse line, Zurich III, was generated (Nuvolone et al., 2016). Zurich III mice showed no overt alteration, except for a chronic peripheral demyelinating neuropathy. Interestingly, a similar phenotype was also observed in Npu PrPKO models (Bremer et al., 2010).

At a more extended analysis Npu KO mice also showed significant alterations in the circadian system, resulting in sleep fragmentation and aberrant response to sleep deprivation. Noteworthy, the phenotype was similar to the sleep alterations in FFI (Tobler et al., 1996). Additionally, several reports pointed out that Zurich I PrP^C-KO mice seem to be more susceptible to excitotoxicity in the retina, in response to damaging light intensities (Frigg et al., 2006) and in the hippocampus following injection with N-methyl-D-aspartate receptors (NMDARs) agonist (Khosravani et al., 2008).

The neuronal loss of PrP^C seems to be also associated with deficits in hippocampal spatial learning and hippocampal synaptic plasticity. Collinge and colleagues (Collinge et al., 1994) showed that Zurich I PrP^C-KO mice have impaired hippocampal long-term potentiation (LTP), abnormal nesting behavior and more pronounced age-related short-term memory decline, as emerged by novel environment exploration tests (Schmitz et al., 2014).

Apart from these few observations obtained with reliable mice models, a vast variety of possible functions have arisen from cellular-based studies; interestingly some of the postulated functions of PrP^C seem to pair and confirm the evidence collected *in vivo*.

1.4.2 Metal Ions Homeostasis

As PrP^C is able to bind Cu²⁺ ions at the plasma membrane through the octapeptide repeat region (Brown et al., 1997a), (Hornshaw et al., 1995), a number of early studies focused on a possible role in Cu²⁺ sensing. Despite the many data collected *in vitro*, the relevance of this interaction *in vivo* is questionable. PrP^C mediates the internalization of Cu²⁺ in cells (Kretzschmar et al., 2000) and conversely binding to Cu²⁺ promotes PrP^C internalization (and cleavage) (Brown et al., 1997a), (Hornshaw et al., 1995). However, it has been argued that the extracellular Cu²⁺ concentration employed to collect these data exceeded physiologically relevant levels (Rachidi et al., 2003). It has also been postulated that PrP^C expression has a cytoprotective effect on a variety of cell lines when exposed to oxidative stress caused by Cu²⁺ overload (Rachidi et al., 2003), (Watt et al., 2007). However, once PrP^C was transfected into the PrP^C null hippocampal cell lines, no protection was observed (Cingaram et al., 2015). Despite that, in a work from Gasperini and colleagues, it has been shown that PrP^C-null mice have reduced serum and spleen Cu²⁺ content (Gasperini et al., 2016). In more recent years PrP^C has been linked also to iron metabolism. N2a cells overexpressing PrP^C showed an augmented physiological iron uptake from the culture medium (Singh et al., 2009b). Also, PrP^C silencing *in vitro* and knockdown *in vivo* seemed to affect the expression of several proteins related to iron metabolism (Singh et al., 2009a). Not surprisingly, Zurich I PrP^C-null mice also have an altered global content of iron in the liver, spleen, brain and kidneys (Gasperini et al., 2016).

1.4.3 Stress-protection

Another early-postulated function of PrP^C is a neuroprotective role against different toxic stimuli, as serum deprivation, oxidative stress and ER stress. Protection against serum deprivation was initially observed on hippocampal cell lines (Nishimura et al., 2007), (Oh et

al., 2008) through the activation of mitochondria-dependent apoptotic signaling driven by Bax (Deckwerth et al., 1996).

Furthermore, in primary neurons, astrocytes and cell lines exposed to different oxidative agents, the expression of PrP^C led to a decrease of cell damage (Anantharam et al., 2008), (Bertuchi et al., 2012), (Brown et al., 1997b), (Dupiereux et al., 2008). It has been hypothesized that PrP^C modulates several antioxidant enzymes scavenging Reactive Oxygen Species (ROS) as superoxide dismutase and glutathione peroxidase, which seem to be less activated in the absence of PrP^C expression (Brown et al., 1997b), (Miele et al., 2002), (Rachidi et al., 2003).

A convincing theory is that since ROS are thought to induce β -cleavage of PrP^C in the presence of Cu²⁺, the resulting C2 or N2 fragments could be responsible for the putative antioxidant properties of PrP^C. Accordingly, it has been reported that N2 lowers ROS production in response to serum deprivation in neuronal cell lines and neural stem cells (NSCs) (Haigh et al., 2015). However, once PrP^C is transfected in a different cell model, as N2a cells, susceptibility to hydrogen peroxide treatment was increased (Vassallo et al., 2005).

1.4.4 Synaptic Functions

As cognitive impairment is one of the major components of the neuropathological symptoms in prion diseases, many putative functions of PrP^C in the synaptic compartment have been investigated. It is widely accepted that PrP^C interacts with several proteins at the synaptic level as neurotransmitter receptors, including $\alpha 7$ nicotinic acetylcholine (Beraldo et al., 2010), kainate (Carulla et al., 2011), α -amino-3-hydroxy-5-methyl-4-isoxazole propionic acid (AMPA receptors) (Kleene et al., 2007), NMDARs (Khosravani et al., 2008) and metabotropic glutamate receptors (mGluRs) (Beraldo et al., 2011). However, none of these interactions have been directly linked to the alterations in memory consolidation (Collinge et al., 1994) and the aberrant behavior observed in Zurich I PrP^C-KO mice (Schmitz et al., 2014).

PrP^C has been reported to inhibit the activity of GluN2D subunit-containing NMDARs, possibly explaining its neuroprotective role during excitotoxic damage also observed *in vivo* (Frigg et al., 2006), (Khosravani et al., 2008). Another explanation has been initially reported by Gasperini and colleagues, who showed that PrP^C regulates the S-nitrosylation of GluN2A

and GluN1 subunits in a Cu^{++} -dependent fashion, likely inhibiting NMDARs activation (Gasperini et al., 2015), (Meneghetti et al., 2019).

Interestingly, during experimental strokes, when excitotoxicity but also oxidative stress are highly predominant, the expression of PrP^{C} in the damaged brain region of both rats and mice appears increased (Shyu et al., 2005), (Weise et al., 2004). Furthermore, Zurich I PrP^{C} -null mice show greater infarct volumes than WT controls after middle cerebral artery occlusion (Spudich et al., 2005), (Weise et al., 2006), which can be reduced by injection of a PrP^{C} -expressing adenovirus (Shyu et al., 2005).

1.4.5 Cellular Differentiation

Several studies have shown that PrP^{C} is implicated in the regulation of neurite outgrowth, cell adhesion, expression of cytoskeletal proteins and proliferation. Such function might be explained by a plethora of potential interactions at the membrane level that have been repeatedly proved in many cell lines (Graner et al., 2000), (Llorens et al., 2013), (Loubet et al., 2012). For example, stress-inducible protein 1 (STI1) binds PrP^{C} (Lopes et al., 2005), promoting neuronal differentiation via the extracellular signal-regulated kinase 1 and 2 (ERK1/2) and cAMP-dependent protein kinase 1 (PKA) pathways (Beraldo et al., 2011), (Caetano et al., 2008), (Llorens et al., 2013). In another report, axonal elongation mediated by PrP^{C} , has been imputed to the activation of PKC and Src kinases (Kanaani et al., 2005). Furthermore, PrP^{C} also directly interacts with laminin, inducing neuritogenesis in hippocampal neurons and PC12 cells (Coitinho et al., 2006), (Graner et al., 2000) through the activation of mGluR1/5, which leads to phospholipase C (PLC) activation and an increase in intracellular calcium levels (Beraldo et al., 2011). Similarly, PrP^{C} directly binds to neural cell adhesion molecule (NCAM) (Schmitt-Ulms et al., 2001), leading to the activation of Fyn kinase and consequent neuritogenesis (Santuccione et al., 2005). Interestingly, in a work from Amin and colleagues it has also been shown that the effect on axonal guidance could be exerted by a homophilic interaction between surface PrP^{C} and soluble PrP released in the medium (Amin et al., 2016), (Nguyen et al., 2019). Other reports observed that casein kinase II (CK2), a serine/threonine kinase involved in neural development, axonal growth, synaptic transmission and plasticity, phosphorylates PrP^{C} via an interaction with its C-terminal domain (Meggio et al., 2000). Moreover, CK2- PrP^{C} pathway seems to trigger a cascade of events, ultimately

leading to microtubule instability and inhibition of the fast axonal transport (FAT) (Zamponi et al., 2017).

1.4.6 Myelin Maintenance

The adult-onset demyelination of the peripheral nervous system (PNS) observed in PrP^C KO models (Bremer et al., 2010), (Nuvolone et al., 2016) provides strong evidence that PrP^C is involved in myelin maintenance. A recent work has proposed that this function might be mediated by a direct interaction between the N-terminal region (residues 23–33) of PrP^C and G-protein coupled receptor 126 (GPR126) on the surface of Schwann cells (Kuffer et al., 2016).

1.5 PrP Paralogs

Human *PRN* gene locus (mapped to band 20p12-3pte in the human genome (Liao et al., 1986) contains three genes: *PRNP*, *PRND*, and *PRNT* (Makrinou et al., 2002). The first prion-related gene discovered is the “downstream prion protein-like gene” Doppel (Dpl) labeled as *PRND*. *PRND* consists of two exons in human (Tranulis et al., 2001) and it was probably lost in birds since the divergence from reptiles (Harrison et al., 2010). The third member of *PRN* locus, *PRNT* gene, was discovered 3 Kb downstream from *PRND*.

Dpl consists of 179 aa and shares 25% of identity with the globular domain of PrP. As PrP, Dpl has an N-terminal signal sequence (1–27 residues) for the exportation to the cell surface and a GPI anchoring signal (from 156 to 179) at its C-terminal. Once processed in the ER and Golgi, Dpl receives two glycosylations (Ciric and Rezaei, 2015). Even though Dpl resides in lipid rafts as PrP^C, it seems to have a distinct microenvironment (Shaked et al., 2002). The NMR structure of the human recombinant Dpl protein displays a short flexibly disordered N-terminal domain encompassing residues 24–51, and a globular domain from residues 52–149. Dpl gained notoriety after the generation of Rcm0 (Moore et al., 1995), Ngsk (Sakaguchi et al., 1996), Rkn (Yokoyama et al., 2001), and Zurich II (Rossi et al., 2001) *Prnp* KO mouse strains, which all developed ataxia due to the overexpression of Dpl (Moore et al., 2001). The physiological function of Dpl however is still unknown, however it seems to be implicated in reproduction and embryonic development, as Dpl KO mice are sterile and KO embryos show

an altered development (Behrens et al., 2002), (Paisley et al., 2004). It seems unlikely that Dpl and PrP^C have a functional overlap since no reproductive defects have been observed in *Prnp* null mice; also *Prnd* null mice show no defects in the development or maintenance of the CNS (Watts and Westaway, 2007).

In 2003, an explorative study for potential homologs of PrP discovered a new gene outside of *PRN* locus (Premzl et al., 2003). The new gene located at chromosome 7 in mice, labeled *Sprm*, encodes for Shadoo, a protein product of 147 residues (Watts and Westaway, 2007). It has been proposed that PrP and Shadoo have evolved from the same ancestral predecessor (Premzl et al., 2004). Murine Shadoo is reminiscent of the N-terminal of PrP^C (Premzl et al., 2003) and retains a single N-glycosylation. Although Shadoo lacks the octapeptide repeat sequences found in PrP^C, it has a series of N-terminal charged tetrarepeats. Interestingly, as the N-terminal region of PrP^C, Shadoo seems to lack any specific secondary structure (Watts and Westaway, 2007). Despite various hypothesis, the physiological function of Shadoo in the CNS is still unknown.

1.6 The Prion Hypothesis

The first attempts to prove the infectivity of prion diseases have been pursued by Alpers and Gajdusek in the late '60s. They observed that brain material derived from Kuru patients injected into chimpanzees produced a series of alterations resembling the human ones (Gajdusek et al., 1966), (Gajdusek et al., 1968), (Gajdusek and Gibbs, 1971). In the same years Gibbs and colleagues (Gibbs et al., 1968) showed that CJD brain homogenate, if inoculated into chimpanzees intracerebrally (IC), caused a similar neuropathological condition within 13 months. Moreover, if the brain of infected primates was used to infect other primates serially, the incubation time was progressively reduced. Few years later, similar evidence have also been reported when sheep scrapie or CJD material have been used on non-primate models (Baringer and Prusiner, 1978), (Hadlow et al., 1980). Interestingly, when the infected material was administered through the intravenous route, the disease progression was slower than if directly injected IC. Given that all these diseases shared similar histopathological and clinical signs, it has then been hypothesized that they all shared a common “subacute spongiform encephalopathies unknown agent” behaving like a “slow virus”. However, such a pathogenic agent was undetectable in the blood or visceral lysates of

affected individuals, and no sign of viral infection, such as raise in the interferon level, was observed (Katz and Koprowski, 1968).

A significant push towards the discovery of the pathogenic agent was given by the development of a procedure for the partial purification of the "scrapie agent" (Prusiner et al., 1978). The particles isolated were resistant to detergents and nucleases, and if inoculated into animal models after such treatments were still able to induce a pathological phenotype. Surprisingly, once analyzed with electrophoresis and sedimentation assays it became obvious that scrapie particles were considerably smaller than any known animal virus (Prusiner et al., 1980) with a Molecular Weight (MW) of approximately 50.000. The nucleic acid enclosed in a globular structure of this dimension would have been too small to code for a protein. Another piece of the puzzle added shortly afterward was the evidence that treatment of the purified scrapie agent by proteinase K (PK), chemical modification and denaturation could reduce its infectivity (Prusiner et al., 1981). Given these peculiar properties distinguishing the scrapie agent from viruses, plasmids, and viroids, in 1982 Prusiner proposed as novel definition, the term "prion", a small proteinaceous infectious particle, resistant to inactivation by most procedures that modify nucleic acids (Prusiner et al., 1982). Further evidence confirmed that the prion corresponded to a protein with a MW around 27/30 kDa, named Prion Protein (PrP), undetectable in non-infected rodent brains (Bolton et al., 1982).

Thanks to the advancements in the purification of PrP 27-30 it was then possible to sequence its N-terminal region (Prusiner et al., 1984), which has then been associated with an mRNA sequence in scrapie-infected animal. By probing the cDNA encoding PrP 27-30, two independent works showed that a single gene for PrP 27-30 was detectable in hamsters and in murine and human DNA. Furthermore, PrP mRNA was clearly traced in normal and scrapie-infected brains at similar levels (Chesebro et al., 1985), (Oesch et al., 1985). As expected, no specific DNA was found in PrP extracts, indicating that prions are not encoded by nucleic acids enclosed in the infective particles. Also, given that the primary sequence of PrP encoded by the gene of a healthy subject does not differ from the one encoded by a scrapie-infected individual, it has then been suggested that the different behaviors of PrP, observed in normal and scrapie-infected brains, might have been determined by post-translational events.

PrP 27-30 purification also led the way to the production of specific antibodies. Thanks to this new tool, Bendheim and colleagues firstly reported that CJD particles from experimental

models could be extracted with the same procedure as scrapie ones and shared biochemical properties as well as reactivity for the same anti-sera (Bendheim et al., 1985). The same results were obtained by using CJD patients brains as a source of material (DeArmond et al., 1985, Kitamoto et al., 1986, Bockman et al., 1985), confirming that the “slow virus” had indeed a shared origin.

A supporting element to the protein-only hypothesis was given by all the pieces of evidence highlighting a possible familial transmission of prion diseases. In a report from Cathala, the pedigree from a French family where multiple cases of CJD have been recorded over six generations was analyzed (Cathala et al., 1980). Considering non-related individuals who lived in the same area and related individuals who moved to other regions, it emerged that among the first, none developed CJD, corroborating the idea that the source of the disease was not environmental, while a number of the relatives who moved to other regions developed CJD. Then after the cloning of PrP cDNA, mutations in the *PRNP* gene have been found in patients with fCJD (Owen et al., 1989) and GSS (Hsiao et al., 1989). Not surprisingly, a form of spontaneous spongiform degeneration was observed in mice carrying transgenic forms of human PrP with mutations associated with GSS and FFI (Collinge et al., 1995), (Hsiao et al., 1990), (Tateishi et al., 1995). Moreover, polymorphisms in the *Prnp* gene affected incubation time and disease duration in scrapie-infected mice (Carlson et al., 1988). Although an aberrant isoform of PrP was ascertained as the origin of TSE, the mechanism by which the disease could spread was still not clear. Multiple pieces of evidence pointed against a possible increase of PrP synthesis, as studies measuring PrP^C mRNA concentration in scrapie-infected animals showed no variation in PrP mRNA levels (Basler et al., 1986), (Oesch et al., 1985). Thus in 1991 Prusiner hypothesized that conversion of PrP^C could be due to a post-translational event:

“A PrP^{Sc} molecule might combine with a PrP^C molecule to produce a heterodimer that is subsequently transformed into two PrP^{Sc} molecules. In the next cycle, two PrP^{Sc} molecules combine with two PrP^C molecules, giving rise to four PrP^{Sc} molecules that combine with four PrP^C molecules, creating an exponential process. In humans carrying point mutations or inserts in their PrP genes, mutant PrP^C molecules might spontaneously convert into PrP^{Sc}” (Prusiner, 1991).

Seminal observations on this regard were made after the first PrP KO models have been produced (Bueler et al., 1992). In 1993, Bueler and colleagues showed that mice lacking the

cellular prion protein were resistant to prion infection, while heterozygous mice have a delayed disease onset if compared to the WT ones (Bueler et al., 1993). Furthermore, after grafting neural tissue overexpressing PrP^C into the brain of PrP-deficient mice and inoculating prion extracts in same animals, Brandner and colleagues observed that the infection could spread only in the tissue graft expressing PrP^C, which developed severe pathological alterations. Conversely, the rest of the brain did not show any pathological alteration and the animal did not develop any symptoms, despite a diffuse accumulation of PrP^{Sc} aggregates all over the brain tissue (Brandner et al., 1996a, Brandner et al., 1996b). While these observations confirmed Prusiner's hypothesis, another seminal concept emerged, that PrP^C was not just necessary as a substrate for PrP^{Sc} conversion, but also to mediate its neurotoxic effects. PrP KO brains, despite their enrichment in PrP^{Sc} aggregates, did not show any histopathological changes, suggesting that PrP^{Sc} might not be toxic *per se*. Neuropathological, molecular, and passage studies in mice inoculated with a particular hamster prion strain (Sc237), not causing clinical manifestations, revealed the presence of a subclinical prion infection with high prion titers in the brain (Hill et al., 2000). Similarly, human prion diseases with little or no detectable PrP^{Sc} have been diffusely described in patients affected by FFI with a mutation at codon 178 and experimental models of FFI, where Congo Red (CR) staining for amyloid deposition and PrP immunohistochemistry were negative (Collinge et al., 1995), (Medori et al., 1992). A striking proof of the role of PrP^C came then from a groundbreaking work by Mallucci and colleagues (Mallucci et al., 2003) where conditionally KO mice, were inoculated with prion extracts and prion infection was allowed to proceed normally. After incubation, all animals showed pathological evidence of neuroinvasive CNS prion infection, with PrP^{Sc} deposition and reactive astrocytosis in thalamus, hippocampus, and cortex. However, the subsequent depletion of neuronal PrP^C in animals with established CNS infection prevented the progression to clinical prion disease and resulted in the long-term survival of infected animals with a reversion of hippocampal neuronal loss and spongiosis.

In 1997 Stanley Prusiner was awarded a Nobel Prize for Medicine "for his discovery of Prions - a new biological principle of infection" and by then the protein-only hypothesis has been universally accepted in the scientific community. Further conclusive proofs came in the early '00s, when A N-terminally truncated recombinant mouse prion protein (recMoPrP89/230) produced in *Escherichia coli* was polymerized into amyloid fibrils and inoculated IC into transgenic (Tg) mice expressing MoPrP(89–231). Mice developed neurologic dysfunction

between 380 and 660 days after inoculation and brain extracts showed protease-resistant PrP (Legname et al., 2004). Additionally, in 2006 Castilla and colleagues described a new method to generate infectious prions (Castilla et al., 2006), showing that the conversion from PrP^C to PrP^{Sc} can be reproduced *in vitro* by cyclic amplification of protein misfolding. Furthermore, inoculation of the newly generated prions in WT hamsters led to the development of a prion disease identical to those developed after inoculation of brain-derived material.

1.7 Structure and Conversion of PrP^{Sc}

According to the prion hypothesis PrP^C is converted to PrP^{Sc} through a conformational change induced by the direct interaction between PrP^C and PrP^{Sc}. However, the atomistic mechanism driving this event is not clarified yet, and neither is the cellular compartment where the conversion occurs. The complete understanding of this phenomenon has been dampened so far by the lack of information on PrP^{Sc} structure at the atomic level. A number of approaches have been pursued over the years, unfortunately the high insolubility, the propensity to aggregate, and the wide heterogeneity of all PrP^{Sc} particles isolated have made high-resolution techniques such as NMR and X-ray crystallography unusable (Rigoli et al., 2019). Therefore, all available information on PrP^{Sc} structure has been produced with low-resolution or indirect experimental methods, such as spectroscopic analyses (e.g. Fourier-transform infrared spectroscopy, FTIR) (Caughey, 1991) and mass spectrometry coupled to biochemical or biophysical approaches as hydrogen/deuterium exchange (Spagnolli et al., 2019) or limited proteolysis (Vazquez-Fernandez et al., 2012). Among the models proposed, two architectures are considered the only plausible ones: the parallel in-register intermolecular beta-sheet model (PIRIBS) and the 4R β S model (Fig. 4).

In the PIRIBS model, PrP^{Sc} monomers appear as a flat succession of β -strands connected by linkers and are aligned onto the preceding misfolded monomer (Grovetman et al., 2014), in a structure similar to other known amyloids. According to this model, each residue is piled on top of the previous one. However, several doubts concerning its limitations and inconsistencies have been raised against this model. First of all, the structure predicted with the PIRIBS model is not able to accommodate the bulky glycans present in PrP^C, as stacking them in-register would generate steric clashes (Grovetman et al., 2014). Moreover, the PIRIBS model cannot explain several pieces of evidence obtained by X-ray fiber diffraction

and cryo-electron microscopy (cryoEM) of infectious PrP^{Sc} preparations, while in turn, the 4R β S architecture seems consistent with these experimental findings (Vazquez-Fernandez et al., 2012). According to the 4R β S model, the structure of PrP^{Sc} is based on a four-rung β -solenoid architecture (Spagnolli et al., 2019). CryoEM and 3D reconstructions revealed a larger assembly unit along the fibril axis, encompassing two monomers in a potential head-to-head/tail-to-tail configuration. Despite the information on the overall architecture of PrP^{Sc} obtained with cryoEM data, the intrinsic resolution of the method was not sufficient to resolve the structure in atomic details.

It is known however that PrP^{Sc} 106, the shortest form of PrP that retains the ability to support the formation of transmissible prions, was also found to contain a 4R β S fold (Supattapone et al., 1999), (Wan et al., 2015)

FTIR spectroscopy and circular dichroism spectroscopy (CD), allowed to measure that PrP^{Sc} and its N-terminally truncated variant, PrP27-30, possess a high β -sheet content (Caughey, 1991), (Pan et al., 1993), (Wille et al., 2002). According to FTIR estimations, the content of β -sheet in PrP27-30 ranges from 43–61%. Furthermore, the FTIR-based data do not support the presence of α -helices in PrP^{Sc}, and it thus can be concluded that the residual 50% amino acids are organized in random coil loops (Requena and Wille, 2014). In the β -solenoid core, the connecting loops are likely very tightly packed against the β -strands. This compact nature well explains the known resistance of PrP27-30 (spanning roughly from 90 to 230aa) to protease digestion, while it has been hypothesized that its N-terminal residues (up to position 86/98), which are rapidly digested, retain the completely unstructured appearance of the N-terminal PrP^C (Prusiner et al., 1998). It is noteworthy that this region is totally dispensable for infectivity. However, shorter PK-resistant PrP^{Sc} fragments have been identified in many “atypical” PrP^{Sc} strains (Di Bari et al., 2013), (Gotte et al., 2011).

The origin of propagation is likely to reside in the β -solenoid structure, which has inherent templating capabilities. Its upper and lowermost rungs contain “unpaired” β -strands that can propagate their hydrogen-bonding pattern into any amyloidogenic peptide they encounter (Vazquez-Fernandez et al., 2017). Once this supplementary β -solenoid rung is formed, it offers a fresh, “sticky” surface that can continue templating the remaining, unfolded portion of the incoming PrP molecule, until a second rung is generated. This process can be repeated two more times until the entire length of the incoming PrP polypeptide chain has been molded into four newly formed rungs, thus completing a new four-rung β -solenoid structure. The newly formed upper or lowermost rungs can then serve as a fresh templating surface for a

new incoming unfolded PrP molecule, in a process that can proceed ad infinitum (Spagnolli et al., 2019).

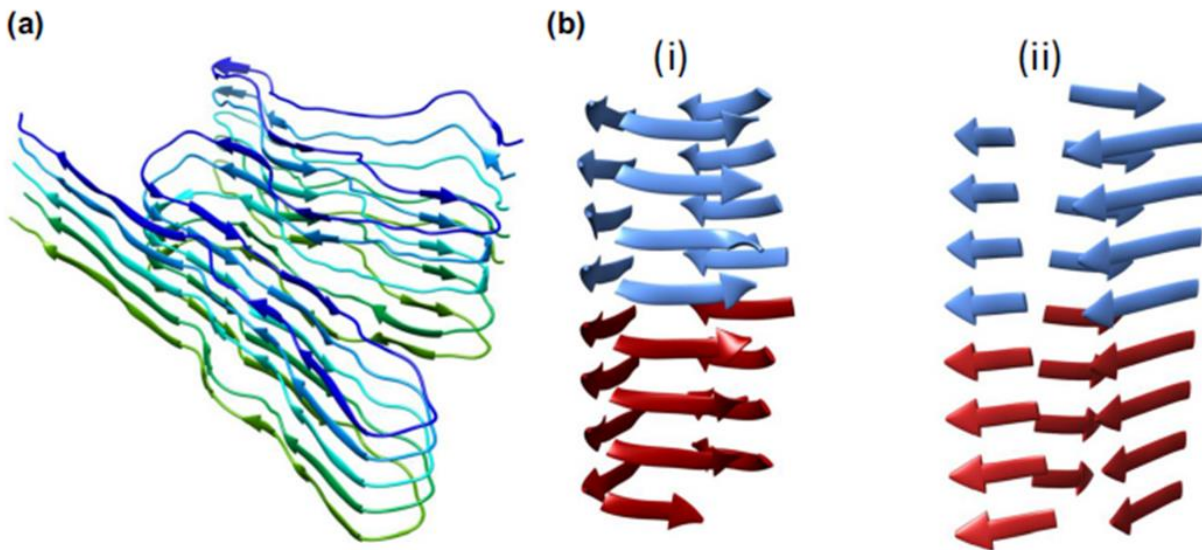


Figure 4: Proposed Architectures for PrP^{Sc}. (a) In the PIRIBS model each misfolded PrP^{Sc} monomer (each color represents one monomer) is perfectly aligned onto the previous misfolded monomer; (b) The 4RβS model (each color reflects one monomer) can be either arranged as in a left-handed (i) or right-handed (ii) conformation). Taken from Rigoli et al., 2019.

1.8 The Cellular Site of Conversion

Another long-time debated and still unclear issue is the subcellular compartment where the conversion from PrP^C to PrP^{Sc} occurs. After the synthesis, PrP^C is immediately translocated in the ER, where it receives double glycosylation. During the following transit through the Golgi apparatus, the glycoside chains are remodeled and once the process is complete, the mature PrP^C is delivered to the plasma membrane. Membrane-resident PrP^C pool undergoes continuous recycling in the endoplasmic system, where the protein is partly degraded after transit into lysosomes, partly recycled to the plasma membrane (see Chapter 1.3). It seems thus likely that the first contact with PrP^{Sc} happens in one of these compartments, especially the plasma membrane, where the majority of PrP^C is exposed. However, considering the conversion site, aspects as the pH of the compartment, PrP^C folding state and consequently the energy necessary for the conversion complicate the picture.

In N2a cells infected with prions as well as infected mouse brains, electron microscopy revealed that PrP^{Sc} is localized in discrete vesicular foci resembling those found when autophagic vacuoles evolve to late lysosomes and into large bodies in the cytoplasm (Arnold et al., 1995), (McKinley et al., 1991). No co-localization was observed with the nucleus, ER, or Golgi compartments. In 1991 Caughey showed that the cellular processing of PrP^{Sc} is blocked if lysosomal proteases are inhibited with leupeptin and NH₄Cl (Caughey, 1991). The evidence that lysosomal proteases are involved in the conversion process suggests that PrP^{Sc} might be translocated to lysosomes, implying that the conversion of PrP^C could occur on the cell membrane or through the endocytic pathway before PrP^{Sc} transits through the endosomal and lysosomal compartment. More recent cryoEM studies on hippocampal sections obtained from prion-infected mice, revealed that during infection, the most prominent increase in PrP labeling was found in the early endosomes compartment, thus suggesting these structures as possible sites of conversion (Godsave et al., 2008). Contrasting evidence came from a contemporary work by Marijanovic and colleagues (Marijanovic et al., 2009), which excluded both early and late endosomes could play a significant role, while identified the endosomal recycling compartment as the likely site of prion conversion. Similarly, another report from Yim and colleagues (Yim et al., 2015), highlighted that when the maturation of the multi-vesicular bodies is impaired (MVBs), the conversion of PrP^{Sc} in chronically infected cell lines is markedly reduced.

However, another conflicting report showed that when the membrane recycling is inhibited or the retrograde transport to the Golgi is hyper-activated in prion-infected N2a cells, a marked increase in the conversion of PrP^C to PrP^{Sc} is detected, suggesting that the prion protein can be retrogradely delivered to the ER, and that this compartment may play a significant role in PrP^{Sc} conversion (Beranger et al., 2002).

One of the major confounding factors affecting the reliability of studies conducted on infected cell models is the impossibility to distinguish PrP^{Sc} species derived from the inocula from the newly formed ones. In an elegant work from Goold and colleagues, the early cellular events right after prion infection were studied inserting an epitope tag into the sequence of the endogenous PrP^C, in order to differentiate *de novo* formed PrP^{Sc}. This strategy allowed to show that prion can infect cells extremely rapidly, just after 1 min of exposure, and that the plasma membrane is the original site of prion conversion (Goold et al., 2011).

Regardless the nature of the final conversion site, the endocytic pathway seems necessary for the conversion of PrP^C to PrP^{Sc}, as the inhibition of endocytosis by a temperature block,

as well as dynamin inhibitors, prevented PrP^{Sc} formation (Borchelt et al., 1992), (Stincardini et al., 2017). The second main requirement for an efficient conversion is the correct localization of PrP^C. Treatment with drugs as lovastatin, which diminishes cellular cholesterol levels, altering the composition of lipid rafts, the membrane subdomain where PrP^C is mostly enriched, inhibited PrP^{Sc} formation (see Chapter 1.17). Similarly, replacement of the GPI-anchor signal sequence, with a sequence coding for a non-raft membrane localization decreased the efficiency of PrP^{Sc} conversion (see Chapter 1.3).

Despite the many contradictory pieces of evidence, the identification of the intracellular trafficking route of PrP^{Sc} is still of vital importance, since the design of specific agents modulating these pathways could represent a possible pharmacological strategy for prion diseases.

1.9 The Concept of Prion Strains

The concept of prion strain progressively emerged after the first attempts of reproducing the disease with experimental models, when it became apparent that prion diseases were characterized by extraordinary variable incubation times, age at the onset, clinical signs, entity and distribution of the anatomic lesions. The prion-strain phenomenon was first described for sheep scrapie, when it was shown that the infectious agent could be propagated in goats as multiple phenotypically distinct entities (Fig. 5a) (Pattison and Jones, 1967). Afterward, studies in mice showed that animals inoculated with different scrapie strains displayed distinct incubation periods and histopathology and that these characteristics were propagated with fidelity on serial passages (Dickinson and Fraser, 1969), (Fraser and Dickinson, 1973). In these early studies, prion strains were distinguished according to their phenotypic features.

After the isolation of the scrapie agent and Prusiner's seminal discoveries, the biochemical and structural properties of the pathogenic agent started to be considered. For example, the characterization of two biologically distinct strains of hamster-adapted TME prions, hyper (HY) and drowsy (DY), proved that the protease-resistant cores of their corresponding PrP^{Sc} structures differed in electrophoretic mobility in denaturing gels (Bessen and Marsh, 1992). This shift in mobility suggested that different prion strains have different 3D conformations that expose different parts of the structure to proteases. Mouse-adapted scrapie strains differed in the relative proportion of PrP^{Sc} isoforms (Kascsak et al., 1991). Other lines of

evidence for the strain theory came from studies of human prion diseases. PrP^{Sc} aggregates associated with FFI were shown to have different electrophoretic mobility when compared with sporadic CJD (sCJD). These observations led to the suggestion that differences in disease outcomes can be associated with differences in the conformation of PrP^{Sc}. It is widely accepted now that PrP conformation is the primary determinant of strain type with glycosylation being involved as a secondary process.

It is thought that the protein structure encoding strain properties is the β -solenoid architecture of PrP^{Sc}. However, it is still unclear how the misfolding of a single protein can determine such a variety of possible disease outcomes and how this happens. It is possible that different threading leads to slight differences in the amino acid composition of the β -strands and loops, thus originating the necessary variability of the main β -solenoid theme (Spagnoli et al., 2019). These variations influence the availability of the upper- and lowermost rungs, thus affecting the templating properties of the specific β -solenoid structure.

Regarding PrP glycosylation state, it is known that transgenic mice expressing PrP with mutations interfering with N-linked glycosylation have different susceptibility to prion infections. Namely, mutations of the first glycosylation consensus sequence failed to support PrP^{Sc} replication. Interestingly, when the second glycosylation site was mutated, prion replication was supported, even though with a significantly longer incubation period for infection (DeArmond et al., 1997). It is thought that different PrP^{Sc} conformations, when inoculated, preferentially recruit and convert specific glycoforms of PrP^C. In a cell-free conversion assay, it has been shown that the glycosylation of PrP^C affects its ability to bind to PrP^{Sc}, and that differences in the primary sequence of the PrP^C and PrP^{Sc} affect the efficiency of conversion (Priola and Lawson, 2001). However, the carbohydrates attached to PrP^C can have a high degree of heterogeneity (Endo et al., 1989), making it extremely difficult to establish if specific carbohydrates play a key role in the replication of distinct prion strains.

1.10 Species Barrier Phenomenon

As for the concept of strain, the species barrier phenomenon has been initially observed when the first attempts of experimentally transmit scrapie to other animal models have been performed. Species barrier results in longer incubation periods, often longer than the lifespan of the animal and generally reduced upon further passage to the same species. Also,

unusual histological and clinical signs together with a global reduction of the death rate in the cohorts of infected animals can occur (Fig. 5b) (Pattison, 1965).

The most extensively characterized barrier is the one between hamsters and mice (Kimberlin and Walker, 1977), (Kimberlin and Walker, 1978). The 263k strain was derived from the DY prion, initially passaged through rats and then in hamsters. During the initial passage in hamsters, the inocula obtained were successfully used to infect mice. However, following further passage in hamsters, the hamster-passaged prion lost the pathogenicity for mice, retaining just the infectivity for hamsters.

As for the strain phenomenon, it seems evident that PrP primary structure can also determine prion species barriers. If a specific prion strain converts PrP^C into one preferred conformer, hosts which express a PrP^C that cannot fold into the preferred conformation of an inoculated prion will be then “immune” to the disease spreading. Conversely, when PrP primary structure of the host allows folding into the conformation of an inoculated prion, the infection will be transmitted in the absence of any barrier (Collinge, 1999). Abrogation of the species barrier was shown in transgenic mice overexpressing PrP sequences from the donor species. In a seminal experiment from Scott and colleagues it has been shown that the species barrier of hamster to mouse prion transmission could be overcome if a hamster PrP transgene was introduced into the recipient mouse line (Scott et al., 1989). Noteworthy, the prions obtained with this paradigm were hamster specific if the inoculum was obtained by hamster and mouse-specific if it was obtained by mice (Prusiner et al., 1990).

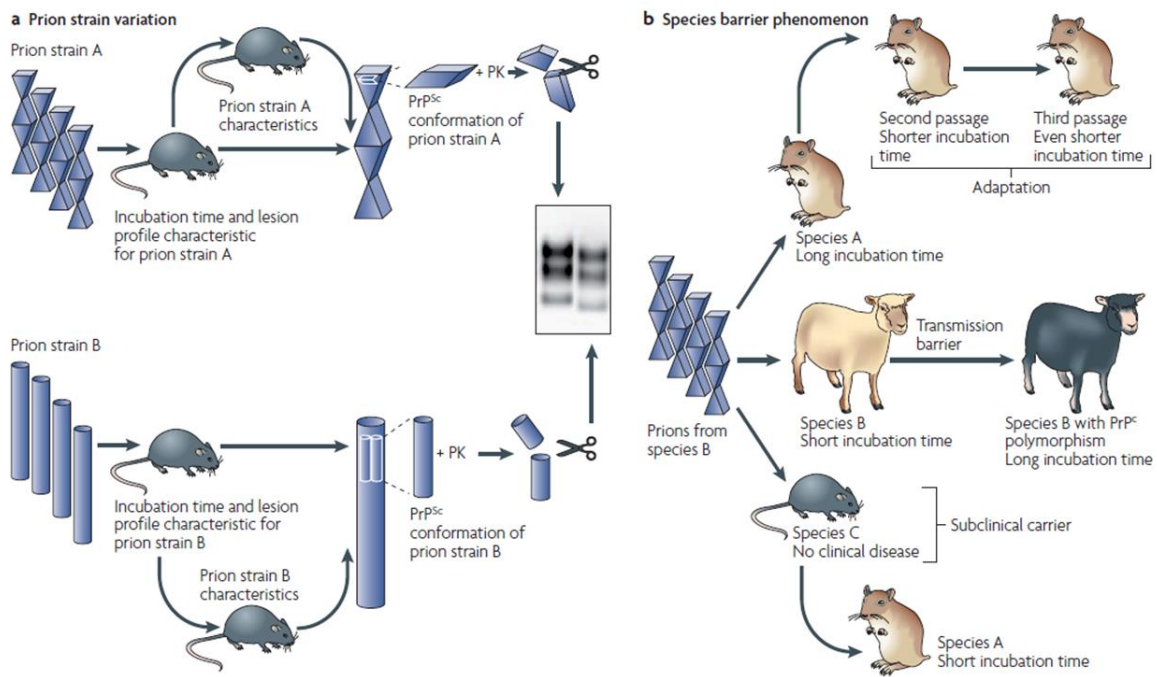


Figure 5: The Concept of Strain and Species Barrier. (a) The transmission of different prion isolates (A B) to genetically identical hosts results in distinct disease phenotypes, such as incubation times and lesion profile, which are determined by the inoculum. These features persist following serial passages to new hosts. In some cases, strains exhibit characteristic biochemical signatures such as electrophoretic mobility of the PK-resistant core (as shown in the western blot insert). This is thought to result from divergent PrP^{Sc} conformations, which lead to the exposure of different sites for enzymatic cleavage (indicated by the scissors). (b) Prions isolated from one species are often less infectious to other species, as evident by longer incubation times and reduced attack rates in these other species. This is thought to depend on dissimilar host prion protein (PrP) sequences, which thereby hinder the conversion process. After serial passages, incubation times gradually decrease — a phenomenon called adaptation. In some cases, the species barrier is so strong that certain hosts do not show any clinical disease following inoculation with prions from other species. Nevertheless, brain isolates of these apparently resistant hosts can transmit disease when inoculated to susceptible hosts. Hosts of the same species as the original inoculum might exhibit remarkably long incubation times that are due to certain polymorphisms of the Prnp gene, a phenomenon that is known as the transmission barrier (Taken from (Aguzzi et al., 2007).

1.11 Mechanisms of Prion Toxicity

1.11.1 PrP^C-Mediated Toxicity

The mechanisms by which prions induce neurodegeneration are still far from being fully clarified. As for other amyloid diseases, PrP^{Sc} oligomers have been the focus of researchers attention for a long time. Despite that, there is little consensus on the nature of oligomeric species involved in prion toxicity. What is widely accepted so far, is that PrP^C plays a crucial role in the pathogenesis of prion diseases, not only by acting as a passive substrate for the generation of PrP^{Sc}. In the absence of endogenous PrP^C, brain tissue is resistant to the neurotoxicity induced by a prion-infected graft tissue (Brandner et al., 1996a, Brandner et al., 1996b). Furthermore, genetic ablation of PrP^C from neurons, in mice with an overt prion infection, reverses the neurodegenerative processes and the development of clinical signs, despite the continuous production of infectious PrP^{Sc} by surrounding astrocytes (Mallucci et al., 2007). Also, when mice expressing an anchorless PrP^C that is secreted in the extracellular space are infected, they do not develop the typical prion pathology despite large amounts of extracellular PrP^{Sc} (Chesebro et al., 2005), (Chesebro et al., 2010), suggesting that PrP^{Sc} oligomers and fibrils are innocuous *per se* (Brandner et al., 1996a, Brandner et al., 1996b) and it is the endogenous PrP^C conversion that causes neuronal dysfunction and death.

In support of this hypothesis, the accumulation of infectious PrP^{Sc} and the neurodegenerative events have been shown to proceed with two different temporal profiles (Sandberg et al., 2011). The overexpression of PrP^C does not change the incubation time until PrP^{Sc} accumulation reaches a plateau, however the interval between the plateau and the terminal disease phase is significantly shortened. Accordingly, a 50% decrease in PrP^C expression does not affect prion replication but decrease the sensitivity of neurons to toxicity (Bueler et al., 1994). It can be evinced that prion disease occurs in two distinguishable phases. In phase 1, non-toxic prions increase until they reach a similar plateau in all mice regardless of PrP^C expression levels. In phase 2, a physically undefined, selectively toxic form of PrP is generated (Aguzzi and Falsig, 2012).

These data provide a possible justification for the poor *in vivo* effects exerted by almost all the anti-prion compounds identified as inhibitors of PrP^{Sc} accumulation in *in vitro* assays. In

fact, these molecules can only disfavor PrP^{Sc} accumulation without hampering the neurotoxicity originating from other toxic conformers (Barreca et al., 2018).

It has been hypothesized that a loss of PrP^C function might be the origin of all the neurotoxic events. Supporting this theory is the implication of PrP^C in several mechanisms leading to neuronal protection from oxidative stress or other types of pro-apoptotic insults (Kovacs and Budka, 2008), (Roucou et al., 2004). PrP^C conversion into PrP^{Sc} might deprive cells of PrP^C physiological function, leading to neurodegeneration. However, this theory is strongly debated by compelling data, showing normal embryonic development and absence of major anatomical or functional phenotypes in mammals where PrP^C expression has been permanently or conditionally knocked out (Benestad et al., 2012), (Bueler et al., 1992), (Mallucci et al., 2002), (Manson et al., 1994), (Richt et al., 2007), (Yu et al., 2006), (Yu et al., 2009).

Prion-induced neuropathology could thus be explained by a “subversion-of-function” hypothesis, where the interaction between PrP^C and PrP^{Sc} (or other pathogenic intermediate species) alters the physiological activity of PrP^C inducing a neurotoxic cascade (Harris and True, 2006).

This hypothesis is also sustained by the evidence collected on mouse models carrying mutant forms of PrP^C lacking specific domains or disease-associated mutations. Studies conducted on cells expressing disease-associated forms of PrP^C have revealed that some of the mutants are more prone to aggregate and resistant to proteases (Lehmann and Harris, 1996), (Priola and Chesebro, 1998). Furthermore, some mutants have aberrant subcellular localizations, as partial retention in the ER (Ivanova et al., 2001) and retro-translocation to the cytoplasm (Lorenz et al., 2002). More interestingly, other disease-associated PrP mutants retain physiological biochemical properties and subcellular localization (Harris et al., 2003), suggesting that they can trigger pathogenic events not because they are more prone to misfold and aggregate, but because the mutation alters the physiological activity of PrP^C. However, cells transfected with disease-associated PrP constructs generally do not show any cytopathic phenotype, making it difficult to analyze the neurotoxic mechanisms underlying these mutants (Solomon et al., 2010).

To gain more insight into the pathological role of PrP^C, several models carrying mutant forms of PrP^C lacking specific domains have been generated. In one of the first seminal reports, Shmerling and colleagues discovered that mice expressing PrP harboring different large, N-terminal deletions (Δ 32-121 and Δ 32-134) developed a spontaneous neurodegenerative

process, independent from prion inoculation, characterized by ataxia and cerebellar granule neurons degeneration (Shmerling et al., 1998). Interestingly, the neurotoxicity of shortened PrP^C mutants was suppressed by sub-stoichiometric co-expression of full-length PrP^C. Similarly, Baumann and colleagues produced a mice line expressing transgenic PrP deleted in residues 94-134 (Baumann et al., 2007). Interestingly, these mice showed a similar neurodegenerative condition, suppressed by the co-expression of WT PrP. In another report, Li and colleagues observed that mice expressing PrP with a smaller deletion, encompassing residues 105-125, within PrP Central Region (PrP Δ CR), develop spontaneous neurodegeneration, particularly evident in the cerebellar granule cells (Li et al., 2007). Surprisingly, PrP Δ CR is neither aggregated nor protease-resistant and its subcellular localization is unaltered, thus neurotoxicity driven by PrP Δ CR rather results from an alteration of the normal activity of PrP^C. As for the other deletions mentioned, the phenotype is reversed in a dose-dependent fashion by coexpression of WT PrP (Christensen and Harris, 2009).

To understand the mechanism underlying PrP Δ CR toxicity Solomon and colleagues measured the membrane activity in different cell lines expressing PrP Δ CR and observed an increase in non-selective ionic currents. The non-selective ion flux was suppressed by co-expression of full-length PrP^C (Solomon et al., 2010), suggesting that PrP itself may give rise to a pore and originate the neurotoxic damage (Solomon et al., 2012). However, there is still no evidence that PrP can autonomously induce pore formation *in vivo* after prion infection.

Another line of evidence suggesting that PrP^C can mediate toxic cascades of events is supported by the findings collected using anti-PrP^C antibodies, which showed that antibodies binding to PrP^C trigger robust neurotoxicity (Solfrosi et al., 2004). Monoclonal antibodies targeting epitopes in the C-terminal of PrP^C induce a fast neurodegenerative process if injected into mouse brain or administered to cultured cerebellar slices (Sonati et al., 2013). Interestingly, neurodegeneration was prevented by antibodies against the N-terminal region, which were also able to compensate the toxicity of PrP Δ 94–134 (Sonati et al., 2013), suggesting that the antibodies targeting the globular domain and the internal deletions activate a similar pathogenic cascade, involving a structural rearrangement of the N terminus. Even though the evidence collected on different cell lines expressing PrP Δ CR suggest that PrP^C toxicity could be an autonomous process, not relying on other interactors, given that PrP^C is an entirely extracellular GPI-linked molecule, it is unclear how it might transmit signals across the plasma membrane (Aguzzi and Falsig, 2012).

A number of different studies, conducted on various cell models, showed that PrP interacts with many membrane proteins, likely affecting their cellular localization and activity (Linden et al., 2008). These include glutamate receptors of the NMDA subclass (Khosravani et al., 2008), γ -aminobutyric acid receptor (GABAR) subunits (You et al., 2012) and voltage-gated calcium channels (VGCCs) (Senatore et al., 2012). The interaction with these channel proteins, might explain some of the neurotoxic events associated with prion pathology, however very few of them have been undoubtedly linked to prion-induced neurodegeneration. Interestingly, a recent work showed an impairment in PrP^C-mediated NMDAR S-nitrosylation in early and late-stage prion-infected mice, a mechanism known to mediate the inhibition of NMDARs, thus offering a possible explanation for the neurotoxicity events characterizing prion diseases (Meneghetti et al., 2019).

1.11.2 Autophagy and Unfolded Protein Response

The accumulation of misfolded proteins, common to a variety of amyloidopathies, is thought to be responsible for several intracellular mechanisms as the Unfolded Protein Response (UPR), autophagy and the activation of proteasomes, which cells activate to promote the clearance of the aggregates. Autophagic vacuoles have been identified in several forms of TSEs, tissues of prion-infected rodents, and in prion-infected cultured cells (Boellaard et al., 1989), (Heiseke et al., 2010), (Joshi-Barr et al., 2014), (Liberski et al., 2008), (Rubinsztein et al., 2005), (Xu and Zhu, 2012), and have been initially interpreted as one of the causes of neurodegeneration (Liberski et al., 2002, Liberski et al., 2004). However the role of autophagy is still debated: some authors consider it a player of neurodegenerative processes (Liberski et al., 2002), while other ones claim it exerts a neuroprotective role, by shifting the equilibrium towards clearance, reducing the intracellular load of PrP^{Sc} deposits (Gilch et al., 2008). Following this latter hypothesis a number of studies in cells and in mice showed that prion infection is efficiently counteracted by induction of autophagy (Abdulrahman et al., 2017), (Ertmer et al., 2004), (Jeong et al., 2012). Namely, treatment of prion-infected cells with trehalose, an extensively characterized inductor of autophagy, dampens PrP^{Sc} aggregation and cell damage (Beranger et al., 2008). Prion-infected mice treated with Imatinib at an early phase of infection have a substantial delay of PrP^{Sc} accumulation in the brain and to a lesser extent a prolonged survival time (Yun et al., 2007). However, Imatinib does not efficiently permeate the Blood-Brain Barrier (BBB) and the small extension of life-

span observed, was achieved only with an early administration (Yun et al., 2007). Rapamycin, the most used mammalian target of rapamycin (mTOR) inhibitor and known autophagy inducer, slightly prolonged the survival prion-infected mice and GSS mouse model (Cortes et al., 2012), with good indications for a potential penetration of the BBB.

As for autophagy, the link between prion spreading and UPR is still not fully understood. UPR seems to play a substantial role in synaptic plasticity reduction and thus in the impairment of long-term memory consolidation. Methionine incorporation experiments on hippocampal slices from infected mice revealed a significant lowering of protein synthesis, not caused by a reduction in the transcriptional activity, but more likely by a blockade at the translational level. Also, an increase in eIF2 α phosphorylation, a common hallmark of UPR activation, can be detected before the neuronal transmission impairment. These pieces of evidence suggest that UPR is activated way before synaptic alterations and is responsible for them (Moreno et al., 2012). The hypothesis that UPR drags on prion disease degeneration is also supported by evidence of ER stress activation in cellular models. N2a cells treated with Rocky Mountains Laboratory (RML) extracts and brain extracts from sCJD patients, show an increase in the protein levels of the chaperones associated with ER stress (Hetz et al., 2003), (Torres et al., 2010). Also, a rise in the processing rate of pro-caspase 12, which has been associated with ER-stress induced apoptosis, has been detected (Hetz et al., 2003), (Nakagawa et al., 2000). The genetic and pharmacologic modulation of UPR, by targeting the protein kinase R (PKR)-like endoplasmic reticulum kinase (PERK) pathway, was tested on a mouse model infected with prions at different stages. If the treatment was administered at a pre-symptomatic stage, it resulted in an extension in mice survival, with preservation of behavioral and memory functions. However, the post-symptomatic administration had no effect (Halliday and Mallucci, 2015), (Halliday et al., 2017), (Moreno et al., 2013). Accordingly, significant prevention of neuronal loss and astrogliosis was observed in the pre-symptomatic treatment group, while the effect of the post-symptomatic treatment was just modest. Nevertheless, treatments have to be forcedly interrupted for severe adverse effects, attributable to the systemic inhibition of PERK (Harding et al., 2001), dampening the transferability of this pharmacological strategy. It is to note also that this kind of approach doesn't account for the problem of infectivity, counteracting only the downstream effects. Also, the relevance of UPR in prion diseases has been questioned: In a study from Unterberger and colleagues, mice injected with RML brain extracts showed no PERK activation during the initial stages of the disease, but just later, when PrP^{Sc} deposition was

highly spread around the brain (Unterberger et al., 2006). These findings arise the doubt that UPR activation might not be among the first pathological events causing synaptotoxicity, but a delayed effect of PrP^{Sc} deposition. In accordance with that, in the same paper, the authors analyzed PERK activation in a cohort of brains from patients with a wide panel of prion diseases. Surprisingly, the immunoreactive signal from P-PERK and other UPR markers was essentially undetectable in the frontal cortex of patients. Further evidence was collected by Wiersma and colleagues, which analyzed UPR activation in brains from a total of 47 cases of prion disease (Wiersma et al., 2016). P-PERK levels, evaluated in the frontal cortex by immunohistochemistry, together with other UPR markers, were undetectable, showing no immunoreactivity. However, it is worth to consider that all the works on human samples proposed here analyze different brain regions with different techniques and also the age of patients is quite heterogeneous. Given these conflicting results, it is clear that a more systematic study on human samples has to be done before considering the application of anti-UPR drugs on prion disease patients.

1.11.3 Synaptic Alterations

Since prion diseases generally manifest with a mental impairment leading to rapid dementia, it is thus likely that, as for the other forms amyloid-driven dementias, synaptic dysfunction may be involved in the pathogenic mechanisms. Electron microscopic studies and examinations with the Golgi method have revealed dendritic varicosities, synaptic vacuolation and loss of dendritic spines in human, animal and experimentally transmitted prion diseases (Ferrer et al., 1982), (Hogan et al., 1987, Landis et al., 1981, Liberski, 1990). From a biochemical standpoint, reduced expression of crucial synaptic proteins linked to exocytosis and neurotransmission, as SNAP-25, synapsin, syntaxin, and α - and β -synuclein, has been reported in human CJD patients and animal prion disease models (Jeffrey et al., 1995), (Siso et al., 2002). Since the first histological analyses of TSE samples, the presence of abnormal accumulations of PrP^{Sc} have been documented in the neuropils (DeArmond et al., 1987) and in the synaptic region (Kitamoto et al., 1992). These pieces of evidence have then been reproduced also in experimental models, where after infection, abnormal PrP aggregates were traced in nerve cell processes and punctate synaptic-like areas (Bruce et al., 1989), (DeArmond et al., 1987, Kitamoto et al., 1992). These pieces of evidence had then been reproduced also in experimental models, where after infection, abnormal PrP aggregates

were traced in nerve cell processes and punctate synaptic-like areas (Bruce et al., 1989, Bruce et al., 1989, DeArmond et al., 1987) Combining the presynaptic marker synaptophysin and PrP immunostaining in patients with CJD, this hypothesis has been confirmed (DeArmond et al., 1987), (Kitamoto et al., 1992). It has been long time unclear however if synaptic damage is just a result of neural death or an early autonomous event and how prion deposition could induce it.

Electrophysiological recordings on hippocampal slices extracted from infected mice at the early stages of the disease revealed a deficit in the ability to induce (LTP) (Chiti et al., 2006), (Johnston et al., 1998b), together with membrane and synaptic abnormalities in the later stages of the disease (Johnston et al., 1998b, Johnston et al., 1998a). Microscopy analyses of hippocampal sections from prion infected mice showed that synaptic and dendritic alterations, together with a massive loss of terminals, are early events of the disease, starting before neuronal loss and fibrils accumulation, suggesting that aggregates are not the cause of synaptic damage (Jeffrey et al., 2000). This observation is also in accordance with all the cases of disease where no detectable PrP^{Sc} was found in the CNS, as seen in some mouse BSE models and sheep scrapie, infective FFI models, human GSS cases and relative transgenic mice (Collinge et al., 1995, Demaimay et al., 1997), (Hsiao et al., 1989). Accordingly, abnormal PrP deposition does not seem to be a predictor of disease severity and does not pair the degree of reduction of synaptic protein expression in the different layers of the cerebellar cortex and in the dentate nucleus (Ferrer, 2002).

In mice injected with ME7 brains homogenates, tested at the beginning of the clinical onset of the disease, no significant increase in neuronal cell loss was observed in the hippocampal region CA1, while a significant loss of synaptic markers and in the number of synapses was observed (Cunningham et al., 2003), suggesting that clinical symptoms may better correlate with synapse loss than with neuronal loss (Gray et al., 2009, Ishikura et al., 2005). Furthermore, two-photon *in vivo* imaging in a mouse model of prion disease revealed that aberrant dendritic dilatations, called varicosities, emerged during the pre-symptomatic phase, leading to the subsequent loss of dendritic spines in the nearby region (Fuhrmann et al., 2007).

It is still unknown however which pathway and which oligomeric form of PrP^{Sc} are the mediators of these processes. Several reports indicated that PrP^C can interact with many synaptic proteins as the glutamate receptors of the NMDA subclass (Khosravani et al., 2008),

GABAR subunits (You et al., 2012) and VGCCs (Senatore et al., 2012), however just few of these proteins has been linked to prion pathological processes so far.

For example, in a recent report from Meneghetti and colleagues, it has been proposed that the first synaptotoxic events observed in prion diseases could be triggered by the loss of the neuroprotective function exerted by PrP^C (Meneghetti et al., 2019). PrP^C in fact, is known to promote the S-nitrosylation of NMDARs in a Cu²⁺-dependent fashion (Gasperini et al., 2016, Gasperini et al., 2015), a mechanism that inhibits the activation of NMDARs, making neurons less susceptible to excitotoxicity (Lipton et al., 1993). Considering the reduction in NMDARs S-nitrosylation observed in early and late stages mice inoculated with different prion strains (Meneghetti et al., 2019), it is possible that the binding to PrP^{Sc} during infection sequesters PrP^C, blocking its synapto-protective activity.

In an attempt to clarify these pathways, some acute models of prion associated synaptic toxicity have been recently developed. In 2016 Fang and colleagues showed that exposure of cultured hippocampal neurons to PrP^{Sc} determined retraction of dendritic spines. Spine loss was dependent on PrP^C expression and more specifically on its N-terminal region (Fang et al., 2016). Furthermore, patch clamp recordings of miniature excitatory postsynaptic currents (mEPSCs), a paradigm of spontaneous synaptic currents evoked by glutamate, revealed a marked reduction in mEPSC frequency, and a less pronounced decrease in mEPSC amplitude (Fang et al., 2018).

Using the same models, the authors showed that PrP^{Sc} triggers a synaptotoxic signaling cascade starting with the activation of NMDA and AMPA receptors, with subsequent calcium influx. The massive increase in intracellular calcium then leads to the activation of p38 mitogen-activated protein kinase (MAPK), and depolymerization of actin filaments in dendritic spines. Synaptic degeneration seems to be restricted to the excitatory post-synapses and can be partially restored by the pharmacological inhibition of any one of the steps involved in the signaling cascade (Fang et al., 2018). It is puzzling however how this dramatic decrease in EPSP frequency can be solely explained by the retraction of dendritic spines, especially considering that EPSP amplitude decrease is just modest, and not also by a concomitant deficit in the pre-synaptic function, which could confirm all the other pieces of evidence pointing out a reduction of presynaptic markers.

In another model developed by Foliaki and colleagues, the LTP in the hippocampal CA1 region was measured on slices briefly superfused with infected brain homogenates. They found that PrP^{Sc} species, with at least modest PK resistance, induce a significant decrease in

the LTP, probably attributable to a heightened presynaptic vulnerability to the synaptotoxic insult, since other electrophysiological parameters, as the post-tetanic potentiation (PTP) and the replenishment of the readily releasable pool (RRP) during the repeated high-frequency stimulation were also impaired. Furthermore, treatment with synaptotoxic PrP^{Sc} reduces many of the proteins necessary for the induction and maintenance of hippocampal LTP such as pERK, pCREB, synaptophysin and vesicular glutamate transporter 1 (VGLUT1), as well as the NMDAR NR2A and NR2B subunits and the GluA2 subunit of AMPAR (Foliaki et al., 2018). These results collectively prove that synaptic dysfunction is an early event in prion diseases. A more global understanding of the molecular determinants of this process could facilitate the development of pharmacological strategies targeting cognitive loss.

1.12 PrP^C as a Receptor for Misfolded Protein Isoforms

The first evidence of a possible role of PrP^C as a receptor for various species of oligomers was raised in a seminal work by Strittmatter group in 2009, where it was proven that A β 1-42 oligomers bind PrP^C (Lauren et al., 2009). The interaction between A β and PrP^C was then confirmed with different approaches in other independent reports (Balducci et al., 2010), (Chen et al., 2010). The importance of this interaction in the context of Alzheimer's disease (AD) pathogenesis was suggested in the same report, since anti-PrP antibodies rescued the synaptic plasticity impairment induced by treatment of hippocampal slices with oligomeric A β , preventing A β oligomers binding to PrP^C (Lauren et al., 2009). Conversely, no effect was observed in PrP null mice slices treated with A β . The significance of this interaction was also confirmed *in vivo* by the same group, when mice encoding a familial mutation in the Amyloid Precursor Protein (APP), crossed with PrP null mice, showed no detectable impairment of spatial learning and memory. Furthermore, significant rescue of synaptic markers, axonal degeneration and early death, however with marked amyloid plaques staining, were observed (Gimbel et al., 2010). More importantly, deletion of *Prnp* in symptomatic AD mice fully reversed hippocampal synapse loss and entirely rescued the preexisting behavioral deficits (Salazar and Strittmatter, 2017).

It is to note however, that the biological significance of the pathway has been argued in a different AD model, based on the acute intra-cerebro-ventricular injection (ICV) of synthetic A β 1-42 oligomers. In this experimental setting, the absence of PrP did not modify the synaptic impairment as seen by novel-object recognition task (Balducci et al., 2010).

In 2013 Strittmatter group proposed that the interaction of A β assemblies with PrP^C activates Fyn kinase via a mGluR5 mediated mechanism, as mGluR5 antagonists prevent A β -induced dendritic spine loss as well as learning and memory deficits in a familial AD mouse model (Um et al., 2013, Um and Strittmatter, 2013). PrP^C and mGluR5 interact physically, and cytoplasmic Fyn forms a complex with mGluR5. Once activated, Fyn signaling promotes the phosphorylation of the NR2B subunit of NMDARs, leading to a synaptic rearrangement process (Um et al., 2013, Um and Strittmatter, 2013) which can also be prevented by the administration of NMDA receptor antagonists (Resenberger et al., 2011).

It has been hypothesized that A β binds to PrP^C in its N-terminal domain (Resenberger et al., 2011) in two distinct regions, the hydrophobic 95–110 segment and the basic residues at the extreme N terminus of PrP residues 23–27 (Chen et al., 2010). Accordingly, administration of synthetic N1 terminal suppresses A β oligomers toxicity in cultured murine hippocampal neurons and in mice (Fluharty et al., 2013).

Multiple groups have started to develop methods to target the A β -PrP^C interaction using different approaches as antibodies directed against the putative A β binding region on PrP^C, small molecules (SMs) or N1 fragments. For example, the infusion of anti-PrP 6D11 in a familial AD mouse model induced a marked improvement in behavioral performances and in cognitive learning (Chung et al., 2010). Similarly, ICV administration of anti PrP^C fragment D13 prevented the inhibition of LTP in the rat hippocampus exerted by injection of AD brain material (Barry et al., 2011). A different paradigm was used by Aimi and colleagues, who using a cell-free assay to screen for compounds inhibiting A β oligomer binding to PrP^C, found that DSS counteracts the interaction in cell-free and in cell cultures and restores the LTP impairment induced by A β oligomers hippocampal slices (Aimi et al., 2015). Finally, Surewicz's group identified two N1-derived synthetic peptides, encompassing residues 23–50 and 90–112, both able to bind to A β 1–42 protofibrillar oligomers and inhibit the formation of fibrils, protecting hippocampal neurons from neurotoxic effects of A β oligomers (Nieznanska et al., 2018, Scott-McKean et al., 2016).

A variety of other reports also indicate that PrP^C can mediate the toxic signalling and facilitate the internalization of various β -sheet-rich conformers other than PrP^{Sc} and A β , as yeast prion proteins, designed β -peptides and α -synuclein aggregates (Aulic et al., 2017), (De Cecco and Legname, 2018), (Ferreira et al., 2017), (Resenberger et al., 2011) making it an even more appealing drug target candidate not just for prion diseases but also for many other amyloidopathies.

1.13 Human Prion Diseases

The vast majority (~85%) of human prion diseases is represented by sporadic forms of CJD (sCJD), while just in 10/15% of the cases has a genetic origin and a very small percentage (>1-2%) iatrogenic transmission (Gambetti et al., 2003a). The genetic forms of prion diseases are all caused by mutations in the *PRNP* gene. Iatrogenic forms of CJD have been reported to occur after surgical procedures with prion-contaminated tools or after transplantation of material from affected donors. In addition, horizontal transmission of prion diseases has been demonstrated for Kuru, a condition caused by ritual cannibalism in tribes of Papua New Guinea, and for variant CJD (vCJD), developed after consumption of (BSE) infected meat (Prusiner et al., 1998).

Globally, prion diseases encompass a wide range of different clinical, neuropathological and histological phenotypes. Interestingly, clinical heterogeneity is also paralleled by different disease duration and age at the onset (Ironsides et al., 2017). However, it is still unknown how the alteration of a single protein can cause such a variety of outcomes.

From a histopathological standpoint the main hallmark of prion diseases is the presence of a variable degree of spongiosis in the brain of affected individuals, hence the definition “transmissible spongiform encephalopathies” also used to define prion diseases (Iwasaki et al., 2017). Spongiform change usually comprises multiple rounded vacuoles within the gray matter, varying from 2 to 20 μm in diameter. Another distinctive feature is the presence of amyloid plaques, composed of abnormal PrP, which occur in some human prion diseases and, unlike AD, are generally more frequent in the cerebellar cortex. These plaques stain with CR and other tinctorial amyloid stains, but are best identified with immunohistochemistry for PrP. The last common pathological hallmark is the diffuse astrogliosis in the absence of inflammation (Fig. 6) (Iwasaki et al., 2017).

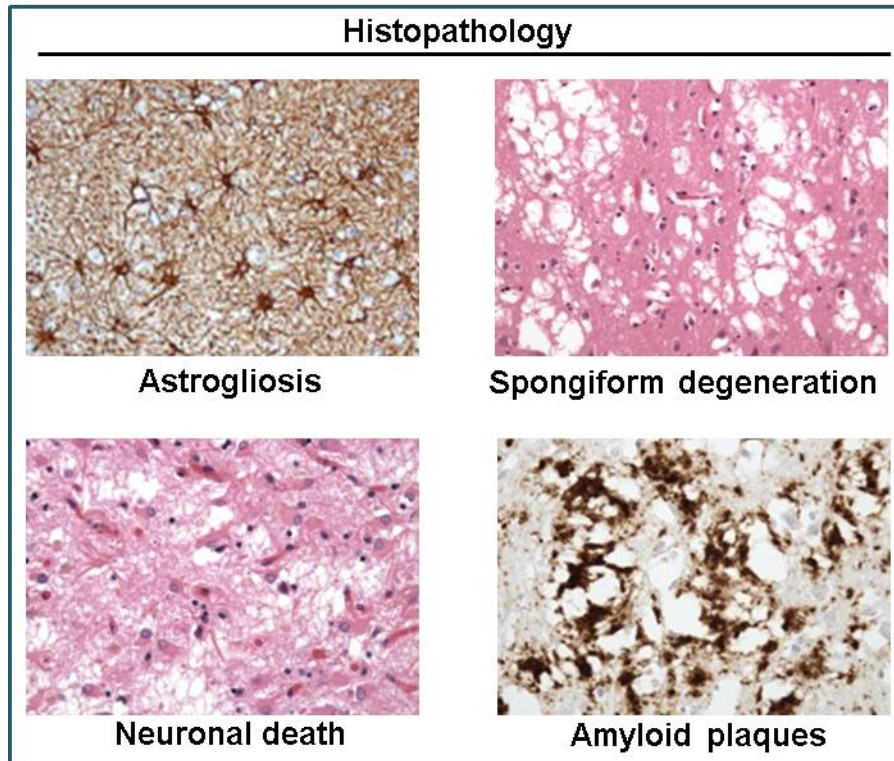


Figure 6: Histopathological Hallmarks of Prion Diseases. *Aberrations in the brains of affected individuals generally consist of astrogliosis (upper left), spongiform degeneration (upper right), neuronal death (lower left) and amyloid plaques (lower right) (taken from Sudano et al., 1984).*

1.13.1 Creutzfeldt-Jakob Disease

CJD has initially been described a century ago in two different reports by Creutzfeldt (1920) and by Jakob (1921) in six patients (Stengel and Wilson, 1946). During the first decades after the discovery, CJD has been considered as a rare pre-senile subacute dementia, and only after 1950, given the increase of the cases reported, this condition has started to be investigated more in detail (Gonatas et al., 1964).

The age at onset largely varies among the affected individuals, although in 90% of the cases the disease occurs between the 35th and the 65th year, with no sex differences. The duration of the disease is also quite heterogeneous amongst the different forms, spanning from few months to five-six years, with an average duration of two years (Gambetti et al., 2003a).

1.13.2 Sporadic CJD

The majority of CJD cases are represented by sporadic forms, which are likely caused by a spontaneous misfolding of PrP^C. Overall sCJD has an incidence of 1–2 cases per million population each year and mainly affect the adults over the age of 60, with a age at the onset of 60/65 years in the majority of patients. Disease progression also varies depending on the subtype, ranging from 3 months to 36 months (Ironsides et al., 2017).

The clinical course of typical CJD follows three phases. The first one is characterized by psychiatric alterations, memory disturbances and visual disorders. During the second phase, patients rapidly develop progressive cognitive impairment, myoclonus and electroencephalography (EEG) alterations. In the last phase, the disease fatally evolves in an a-kinetic mutism state (Iwasaki et al., 2017). On macroscopic examination, autopsic brains show a non-pronounced atrophy in some areas of the cortex such as the frontal, parietal or occipital lobe (Gonatas et al., 1964). Neuropathological evaluation by Hematoxylin Eosin staining usually reveals a marked spongiform change, with diffuse vacuolation, followed by astrocytic hyper-proliferation and gliosis. Afterward, neuropil rarefaction is observed and leads to massive by neuron loss (Iwasaki et al., 2017). As the disease progresses also an increase in PrP aggregates deposition can be traced. Interestingly, the different forms of CJD are associated with a different distribution and shape of PrP deposits.

A systematic classification of sCJD subtypes was proposed in 2003 by Gambetti and colleagues (Table 1) who identified five distinct forms: Typical (MM1/MV1), Early-onset (VV1), Long duration (MM2), Kuru plaques (MV2) and Ataxic (VV2) (Gambetti et al., 2003a). This classification takes into account the different disease phenotypes, the polymorphism on codon 129 of *PRNP* and Western blot profile of PrP^{Sc} after treatment with PK. Codon 129 is the site of a common methionine (M)/valine (V) polymorphism. In the Caucasian population, 52% of individuals are M homozygous (MM), 36% are heterozygous (MV) and 12% are V homozygous (VV) (Collinge et al., 1991). The phenotype of each prion disease subtype depends on the genotype at codon 129, which appears to act as a disease modifier. Gambetti and colleagues also observed that after PK treatment and Western blot two types of PrP^{Sc} were distinguishable according to their MW: In PrP^{Sc} type 1 the PK-resistant fraction has a gel mobility of about 21 kDa, while in PrP^{Sc} type 2, of approximately 19 kDa (Gambetti et al., 2003a). Patients with type 1 or type 2 PrP^{Sc} have different clinical features, also relatable to codon 129 polymorphism: MM homozygous patients have PrP^{Sc} type 1 whereas VV homozygous or MV heterozygous patients have PrP^{Sc} type 2, suggesting that *PRNP*

genotype affects PrP^{Sc} structure and thus disease's phenotype (Parchi et al., 1996, Parchi et al., 1999).

Subtype	Frequency (%)	Median age at onset (years)	Median duration of illness (months)	Diagnostic neuropathological features	Characteristic patterns of PrP deposits
MM1, MV1	57, 6	66, 73	3, 5	Microvacuolar spongiform change (cerebral cortex and cerebellum)	Synaptic, granular
MM2 cortical	7	52	17	Confluent spongiform change (cerebral cortex, enthorinal cortex)	Perivacuolar
MM2 thalamic	<1	53	16	Limited spongiform change (cerebral cortex, cerebellum). Marked anterior thalamic gliosis and neuronal loss	Synaptic, granular
MV2	14	65	11	Diffuse microvacuolar spongiform change. Kuru plaques (cerebellar cortex)	Kuru plaques, synaptic plaques-like
VV1	2	53	10	Diffuse microvacuolar spongiform change.	Synaptic, with pale staining
VV2	14	66	6	Diffuse microvacuolar/confluent spongiform change	Synaptic, perineuronal, plaque-like

Table 1: Classification of sCJD Subtypes: sCJD are classified according to disease phenotypes, the polymorphism on codon 129 of PRNP and Western blot profile of PrP^{Sc}. Readapted from (Gambetti et al., 2003a).

1.13.3 Familial CJD

The first case of fCJD was reported in 1924 by Kirshbaum, but a few years later Meggendorfer proved that patient zero was actually member of a large family carrying an inherited form of CJD (Jacob et al., 1950). Other cases of fCJD were then reported by Buge in 1978, and followed by Cathala, who studied the same family (Buge et al., 1978), (Cathala et al., 1980). Only after the discovery and the cloning of *PRNP* gene it has been proven that fCJD are caused by pathogenic mutations in *PRNP* (Prusiner et al., 1998) and, taking into account the prion hypothesis, it has been hypothesized that mutated PrP^C possesses a higher propensity to spontaneously convert to the infectious isoform, compared to non-mutated PrP^C (Prusiner, 1989). A large variety of mutations has been identified over the decades (Table 2), encompassing 24 missense point mutations, 27 insertions of additional repeats in the octapeptide region, two deletions of repeats and two nonsense mutations in the same area (Gambetti et al., 2003b). Additionally, three missense polymorphisms located at codons 129 (M/V), 171 (N/S), and 219 (E/K), 12 silent polymorphisms and the deletion of one 24-bp octapeptide are known. From a clinical standpoint, as for sCJD, also fCJD forms present a variety of different phenotypes, ranging between sCJD-like to forms causing personality changes coupled to dementia and Parkinsonism (T183A–129M) (Gambetti et al., 2003b).

The most common mutation is the E200K, with an incidence of CJD about 100 times higher than the worldwide average and a marked prevalence in Jews of Libyan and Tunisian origin. E200K forms resemble sCJD and manifest as spongiform degeneration, astrogliosis and neuronal loss (Parchi et al., 1996, Parchi et al., 1999). Histopathological analyses reveal multicentric plaques, which are also associated with several GSS-linked mutations on *PRNP* and appear as large irregular aggregates with a multicentric structure. Plaques are generally severe and widespread in the cerebral cortex and milder in the striatum, diencephalon, and cerebellum. Another common mutation is the D178N, also associated with FFI and the V210I, which causes a fast progressing fCJD, with sudden confusion, hallucinations, abnormal motor functions and myoclonus (Gambetti et al., 2003b).

Genotype	Onset (years)	Duration	Clinical and pathological features
Familial CJD			
P105T	30–42	NA	* NA ** NA
R148H–129M	63	18 months	* Like sCJDMV2 ** Like sCJDMV2
D178N–129V	26–56	9–51 months	* Dementia, ataxia, myoclonus, extrapyramidal and pyramidal signs ** Spongiosis, neuronal loss and astrogliosis in the cerebral cortex (most severe), striatum, and thalamus (least severe), while the cerebellum is spared
V180I–129M	66–85	1–2 years	* Similar to typical sCJD but with a slower progression ** Like typical sCJD
T183A–129M	45	4 years	* Personality changes followed by dementia and Parkinsonism ** Atrophy with spongiform degeneration in the cerebral cortex and, to a lesser extent, in the basal ganglia
T188A–129M	82	4 months	* Like sCJDMM1 ** Immunohistochemistry for PrP negative, no immunoblot
T188K	59		* Dysphasia, rapidly progressive dementia, and negative family history ** NA
T188R			* NA ** NA
E196K–129M	63–77	~1 year	* Rapidly progressive dementia, ataxia, no PSW on EEG ** NA
E200K–129M	35–66	2–41 months	* Similar to typical sCJD; atypical signs such as supranuclear palsy and peripheral neuropathy in some cases ** Like typical sCJD
V203I–129M	69	~1 month	* Sudden confusion hallucinations, abnormal motor functions, myoclonus, PSW on EEG, negative family history ** NA
H208R–129M	60	7 months	* Like typical sCJD ** Like typical sCJD
V210I–129M	49–70	3–5 months	* Like typical sCJD ** Like typical sCJD
E211Q–129M	42–81	3–32 months	* Like typical sCJD, PSW on EEG ** NA
M232R–129M	55–70	4–24 months	* Like typical sCJD ** Like typical sCJD
FFI			
D178N–129M	20–71	6–33 months	* Reduction of total sleep time, enacted dreams, sympathetic hyperactivity, myoclonus, ataxia; late dementia, pyramidal and extrapyramidal signs in the cases with a relatively long duration (> 1 year) ** Preferential thalamic and olivary atrophy; spongiform changes in the cerebral cortex in the subjects with a duration of symptoms longer than 1 year

*Clinical and **pathological features. NA, not available.

Table 2: Genotype and Phenotype of fCJD and FFI. *Different forms of fCJD and FFI classified according to the mutations on PRNP gene and 129M polymorphism. Taken from (Gambetti et al., 2003b).*

1.13.4 Variant CJD

The first ten cases of vCJD have been identified in the UK between 1994 and 1995, shortly after the first cases of BSE. vCJD patients manifested a new neuropathological profile, rather different from canonical CJD, with an unusually young age of onset and death (median 29 years), an EEG characterized by the absence of the typical CJD alterations, early ataxia and behavioral changes with no dementia (Will et al., 1996). From a histological standpoint brains

showed uniform spongiform change throughout the cerebral cortex. Interestingly PrP deposits showed a completely different aggregation behavior, giving rise to “florid” plaques, which could be markedly traced in the cerebral and cerebellar cortex and are structured as a central eosinophilic amyloid core with radiating fibrils surrounded by spongiotic tissue (Iwasaki et al., 2017). Given the concomitant widespread epidemic of BSE in UK and the absence of vCJD cases in other European countries where BSE was not reported, it was immediately suggested that vCJD could have been caused by the ingestion of infected meat (Baker and Ridley, 1996). Furthermore, some of the clinical and neuropathological features observed in vCJD, as the age of onset and the plaque deposits, resemble the ones associated with Kuru and Human Growth Hormone (HGH)-treatment derived iCJD, both having a peripheral transmission route (Baker and Ridley, 1996). Since 1994, 130 people have been diagnosed with vCJD, with the vast majority of cases in the UK, and few other victims in France, Ireland, and Italy (Bosque, 2002).

1.13.5 Iatrogenic CJD

Iatrogenic forms of CJD are due to exposure to infectious brain material, as dura mater and corneal grafts, cadaveric pituitary hormone extracts, or contaminated surgical instruments during medical procedures (Pedersen and Smith, 2002). The first evidence of iCJD was reported in 1974 in a patient who received corneal transplantation from a donor affected by CJD (Duffy et al., 1974). In the same period, two cases of CJD were reported in patients who underwent procedures with stereotactic IC EEG electrodes previously used on known CJD patients (Bernoulli et al., 1977). The first case of iatrogenic CJD transmitted through cadaveric pituitary HGH was reported in 1985 (Powell-Jackson et al., 1985). The highest number of iatrogenic CJD cases registered so far has been seen in recipients of HGH and dura mater grafts, with a global number of 139 cases derived by HGH treatment and 114 cases caused by dura mater grafts till the year 2000 (Brown et al., 2000). However, the risk of transmission was eliminated at the end of the 1980s through the use of recombinant hormones and urea-treated native hormone. iCJD cases caused by HGH infusion generally present with a progressive cerebellar syndrome and late dementia. Dura madre grafts cases on the other hand present a rapidly progressive dementia (Brown et al., 2000).

1.13.6 Kuru

Kuru has been firstly described by Gajdusek in 1957 (who has been awarded in 1977 a Nobel Prize for his pioneering discoveries in the field), as an acute progressive degenerative disease of the central nervous system, affecting the Fore tribes of the highlands of Papua New Guinea, with unprecedented records in western medicine (Gajdusek and Zigas, 1957). By the time of the first investigations almost half of the deaths among the Fore population were imputable to Kuru, with an incidence of 5-10% and a male to female ratio of 1:4. The word Kuru in the Fore language means “shaking with fear” and refers to the uncontrolled shaking that characterized the affected individuals (Gajdusek and Zigas, 1957). From a pathological point of view, Kuru is characterized by an extremely specific set of symptoms and clinical features, which inevitably end with death within 9 to 12 months. The first symptom is progressive locomotor ataxia, often coupled to headache, fever and cough. As ataxia progresses, subjects develop the distinctive tremor, which occurs during voluntary movements and recedes during rest and sleep. Tremor causes a progressive motor and speech invalidation with no sign of cognitive decline but a marked emotionalism with excessive laughter (Gajdusek and Zigas, 1957). From a histological standpoint brains are characterized by spread neuronal degeneration, astroglia and microglia proliferation, and the presence of specific Kuru-type plaques, with a compact central core, surrounded by radiating fibrils (Gajdusek and Zigas, 1959). The first evidence of a possible infectious transmission raised from latter works by Gajdusek, who produced a kuru-like syndrome in chimpanzees after IC inoculation of brain suspension from Kuru patients (Gajdusek et al., 1966). Similar results were also obtained by Fields and colleagues, who injected homogenates of kuru-infected chimpanzee brains into mice and again observed a kuru-like phenotype (Field, 1968). Interestingly the same authors also suggested several similarities between this kuru-like condition and sheep scrapie. In 1980 Gibbs and colleagues showed that monkeys could develop a Kuru-like pathology after ingestion of infected brain material, supporting the idea that the infection route might be oral (Gibbs et al., 1980). This hypothesis has also been suggested in a precedent report, where it was proposed that cannibalistic rituals of victims affected by Kuru were responsible for the epidemic spread of the disease in the Fore population (Mathews, 1968, Mathews et al., 1968). The same theory was also confirmed by the gradual disappearance of Kuru after the 60s, after the cessation of mourning ritual cannibalism in Fore tribes (Gajdusek, 1977). It is likely that the infection originated from the brain from an individual affected a sporadic form of CJD, ingested during the funerary rituals

in the early '900, and then spread through the entire population within 50 years, particularly in female and child patients, which were more involved in ritual cannibalism.

1.13.7 Fatal Familial Insomnia

FFI was described by Lugaresi in 1986 as a rapidly progressing untreatable insomnia, caused by a complete disruption of the circadian rhythm as clearly revealed by EEG analysis, showing a complete absence of the electrical patterns associated with physiologic sleep (Lugaresi et al., 1986). Patients affected by FFI also develop severe dysautonomia, which appears as a vegetative dysfunction of the autonomic motor and endocrine systems. In the more advanced stages patients progressively show occasional fluctuations of vigilance, then complex hallucinations, stupor and coma. However, no global impairment of memory and cognition is observed (Lugaresi et al., 1986). Histological analysis reveals marked atrophy of the anterior and dorsomedial thalamic nuclei, with neural loss and reactive astrogliosis, and occasional spongiosis, unlike thalamic forms of CJD. Other thalamic areas, as well as cortical and cerebellar cortexes, showed less severe when not even traceable alterations (Medori et al., 1992).

FFI has an autosomal dominant transmission, affecting man and women with the same rate, with a mean age at onset of 49 years and mean duration of 11 months (Gambetti et al., 2003b).

Few similarities with CJD and the familiar transmission prompted Medori and collaborators to investigate whether the origin of FFI was ascribable to a mutation on *PRNP* gene, as for fCJD forms. Two seminal works conducted by analyzing three different familiar clusters showed that proteinase resistant PrP aggregates were traceable in patients brains, even if Western blot signals appeared weaker if compared to CJD (Medori and Tritschler, 1993, Medori et al., 1992). Furthermore, *PRNP* gene sequencing proved that FFI is caused by a nucleotide substitution at codon 178 of *PRNP*, leading to an Asp to Asn mutation (D178N) (Medori and Tritschler, 1993, Medori et al., 1992). The final proof was given by Collinge and colleagues in 1995, who showed that, as for all the other prion diseases, brain homogenates from FFI patients induced an FFI-like condition once IC-injected into two different mouse models (Collinge et al., 1995).

1.13.8 Gerstmann-Straussler-Scheinker Syndrome

GSS syndrome is an autosomal dominant disorder with a broad spectrum of clinical presentations, which has been firstly described by neurologists Gerstmann Straussler and Scheinker in 1936 (Boellaard and Schlote, 1980). GSS is characterized by a marked cerebellar dysfunction with mild pyramidal and extrapyramidal symptoms. Symptoms include ataxia, spastic paraparesis, dementia and dysarthria (Ghetti et al., 1995). Symptoms generally occur in the third to sixth decade of life and the mean duration of illness is five years. A common hallmark of GSS is the presence of massive unicentric and multicentric amyloid deposits appearing throughout the brain, particularly in the cerebellar and cerebral cortices (Dolman and Daly, 1982). The tight similarity between these plaques and Kuru-CJD ones lead researches to investigate a possible link between GSS and prion diseases. In 1988 Kitamoto and colleagues showed that GGS plaques were immunoreactive for PrP (Kitamoto et al., 1988); interestingly, misfolded PrP^{Sc} conformers showed an atypical protease-resistant core. At a histopathological analysis amyloid deposition is accompanied by atrophy, neuronal loss and glial proliferation, with occasional spongiosis as for the other TSE (Dolman and Daly, 1982). Given the familiar transmission of GSS it was then easy to speculate a genetic transmission route. The first mutation linked to the typical ataxic presentation of GSS was a substitution at codon 102 of the *PRNP* gene, resulting in an amino acid change from proline to leucine (P102L) (Hsiao et al., 1989). Later on, GSS has been associated with other mutations as P105L, F198S, Q217R and several other rarer mutations (Ghetti et al., 1995). Such a variety of mutations is likely to contribute to the wide spectrum of manifestations associated with GSS.

GSS infectivity has been long-time debated, since numerous attempts to infect rodent models with human material failed or showed scarce efficiency. In 1981 Masters and colleagues reported that brain homogenates from GSS-affected patients could induce spongiform encephalopathy if inoculated in non-human primates (Masters et al., 1981). Afterwards, P102L patients brain material have been successfully used to infect mice and other rodent models (Baker et al., 1990), (Tateishi et al., 1988), however other mutations as F198S and A117V showed no proof of infectivity (Hsiao et al., 1992), (Tateishi et al., 1990).

1.14 Animal Prion Diseases

Animal prion diseases include scrapie of sheep and goats, BSE or mad cow disease, TME, feline spongiform encephalopathy, exotic ungulate spongiform encephalopathy, CWD and spongiform encephalopathy of primates.

1.14.1 Scrapie

Scrapie has been well-known since the 18th century as a disease affecting sheep, goats and mouflons in several countries throughout the world, with the exception of Australia and New Zealand. Clinical symptoms generally encompass behavioral changes, lack of coordination, ataxia, blindness, tremors and hyper-excitability. The most characteristic hallmark of scrapie is the intense pruritus, which usually leads the affected animals to compulsively rub and scrape their wool off (Imran and Mahmood, 2011). As for its human counterparts, pathology consists of brain vacuolation, gliosis and accumulation of PrP deposits; however, unlike human TSE, scrapie affected individuals show no significant neuronal loss (Jeffrey and Gonzalez, 2007). The incubation period of scrapie is 2-5 years and death occurs within 2 weeks to 6 months after clinical onset. Classical scrapie is endemic in flocks, as milk and uterine discharges have been established as likely sources of infection and environmental contamination (Andreoletti et al., 2002), (Konold et al., 2008), (Pattison et al., 1972). However, it has been proved that also genetic predisposition is necessary for the development of the disease (Dickinson et al., 1968), (Nussbaum et al., 1975), (Parry, 1979), as many polymorphisms in PrP gene can influence the risk of infection (Hunter, 1997). So far no apparent evidence of transmission to humans has been found, even though the possibility cannot be excluded (Chatelain et al., 1981), (Gibbs and Gajdusek, 1971), (Wadsworth et al., 2013).

1.14.2 Bovine Spongiform Encephalopathy

BSE or “Mad Cow disease” is a progressive and fatal neurodegenerative condition affecting cattle and noteworthy the only animal prion disease whose transmission to human has been ascertained so far. The first stages of the disease are characterized by aggressive behavior, fine head tremor, exaggerated startle reflexes and reluctance to handling. Later clinical signs

encompass ataxia and stumbling. The average incubation period is around 5 years; after the onset, the clinical phase lasts several weeks (Wilesmith et al., 1992). As for the other prion diseases, histopathological evaluation generally reveals PrP^{Sc} accumulation and spongiform vacuolation (Novakofski et al., 2005).

The first cases of BSE likely occurred in the UK in the early '80s, however, the condition was recognized as a prion disease only in 1988 (Hope et al., 1988). The number of cases increased until 1992, when roughly 37,000 cattle were diagnosed with BSE. The cause of BSE has been attributed to the use of meat and bone meal (MBM) derived from rendered cattle as protein supplements (Fraser, 2000). MBM supplements were first rendered (heated) and extracted with hydrocarbon solvents to recover animal fats. It is likely that heating favored prions denaturation, blocking the infective potential (Wilesmith, 1988). For this reason in 1988, the use of cattle-derived protein supplements on animal of the same species was banned by the "Feed ban", which was further improved in 1996, when feed containing cattle-derived material were prohibited also for the other farmed species.

Since then, the incidence has steadily declined (Bosque, 2002), with an approximate global number of 0.2 million cases. Besides UK BSE has been found in several European countries, Israel and Japan. It is likely that contaminated cattle food imported from UK spread BSE to other countries. Even though the origin of BSE is unknown, it is widely accepted that the origin of the infection was the rendered remains of sheep with scrapie (Bosque, 2002). However, cattle experimentally inoculated with sheep scrapie develop a different form of prion disease, whose properties are different from BSE (Clark et al., 1995).

1.14.3 Chronic Wasting Disease of Cervids

CWD affects deer and elk and has originally been reported in 1967 in captive animals in Colorado. Since then, the epidemic has been initially found in farmed and free-ranging deers and elks only in northeastern Colorado (Williams and Young, 1980). Alarmingly, a few years ago CWD surveillance revealed that the epidemic is progressively spreading to other regions of the USA and Canada, with a prevalence ranging from 0.1 to 50%, sometimes 100%, making CWD the only truly endemic prion disease (Gilch et al., 2011). As the name suggests, affected animals commonly show chronic wasting of carcasses or weight loss. Other symptoms are behavioral changes, sudden death and loss of fear of humans. When the diseases progress animals develop ataxia, tremors, hypotonia, and die of consumption (Gilch

et al., 2011). The incubation time ranges between 16 months to 5 years, while animals normally die within one year after the onset. Histopathological analysis reveals neuronal vacuolation and loss, with diffuse astrocytosis and spongiosis, and occasional amyloid plaques (Spraker et al., 1997). Even though the spreading mechanism is not fully understood yet, it seems possible that CWD has an airborne transmission. The experimental use of saliva in fact, could generate an infection in target animals. Moreover, PrP^{Sc} and CWD-infectivity have been found in the lymphoreticular system and in various body fluids (Mathiason et al., 2006). Interestingly, CWD can be experimentally transmitted to transgenic mice over-expressing cervid PrP genes (Browning et al., 2004), but transgenic mice expressing either the human, ovine or bovine PrP^C do not develop CWD if inoculated with the agent (Tamguney et al., 2006).

1.14.4 Transmissible Mink Encephalopathy

TME outbreaks in the US have occurred sporadically in ranch-reared mink North America in the 60s and 70s till the last outbreak occurred in 1985 (Bessen and Marsh, 1992). The disease has been and imputed to the use of scrapie-affected sheep meat as mink feed, even though there is still scarce evidence of minks experimentally infected after scrapie-derived material consumption, and no explanation why the outbreaks apparently stopped. After the generation of transgenic mice susceptible to TME, a phenotypic similarity BSE was described (Baron et al., 2007), (Windl et al., 2005).

The clinical features of TSE encompass behavioral changes such as increased aggressiveness, restlessness and neglect in parental care and grooming. In the early phases, animals exhibit eating and swallowing problems, while in the last phases ataxia, incoordination, tremors, and compulsive biting appear. By the end stage of the disease minks develop convulsions, sleepiness and unresponsiveness. The incubation time ranges from 6 to 12 months, and animals normally die within 2 to 8 weeks after the onset. As for the other TSE, histological analysis of TME brains reveals widespread spongiform degeneration, astrocytosis and PrP deposition (Bessen and Marsh, 1992).

1.14.5 Exotic Ungulate Spongiform Encephalopathy

EUE is a TSE registered in exotic ruminants from the Bovidae family during the same period of BSE epidemic. The affected animals (6 elands, 6 greater kudu, 2 each of ankole cattle and Arabian oryx, and 1 each of nyala, gemsbok, bison and scimitar-horned oryx) were all hosts of zoo and sanctuaries in the UK, and fed with MBM derived from ruminants (Imran and Mahmood, 2011). As expected, once inoculated with EUE-infected brain homogenates from greater kudu and nyala, mice developed a BSE-like form of TSE, supporting the idea that the origin of the epidemic was indeed BSE-infected material. After the Feed ban and the further restrictions on animal feed processing, no other cases of EUE have been reported (Sigurdson and Miller, 2003).

1.14.6 Feline Spongiform Encephalopathy

FSE is a form of TSE affecting domestic cats and captive Felidae family members. Since the first diagnosis in 1990, roughly 100 domestic cats, mostly from the UK, and 29 captive wild cats in zoos of the UK, France, Australia, Ireland, and Germany (though actually originated from UK) have been diagnosed with FSE. As for EUE, most of the FSE cases occurred during the BSE epidemic; thus exposure of affected cats to feed contaminated with BSE agent was taken as causative of the disease. Further supporting evidence is the decline in the number of recorded cases of FSE after the Feed ban (Sigurdson and Miller, 2003). Additionally, mice inoculated with brain homogenates from cats with FSE and cattle with BSE developed similar TSE profiles. The clinical manifestation of the disease includes severe behavioral changes as unusual aggressiveness or timidity, depression, restlessness and neglect in coat grooming. Abnormal or hypermetric gait and ataxia, hyperesthesia and tremors are also characteristics of FSE and by the end of the disease course, convulsions and somnolence are usual. Death occurs after 3-10 weeks from the clinical onset (Bencsik et al., 2009). Neuropathological alterations include spongiform degeneration and PrP deposits, with the characteristic vCJD-associated florid plaques (Eiden et al., 2010).

1.15 Experimental Models of Prion Diseases (animal, *ex vivo*, cellular, cell-free)

1.15.1 Animal Models of Prion Diseases

Compared to other neurodegenerative disorders, prion diseases offer the unique opportunity to study the pathology directly into the original recipients. Also, when other experimental models are used, they actually develop *bona fide* prion disease, which recapitulates all the clinical and histological features of the disease and not just some of the pathological processes related to it, as it happens for example in AD and Parkinson's disease (PD) models.

The first attempts to experimentally transmit prion diseases were performed in the '30s by Cuille and Chelle, who studied the transmission of scrapie, inoculating goats and sheep (Plummer, 1946) When the infective nature of Kuru and CJD was firstly hypothesized, different primate models as spider monkeys and chimpanzees were used to reproduce disease-like phenotypes (Gajdusek et al., 1966), (Gajdusek et al., 1968), (Gibbs et al., 1968). Additionally, the link between BSE and vCJD has been established after the inoculation of BSE extracts in primate models (Lasmezas et al., 1996).

However, the majority of the experimental observations, especially after the discovery of the prion protein, has been conducted on mice and to a lesser extent on hamsters. After IC inoculation mice start to develop symptoms within a 4–5 months long incubation period, dependent on the strain used (while in hamsters the incubation can be shorter (Kimberlin et al., 1977). When the infection follows a peripheral route the incubation period is generally longer (Watts and Prusiner, 2014). Mice develop a very specific set of clinical features including progressive ataxia, tail rigidity, hunched back and eventually die within a period depending on the prion titration of the inoculum. At a neuropathological analysis, mice brains present all the typical hallmarks of prion diseases as spongiosis, misfolded PrP deposition and astrogliosis (Watts and Prusiner, 2014).

However, given the long incubation period required to reach the clinical onset researchers started to use transgenic mice overexpressing mouse PrP in CNS, which show a much shorter incubation period, for example around 50–60 days when mice are infected with the mouse-adapted RML scrapie strain (Carlson et al., 1994).

Prion disease	Line	Type of mouse	PrP sequence	Expression level ^a	Incubation period (in days)
Mouse-passaged scrapie	Tg4053	Transgenic	Mouse	4x	~50
Mouse-passaged scrapie	Tga20	Transgenic	Mouse	10x	~60
Mouse-passaged scrapie	Tg37	Transgenic	Mouse	3x	~80
Hamster-passaged scrapie	Tg7	Transgenic	Syrian hamster	8x	~50
Sheep scrapie	Tg338	Transgenic	Sheep (VRQ)	8–10x	~70
Sheep scrapie	Tg(OvPrP)14882	Transgenic	Sheep (VRQ)	1.4x	~75
Sheep scrapie	Tg(OvPrP-V136)4166	Transgenic	Sheep (VRQ)	1x	~130
CWD	Tg(CerPrP)1536	Transgenic	Deer	5x	~230
CWD	Tg10969	Transgenic	Deer	1x	~320
CWD	Tg33	Transgenic	Deer	1x	~300
CWD	Tg12584	Transgenic	Elk	6x	~120
CWD	Tg12	Transgenic	Elk	2x	~120
CWD	Tg5037	Transgenic	Elk	5x	~170
BSE	Tg4092	Transgenic	Cow	8x	~230
BSE	TgBovXV	Transgenic	Cow	8x	~250
BSE	boTg110	Transgenic	Cow	8x	~290
BSE	BovTg	Knock-in	Cow	1x	~550
Sporadic CJD (MM1)	Tg2669	Transgenic	Human (M129)	5x	~150
Sporadic CJD (MM1)	Tg35	Transgenic	Human (M129)	2x	~230
Sporadic CJD (MM1)	Tg1	Transgenic	Human (M129)	2x	~230
Sporadic CJD (MM1)	Tg650	Transgenic	Human (M129)	6x	~160
Sporadic CJD (MM1)	HuMM	Knock-in	Human (M129)	1x	~450
Sporadic CJD (VV2)	Tg152	Transgenic	Human (V129)	8x	~200
Sporadic CJD (VV2)	HuVV	Knock-in	Human (V129)	1x	~270

Table 3 Commonly Used Transgenic and Knock-in Mouse Models for Bioassays of Prion Diseases (readapted from Watts and Prusiner, 2014).

The main issue related to the use of native and transgenic mouse models expressing murine PrP is that disease transmission can be dampened by species-barrier effect; thus they can be used only to study mouse-passaged prion strains (Collinge and Clarke, 2007) (Pattison, 1965), (Tateishi et al., 1996). This issue has been overcome utilizing mice with a transgenic PrP gene matching the strain inoculated on a *Prnp* null background. More recent knock-in approaches prevented the risk of late-onset spontaneous diseases (Westaway et al., 1994) and confounding phenotypes driven by the ectopic insertion of PrP or the use heterologous promoters (Fischer et al., 1996). However, when heterologous PrP is expressed at physiological levels and under the control of its native promoter, the incubation period can become very long (Bishop et al., 2006, Bishop et al., 2010).

Transgenic and knock-in models can also be used to reproduce familial prion diseases (Table 3). Tg mice overexpressing the mouse equivalent (P101L) of a punctiform mutation associated with GSS (P102L) develop a spontaneous neurodegenerative disease and exhibit deposition of misfolded PrP in their brains (Hsiao et al., 1990) (Telling et al., 1995). However, knock-in or transgenic models with a lower PrP copy number and thus a physiological-like expression of PrP, do not develop any pathological sign (Manson et al., 1999, Nazor et al., 2005), suggesting that HuPrP is less prone to misfold than MoPrP. Other GSS-related mutations include A117V (Yang et al., 2009) and a nine-octapeptide repeat insertion in the N terminus of PrP (Chiesa et al., 1998), while the D178N model undergoes a CJD-like disease (Dossena et al., 2008). Another model of fCJD, carrying the E200K mutation develops a spontaneous neurological phenotype only when inserted into a chimeric mouse/ human PrP molecule (Friedman-Levi et al., 2011), but not in mouse PrP (Telling et al., 1996) or human PrP (Asante et al., 2009).

Another widely used rodent model is the bank vole (BV), a wild rodent highly susceptible to a wide range of prion strains isolated from numerous species and also humans (Agrimi et al., 2008), (Cartoni et al., 2005) (Di Bari et al., 2013) (Nonno et al., 2006). These properties have partly been imputed to a polymorphism at codon 109 in the *Prnp* gene and can be indeed reproduced in Tg mice expressing BVPrP (Espinosa et al., 2016). Transgenic mice overexpressing BVPrP M109 propagate a number of prion strains with high efficiency and shorter incubation times (Watts et al., 2014). Additionally, Tg mice expressing the I109 polymorphic variant of bank vole PrP undergo a spontaneous neurodegenerative process encompassing all of the neuropathological features of prion disease without the need for inoculation with exogenous prions, thus reproducing the stochastic misfolding event that is

thought to origin PrP^{Sc} in sporadic prion disease (Watts et al., 2012). For these reasons this model could be particularly suitable to test the efficacy of molecules targeting the spontaneous misfolding of PrP^C, as pharmacological chaperones (Barreca et al., 2018).

Invertebrate models as *D. melanogaster* have scarcely been used so far in prion diseases research. Since *D. melanogaster* does not possess an endogenous PrP, mammalian PrP is usually expressed. The reports obtained so far outline different outcomes, from no phenotype to progressive degeneration (Fernandez-Funez et al., 2009, Fernandez-Funez et al., 2017, Fernandez-Funez et al., 2010), (Raeber et al., 1995), (Thackray et al., 2012). Namely, when the P101L mouse PrP is expressed in cholinergic neurons, flies show severe locomotor and electrophysiological alterations compared to controls expressing WT moPrP (Murali et al., 2014).

Only recently *Drosophila* has been proven to be able to propagate prion infection. When flies expressing ovine PrP under a neuronal promoter are exposed to sheep scrapie during the larval stage, prions can replicate and retain the infectivity to flies and mice expressing the same transgene (Thackray et al., 2016, Thackray et al., 2018). Given the short lifespan and reproductive cycle as well as the relatively easy genetic manipulation of flies, this finding opens new avenues to possible drug screening campaigns and shorter discovery pipelines.

1.15.2 Ex Vivo Models of Prion Diseases

A good compromise exploited to study prion propagation *in vitro* on intact brain cytoarchitecture are organotypic slices, which retain a well-preserved morphology for several months. In 2008 Falsig and colleagues showed for the first time that chronically cultured organotypic cerebellar slices (COCS) from 10 days-old pups, overexpressing PrP^C, can propagate prion infection if briefly exposed to RML homogenates. PK resistant fraction can be traced in the infected slices starting from 3 weeks after RML exposure and its amount correlates with PrP^C expression levels (Falsig et al., 2008). Progressive neurodegeneration starts 5 weeks post-inoculation, with loss of synaptophysin and NeuN in the cerebellar granule layer (CGL). Typical spongiform changes as vacuolation, tubulovesicular structures, together with neurites dystrophy and astrogliosis also appear. As observed in mice models,

the selective ablation of PrP on CGCs tackles neurodegeneration and prion spreading (Falsig et al., 2012), (Wolf et al., 2015).

Interestingly, when organotypic non-cerebellar brain sections, as cortico-striatal slices, have been tested with the same paradigm, these slices showed a seeding activity comparable to the one obtained from cerebellar slice cultures (Kondru et al., 2017).

COCS have been used to compare the morphological alterations of different strains (Campeau et al., 2013), identify early neuronal damage and neurotoxic pathways (Campeau et al., 2013), (Goniotaki et al., 2017), kinetics of PrP^{Sc} conversion (Kondru et al., 2017) and test possible drugs on an intact brain system (Falsig et al., 2012), (Goniotaki et al., 2017), (Kondru et al., 2017). Compared to cellular models, organotypic slices offer a more complex paradigm, taking into account neuronal wiring and a tissue architecture. However, it is to note that, especially if used for pharmacological research, organotypic cultures do not account for the contribution of the blood flow and the BBB. Also, the experimental time-points are still quite long and sacrifice of mice is still required.

1.15.3 *In Vitro* Models of Prion Diseases

As for the other neurodegenerative conditions, also for prion diseases many cellular models have been developed over the decades. Unlike animal models and *ex vivo* approaches, cell cultures are generally devoid of ethical issues and offer a cheaper and faster tool to both study pathological mechanisms and test possible drugs. At this aim several cell lines have been infected with prion extracts, resulting in the identification of roughly 20 different lines stably propagating a detectable prion infection once exposed to different prion strains (Vorberg and Chiesa, 2019).

The first cell culture was generated in 1970 (Clarke and Haig, 1970b, Clarke and Haig, 1970a), before the discovery and isolation of the prion agent. In the late '80s, after the development of the protocol for the isolation of PrP^{Sc}, N2a cells have been exposed to mouse-adapted scrapie and the stable replication of the prion agent over multiple passages was firstly shown (Butler et al., 1988), (Caughey et al., 1989). In the following years N2a cells have been stably infected with other mouse-adapted prion strains, and other cell lines of neuronal and non-neuronal origin, as microglial cells, epithelial cells, fibroblasts and myoblasts, have been employed (Courageot et al., 2008), (Iwamaru et al., 2007), (Lawson et al., 2008), (Vella et al., 2007), (Vilette et al., 2001), (Vorberg et al., 2004). In the majority of

cases the infection is virtually chronic and non-cytopathic (Grassmann et al., 2013). N2a cells are still the most used cell model for anti-prion drug discovery (Karapetyan et al., 2013) (Kocisko et al., 2003). Notwithstanding this, it is worthy of considering that many cell lines expressing PrP^C are resistant to prion infection and for many prion it seems impossible to stabilize a chronic infection (Butler et al., 1988), (Gibson et al., 1972, Polymenidou et al., 2008). Furthermore, despite many efforts, the replication of human prion strains in cell lines has never been successful without a previous step of adaptation in mice (Courageot et al., 2008, Vella et al., 2007), thus raising the possibility that any drug developed with these models could retain some strain-specificity. It is also to note that the translational relevance of these models might be dampened by the intrinsic nature of the assay, which relies on cell often very phenotypically distant from neurons and in active replication.

To partially overcome this issue, primary cell culture models have been generated. In some of them, unlike for cell lines, a marked cytopathic effect was detectable upon infection (Cronier et al., 2004), (Giri et al., 2006), (Herva et al., 2010). However, considering primary neuronal cultures, only a few models are available. In a report from Hannaoui and colleagues, primary cerebellar granule cells from mice expressing human PrP were infected with CJD prions (Hannaoui et al., 2014).

The generation of iPS cells from a human source partially overcomes the problem of translatability associated with mouse and mouse-derived models. In a first study using iPS cells from a GSS patient, marked cytopathic alterations, resembling the human pathology, have been reported although in absence of PK resistant PrP accumulation (Matamoros-Angles et al., 2018) .

1.15.4 Cell-free Assays

Cell-free PrP conversion techniques have been developed to study the mechanisms of strain and species specificity (Bessen et al., 1995), (Raymond et al., 2000, Raymond et al., 1997), as well as to screen anti-prion compounds and clarify their mechanism of action (Caughey et al., 1998). Caughey's laboratory developed the first cell-free PrP conversion method in 1994. PrP^{Sc} isolated from prion-infected mouse brain was incubated with radioactively labeled PrP^C extracted from uninfected cells and then treated with (PK). The newly generated protease-resistant PrP was then revealed after SDS-PAGE with autoradiography (Kocisko et al., 1994).

Despite the efficacy of prion conversion, this method cannot actually generate infectious PrP (Hill et al., 1999a). Furthermore, its long experimental time and the necessity to use radioactive labeling, prompted researches to develop new methods.

In 2001 Soto and colleagues obtained *bona fide* cell-free PrP^{Sc} replication with the protein misfolding cyclic amplification (PMCA) technique (Saborio et al., 2001). This method relies on the nucleation-dependent polymerization model that has been proposed as the primary mechanism for the propagation of amyloid structures, which allows the amplification of small amounts of PrP^{Sc} derived from infected brains, using uninfected brain homogenates as a source of PrP^C substrate. The amplification requires repeated cycles of incubation at 37 °C followed by a sonication step. During the first step, PrP^{Sc} seeds can convert PrP^C, forming larger amyloid fibrils after the recruitment of the newly formed PrP^{Sc} molecules. The subsequent sonication breaks PrP^{Sc} fibrils, thus creating new nucleation seeds. Noteworthy, PrP^{Sc} molecules obtained by PMCA retain the same structure and biochemical properties of the original PrP^{Sc} seed, and its infectivity as well (Castilla et al., 2006). PMCA is now used as diagnostic tool (Barria et al., 2018, Concha-Marambio et al., 2016), to screen anti-prion compounds (Massignan et al., 2016), (Stincardini et al., 2017), to study the involvement of possible co-factors in prion replication (Fernandez-Borges et al., 2018) and to generate PrP^{Sc} molecules (Noble and Supattapone, 2015).

Another cell-free prion detection assay called real-time quaking-induced conversion (RT-QulC), developed by Caughey and collaborators in 2014, substitutes sonication with shaking, and monitors PrP amyloid formation in real-time with the fluorescent dye thioflavin-T (ThT) (Orru et al., 2014). The high sensitivity and specificity allow this assay to be used to diagnose prion diseases (Franceschini et al., 2017) as well as to screen PrP conversion inhibitors in high-throughput platforms (Hyeon et al., 2017) although less accurately than PMCA, since it cannot produce infective prions.

1.16 Diagnosis of Prion Diseases

As for many other neurodegenerative conditions, a definitive diagnosis of prion diseases can only be performed post-mortem, evaluating by histological analysis the presence of prion deposits, spongiform degeneration and astrogliosis (Budka, 2003). As biopsy procedures are extremely dangerous, less invasive options have been recently evaluated, by using the olfactory mucosa and skeletal muscle (Glatzel et al., 2003). None of them however has been validated so far. It is also known that PrP^{Sc} can be detected in tonsils from vCJD, but not sCJD patients (Hill et al., 1999b). Whatever the source, the presence of prions in biopsies is detected by Western blot after PK treatment. The recent development of *in vitro* protein misfolding amplification assays as PMCA and RT-QuIC allowed the detection of a very low amount of PrP^{Sc} from several types of patients tissues and biological fluids, such as brain homogenates, blood, urine and olfactory mucosa, with a robust, reproducible and automated system, possibly facilitating the diagnosis (Atarashi et al., 2011), (Cramm et al., 2016), (McGuire et al., 2012).

RT-QuIC for example has been used in several reports conducted on the CSF of sCJD and fCJD patients (Cramm et al., 2016), (Sano et al., 2013), showing high sensitivity and specificity. Also, different works reported the detection of prion seeding activity in nasal lavages by RT-QuIC (Bongianni et al., 2017), (Orru et al., 2016), (Wilham et al., 2010). Interestingly, a further development of this method, called eQuIC, made it possible to visualize PrP^{Sc} also in plasma samples from vCJD subjects (Orru et al., 2011) and it could be useful in the future to prevent further transfusion-based transmissions of vCJD. In the last years also PMCA has been considered for diagnostic purpose. Noteworthy, several groups revealed, by means of PMCA, the presence of PrP^{Sc} in urine samples from vCJD and sCJD patients (Luk et al., 2016), (Moda et al., 2014).

The EEG has also been used to discriminate CJDs since 1954, thanks to distinct hallmarks, as periodic sharp wave complexes, present in the EEG recordings of CJD patients. However the high rate of variability and the differences between the different forms of CJD, do not allow a definitive diagnosis, and this technique has low sensitivity and high rate of false positives (Steinhoff et al., 1996).

Another non-invasive technique used to diagnose prion diseases in humans is magnetic resonance imaging (MRI). However, also in this case, characteristic changes in MRI features are different for each prion disease, making MRI useful mainly to exclude other causes of pathology (Collins et al., 2000). Also the interpretation of MRI largely relies on the skills and

experience of clinicians, suggesting that even if an initial MRI is regarded as normal, a specialized review should still be carefully considered.

Another possible source of diagnostic material is the CSF. It has been reported that in the CSF of TSE patients there is a marked increase of many neuronal and astroglial proteins (Bahl et al., 2009), (Chohan et al., 2010), (Jimi et al., 1992). However, also in this case, there is a great variability between the different forms of TSE (Hsich et al., 1996).

As no sensitive and specific diagnostic tool has been generated so far, diagnosis is performed combining the use of these techniques with an assessment of clinical signs and symptoms.

1.17 Therapies for Prion Diseases

1.17.1 Therapeutic Agents Targeting Prion Propagation

As for many other amyloidoses, targeting PrP^{Sc} aggregates initially appeared to be the most logical approach. For this reason all the first attempts to search for anti-prion agents have been conducted in infected cells or mice, measuring the propagation of PrP^{Sc} isoform. Unfortunately, once tested in mouse models or directly into patients, none of these molecules exerted a significant therapeutic effect, suggesting that targeting PrP^{Sc} and its propagation as selection criteria in drug screening paradigms might not be a winning strategy (Barreca et al., 2018).

Polyanionic compounds: Glycosaminoglycans (GAGs), linear polymers of repeating disaccharide units, constitute the polysaccharide sidechains of proteoglycans (PGs) and retain the ability to bind PrP^{Sc} deposits. This structure is also shared by semisynthetic analogues as pentosan polysulphate (PPS) and dextran sulphate (DS), which are thought to counteract prion replication by competitive inhibition of the interaction between endogenous GAGs and PrP^{Sc}. DS and PPS treatment decreases PrP^{Sc} levels in prion-infected cells (Birkett et al., 2001, Caughey and Raymond, 1993), (Caughey et al., 1994) and delays disease onset in mice, if administered at the moment of the infection (Diringer and Ehlers, 1991), (Ehlers and Diringer, 1984). However, once tested in mice, PPS showed severe adverse effects (Doh-ura et al., 2004).

Congo Red: CR is a dyazo dye normally employed to stain amyloid deposits, including PrP^{Sc} ones. It has been shown to prevent prion accumulation in prion-infected cells (Caughey et al., 1993, Caughey and Race, 1992), (Caspi et al., 1998, Demaimay et al., 1998), (Milhabet et al., 2000). However, once tested *in vivo*, CR delays the disease onset only when administered around the time of infection (Poli et al., 2004). Despite numerous attempts with different approaches, it is still not clear if the molecule binds specifically PrP (Nakagaki et al., 2013, Kawatake et al., 2006)). Additionally, CR is toxic, non-specific and does not cross the BBB (Klunk et al., 1998, Klunk et al., 1994). Many analogues and derivatives of CR have been studied in both cell and cell-free systems in order to identify compounds with improved properties (Poli et al., 2003, Rudyk et al., 2003).

Polyene antibiotics as methotrexate and amphotericin B were tested on infected hamsters in the '80s, together with a large panel of other anti-viral and antibacterial drugs. Both molecules lead to an extension of the incubation time when administered to hamsters and mice, although with no effect on the disease progression (Adjou et al., 1999, Adjou et al., 1995, Adjou et al., 2000) (Pocchiari et al., 1989, Pocchiari et al., 1987). Interestingly, treatment was effective even if administered at late stages, when the infectivity and PrP^{Sc} accumulation are already significant (Demaimay et al., 1997).

Tetracyclic compounds The anthracycline 40-iodo-40-deoxy-doxorubicin (IDOX) is an anticancer drug with anti-amyloidogenic properties, showing a positive effect in delaying the clinical onset of the disease and preventing the histopathological damage when tested in experimental models (Tagliavini et al., 1997). However, IDOX has also high cytotoxicity and a low BBB penetration rate, making it an unsuitable drug candidate (Tagliavini et al., 1997). Similarly, other chemically related molecules, like tetracycline and doxycycline, induced a delay in the disease onset if incubated together with the prion inoculum before the infection, thus showing potential for decontamination rather than for therapeutic use (Forloni et al., 2002).

Acridine and Phenothiazine Derivatives: Tricyclic derivatives of acridines and phenothiazines like Chlorpromazine (CPZ) and Quinacrine (QNC) have been proposed by Doh-Ura and colleagues as promising candidates for the treatment of prion diseases in a repurposing perspective (Doh-Ura et al., 2000). QNC, an antimalarial agent and CPZ, an antipsychotic drug, showed inhibition of PrP^{Sc} formation in prion-infected cells, with half-maximal effective concentration (EC50) values in the low micromolar range (Korth et al., 2001), (Ryou et al.,

2003). However, once tested in prion-infected rodent models, QNC showed no beneficial effect (Collins et al., 2002, Barret et al., 2003). Noteworthy, the activity and safety of QNC were also assessed in clinical trials on CJD patients, with no prolongation of survival or modification of the clinical course of the disease (Collinge et al., 2009, Geschwind et al., 2013). It has been hypothesized that such a lack of clinical efficacy was mainly attributed to QNC intrinsic metabolic instability and scarce accumulation into the brain, as also suggested by pharmacokinetic studies (Ahn et al., 2012).

Similarly, the tricyclic phenothiazine derivative CPZ inhibits PrP^{Sc} formation in infected cultures, however less effectively if compared to QNC (Korth et al., 2001). As for QNC, once tested *in vivo*, CPZ showed no effect (Barret et al., 2003). Accordingly, when administered to FFI patients in combination with QNC no beneficial effect was observed (Benito-Leon, 2004).

Tetrapyrrolic compounds: A variety of tetrapyrroles, including porphyrins and phthalocyanins, were investigated by Caughey and co-workers as potential anti-prion compounds using prion-infected N2a cell culture system and were found to decrease PrP^{Sc} levels (Caughey et al., 1998), as well as to prevent propagation of PrP^{Sc} in a cell-free conversion system, with submicromolar half-maximal inhibitory concentration (IC50) (Caughey et al., 1998), (Massignan et al., 2016). The most efficient compounds were then examined using different infected mouse models (Priola et al., 2003, Priola et al., 2000), showing a delay in the onset of disease if the compounds were repeatedly administered over the first month after infection. However, no significant effect was seen after treatment at a later stage in the disease progression (Priola et al., 2003, Priola et al., 2000).

1.17.2 Therapeutic Agents Targeting PrP^C

PrP synthesis

The most intuitive therapeutic approach for prion diseases is the removal of PrP^C, the substrate for PrP^{Sc} conversion, with RNA silencing approaches. Many pieces of evidence collected on PrP^C KO animals support this notion. PrP^C null mice in fact are completely resistant to infection and at first glance phenotypically and behaviorally normal (Brandner et al., 1996a, Brandner et al., 1996b, Bueler et al., 1993). Mice treated with a lentiviral vector expressing an anti-PrP shRNA showed a marked extension of survival when infected (Pfeifer et al., 2006). Similar results were obtained on livestock and cattle (Golding et al., 2006),

(Wongsrikeao et al., 2011). More importantly, silencing of PrP^C not just before, but also after prion infection exerted comparable neuroprotection (White et al., 2008). However, despite being quite promising, RNA silencing of PrP^C is still far from being clinically relevant. The effects of the lack of PrP^C in humans are still unknown and the safety of viral vectors is yet to be ascertained.

Interestingly, in a recent work Vallabh and collaborators tested the efficacy of antisense oligonucleotides (ASOs) ICV delivered to prion-infected WT mice. They observed a 61%–98% extension of survival time after multiple treatments and a 55% extension after single injection by the onset of clinical signs, providing a clear demonstration of the potential for ASOs (Raymond et al., 2019).

PrP^C ligands

The concept of chemical chaperones has been initially proposed by Tatzelt and colleagues to define molecules directly binding PrP^C and stabilizing it in its native conformation, thus reducing the rate of conversion into PrP^{Sc}. Although the chemical chaperones do not affect the existing population of PrP^{Sc}, they interfere with the formation of PrP^{Sc} from newly synthesized PrP^C (Tatzelt et al., 1996).

One of the most exploited paradigms to screen for pharmacological chaperones is to use surface plasmon resonance (SPR) to detect the direct binding to PrP^C of libraries of chemicals and then test the anti-prion activity of the candidate hits with cellular-based assays (Guo et al., 2008), (Touil et al., 2006). Based on a similar approach Kawatake and colleagues proposed, thanks to NMR and SPR studies, that QNC binds to the globular domain of human recombinant PrP (residues 121–230) with a KD similar to its IC50 (Nakagaki et al., 2013, Kawatake et al., 2006), however, other SPR studies reported a KD tenfold higher (Touil et al., 2006). It has been hypothesized that QNC binding to PrP^C induces a conformational change in the latter, disfavoring PrP^{Sc} formation (Georgieva et al., 2006). However, once tested in cell-free conversion systems, QNC seems to have no effect on PrP^{Sc} propagation according to the majority of the reports (Doh-Ura et al., 2000), (Kirby et al., 2003).

Similarly, the binding of CPZ to PrP^C was originally investigated by NMR (Vogtherr et al., 2003) and SPR (Touil et al., 2006), showing a weaker interaction with recombinant PrP, if compared to QNC. The proposed binding site of phenothiazines on PrP^C is located in a hydrophobic pocket formed by helix-2 (H2) and the two anti-parallel sheets (Baral et al., 2014). However, in a recent report from Stincardini and colleagues, it was shown by dynamic

mass redistribution (DMR) and SPR that CPZ binds to PrP^C only at very high, non-pharmacologically relevant, concentrations. Additionally CPZ was not able to counteract prion replication in cell-free systems, as expected from a pharmacological chaperone, while its activity seemed more likely to rely on the re-localization of PrP^C from the plasma membrane (Marella et al., 2002), (Stincardini et al., 2017). In contrast, another recent report from Yamasaki and colleagues highlighted that CPZ promotes the redistribution of PrP^{Sc} from organelles in the endocytic-recycling pathway to late endosomes/lysosomes without affecting the distribution of PrP^C (Yamasaki et al., 2014).

A further well-characterized anti-prion compound, FeTMPY, was shown to bind human recombinant PrP in the C-terminal, with a KD consistent with its cellular EC50 (Massignan et al., 2016). As expected, FeTMPY exerted a consistent inhibition of prion replication in cell-free systems once tested with PMCA (Massignan et al., 2016), (Nicoll et al., 2010).

A recently developed approach to identify pharmacological chaperones is the application of the RT-QuIC technology as a screening test for molecules inhibiting the conversion and aggregation of PrP^{Sc}. In recent works doxycycline as well as acridine, dextran, and tannic acid were tested with this approach, with positive results (Hyeon et al., 2017, Schmitz et al., 2016).

Compounds Targeting PrP^C Localization

The concept of altering the correct membrane localization of PrP^C as a potential therapeutic strategy for prion diseases have been initially explored studying the effect of the perturbation of lipid rafts environment. At this aim, a variety inhibitors of cholesterol synthesis as statins have been tested *in vitro* and *in vivo*. In the first report by Taraboulos and colleagues, treatment with lovastatin reduced the formation of PrP^{Sc} in prion-infected N2a cells (Taraboulos et al., 1995). Similarly, squalestatin reduced the cholesterol content of cells promoting the redistribution of PrP^C from lipid rafts and preventing the accumulation of PrP^{Sc} in infected lines (Bate et al., 2004). However, chronic and global inhibition of cholesterol synthesis can also induce a variety of side effects due to the global perturbation of cholesterol levels, dampening the possible clinical use of this pharmacological strategy. Additionally, when tested *in vivo*, statins induced no reduction in the progression of the disease (Hagiwara et al., 2007) or just a modest prolongation of the incubation time (Kempster et al., 2007), (Mok et al., 2006). However, this effect has actually been imputed to the neuroprotective effect of the drug (Haviv et al., 2008).

In a similar attempt, Bate and colleagues used synthetic GPI analogues to treat prion-infected neuronal cell lines. GPI analogues altered the composition of cell membranes and reduced PrP^{Sc} content in a dose-dependent fashion (Bate et al., 2010).

The same group also evaluated the release of GPI-anchored proteins from the cell surface as a possible therapeutic approach by testing the effect of glimepiride. Glimepiride is a sulphonylurea used to treat diabetes, which acts by promoting the release of some GPI-anchored proteins from the plasma membrane. Once tested in infected cells, glimepiride induced a reduction of PrP^{Sc} formation and an increase of PrP^C levels in the culture medium (Bate et al., 2009).

The paradigm of PrP^C removal from the plasma membrane has been further exploited through the development of new screening approaches. In a paper from Lazmesas group, a new FRET-based high throughput assay (PrP–FEHTA) was employed to screen for compounds decreasing the expression of PrP^C. The campaign led to the identification of two hit compounds, astemizole and Tacrolimus (TAC), which reduced cell-surface PrP and inhibited prion replication in N2a cells. Further evaluations suggested that TAC might reduce total PrP levels by a non-transcriptional mechanism while astemizole stimulates autophagy. However, once tested *in vivo* only astemizole induced a slight prolongation of the survival time of prion-infected mice, while TAC was completely ineffective (Karapetyan et al., 2013). Similarly, Silber and colleagues used an HTS ELISA cellular assay to identify SMs lowering PrP^C surface levels without any cytotoxic effect (Silber et al., 2014).

More recently, the concept of removing PrP from the cell surface has been exploited by Stincardini and colleagues, who took advantage of an Enhanced Green Fluorescent Protein (EGFP) tagged PrP construct stably transfected in cells, to monitor PrP localization with an automated plate reader. Interestingly the authors observed that CPZ, the already widely-known anti-prion compound, promotes the internalization of PrP^C from the cell surface at low micromolar concentrations (Stincardini et al., 2017). Noteworthy, no binding to PrP^C was observed in that concentration range, suggesting that CPZ might actually not be a pharmacological chaperone of PrP^C but more likely a modulator of endocytosis through a dynamin-dependent mechanism (Marella et al., 2002), (Stincardini et al., 2017), (Wang et al., 1993). In accordance with these observations, when a set of dynamin inhibitors was used on the same experimental models, the authors observed a significant decrease in the surface levels of PrP, also confirming the role of dynamin-dependent endocytosis in the trafficking of PrP (Stincardini et al., 2017).

Antibodies

As for the other amyloidopathies, the development of antibodies targeting PrP^{Sc} aggregates has been initially proposed. However, such antibodies showed poor therapeutic effect once tested into *in vivo* or *in vitro* (Antonyuk et al., 2009), (Kubota et al., 2012), (Petsch et al., 2011), confirming the idea that the amyloid deposits per se are not the major toxic species in prion diseases. Conversely, more evidence collected *in vitro*, suggest that antibodies targeting PrP^C could be an effective treatment (Antonyuk et al., 2009), (Enari et al., 2001), (Feraudet et al., 2005), (Peretz et al., 2001). Antibodies can be used to sterically prevent the interaction of PrP^C with PrP^{Sc} (Heppner et al., 2001, Peretz et al., 2001), but also to perturb PrP^C trafficking, promoting its internalization, degradation and redistribution from the cells surface (Feraudet et al., 2005), (Jones et al., 2010), (Pankiewicz et al., 2006), (Perrier et al., 2004), or stabilizing it in order to prevent the conversion (Nicoll and Collinge, 2009).

1.18 Clinical Trials for Prion Diseases

Since 1971, only fourteen clinical trials for prion diseases have been designed, and in none of them molecules specifically designed for the disease have been tested, but mainly antivirals, antimalaria and antifungals (Gandini and Bolognesi, 2017). As prion diseases were initially considered slow viral infections, the first drugs tested in clinic were antivirals as Amantadine. Amantadine was tested in two distinct trials on CJD patients, showing no prolongation of survival (Neri et al., 1984, Terzano et al., 1983). Similarly, the nucleoside analogs Acyclovir (David et al., 1984, Newman, 1984) and vidarabine (Furlow et al., 1982), as well as the anti-viral interferon (Kovanen et al., 1980), exerted no effect. Following the same principle, the antibiotic Amphotericin B was initially tested after the promising results obtained in hamsters infected with 263K strain and CJD monkeys (Pocchiari et al., 1989, Pocchiari et al., 1987), where Amphotericin B induces a significant extension of survival. However, once administered to two CJD patients also this molecule was ineffective (Masullo et al., 1992).

In the early '00s the promising results obtained *in vitro* by Korth and colleagues with the tricyclic acridine derivative QNC (Korth et al., 2001), together with its good safety and bioavailability profile, encouraged the design of new clinical trials to test QNC on CJD patients. The first clinical trial with QNC, conducted in France in 2004 (32 CJD patients), led to no positive effect (Haik et al., 2004). Similarly, a bigger trial (PRION-1, 107 patients) was

opened in the UK in 2009 by Collinge and colleagues and also in this case QNC showed no significant effect (Collinge et al., 2009). The last QNC trial was performed between 2005 and 2009 at the University of San Francisco (425 patients), and no significant differences between the placebo and QNC treated patients were reported (Collinge et al., 2009, Geschwind et al., 2013). It is to note however, that such failure could have been prevented if a careful evaluation of the *in vivo* results have been conducted. In fact, when QNC was tested in mice models, induced just a modest extension in survival time despite the strong efficacy described in cells (Collins et al., 2002, Barret et al., 2003). Additionally, in the same years, several *in vitro* studies demonstrated that a chronic treatment with QNC results in a strain selection of PrP and drug resistance (Ghaemmaghami et al., 2009).

In 2004 the nonopioid analgesic Flurpirtine was used to treat 28 patients with a probable CJD thanks to its promising results *in vitro* (Perovic et al., 1997). Although tests demonstrated a slowdown of cognitive decline, Flurpirtine did not seem to induce any significant extension in the survival time (Otto et al., 2004).

More promising results were obtained with PSS, which once tested on patients significantly increased the survival time (Todd et al., 2005). Unfortunately, given its scarce penetration of the BBB, the administration of PSS required an ICV procedure, dampening its clinical use due to adverse effects (Bone et al., 2008).

Recently, after the good results *in vitro* and *in vivo* (Forloni et al., 2009), the antibiotic Doxycycline was tested in two clinical trials in Italy and Germany. In both cases an increase in the survival time was recorded (De Luigi et al., 2008), (Zerr, 2009), prompting the design of another trial conducted between Italy and France. Unfortunately, in this case, the results were not confirmed (Haik et al., 2014). However a new trial, started in Italy in the last years and ending in in 2023 (Gandini and Bolognesi, 2017), targeted patients with the genetic risk of developing FFI preventively treated with Doxycycline (Forloni et al., 2015).

Drug	Country	Patient recruitment	Number	Primary endpoint
Flupertine	Germany	sCJD and genetic TSEs	28	ADAS-cog
PPS	UK	vCJD, iCJD and genetic TSEs	7	Survival
PPS	Japan	sCJD and iCJD	11	Survival
QNC	France	sCJD and genetic TSEs	32	Survival
QNC	UK	sCJD and genetic TSEs	107	Survival and rating scales
QNC	USA	sCJD	51	Survival
Doxycycline	France/Italy	sCJD and genetic TSEs	121	Survival
Doxycycline	Germany	sCJD	100	Survival

Table 4: Overview of the Most Relevant Clinical Trials for Prion Diseases Conducted so far.

CHAPTER 2: AIMS AND OBJECTIVES

Despite many decades since the formulation of the prion hypothesis, prion diseases are still incurable. Multiple previous data indicate that exclusively targeting PrP^{Sc} might not be a viable strategy. PrP^{Sc} conformers in fact have a great and not fully understood structural diversity, which made impossible so far to rationally design drug candidates effective for all the existent strains (Giles et al., 2017). More recently, several reports pointed out that PrP^C, whose structure has been defined at high resolution, might be a more suitable drug candidate (Barreca et al., 2018). It is now widely accepted that PrP^C is not just a passive substrate for prion conversion, but is also primarily involved in the neurodegenerative events triggered by PrP^{Sc}. Genetic ablation of PrP^C in infected brains in fact fully recovers histological alterations (Mallucci et al., 2003), furthermore mutated variants of PrP^C associated with genetic forms of prion diseases show marked cytotoxic features (Solomon et al., 2010). Additionally, other pieces of evidence suggest that PrP^C could bind many diseases-associated aggregates, as A β and α -synuclein oligomers, acting as a transducer of neurotoxicity (Ferreira et al., 2017), (Lauren et al., 2009). In this thesis, in an attempt to explore novel therapeutic strategies for prion diseases, I tested different experimental paradigms to target PrP^C.

2.1 Part I

In Part I, I exploited the rationale of removing PrP^C from the cell surface, to prevent PrP^{Sc} conversion and tackle prion-related cytotoxicity. This strategy has already been validated in previous reports (Bate et al., 2004), (Gilch et al., 2008), (Korth et al., 2001), (Ryou et al., 2003), (White et al., 2008), however only one systematic screening campaign has been conducted so far (Karapetyan et al., 2013). In a previous study from my laboratory, we used a fluorescently tagged version of PrP^C to prove that CPZ exerts its anti-prion effect by removing PrP from the cell surface (Stincardini et al., 2017). Here I took advantage of this new cellular tool to carry out a high-content screening campaign and subsequent secondary assays, testing two chemical libraries, with the ultimate objective of identifying non-cytotoxic compounds specifically removing PrP^C from the cell surface and blocking prion accumulation and toxicity.

2.2 Part II

In Part II, I followed the concept of uncoupling prion toxicity and replication pharmacologically by capitalizing on a previously described cellular assay called the Drug Based Cellular Assay (DBCA). This assay, which is based on the intrinsic toxicity of an artificial mutant of PrP^C (Massignan et al., 2011), previously allowed the identification of a promising anti-prion compound, referred as LD24 (Imberdis et al., 2016). Here, I coupled serial cycles of chemical rearrangement to DBCA screening steps, to optimize derivatives of LD24, enhance their potency and reduce their toxicity, evaluating their effect in disease-relevant cell-based and *ex vivo* models.

CHAPTER 3: MATERIALS AND METHODS

3.1 Institutional Ethical Approval

Regarding the MEA section all animal handling was in accordance with Australian National Health and Medical Research Council (NHMRC) guidelines. All experimental procedures were approved by The Florey Institute of Neuroscience and Mental Health Animal Ethics Committee (Ethics number: 13-048) or the Biochemistry & Molecular Biology, Dental Science, Medicine (RMH), Microbiology & Immunology, and Surgery (RMH) Animal Ethics Committee, The University of Melbourne (Ethics number: 1312997.1). The animal handling and the experimental procedures regarding the preparation of the primary neuronal cultures were carried out according to the Italian legislation guidelines (L.D. no. 26/2014), reviewed by the Animal Welfare Committee of the University of Milan, and approved by the Italian Ministry of Health.

3.2 Compounds Synthesis

Synthesis schemes for the different derivatives have been conceived and executed by the group of Prof. Giuseppe Manfroni, Department of Pharmacy, University of Perugia. The synthesis of novel compounds has been carried out using newly developed synthetic protocols, as well as parallel, combinatorial and microwave-assisted synthetic methods. The structure and stereochemistry of all synthesized molecules have been assigned by NMR, FT-IR, GC-MS, LC-MS and/or X-ray crystallography. Computational methods aided the design of some derivative compounds. Chemoinformatics tools have been used to select candidate molecules on the basis of their calculated physical-chemical properties, eliminating compounds with poor predicted ADMET values. Briefly, the structure of LD24 [dibenzo[3,4][c,e]thiazine 5,5-dioxide] provided a convenient chemical scaffold to perform structure-activity relationship (SAR) experiments. Four chemical regions of the compound were explored, with the dual objective of improving potency and acquiring SAR information. The bromine atom at position 9 (C ring) was shifted at position 7, 8 and 10, deleted or replaced by substituents with similar or different steric/electronic properties. The cyclohexyl

moiety was replaced with a wide panel of substituents, rationally chosen to explore chemical diversity. Finally, we also modified the linker at N-6 position.

3.3 Plasmids

Cloning procedures used to generate the cDNAs encoding WT and Δ CR have been described in (Massignan et al., 2010). The EGFP-PrP construct has been described in (Stincardini et al., 2017). Sequencing of the entire coding region was used to confirm the identity of all constructs. The structure of WT PrP, Δ CR PrP, EGFP-PrP, GPI-GFP and Negr1 constructs is depicted in the supplementary information section. All protein constructs were cloned into the pcDNA3.1(+)/hygro expression plasmid (Invitrogen, Carlsbad, CA, USA) and express mouse proteins.

3.4 Cell Cultures

All the cell lines used in this manuscript are not listed as a commonly misidentified cell lines by the International Cell Line Authentication Committee (ICLAC) and have not being authenticated for this study. Cells have been cultured in Dulbecco's Minimal Essential Medium (DMEM, Corning, New York, USA, #15-017-CVR), 10% heat-inactivated fetal bovine serum (FBS), Penicillin/Streptomycin (Pen/Strep, Corning, New York, USA, #20-002-CI), non-essential amino acids (NEAA, Gibco, #11140-035) and L-Glutamine (Corning, New York, USA, #25-005-CI). All cell lines were cultured in T25 flasks or 10mm Petri dishes and split every 3-4 days. Cells employed in all the experiments have not been passaged more than 20 times. For the primary and secondary HCS screenings (Part 1) and to evaluate PrP internalization (Part 2), we used a subclone (A23) of HEK293 (ATCC CRL-1573) stably expressing a mouse EGFP-PrP^C construct, already characterized in Stincardini et al. 2017. For the internalization specificity assay (Part 1) another stable line of HeLa (ATCC CCL-2) expressing a GPI-EGFP construct was generated (clone A1). To control effect specificity (Part 1) we also employed HEK293 cells stably expressing a Flag-Negr1 construct. For the DBCA screening (Part 2), the DBCA-based secondary assays (Part 1) and patch clamp recordings (Part 2), we used HEK293 cells stably expressing Δ CR PrP, (ATCC CRL-1573). For the evaluation of PrP levels (Part 1 and 2) we used HEK293 cells stably expressing WT

PrP. The Scrapie Cell Assay (SCA) was performed (Part 1 and 2) using a specific sub-clone (called N2a.3) of mouse neuroblastoma (N2a) cells (ATCC CCL-131). As a source of PrP scrapie for the MEA recordings, Rabbit kidney epithelial (RK) cells expressing murine PrP^C (MoRK13, Vella et al. 2007), either mock-infected with Normal Brain Homogenate (NBH, control) or with M1000 mouse-adaptor human prion strain were used.

3.5 Treatments

All the dose-response treatments with the different compounds have been performed by adding each molecule, dissolved in DMSO, directly to the cell medium in an 8-point dose-response curve in Part 1 (0.01, 0.03, 0.1, 0.3, 1, 3, 10, 30 μ M) or at different concentration ranges in Part 2. The hit compounds tested in the HCS screening (Part 1) are: BFA (B7651), QNC (Q3251), TAC (F4679), Hematein (HM, 51230), all from Sigma Aldrich (Saint Louis, MO, USA), Harmalol Hydrochloride (HRO. 0215122680, Merck Millipore, Burlington, MA, USA) and SU11652 (572660, Merck Millipore, Burlington, MA, USA). LD24 and all its derivatives have been synthesized as briefly summarized in paragraph 3.2. Imynodin-17 (ab120462, Abcam, Cambridge, UK) was used as positive control for the imaging experiments in Part 1. CPZ (Chlorpromazine Hydrochloride, #C3138, Sigma Aldrich, Saint Louis, MO, USA) was used as positive control for the imaging experiments and for the DMR in Part 2. TP (#75854, Cayman Chemicals, Ann Arbor, MI, USA) was used as positive control for the DMR (Part 1 and 2) and for both the Scrapie Cell Assay and the A β oligomers synaptotoxicity (Part 2).

3.6 HCS Screening

For the primary screening, cells were automatically plated with a Tecan Freedom EVO liquid handler (Tecan, Mannendorf, Swiss) on CellCarrier-384 Ultra microplates (Perkin Elmer, Waltham, MA, USA, #6057300) at a concentration of 12,000 cells/well and grown for approximately 24 h, to obtain a semi-confluent layer (60%). The primary screening was performed administering the different compounds at a final concentration of 3 μ M, in two replicate wells. Imynodin-17 was used as positive control at a final concentration of 30 μ M, while the vehicle DMSO, at a final concentration of 0.2% was used as negative control. Cells

were treated for 24 h and then fixed for 12 min at room temperature by adding methanol-free paraformaldehyde (Thermo Fisher Scientific, Waltham, MA, USA, #28908) to a final concentration of 4%. Plates were then washed twice with PBS and counterstained with Hoechst 33342 (Thermo Fisher Scientific, Waltham, MA, USA, #62249). All these procedures have been performed with Biotek EL406 Washer Dispenser (Biotek, Winooski, Vermont, USA).

3.7 HCS Dose-Response Assays

For all the imaging-based dose-response assays, cell seeding, treatment and fixation were manually performed. Each compound was administered in 2 replicates for each point, positive and negative controls were as described above. Cell confluency was 12,000 and 8,000 cells/well for the EGFP-PrP^C dose-response internalization assay and for the GPI-EGFP specificity assay, respectively.

3.8 Cell Imaging

The localization of PrP^C was monitored using an Operetta High-Content Imaging System (Perkin Elmer, Waltham, MA, USA). Imaging was performed in a wide field mode using a 20X High NA objective (0.75). For reliable statistical analysis, five predefined field regions were consistently considered for all the wells and acquired with two different channels (380-445 Excitation-Emission for Hoechst and 475-525 for EGFP). Image analysis was performed using the Harmony software version 4.1 (Perkin Elmer, Waltham, MA, USA). The segmentation of the images consisted of two steps: nuclei identification by the Hoechst staining, and selection of the regions of interest relying on the signal given by the EGFP. The average fluorescence intensity of the EGFP was detected in the membrane region (enlarged border of the cell), as well as inside the cell. As a measure of the degree of PrP^C internalization from the plasma membrane to intracellular compartments, the membrane/cellular (surface/internal, S/I) fluorescence intensity ratio was calculated for each cell. The mean S/I was estimated for each condition and normalized to the control samples (% Surface/Internal EGFP-PrP^C). Cell viability was quantified by counting cell nuclei and expressed as the percentage of cells relative to vehicle-treated controls. As a parameter for

screening quality control, Z prime values (Z' between positive and negative controls) were calculated for each plate. Screening plates have been considered acceptable when exhibited Z' for S/I higher than 0.35, while no significant difference in cell number was detected between the positive and negative controls.

3.9 DBCA Screening

The DBCA was performed as described previously (Massignan et al., 2011). Briefly, HEK293 cells (ATCC, CRL-1573) expressing Δ CR PrP were seeded on day 1 in 24-well plates at approximately ~60% confluence. On day 2, cells were treated with each compound (1 μ M) and Zeocin (Invivogen, San Diego, CA, USA, #ant-zn-05) at a final concentration of 500 μ g/mL. On day 3 medium with fresh compounds was replaced and at day 4, after removing the medium, cells were incubated with 1 mg/mL of 3-(4,5-dimethylthiazol-2-yl)-2,5-diphenyltetrazolium bromide (MTT, Sigma Aldrich, Saint Louis, MO, USA, #M5655) in PBS for 20 min at 37°C. After carefully removing MTT solution, cells were resuspended in 300 μ L of dimethyl sulfoxide (DMSO), and cell viability was measured with a spectrophotometer (Tecan, Mannendorf, Swiss) by detecting absorbance at 570 nm.

3.10 DBCA

The DBCA protocol was performed as described previously with minor modifications. HEK293 Δ CR cells (ATCC, CRL-1573) were seeded on 24-well plates at roughly ~60% confluence (day 1). On day 2, cells were treated with different concentrations of each compound or vehicle control and after 6h (Part 1) or at the same time (Part 2) Zeocin (500 μ g/mL) was added. Intrinsic toxicity of the different molecules was also evaluated using the same experimental conditions without adding Zeocin. After 24h (Part 1) or 48h (Chaper 2) medium was removed, and cells were incubated with 1 mg/mL MTT in PBS for 20 min at 37°C, resuspended in 300 μ L of DMSO, and cell viability was measured as above.

3.11 Prion-Infected Cells

For the Scrapie Cell Assay (Part 1 and 2), a subclonal population of mouse neuroblastoma N2a cells, previously selected as highly prone to prion infection (called N2a.3) was grown in culturing medium, and passaged 5-7 times after infection with 22L or RML prion strains (both derived from corresponding prion-infected mice). To test the anti-prion effects of the compounds, cells were seeded in 24-well plates (day 1) at approximately 50% confluence, with different concentrations of each compound, vehicle (DMSO, volume equivalent) or positive control (TP, 50 μ M, Part 2). Medium containing vehicle or fresh compounds was replaced on day 2, and cells were split (1:2) on day 3, by directly pipetting onto the well surface, avoiding the use of trypsin. Cells were collected on day 4 by washing the wells with phosphate-buffered saline (PBS). Cell pellets were obtained by centrifuging at 3.500 rpm x 3 min, and then rapidly stored -80°C.

For the MEA recordings (Part 2) MoRK13 cells previously infected with NBH and M1000 were harvested, lysed in aCSF through needles to a final concentration 4% (w/v) and stored at -80 °C for further use as in (Foliaki et al., 2018).

3.12 PK Digestion

To perform the PK digestion (Part 1 and 2) N2a.3 cell pellets were resuspended in 20 μ L of lysis buffer (Tris 10 m M. NaCl 150 mM, pH 7.4, 0.5% NP-40, 0.5% TX-100 plus complete EDTA-free Protease Inhibitor Cocktail Tablets, Roche, Roche Applied Science, Penzberg, Germany #11697498001) and incubated for 10 min at 37°C with 2,000 units/mL of DNase I (New England BioLabs, Ipswich, MA, USA, #M0303). Half of the sample was incubated with 10 μ g/mL of PK (Sigma Aldrich, Saint Louis, MO, USA, #11195) for 1h at 37°C, while the remaining half was incubated in absence of PK in the same conditions. Both PK-treated and untreated samples were then added with 4X Laemmli sample buffer (Bio-Rad Hercules, CA, USA, #151-0747) and 100 mM DTT, boiled for 10 min at 95°C, and ran by SDS-PAGE.

3.13 Western Blots

For the Scrapie Cell Assay and the evaluation of PrP levels (Part 1 and 2), samples were loaded on SDS-PAGE, using 12% acrylamide pre-cast gels (Mini-Protean TGX Stain Free Gels, Bio-Rad, Hercules, CA, USA, #4568043) and then transferred to PVDF membranes (Thermo Fisher Scientific, Waltham, MA, USA, #88518). Membranes were blocked for 20 min in 5% (w/v) non-fat dry milk in Tris-buffered saline containing 0.01% Tween-20 (TBST). Blots were incubated with anti-PrP antibody D18 (1:5,000) 1h at room temperature, washed 3 times with TBST 10 min each, then probed with a 1:8,000 dilution of horseradish conjugated goat anti-human IgG (Santa Cruz Biotechnology, Dallas, TX, USA, sc-2934) for 1h at RT. After 2 washes with TBS-T and one with Milli-Q water, signals were revealed using the Amersham ECL Prime Western Blotting Detection Kit (GE Healthcare, Chicago, IL, USA, #RPN2232), and visualized with a ChemiDoc Touch Imaging System (Bio-Rad, Hercules, CA, USA). PrP levels in PK-treated samples were normalized on total protein levels of untreated samples.

3.14 Immunocytochemistry

Immunocytochemistry on EGFP-PrP^C cells was performed on 384 plates treated as described above. After fixing, methanol-free paraformaldehyde (PFA) was washed three times with PBS. Permeabilization was performed by incubating cells for 1 min with a wash solution containing a final concentration of 0.1% Triton X-100. Wells were then washed three times with PBS and cells were incubated with blocking solution (FBS 2% in PBS) for 1h at room temperature. The anti-PrP primary antibody (6D11, Santa Cruz Biotechnology, Dallas, TX, USA, sc-58581) was diluted in the blocking solution and added to the wells to a final concentration of 1:100. After three washes with PBS, the secondary antibody (Irdye 680 RD Li-Cor Biosciences, Lincoln, NE, USA #926-32222, diluted 1:500 in blocking solution) was incubated for 1h at room temperature. Hoechst 33342 (Thermo Fisher Scientific, Waltham, MA, USA, #62249, 0.5mM in PBS) was then added after two additional washes and left in the wells. Image for the far-red signal was performed by using a 630-705 Excitation-Emission. Images were then analyzed following the workflow described for the screening, including the quantification of far-red signal intensities in the segmented regions.

For surface staining of PrP^C- or Negr-1 (Part 1), stably transfected HEK293 cells were seeded on glass coverslips, grown for 24h and treated with HM, Imynodin-17 or DMSO. After 24h cells were incubated for 15 min on ice with the D18 or anti-Flag (Sigma Aldrich Saint Louis, MO, USA, #F7425) antibodies diluted 1:500 in culture medium, then washed with PBS and fixed in 4% paraformaldehyde for 15 min. After another wash with PBS, coverslips were then incubated with blocking solution (10% NGS, Sigma Aldrich, Saint Louis, MO, USA #G9023, and 2.5% FBS in PBS) for 30 min at room temperature and then with Alexa 488-conjugated goat anti-human or anti rabbit IgG (Invitrogen, Carlsbad, CA, USA #A11013 and #A11034) diluted 1:500 in blocking solution for 1h at room temperature. After washing with PBS, coverslips were then incubated with Hoechst 33342 (0.5mM in PBS, Thermo Fisher Scientific, Waltham, MA, USA, #62249), mounted with Aqua Poly/Mount (Polysciences Inc, Warrington, PA, USA, #18606), and analyzed with a Zeiss Imager M2 microscope.

3.15 Dynamic Mass Redistribution

The interaction of the different molecules with PrP^C (Part 1 and 2) was measured by detecting the binding events at the equilibrium with label-free DMR Module using the EnSight Multimode Plate Reader (Perkin Elmer Waltham, MA, USA). Human full-length recPrP (residues 23-230) or mouse full length (residues 23-230) PrPC were immobilized onto the surface of DMR plates (EnSpire-LFB high sensitivity microplates, Perkin Elmer, Waltham, MA, USA, #6057460) using amine-coupling chemistry (2.5µM in 10mM sodium acetate buffer, pH5) overnight at 4°C. The interaction between each compound and recPrP was evaluated by incubating for 30 min at room temperature different concentrations of each molecule (0.03-100 µM, eight serial dilutions in Part 1, 12-1000 µM, eight serial dilutions in Part 2) re-suspended in assay buffer (PBS pH 7.5, 0.005% Tween-20). All steps were performed using a Zephyr Compact Liquid Handling Workstation (Perkin Elmer, Waltham, MA, USA). Final signals were obtained by normalizing each signal on the intra-well empty surface, and then by subtraction of the control wells signal. The Kaleido software (Perkin Elmer Waltham, MA, USA) was employed to acquire and process the data.

3.16 Patch Clamp

The spontaneous ion channel activity induced by the Δ CR PrP mutant in HEK293 cells was detected by whole-cell patch clamping (Part 2) as already described (Massignan et al., 2010), (Solomon et al., 2012). Cells were seeded at a low confluence on plastic coverslips (Thermanox #174950, Nalge Nunc International, Rochester, NY, USA) and treated with vehicle (DMSO 0.1%), SM231 3 or 10 μ M for 18 h before the recording. Borosilicate electrodes with a 3-6 M Ω electrical resistance were employed. Cells were visualized with a 40X objective using an Olympus BX51WI microscope costumed with reflected fluorescence, and differential interference contrast observation systems. All the experiments were conducted at room temperature with the following solutions (All components were purchased from Sigma Aldrich, Saint Louis, MO, USA) Internal solution: 140 mM Cs-glucuronate, 5 mM CsCl, 4 mM MgATP, 1 mM Na₂GTP, 10 mM EGTA, and 10 mM HEPES (pH 7.4 with CsOH); External solution: 150 mM NaCl, 4 mM KCl, 2 mM CaCl₂, 2 mM MgCl₂, 10 mM glucose, and 10 mM HEPES (pH 7.4 with NaOH). Data were acquired using a Multiclamp 700B amplifier and pClamp 10 software (Molecular Devices, Foster City, CA), and sampled at 5 kHz with a Digidata 1440 (Molecular Devices, Foster City, CA). Data were analyzed off-line using the Clampfit 10 software (Molecular Devices, Foster City, CA).

3.17 Primary Neuronal Cultures

For the synaptotoxicity experiments (Part 2), primary neuronal cultures were derived from the hippocampi of 2-day-old postnatal mice, and cultured as described in (Balducci et al., 2010). Neurons were plated (500,000 cells/dish) on 35-mm dishes pre-coated with 25 μ g/mL poly-D-lysine (Sigma Aldrich, Saint Louis, MO, USA, #P6407) in B27/Neurobasal-A medium supplemented with 100 units/mL penicillin, 100 μ g/mL streptomycin and 0.5 mM glutamine, (all from Invitrogen, Carlsbad, CA, USA). Experiments were performed 12 days after plating (DIV12).

3.18 Preparation of A β Oligomers

Synthetic A β (1-42) peptide (Karebay Biochem., Rochester, NY) was dissolved in hexafluoro-2-propanol, incubated in a bath sonicator for 10 min at maximum power, then centrifuged at

15.000 x g for 1 min, aliquoted, dried, and stored at -80 °C. Before use, the dried film was dissolved in DMSO and diluted to 100 µM in F12 Medium (Invitrogen, Carlsbad, CA, USA). Oligomers were obtained by incubating the peptide at 25°C for 16 h. This procedure routinely produces oligomers that elute near the void volume of a Superdex 75 10/300 size exclusion column (GE Healthcare, Chicago, IL, USA, 17-5174-01), and that react with oligomer-specific antibody A1133. Final Aβ oligomers concentration was considered as monomer equivalents, since the size of the oligomers is heterogeneous.

3.19 Detection of Aβ Toxicity in Primary Neurons

The synaptotoxicity paradigm employed in Part 2 has been already described in (Massignan et al., 2016). Neurons were pre-treated for 20 min with vehicle (DMSO 0.1%), TP (10 µM) or SM231 3 µM and then exposed for 20 mins or 3 hr to Aβ oligomers (3 µM). Subcellular fractionation was performed as reported in (Balducci et al., 2010), with minor modifications. Tissues were homogenized using a Potter-Elvehjem homogenizer in 0.32 M ice-cold sucrose buffer (pH 7.4) additioned with 1 mM HEPES, 1 mM MgCl₂, 10 mM NAF, 1 mM NaHCO₃, and 0.1 mM PMSF (All from Sigma Aldrich, Saint Louis, MO, USA) and protease inhibitors (Complete mini, Roche Applied Science, Penzberg, Germany, #11697498001) and phosphatase inhibitors (PhosSTOP, Roche Applied Science, Penzberg, Germany, #4906845001). Samples were centrifuged at 13.000 x g for 15 min to extract a crude membrane fraction. The pellet was re-suspended in buffer containing 150 mM KCl and 0.5% Triton X-100 and centrifuged at 100,000 x g for 1 hr. The final pellet, referred to as the Triton-insoluble fraction, was re-suspended in 20 mM HEPES supplemented with protease and phosphatase inhibitors and then stored at -80 °C or directly used in further experiments. Protein concentration in each sample was quantified using the Quick Start™ Bradford Assay (#5000201, Bio-Rad, Hercules, CA, USA), and proteins (5 µg) were then analyzed by Western blotting. Primary antibodies were as follow: phospho-SFK (Tyr 416, #2101, Cell Signaling Technology, Danvers, MA, USA) or Fyn (ab125016, Abcam, Cambridge, UK). The phospho-SFK antibody detects pY416 in many SFKs, however previous studies showed that PrP^C activates specifically Fyn). Anti-GluN2A and anti-GluN2B (#480031 and #71-8600 respectively, both 1:2000; Invitrogen, Carlsbad, CA, USA), anti-GluA1 and anti-GluA2 (MAB2263 and MAB1768-I respectively, both 1:1000; Merck Millipore, Burlington, MA, USA), anti-PSD-95 (post-synaptic density protein 95; #10009506, 1:2000; Cayman Chemicals, Ann

Arbor, MI), and anti-actin (#A2228, 1:5000; Merk Millipore, Burlington, MA, USA). Western blots were analyzed by densitometry with Quantity One software (Bio-Rad, Hercules, CA, USA), actin was used as loading control.

3.20 Prion Toxicity in Brain Slices

Hippocampal slices for multi-electrode array (MEA) studies were prepared as in (Foliaki et al., 2018). 12-week-old C57 black 6J (C57BL/6J) female mice were used (Animal Resource Centre, Western Australia). Mice were group caged, with 12-hour day-night light cycles and food and water provided ad libitum. Mouse brains were rapidly extracted after decapitation while under isoflurane-induced deep anesthesia. 300µm dorsal horizontal brain slices were sliced using a vibratome (VT1200S, Leica Biosystems, Wetzlar, Germany) continuously carboxygenated in ice-cold c (5% CO² and 95% O²) cutting solution (3mM KCl, 25mM NaHCO₃, 1.25mM NaH₂PO₄, 206mM Sucrose, 10.6mM Glucose, 6 mM MgCl₂·6H₂O, 0.5mM CaCl₂·2H₂O, all from Sigma Aldrich, Saint Louis, MO, USA). Slices were then stabilised at 32°C by incubation for 40 min in carboxygenated aCSF (126mM NaCl, 2.5mM KCl, 26mM NaHCO₃, 1.25mM NaH₂PO₄, 10mM Glucose, 1.3mM MgCl₂·6H₂O, 2.4mM CaCl₂·2H₂O, all from Sigma Aldrich, Saint Louis, MO, USA) before mounting onto 60MEA200/30iR-Ti-pr-T multi-electrode arrays (MEA; Multichannel Systems; Germany). Hippocampal field EPSP (fEPSP) were evoked by stimulating the Shaffer collateral pathway and recording from the stratum radiatum of the CA1 region. For each slice an average of six recorded electrodes was used for analysis. The amplitude of fEPSP was recorded as a paradigm of the synaptic response. An input-output (I-O) curve was used to determine a basal stimulus intensity sufficient to induce a fEPSP of ~40% of the maximum response and the baseline was recorded by stimulating every 30 sec for 35 min. After approximately 10 min during the baseline, the M1000 or NBH lysates were superfused in the recording chamber for 5 min, the baseline was then allowed to stabilize for other 20 min of recording in aCSF. To induce the LTP 3 trains of high frequency stimulation (HFS), three 100Hz trains, 500 millisecond each, 20 sec apart) were delivered. After the HFS slices were stimulated every 30 sec for 30 mins. SM884 (final concentration 0.03 µM) or vehicle (DMSO 0.002%) were perfused during the entire duration of the recording. The responses recorded starting from five min post-HFS were normalized on the last 5 mins of baseline and considered as LTP. The last 10 mins of LTP were used for analyses

3.21 In Silico Analyses

Different physicochemical and absorption, distribution, metabolism, elimination (ADME) descriptors were in silico calculated to evaluate the “druglikeness” of HM by using Optibrium models (<http://www.optibrium.com/stardrop>) imported in SeeSAR (SeeSAR version 8.1, BioSolveIT GmbH, Sankt Augustin, Germany; www.biosolveit.de). The computed parameters were as follow: 1) MW: molecular weight; 2) HIA category: Human Intestinal Absorption (HIA) Classification. Predicts a classification of ‘+’ for compounds which are $\geq 30\%$ absorbed and ‘-’ for compounds which are $< 30\%$ absorbed; 3) LogS: Intrinsic aqueous solubility. A LogS > 1 corresponds to intrinsic aqueous solubility of greater than $10 \mu\text{M}$; 4) LogP: Partition coefficient. LogP > 3.5 significantly increases the chance of metabolism, particularly by CYP3A4. LogP < 0 can cause problems with membrane permeation; 5) cLogBB: blood-brain barrier penetration log. It takes into account only passive transport of molecules, not addressing the possible role of active transporters. Worth noting, a recent analysis performed on approved drugs for CNS diseases showed that $\sim 84\%$ are natural products (NP) or NP-inspired compounds and $\sim 35\%$ of NPs/NP-inspired drugs, all characterized by a cLogBB ≥ -1 (Bharate et al., 2018); 6) P-gP category: Classification of P-glycoprotein transport. To evaluate CNS exposure, the compound must belong to the ‘-’ category to avoid the active efflux; 7) hERG pIC50: Predicts the pIC50 values for inhibition of hERG K⁺ channels expressed in mammalian cells. pIC50 ≤ 5 might avoid hERG interactions. 8) 2C9 pKi: ability of the compound to inhibit cytochrome P450 CYP2C9. pKi ≤ 6 is to avoid drug-drug interactions due to inhibition of CYP2C9; 9) 2D6 affinity category: Cytochrome P450 CYP2D6 affinity. Predicts a classification of ‘low’ for compounds with a pKi < 5 , ‘medium’ for compounds with a pKi between 5 and 6, ‘high’ for compounds with a pKi between 6 and 7, and ‘very high’ for compounds with a pKi > 7 . Values low to medium are required to avoid drug-drug interactions; 10) PPB90 category: Plasma Protein Binding Classification. Ideally would like low PPB to increase free concentration and brain exposure.

3.22 Statistical Analyses

All the data have been acquired and analyzed by at least two different operators. Statistical analyses, performed with the Prism software version 7.0 (GraphPad), included all the data points obtained, with the exception of experiments in which negative and/or positive controls did not give the expected outcome. No normality test was used. Results were expressed as the mean \pm standard errors. Dose-response experiments were fitted with a 4 parameter logistic (4PL) non-linear regression model. Fitting was estimated by calculating the R^2 value for each compound. All the other experiments have been analyzed with the Student's t-test or one-way ANOVA test, including an assessment of the normality of data, and corrected by the appropriate post-hoc tests. Probability (p) values < 0.05 were considered as significant (* <0.05 , ** <0.01 , *** <0.001).

CHAPTER 4. RESULTS PART I: RE-LOCALIZING PRP^C

4.1. Specific Aims and Rationale

In the last decade various reports highlighted the concept of removing PrP^C from the plasma membrane as a possible therapeutic strategy for prion diseases (Bate et al., 2009), (Karapetyan et al., 2013), (Taraboulos et al., 1995). The decrease of the surface levels of PrP^C in fact could result not just in the reduction of its availability for conversion into PrP^{Sc}, but also in a lowered activation of the neurotoxic cascade mediated by it. In a recent report from our laboratory it was shown that CPZ, a previously identified anti-prion agent, acts by removing PrP^C from the cell surface (Stincardini et al., 2017). When administered to HEK293 cells stably expressing a fluorescently-tagged PrP^C construct, CPZ induced a significant re-localization of PrP^C from the plasma membrane. Interestingly, the same effect was reproduced by the administration of an inhibitor of the GTPase activity of dynamins, Imynodin-17. However, both CPZ and Imynodin-17 are unsuitable drug candidates, as they induce a global perturbation of membrane dynamics, resulting in a generally non-specific and toxic effect. In this work we aimed at applying this rationale to build an assay for the rapid screening of compounds capable of specifically induce the removal of PrP^C from the cell membrane. To pursue this objective, we designed an experimental workflow based on the same HEK293 cell line stably expressing an EGFP-PrP^C, which allowed the detection of PrP^C cellular distribution upon compound treatment using a semi-automatic high-content imaging platform (Operetta, Perkin Elmer).

4.2 Experimental layout

To set up the experimental procedures for the screening campaign we proceeded by optimizing a previously described protocol (Stincardini et al., 2017). Cells were seeded at day 0 in 384-well plates and grown for 24h to reach an approximate 60% confluency. At Day 1, cells were exposed to each compound (3 μ M) for 24h, and then fixed and stained with Hoechst to detect cell nuclei. Acquisition and analysis of the EGFP signal, reflecting PrP^C distribution, were automatically performed by the Harmony software (Perkin Elmer, Fig. 1). In physiological conditions, PrP^C decorates the outer leaflet of the plasma membrane, giving

rise to a typical honeycomb pattern (Fig. 2b). Relying on this information, cells segmentation was performed in two key steps: nuclei identification by the Hoechst signal (Fig. 2a), and selection of the regions of interest based on the EGFP signal (Fig. 2c, d). Only the nuclei surrounded by an EGFP signal-defined membrane were considered as objects and counted. The number of counted objects was considered as an estimation of the number of cells per well. The average fluorescence intensity of the EGFP signal was detected in the membrane region (enlarged border of the cell), as well as the region inside the cell. Next, the intensity of EGFP signals at the surface (S) or inside each cell (I) was compared. PrP^C re-localization was then estimated as the mean ratio between S and I signals (S/I) of five pre-assigned fields for each of two replicate wells.

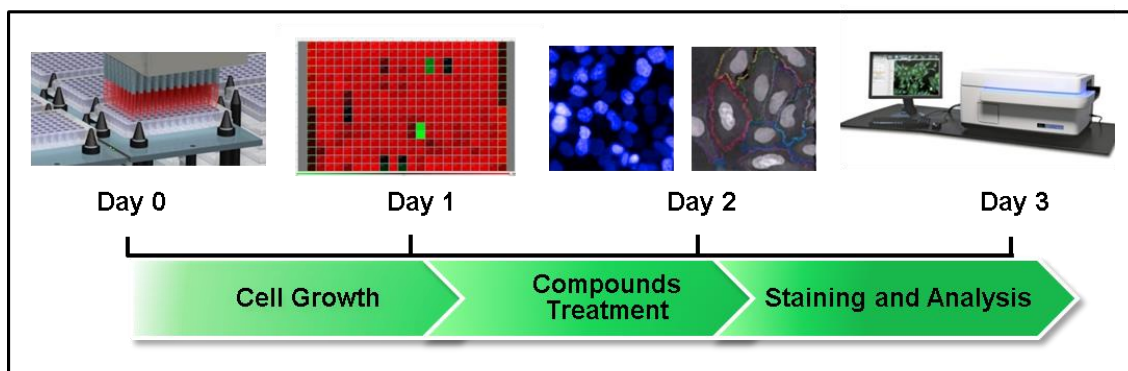


Figure 1: Workflow of the Primary Screening. Cells were automatically seeded on Day 0 with a liquid handler; exposed to the different compounds for 24h on Day 1, and then fixed and stained with Hoechst on Day 2. Image acquisition was performed with Operetta Imaging System (Perkin Elmer) and the analysis with Harmony software (Perkin Elmer).

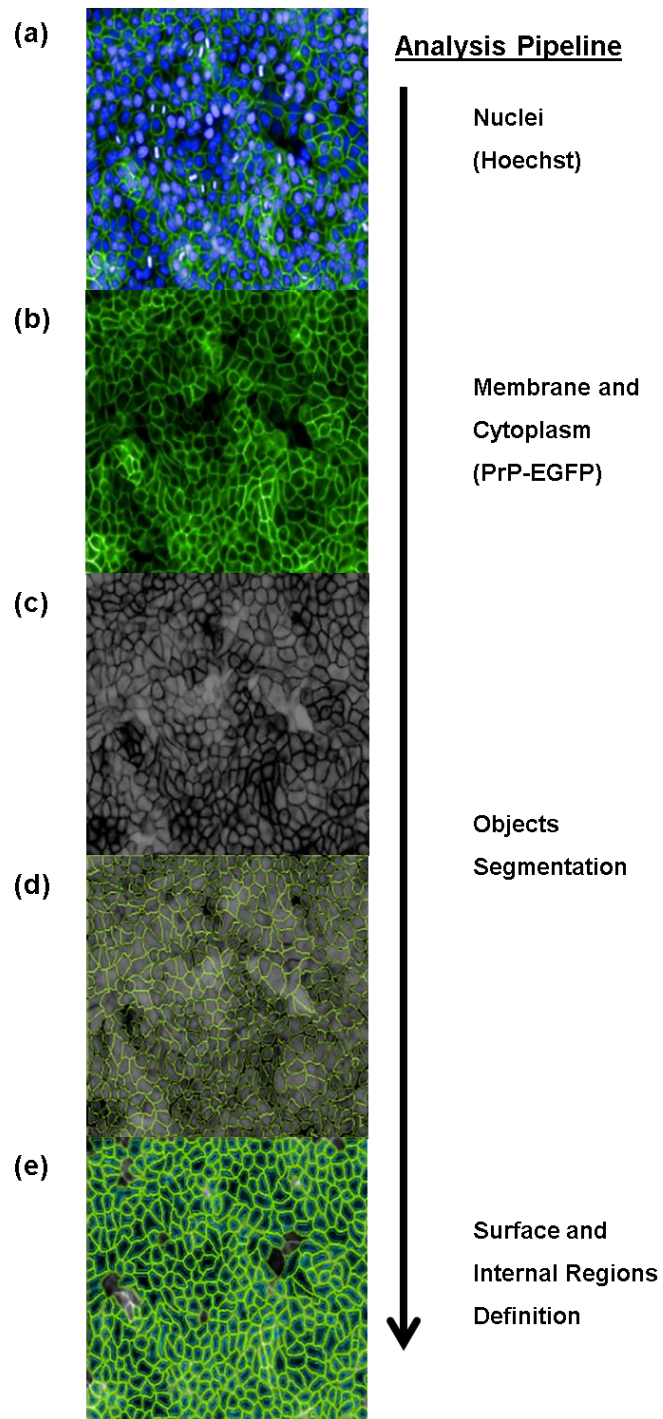


Figure 2: Segmentation Steps. Acquisition and analysis of images were automatically performed by Operetta Imaging System with the Harmony software (Perkin Elmer). **(a)** Image showing both nuclei (Hoechst blue signal) and PrP (EGFP green signal). **(b)** In physiological conditions, PrP^C decorates the outer leaflet of the plasma membrane, giving rise to a typical honeycomb pattern. **(c-d)** segmentation of the cells, performed by coupling the detection of EGFP (green) and Hoechst (blue) signals. **(e)** Definition of the surface (S) PrP signal (green areas) and the internal (I) PrP signal (cyan areas).

4.3 Definition of the Z prime

Since the all the SMs which were be tested are dissolved in DMSO, we set as negative control (hereon referred as VHC) a final concentration of 0.2% DMSO. At such concentration, as already seen in (Stincardini et al., 2017), PrP^C retains a physiological honeycomb localization (Fig. 3a). Taking advantage of the information collected we decided to use as positive control the dynamin inhibitor Imynodin-17 at a final concentration of 30 μ M (hereon referred as CTR+). As shown in Figure 3b the membrane localization of the EGFP-PrP signal appears reduced if compared to negative controls (Fig. 3a). To firstly establish the reliability of our assay a Z' analysis was performed between VHC and CTR+. As displayed in Figure 3d, when the S/I parameter was considered, the Z' between VHC and CTR+ was 0.45, indicating a sufficient discrimination. Conversely, when the Number of Cells was considered, the Z' between VHC and CTR+ was below zero.

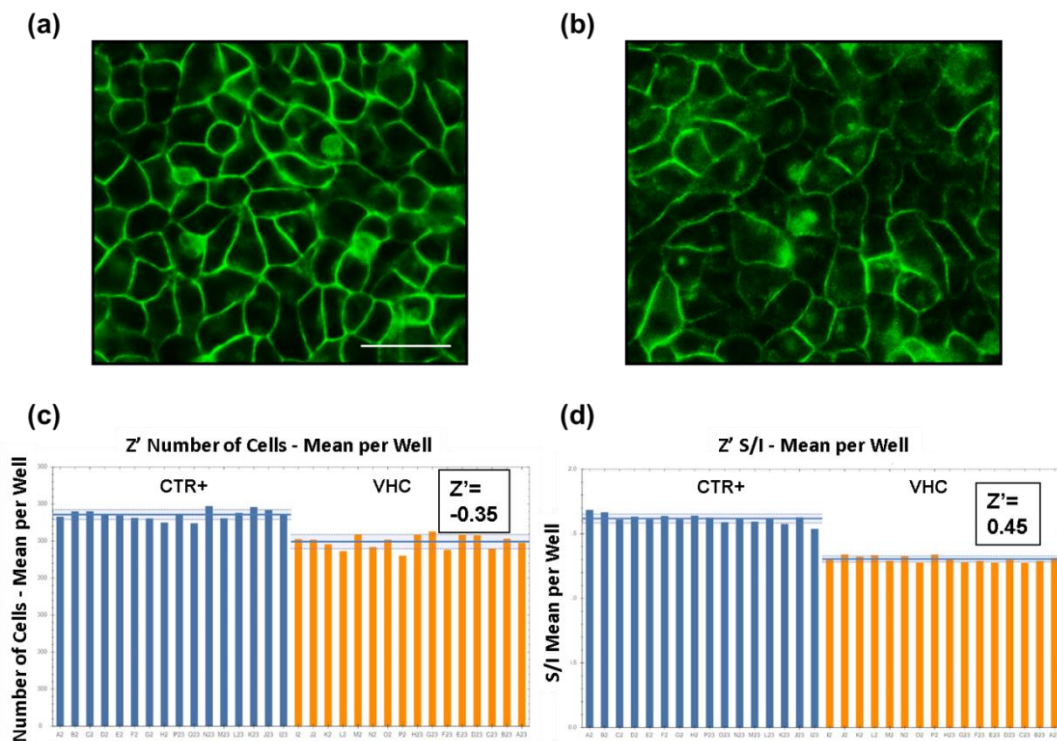


Figure 3: The Definition of the Z Prime. (a) Representative image of the vehicle-treated negative controls (VHC). (b) Representative image of Imynodin-17-treated cells, used as positive controls (CTR+), scale bar 50 μ m. (c) Quantification of the number of cells for each well (represented by a single histogram column) in CTR+ treated wells (blue columns) and VHC treated wells (orange columns). The Z' between CTR+ and VHC is below zero. (d) Quantification of the S/I for each well (represented by a single histogram column) in CTR+ treated wells (blue columns) and VHC treated wells (orange columns). The Z' between CTR+ and VHC is 0.45.

4.4 Identification of PrP^C-re-localizing compounds

Once completed the set-up phase, the assay was employed to screen two different chemical libraries. The Microsource Spectrum Collection, which includes 2050 FDA/EMA-approved drugs, natural compounds and molecules in preclinical stages, selected for their biological relevance, was chosen in a repurposing perspective. The Screen-Well Autophagy Library, encompassing a number of 94 molecules involved in the regulation of autophagy at different levels, was chosen considering the importance of autophagy in the pathogenesis of prion diseases, as well as the effect of several inducers of autophagy, promoting the clearance of PrP^{Sc} (Aguib et al., 2009), (Heiseke et al., 2009), (Thellung et al., 2018). Interestingly, one of these compounds also reduced the levels of PrP^C, thus limiting the substrate available for conversion into PrP^{Sc} (Heiseke et al., 2009). The entire procedure was performed as shown in Figure 1, SMs of both libraries were administered at a final concentration of 3 μ M. After the fixation images were acquired and analyzed as explained above. The number of cells and S/I values for each well were expressed as the percentage over VHC-treated controls, then % S/I values were plotted against the % Cells (Fig. 4). As shown in the scatter plot depicted in Figure 4, VHC (red dots) and CTR+ (green dots) controls correctly segregate as two distinct populations. As also seen in Figure 3 CTR+ show a lower number of cells compared to VHC, imputable to a modest intrinsic toxicity. To select the primary hits, we then set the cell number cutoff to 60% and for the S/I EGFP-PrP^C <90%. After manually removing technical artifacts (e.g. largely altered cell segmentation due to non-uniform seeding) we identified 23 primary hits, which were further characterized in subsequent experiments.

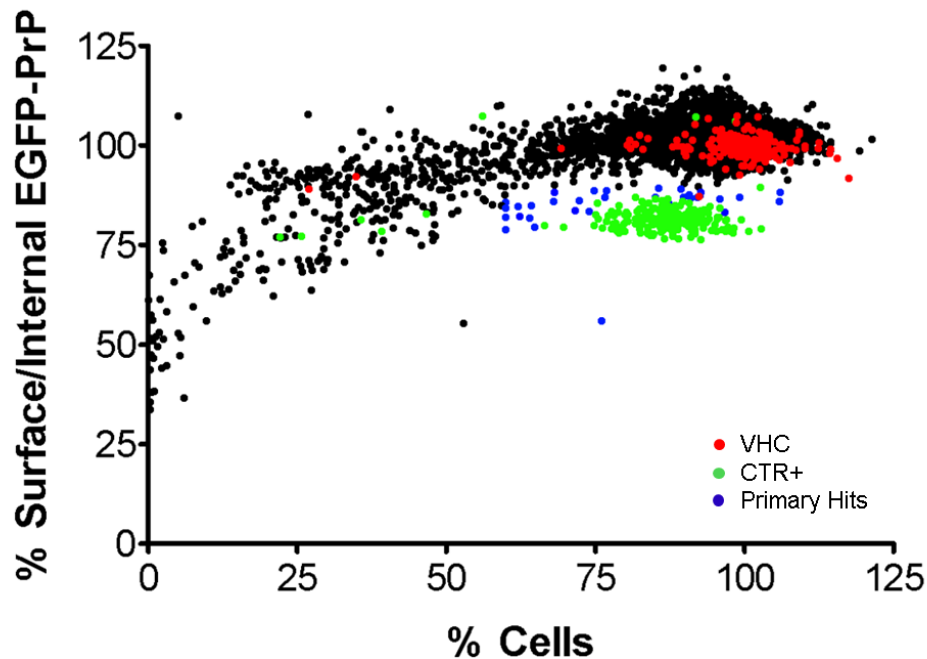


Figure 4 High Content Screening Data Distribution. Scatter plot representation of the different compounds tested, plotted for the number of cells over controls (X axis) and the Surface/Internal EGFP-PrP^C ratio over controls (Y axis). Each dot represents a well, red dots are VHC controls. Green dots are CTR+ controls. Blue dots are the primary hits, selected by imposing the following cutoffs: % cells >60%, % S/I EGFP-PrP^C <90%.

4.5 Validation of the Hits

To validate the hits identified in the HCS campaign, we performed four different assays (Fig. 5). As first hits were tested in a dose-response assay, using the same experimental paradigm employed in the screening, to select the SMs with a relevant pharmacological profile (i.e. inducing a dose-dependent re-localization). Then the false positive hits selected because of an intrinsic green autofluorescence were eliminated evaluating the localization of PrP^C using an immunofluorescence (IF)-based approach. Also, the specificity of PrP internalization was studied employing cells stably expressing a GPI-EGFP construct. Furthermore, a direct binding between the hits and recombinant PrP^C was tested with DMR and lastly a possible effect on the synthesis of PrP^C was investigated by Western blotting.

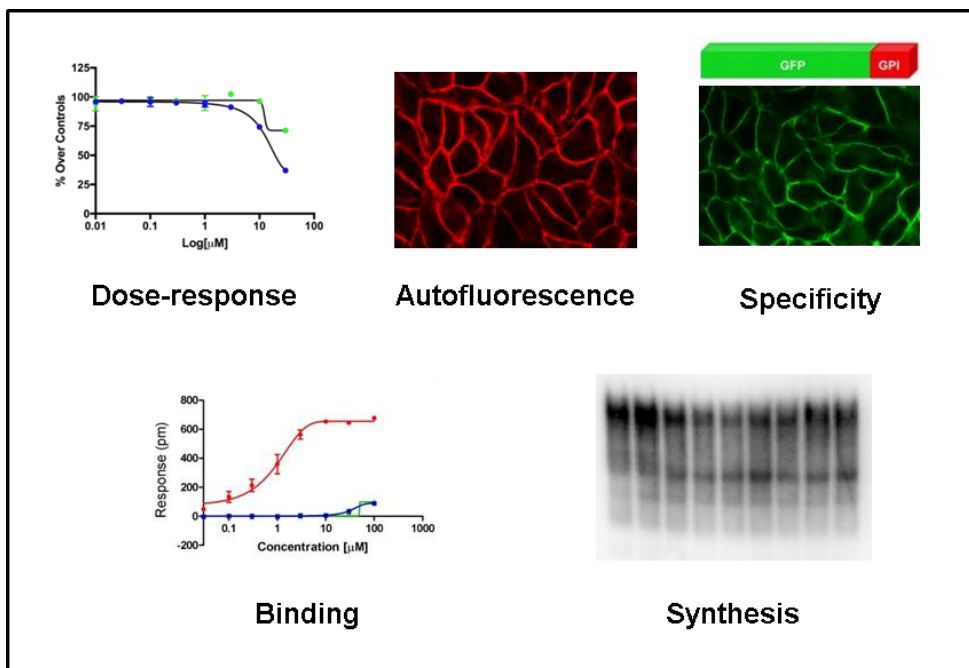


Figure 5: The Validation Steps. The 23 primary hits have been validated in five different assays, measuring the dose-response effect, the autofluorescence, the specificity of internalization, the binding to PrP and the effect on PrP synthesis.

4.6 Dose-response assays

To select the hits with a relevant pharmacological profile, we tested each compound in an 8-point dose-response curve (0.01, 0.03, 0.1, 0.3, 1, 3, 30 μM), comparing in parallel PrP^C relocalization and cytotoxicity, using the same experimental setting employed in the primary screening step. To better evaluate the dose-response effect for each compound the % S/I and the % Cells have been fitted to a 4PL sigmoidal-curve (Fig. 6 and Fig. S2). By imposing two cutoff criteria to the S/I curves, an $R^2 > 0.60$ and a reduction of $\geq 10\%$ at $10\mu\text{M}$, we detected statistically significant dose-response distributions for 6 molecules (Fig. 6), while we observed no significant dose-response correlation for 17 compounds (Fig. S2).

Among the compounds of the Screen-Well Autophagy Library, we found BFA and SU11652. BFA is a molecule known to block protein transport from the ER to the Golgi apparatus (Orci et al., 1991). In our assay, this compound induced an evident decrease of cell surface EGFP-PrP^C, starting at $0.03\mu\text{M}$ ($>10\%$) and rapidly reaching a plateau at $0.1\mu\text{M}$ ($>25\%$; Fig. 3a and d). The same trend however was observed also when % Cells was analyzed. SU11652,

a tyrosin kinase receptor inhibitor, decreased cell surface EGFP-PrP^C starting at 0.3 μM (~15%) in the absence of cytotoxicity, which was instead prominent at concentrations higher than 3 μM (Fig. 3b and e). We found four additional positive compounds from the Microsource Spectrum Collection. These included QNC, TAC, HRO and HM. QNC, a tricyclic acridine derivative, traditionally used as an anti-malaria drug, is also well-known for its potent anti-prion activity in cell cultures (Collins et al., 2002, Barret et al., 2003, Korth et al., 2001). This molecule induced a dose-dependent decrease of surface-exposed EGFP-PrP^C above 3 μM (~20%), while showing evident cytotoxicity only at much higher concentrations (30 μM; Fig. 3c and f). TAC, a widely used immunosuppressant, showed an effect only at 10 μM (~12%) without dampening cell viability (Fig. 3g and j). HRO, a β-carboline of natural origin, reported as a mono-amino-oxidase inhibitor (Herraiz et al., 2010), lowered the amount of surface EGFP-PrP^C by more than 35% at the highest concentration (30 μM) without showing any effect on cell viability (Fig. 3h and k). Finally, HM, an hematoxilyn derivative commonly used to stain nucleic acids (Cooksey, 2010), reduced EGFP-PrP^C from the cell membrane of ~15% starting at 10 μM, in the absence of toxicity (Fig. 3i and l).

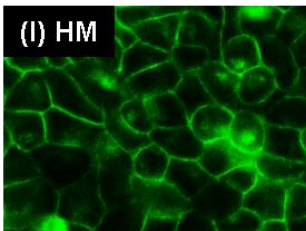
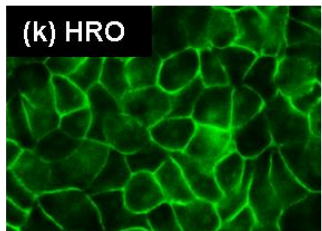
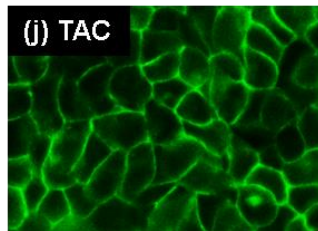
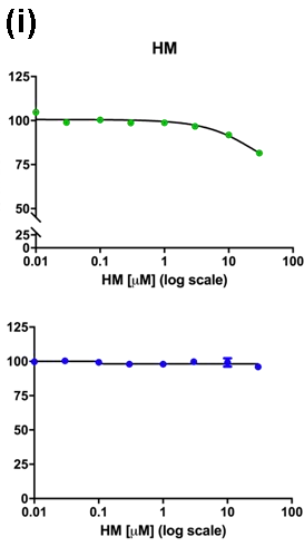
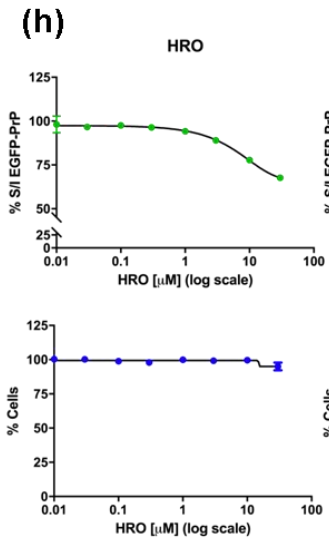
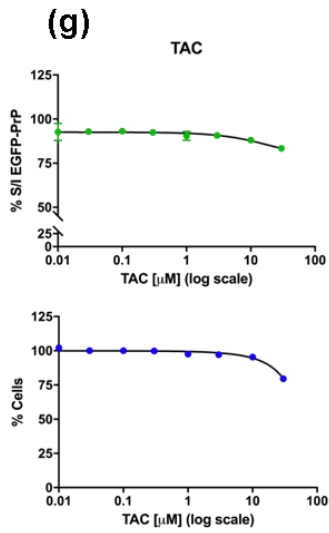
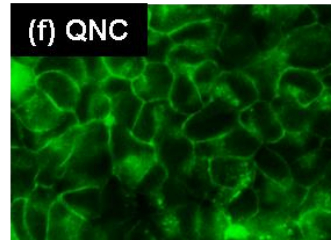
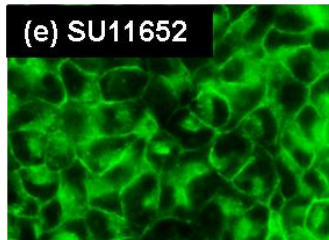
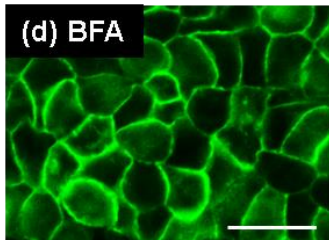
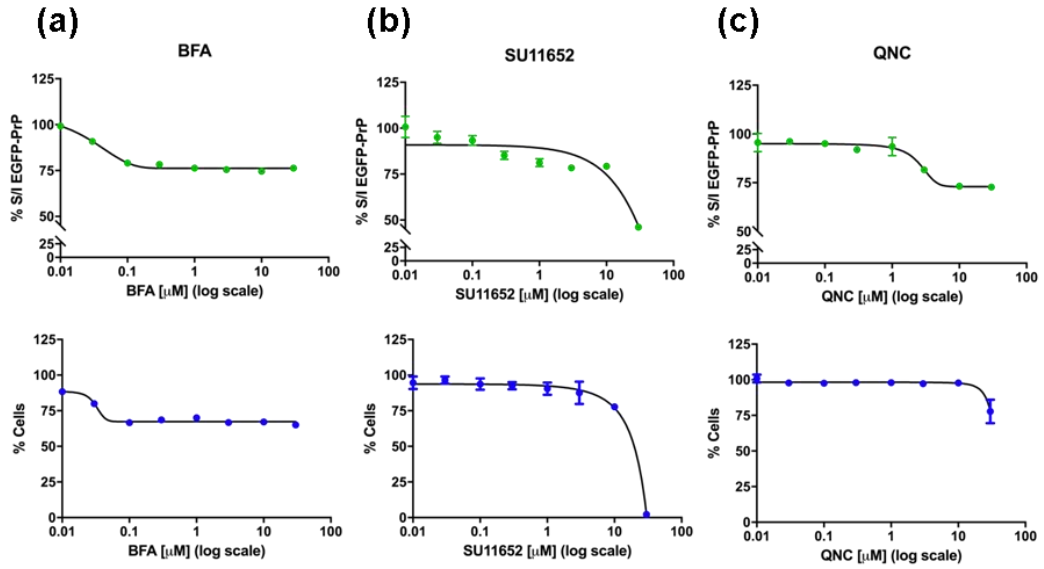


Figure 6: Dose-Response Assays to Validate Compound Hits. Graphs depict the quantification of EGFP-PrP^C re-localization (green dots) or cytotoxicity (blue dots) upon compound treatments, both acquired with Operetta Imaging System and quantified with the Harmony software. Data from three independent cell culture preparations were fitted by using the 4PL non-linear regression model. Statistical analyses were as follow: **(a)** BFA, % S/I EGFP-PrP^C $R^2=0.97$, % Cells $R^2=0.94$; **(b)** SU11652, % S/I EGFP-PrP^C $R^2=0.83$, % Cells $R^2=0.98$; **(c)** QNC, % S/I EGFP-PrP^C $R^2=0.92$, % Cells $R^2=0.80$; **(g)** TAC, % S/I EGFP-PrP^C $R^2=0.66$, % Cells $R^2=0.95$; **(h)** HRO, % S/I EGFP-PrP^C $R^2=0.97$, % Cells $R^2=0.55$; **(i)** HM, % S/I EGFP-PrP^C $R^2=0.90$, % Cells $R^2=0.16$. Representative images for each molecule are also shown below the graphs (**d-f** and **j-l**; **d**: BFA 0.03 μ M; **e**: SU11652 3 μ M; **f**: QNC 10 μ M; **j**: TAC 10 μ M; **k**: HRO 10 μ M; **l**: HM 30 μ M; VHC and CTR+ are not shown; Scale bar 50 μ m).

4.7 Elimination of False Positives

Next, to further exclude false positives possibly derived from the cleavage of the EGFP attached to the N-terminus of PrP^C, or to the intrinsic autofluorescence of the compounds, we performed a classical IF staining using an anti-PrP^C antibody (called 6D11) recognizing the central region of the protein (See Fig. S1). We used the same experimental setting exploited in the screening, and in this case IF signals were revealed with a secondary antibody coupled to a near-infrared dye (Fig. 7). As for the previous steps, images were acquired and analyzed with Operetta Imaging System and Harmony software, % S/I and the % Cells were fitted to a 4PL sigmoidal-curve. As expected, in VHC treated-cells we detected the honeycomb-like pattern consistent with a cell surface distribution of PrP^C (Fig. 7n). Conversely, the CTR+ altered PrP^C distribution toward a more widespread intracellular localization (Fig. 7m). Importantly, among the six candidate hits, we found consistency between EGFP- and antibody-derived signals only for BFA, QNC, TAC and HM (Fig. 7a, c, d and f), while the other two compounds SU11652 and HRO showed a largely lower PrP^C-re-localizing effect when the protein distribution was monitored by IF staining (Fig. 7h and k, respectively). Also, the trend of the EGFP- and antibody-derived S/I curves was not overlapping (Fig. 7b and j respectively). For this reason, we decided to exclude SU11652 and HRO from the further analyses.

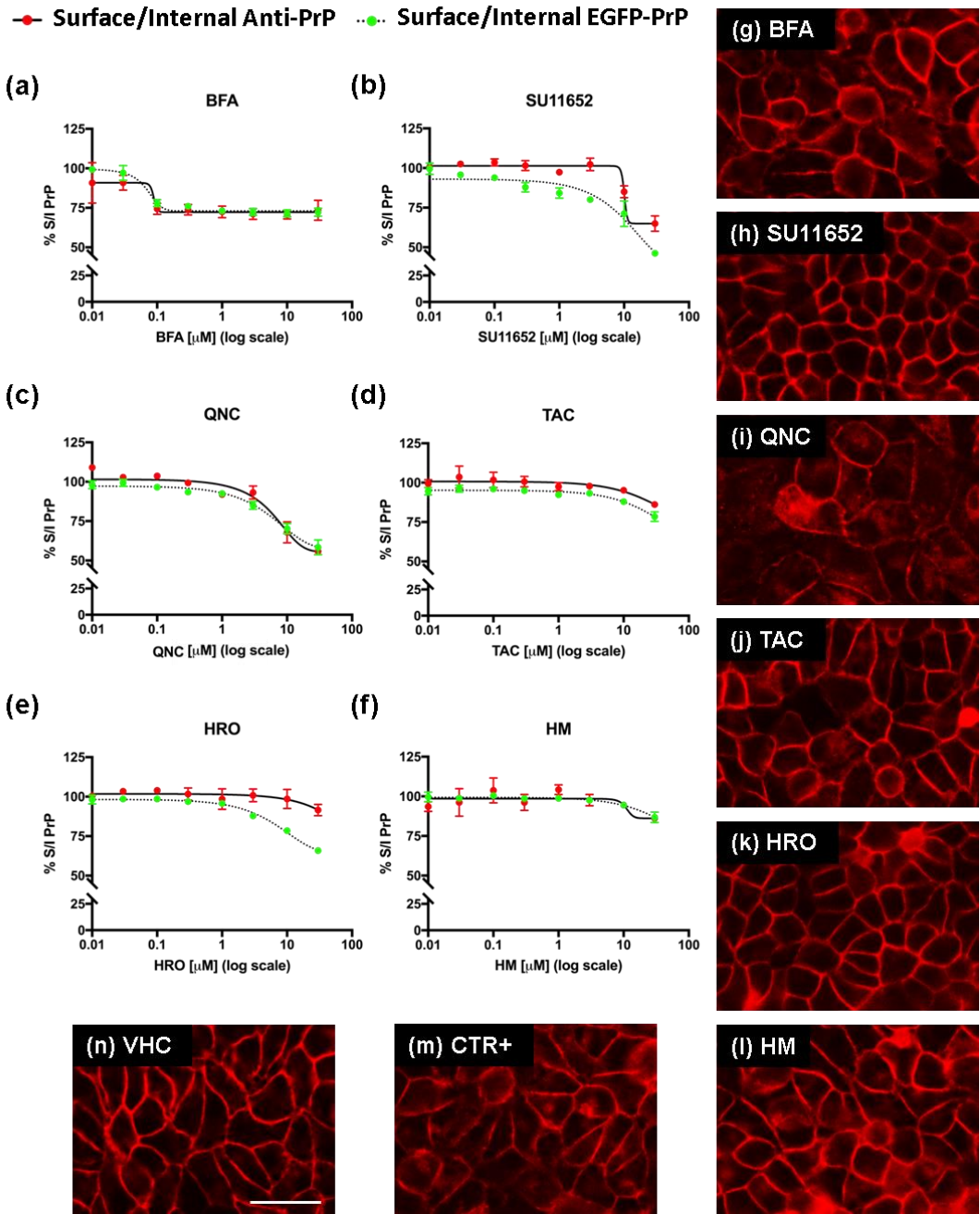


Figure 7: Dose-Response Assay to Eliminate False Positives. Graphs show the quantification of EGFP-PrP^C re-localization obtained by detecting the intrinsic fluorescence of EGFP (green dots) or by staining with an anti-PrP antibody (6D11, red dots). Data from three independent cell culture preparations were fitted by using the 4PL non-linear regression model. Statistical analyses were as follow: **(a)** BFA, % S/I of EGFP-PrP^C $R^2=0.84$, % S/I of anti-PrP antibody $R^2=0.63$; **(b)** SU11652, % S/I of EGFP-PrP^C $R^2=0.85$, % S/I of anti-PrP antibody $R^2=0.88$; **(c)** QNC, % S/I EGFP-PrP^C $R^2=0.85$, % S/I of anti-PrP antibody $R^2=0.90$; **(d)** TAC, % S/I EGFP-PrP^C $R^2=0.70$, % S/I of anti-PrP antibody $R^2=0.60$; **(e)** HRO, % S/I EGFP-PrP^C $R^2=0.95$, % S/I of anti-PrP antibody $R^2=0.24$; **(f)** HM, % S/I EGFP-PrP^C $R^2=0.60$, % S/I of anti-PrP antibody $R^2=0.31$. Representative images for each molecule are also shown on the right **(g-n)**; **g**: BFA 0.03 μ M; **h**: SU11652 3 μ M; **i**: QNC 10 μ M; **j**: TAC 10 μ M; **k**:

HRO 10 μ M; l: HM 30 μ M; n: VHC and m: CTR+ indicate vehicle (DMSO 0.2%) and Imynodin-17 (30 μ M) respectively; Scale bar 50 μ m).

4.8 Specificity of the internalization

Then, in order to estimate the effect specificity for each candidate hit, we monitored the localization of a control protein construct (GPI-anchored EGFP) mimicking PrP^C trafficking and localization (Mayor and Riezman, 2004) and stably expressed in HeLa cells. Consistently with the previous setting, we tested each molecule in an 8-point dose-response curve (0.01, 0.03, 0.1, 0.3, 1, 3, 30 μ M), and measured GPI-EGFP re-localization after 24 h of treatment. As for PrP^C re-localization, to evaluate the dose-response effect of each compound the % S/I has been fitted to a 4PL sigmoidal-curve (Fig. 8). Not surprisingly, BFA and QNC, both known to act by altering steps of the secretory pathway (Klingenstein et al., 2006), (Orci et al., 1991), induced the re-localization of GPI-EGFP from the cell surface (Fig. 8a, g and b, h, respectively). A similar effect was detected for TAC (Fig. 9c and i), indicating that all these molecules likely alter the membrane localization of several GPI-anchored proteins in addition to PrP^C. Conversely, we observed no alteration of the amount of GPI-EGFP at the cell surface for HM (Fig. 9d and j).

Collectively, these data validated PrP^C-re-localizing effects for compounds BFA, QNC, TAC and HM, although only the latter showed the ability to specifically redistribute PrP^C in absence of cytotoxicity.

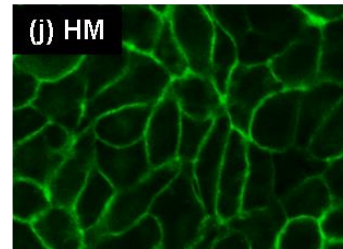
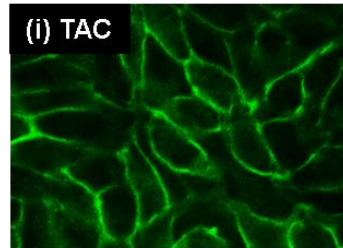
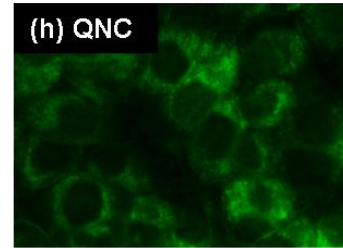
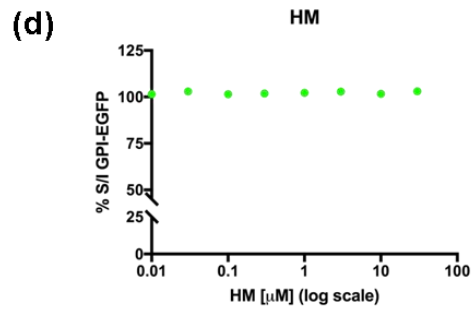
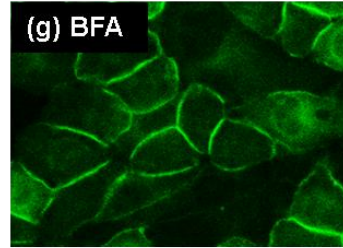
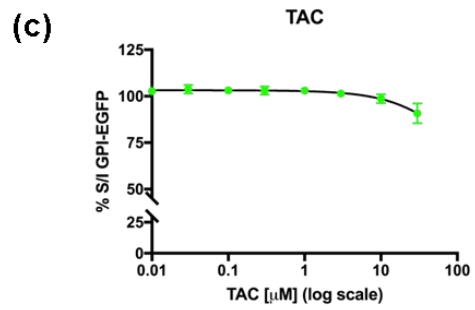
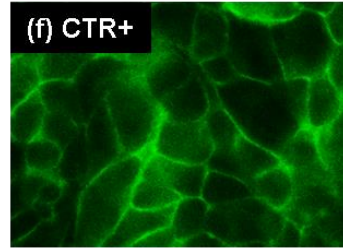
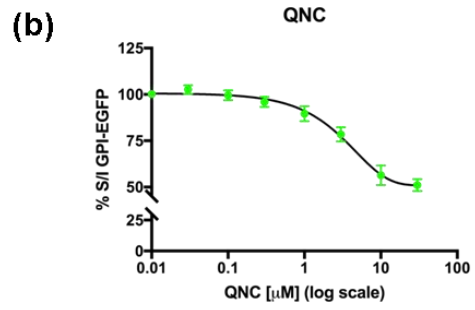
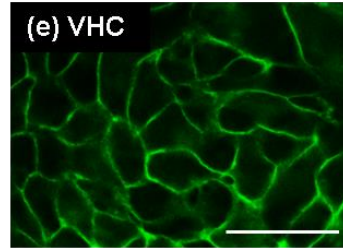
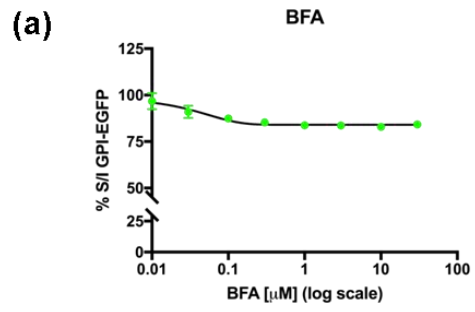


Figure 9: Evaluation of PrP^C Internalization Specificity. Graphs show the quantification of GPI-EGFP re-localization obtained by detecting the intrinsic fluorescence of EGFP (green dots). Data from three independent cell culture preparations, two replicates each, were fitted by using the 4PL non-linear regression model. Statistical analyses were as follow: **(a)** BFA, % S/I of GPI-EGFP R²=0.44; **(b)** QNC, % S/I of GPI-EGFP R²=0.86; **(c)** TAC, % S/I of GPI-EGFP R²=0.31, **(d)** HM, % S/I of GPI-EGFP, not fitted. Representative images for each molecule are shown on the right (**e-j**; **g**: BFA 0.03μM; **h**: QNC 3μM; **i**: TAC 10μM; **j**: HM 30μM; VHC and CTR+ indicate vehicle and Imynodin-17 at 30 μM, respectively; Scale bar 50 μm)

4.9 Evaluation of PrP^C binding

To test the hypothesis that these four remaining hits might act by directly binding to PrP^C we employed DMR, a biophysical technique previously used to monitor binding of putative ligands to the protein. This assay relies on the physical principle of SPR (i.e. monitoring the change in refraction index upon a binding event occurring at a surface and detected as a shift in wavelength) although in contrast to other SPR techniques, classically based on kinetic measurement of binding constants, it allows the estimation of binding affinity at the equilibrium. Human recombinant PrP (recPrP) was immobilized on 384-well microplates by amine-coupling, then incubated for 30 min with each molecule (0.03-100 μM). The porphyrin Fe(III)-TMPyP (TP), previously shown to interact with PrP^C (Massignan et al., 2016), was used as positive control, while vehicle injections and empty surfaces were used to normalize the signals. These analyses revealed a detectable binding to recPrP for QNC and HM, although the affinity values ($K_d > 100 \mu\text{M}$, Fig.9a, blue and green line respectively) were too high to justify their effects on PrP^C re-localization by direct interaction. None of the other molecules showed binding to recPrP (Fig.9b, yellow and purple lines), with the exception of the positive control TP (Fig. 9, red line).

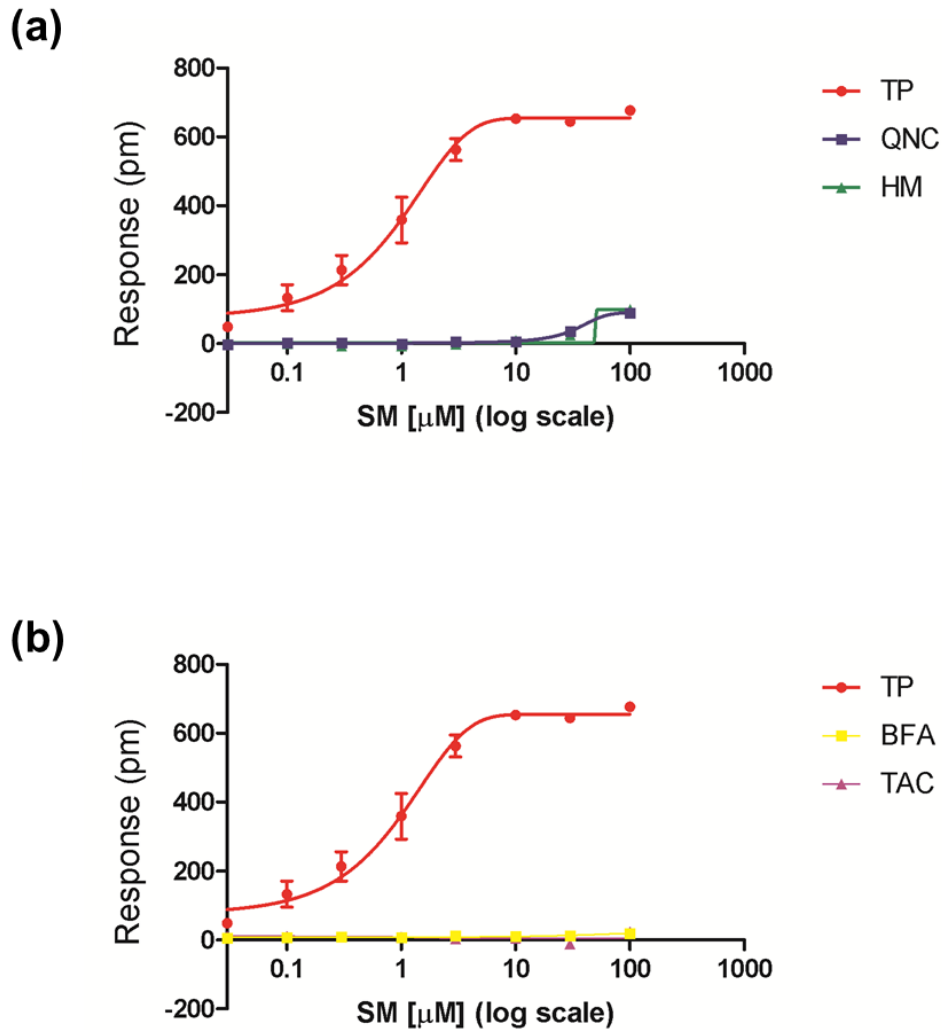


Figure 9: DMR-Based Detection of Binding to PrP^C. Different concentrations of compounds (0.03 - 100 μM) were added to label-free microplate well surfaces on which full-length, human recPrP^C have previously been immobilized. Measurements were performed before (baseline) and after adding each compound. The output signal for each well was calculated by subtracting the signal of the protein-coated reference area to the signal of the uncoated area. The final response (pm) was obtained by subtracting the baseline output to the average of three final output signals. TP (red dots) was used as positive control. All signals were fitted (continuous lines) to a sigmoidal function using a 4PL non-linear regression model. **(a)** TP, $R^2=0.97$; QNC, $R^2=0.98$; HM, $R^2=0.87$ **(b)** TP, $R^2=0.98$; BFA, $R^2=0.38$; TAC, $R^2=0.53$.

4.10 Effect on PrP^C Synthesis

As a further validation step we then evaluated if the re-localizing effect exerted by the hits was attributable to a global change in the expression levels of PrP^C. HEK293 cells stably expressing a murine WT PrP construct were treated for 24 h with different concentrations of each molecule (0.01, 0.03, 0.1, 0.3, 1, 3, 30 μ M), lysated and PrP levels were analyzed by Western blotting. Of note, none of the molecules altered the expression levels of PrP^C in HEK293 cells (Fig. 10) at non-toxic concentrations (Fig. 6) as treatment with BFA, QNC and TAC induced a detectable and/or significant decrease in PrP^C signal only at the higher concentrations (Fig. 10a, b and c respectively), when cytotoxicity was already marked.

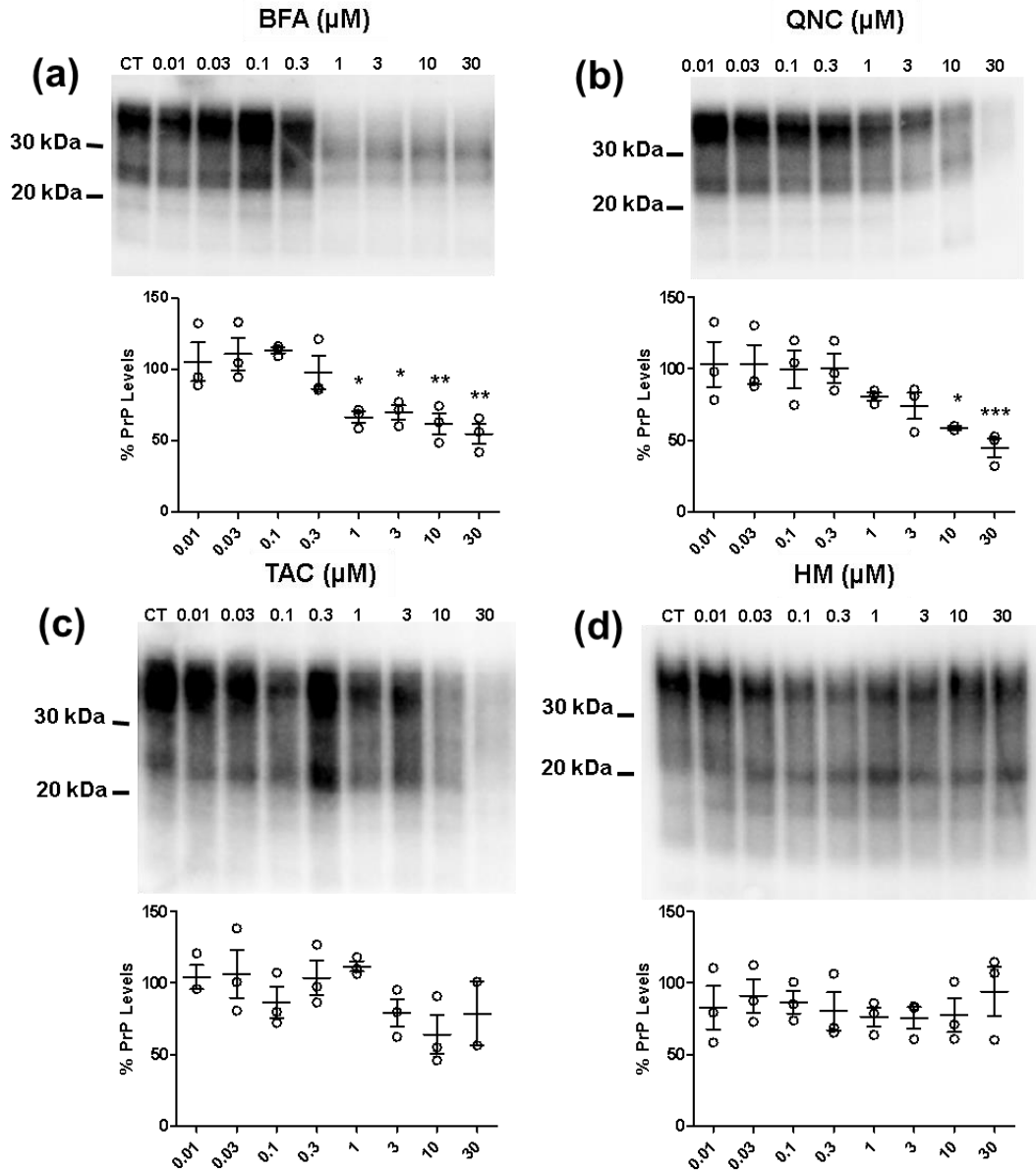


Figure 10: Evaluation of PrP^C levels by Western Blotting. (a-d) Representative blots of total PrP^C molecules in HEK293 cells stably expressing WT PrP and exposed to different concentrations of each compound (as indicated), detected by probing membrane blots with an anti-PrP antibody (D18). Graphs show the quantification of three independent cell culture preparations. Data were acquired by densitometric analysis of PrP bands, and expressed as percentage of signal over vehicle (DMSO) control. Statistical differences were estimated by one-way ANOVA, Dunnet post-hoc test. *p* values are: **p*<0.05, ***p*<0.01, ****p*<0.001.

4.11 Secondary Assays to assess efficacy

After the validation of the hits we sought to evaluate their anti-prion activity in different cell-based secondary assays. The inhibition of prion propagation was tested in cells chronically infected with two different prion strains. Then, the inhibitory effect against prion-induced cytotoxicity was studied by DBCA in HEK293 cells stably expressing a mutant form of PrP (Δ CR). Furthermore, the intrinsic toxicity of each molecule was monitored on both the cell lines used for the secondary assays.



Figure 11: The Secondary Assays. Representation of the secondary assays employed to characterize the anti-prion activity of the different compounds: molecules were tested on cells chronically infected with two different prion strains to evaluate anti-prion properties, by DBCA to evaluate the ability to suppress mutant PrP toxicity, as well as by MTT to monitor the intrinsic cytotoxicity.

4.12 HM Inhibits Prion Accumulation in Cell Cultures

In light of the observed ability of BFA, QNC, TAC and HM to induce the re-localization of PrP^C from the cell surface, we sought to test the efficacy of these compounds against two different prion strains in cell cultures. N2a cells stably-infected with the 22L or the RML prion strains were seeded on 24-well plates and exposed for 72 h to different concentrations (0.01-30 μ M) of each compound, or vehicle control (DMSO, volume equivalent). We then evaluated in parallel the amount of PK-resistant PrP by Western blotting, and cell viability by MTT assay. Consistent with previous reports (Daude et al., 1997, Klingenstein et al., 2006, Ryou et al., 2003), BFA and QNC drastically reduced PK-resistant PrP starting at 0.1 μ M concentration in both 22L and RML-infected cells, although no evident dose-response was

observed in RML-infected cells for BFA (Fig. 12a, b and Fig. 13a, b). However, these molecules also showed high cytotoxicity at comparable concentrations (Fig. 14a, b). TAC inhibited replication of both prion strains starting at 1 μM concentration, while it was toxic only at higher concentrations ($>10 \mu\text{M}$, Fig. 12c, Fig. 13c and Fig. 14c). Interestingly, HM was the only compound showing potent, dose-dependent inhibition of both 22L and RML prions in the almost complete absence of toxicity (Fig. 12d, Fig. 13d and Fig. 14d).

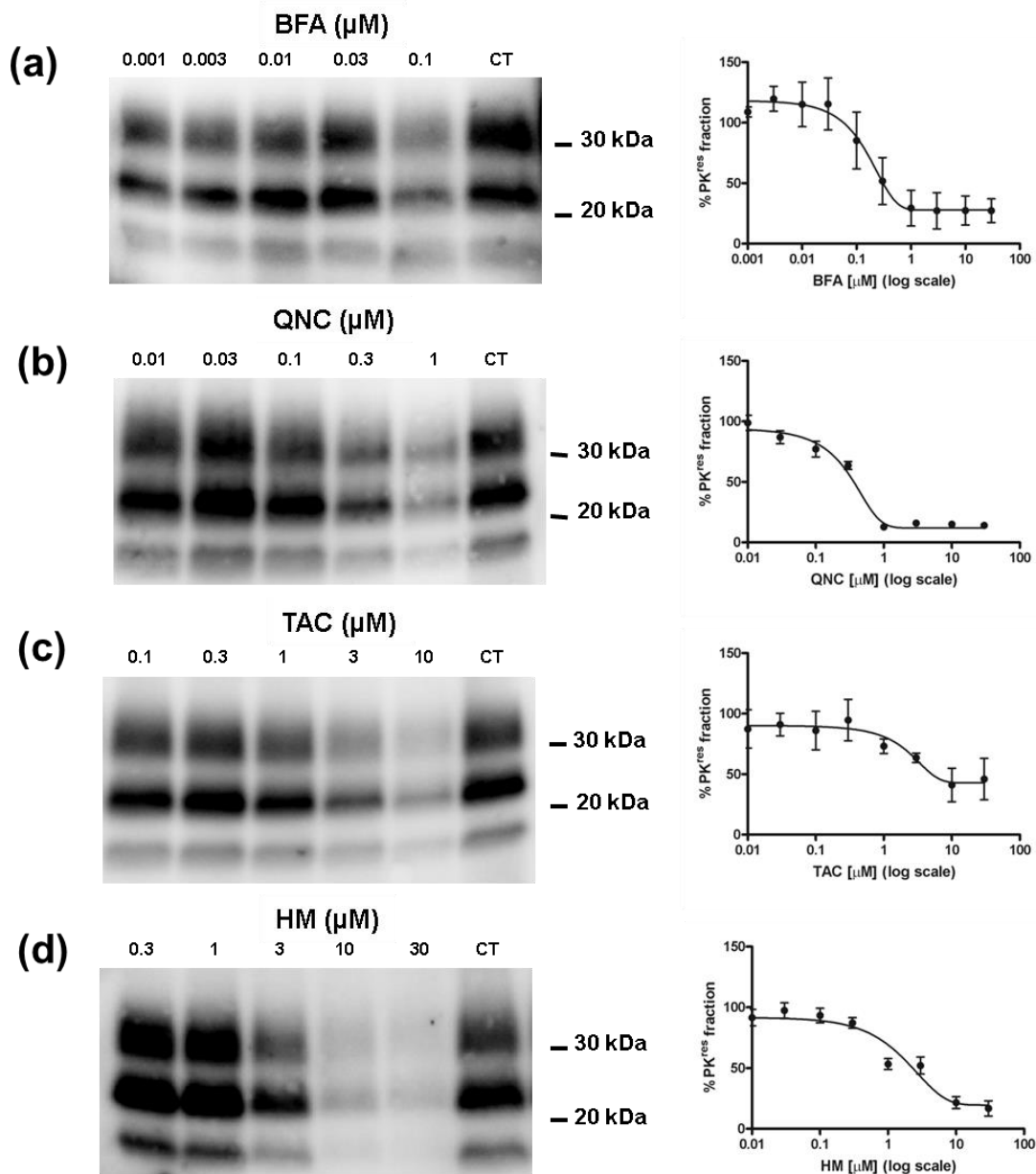


Figure 12: Test of Anti-Prion Activity in Cells Infected with 22L Prion Strain. (a-d) Representative blots of PK-resistant PrP molecules in N2a.3 cells chronically infected with the 22L mouse prion strains exposed to different concentrations of each compound (as indicated). Signals were detected by probing membrane blots with an anti-PrP antibody (D18). Graphs show the quantification of at least four independent cell culture preparations. Data were normalized over VHC (DMSO) controls, and fitted by a 4PL non-linear regression model (BFA, $R^2=0.70$; QNC, $R^2=0.83$; TAC, $R^2=0.38$; HM, $R^2=0.80$).

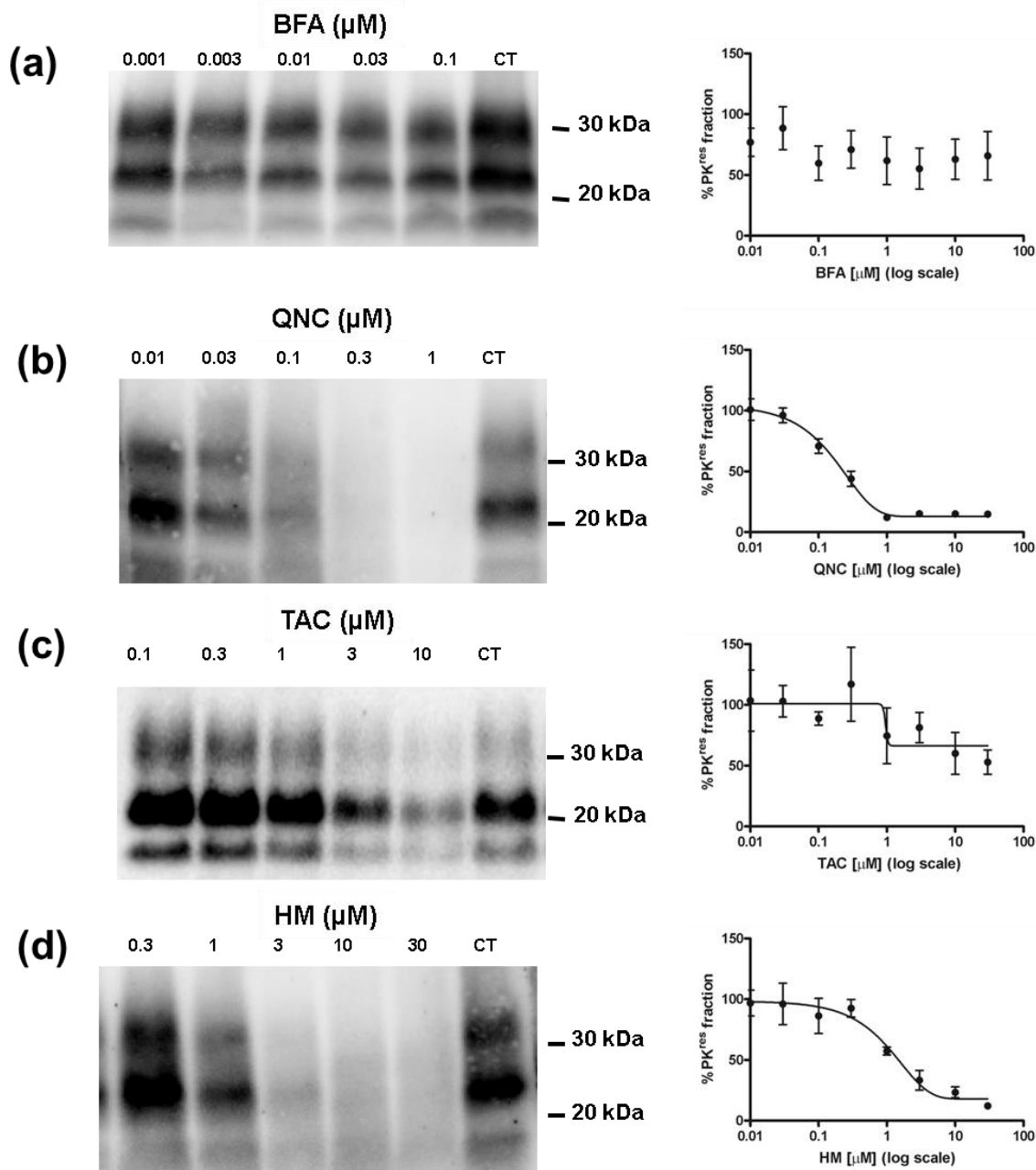


Figure 13: Test of Anti-Prion Activity in Cells Infected with RML Prion Strain. (a-d) Representative blots of PK-resistant PrP molecules in N2a.3 cells chronically infected with the RML mouse prion strains exposed to different concentrations of each compound (as indicated). Signals were detected by probing membrane blots with an anti-PrP antibody (D18). Graphs show the quantification of at least four independent cell culture preparations. Data were normalized over VHC (DMSO) controls, and fitted by a 4PL non-linear regression model (RML: BFA, not fitted; QNC, $R^2=0.81$; TAC, $R^2=0.27$; HM, $R^2=0.80$).

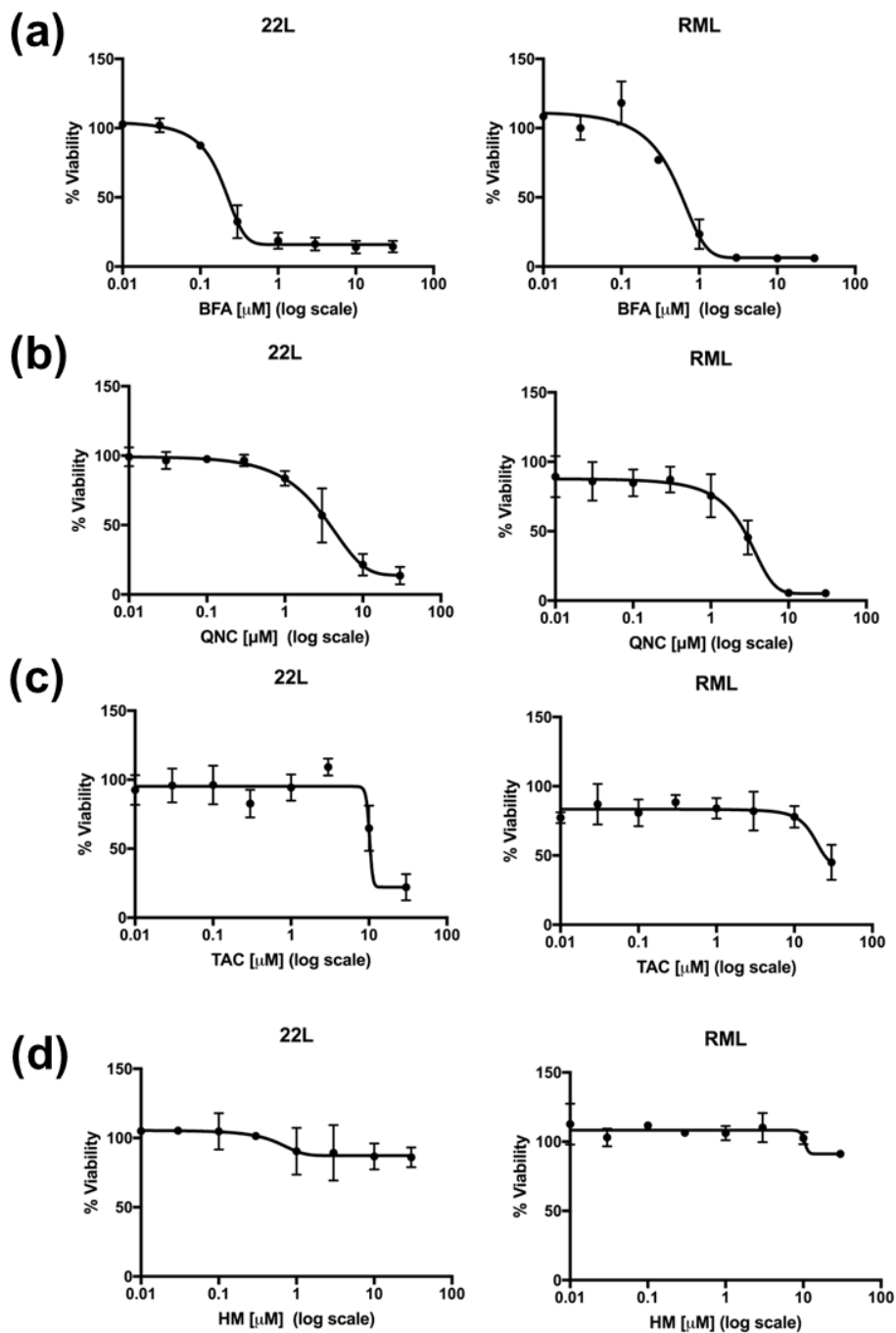


Figure 14 Cytotoxicity of Candidate Hits in Prion-infected N2a Cells. *Quantification of cell viability in N2a.3 chronically infected with the 22L or RML mouse prions upon incubation with the different compounds at various concentrations (1:3 dilutions from 0.01 to 30 μ M), detected by MTT assay. Graphs show the quantification of three independent cell culture preparations. Data were normalized over vehicle (DMSO) controls, and fitted by a 4PL non-linear regression model (BFA, 22L $R^2=0.95$, RML $R^2=0.5$; QNC, 22L $R^2=0.89$, RML $R^2=0.9$; TAC, 22L $R^2=0.66$, RML $R^2=0.58$; HM, 22L $R^2=0.21$, RML $R^2=0.35$)*

4.13 HM Inhibits Prion Toxicity in Cell Cultures

To further extend the characterization of the anti-prion properties of the identified compounds, we relied on the DBCA, a surrogate tool to study mutant PrP-dependent toxicity, previously employed to identify novel anti-prion compounds (Massignan et al., 2011). This assay is based on the ability of PrP molecules carrying artificial deletions or naturally-occurring mutations, to hypersensitize cells to the toxicity of several cationic antibiotics, such as bleomycin analogues (e.g. Zeocin) or aminoglycosides (e.g. hygromycin or G418). Since the cytotoxic activity of mutant PrP molecules has been shown to be dependent on their cell surface expression (Solomon et al., 2011), we employed the DBCA to evaluate the PrP-re-localizing effects of our compounds. To test the potential rescuing activity of BFA, QNC, TAC and HM, HEK293 cells stably expressing a PrP mutant carrying Δ CR deletion in the central region (Massignan et al., 2010) were exposed to each compound (0.001-50 μ M) for 6 h, and then treated with Zeocin (400 μ g/mL) for 24 h. Cell viability in the different conditions was then evaluated by MTT assay (Fig. 15). We observed no significant rescuing effects for BFA, QNC, TAC in the range of non-toxic concentrations (with the exception of QNC at 0.3 and 1 μ M, which showed modest rescuing effects, Fig. 15a, b, c and 16a, b, c). Conversely, HM showed a robust, dose-dependent rescue of mutant PrP-dependent toxicity (Fig. 15d), once again in the near-complete absence of cytotoxicity (Fig. 16d).

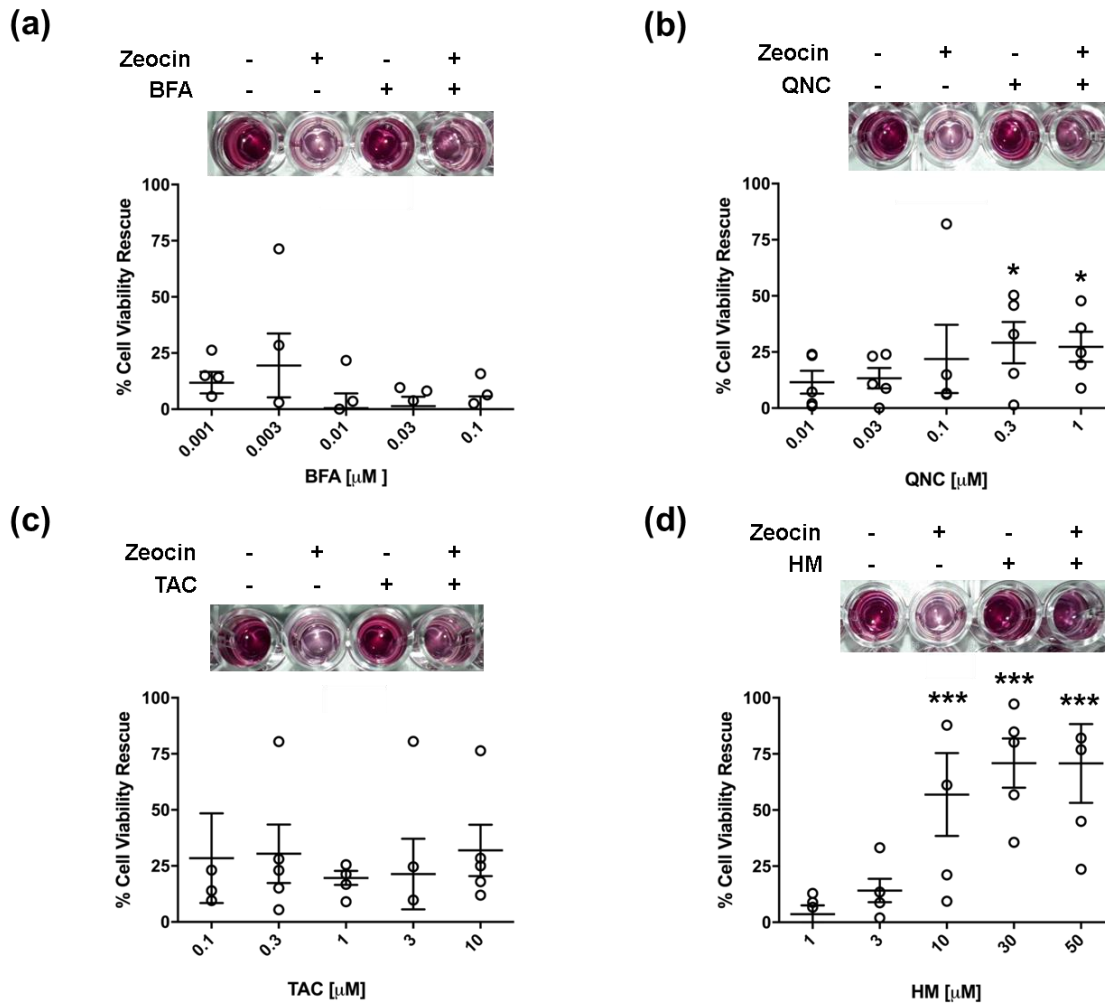


Figure 15: Evaluation of Rescuing Activity by DBCA. The DBCA was employed to evaluate the ability of each compound, tested at different concentrations (indicated), to rescue the Zeocin hypersensitivity conferred by the expression of mouse Δ CR PrP molecules expressed in HEK293 cells. The picture above the graphs show examples of wells after MTT assay. **(a-d)** Bar graphs illustrate the quantification of the dose-dependent rescuing effect of each molecule. Mean values were obtained from a minimum of 4 independent cell culture preparations, and expressed as percentage of cell viability rescue, using the following equation: $R = (T-Z)/(U-Z)$ (R : rescuing effect; T : cell viability in compound-treated samples; Z : cell viability in zeocin-treated samples; U : cell viability in untreated samples). Statistically-significant differences (*) between compound-treated and untreated cells were estimated by One-way ANOVA, Dunnet post-hoc test (p values are indicated as $* < 0.05$, $** < 0.01$, $*** < 0.001$).

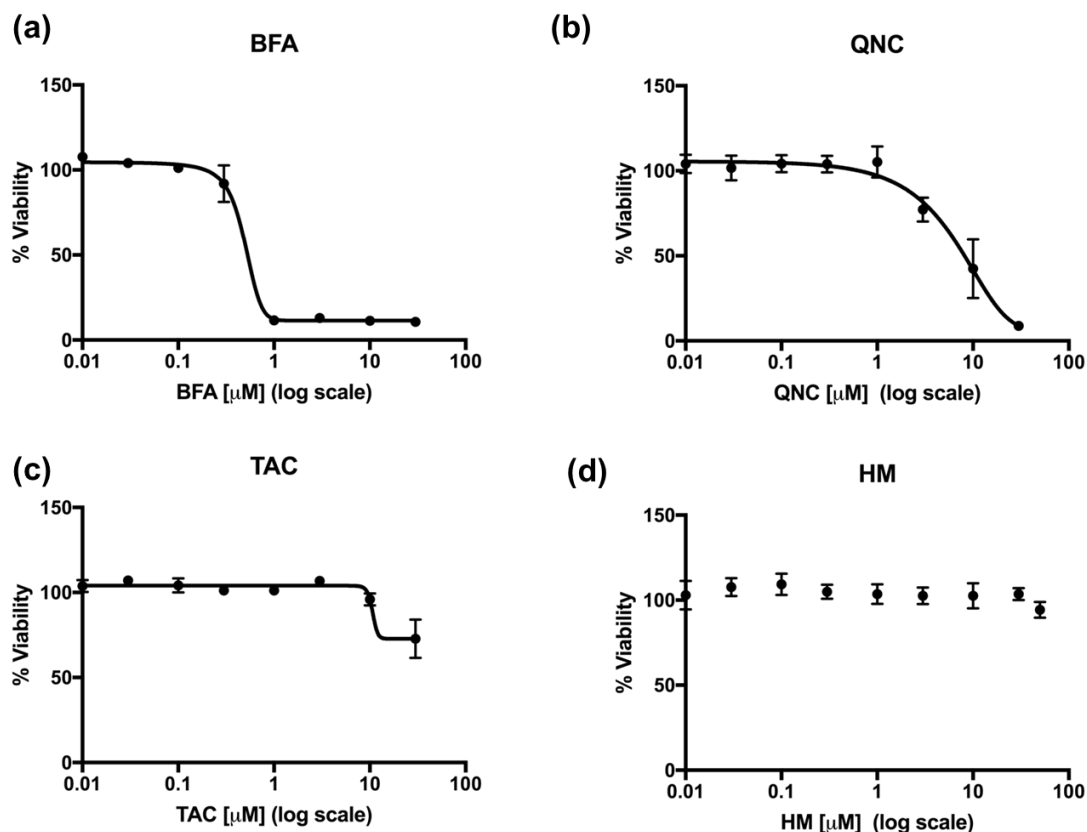


Figure 16: Cytotoxicity of the Candidate Hits in HEK293 Cells. (a-d) Quantification of cell viability in HEK293 cells stably expressing $\Delta\text{CR PrP}$ upon incubation with the selected compounds at different concentrations (1:3 dilutions from 0.01 to 30 or 50 μM), detected by MTT assay. Graphs show the quantification of three independent experiments. Data were normalized over vehicle (DMSO) controls, and fitted by a 4PL non-linear regression model (BFA, $R^2=0.98$; QNC $R^2=0.88$; TAC $R^2=0.68$; HM not fitted).

4.14 Overview of the Hits

A great deal of evidence in the past decades had reported that QNC is an efficient anti-prion molecule (Korth et al., 2001, Ryou et al., 2003). However, once tested both *in vivo* and in patients, QNC exerted no significant amelioration in disease progression and pathology (Barret et al., 2003, Collinge et al., 2009, Collins et al., 2002, Geshwind et al., 2013). Similarly, TAC showed no effect in prion animal models (Karapetyan et al., 2013). Our results indicated that HM is a potent, non-toxic anti-prion compound, capable of blocking prion replication in a strain-independent manner, as well as rescuing mutant PrP toxicity. Interestingly, HM has never been studied against prion diseases before, although few reports

indicate that its chronic administration in rodent models exerts no toxicity (Choi et al., 2003), (Hung et al., 2013), as we observed in cellular models. For these reasons we decided to continue our investigations focusing on a better characterization of the effect of HM, by considering more accurately its specificity, its pharmacological properties and a possible mechanism of action.

HITS				
	BFA	QNC	TAC	HM
Specificity for PrP	Non-specific	Non-specific	Non-specific	Specific
Binding to PrP	No	No	No	No
PrP Expression Levels	Unaltered (At non-toxic concentrations)	Unaltered (At non-toxic concentrations)	Unaltered (At non-toxic concentrations)	Unaltered
Anti Prion Accumulation Activity	No	Yes	No	Yes
Anti Prion Toxicity Activity	No	Moderate	No	Yes
Intrinsic Cytotoxicity	High	High	High	Low
Already Tested in Prion Models	Effective but toxic <i>in vitro</i>	No effect <i>in vivo</i>	No effect <i>in vivo</i>	-

Table 1: Summary of the properties of each selected hit.

4.15 HM Doesn't Alter the Membrane Dynamic of an Endogenous Protein

To better evaluate the specificity of action of HM we investigated the effect on the localization of another cell surface GPI-anchored protein, the Neuronal growth regulator 1 (Negr1), a cell adhesion molecule highly expressed in neurons (Noh et al., 2019). HEK293 cells stably expressing either WT PrP^C or a Negr1-Flag construct were treated for 24 hours with two different concentrations of HM (10 and 30 μ M) and the localization of both proteins was evaluated by an IF surface staining. As shown in Figure 17, HM induced a detectable

decrease in the intensity of PrP^C surface signal at both concentrations tested (Fig. 17c, d), confirming the hypothesis that HM acts by removing PrP from the cells surface. Furthermore, HM treatment did not decrease the cell surface levels of Negr1, (Fig. 17g, h), suggesting a PrP^C-specific effect for this compound.

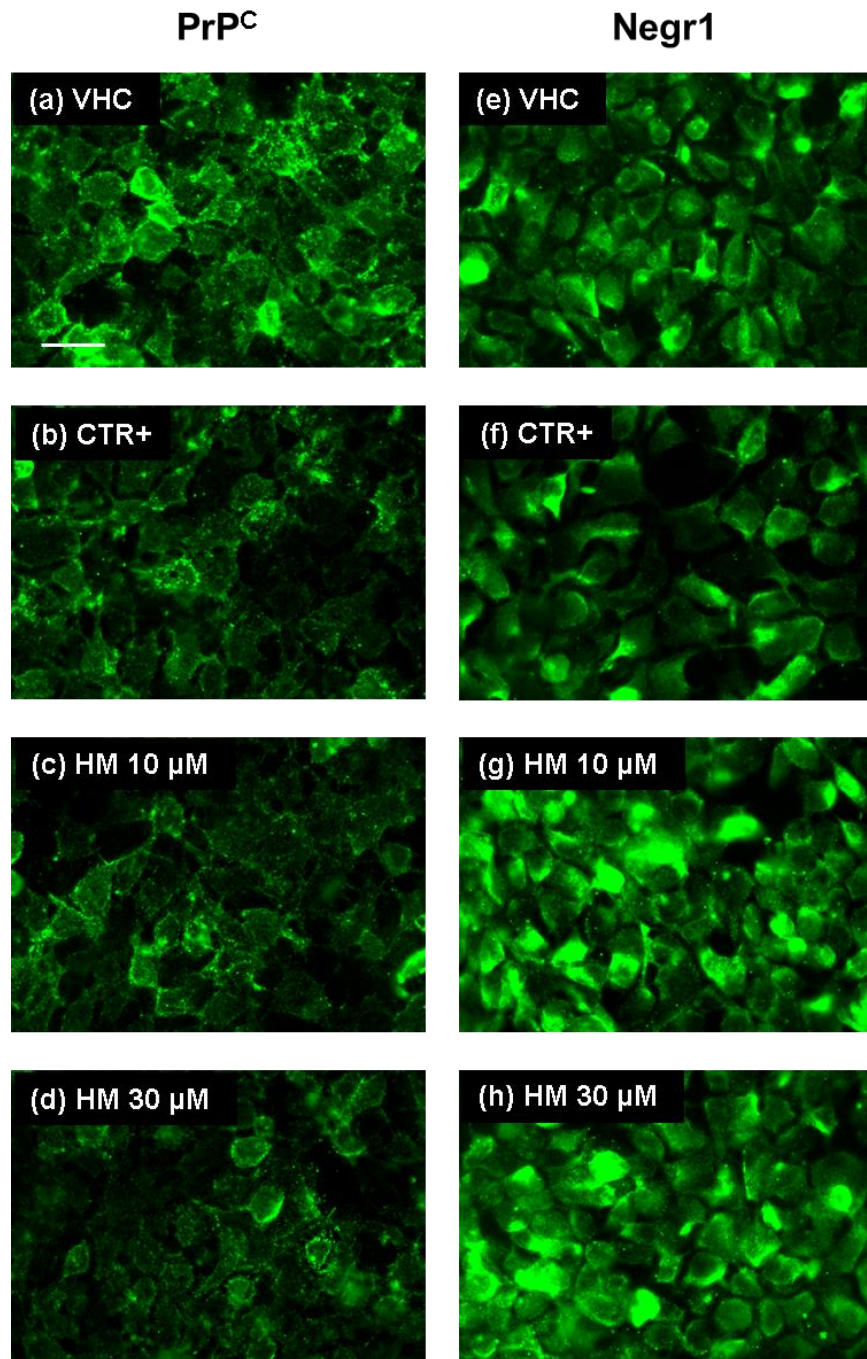


Figure 17: HM alters the cell surface localization of PrP^C but not Negr1. Cells were seeded on glass coverslips and grown for 24h to ~50% confluence, then treated for additional 24h with VHC (DMSO volume equivalent, **a** and **e**), CTR+ (Iminodine-17, 30 μ M, **b** and **f**) or HM at the indicated concentrations (**c**, **g**, **d** and **h**). Surface staining of PrP^C or NEGR-1 was achieved by incubating cells at 4°C with appropriate primary antibody, fixing with paraformaldehyde and then adding fluorescently-labelled secondary antibody. Images were acquired with a Zeiss Imager M2 microscope. Scale bar 30 μ m.

4.16 *In Silico* Pharmacokinetic Profiling of HM

In an attempt to predict the pharmacokinetic properties of this molecule, we carried out an *in silico* profiling and observed promising absorption, distribution, metabolism and excretion (ADME) values (Table 2). Moreover, *in silico* estimation of its BBB penetration ability, as evaluated by using two different software for ADME prediction, showed that HM's likelihood to cross the BBB lies within the range of many NPs or derived drugs targeting the CNS (Bharate et al., 2018). Together, these considerations suggest that although HM does not immediately appear as an ideal candidate molecule from a pharmacological standpoint, it may still be worth in the future to evaluate the therapeutic potentials of this compound in mouse models of prion diseases.

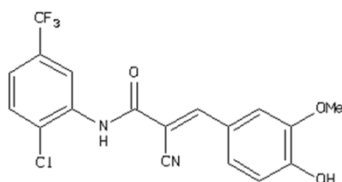
PARAMETERS	IDEAL VALUE/RANGE ^[a]	HM
MW (Da) ^[b]	<500	300
LogS ^[c]	>1	3.3
LogP ^[d]	0-3.5	0.36
cLogBB ^[e]	\geq -1	- 0.9
HIA ^[f]	+	-
P-gP category ^[g]	No	No
hERG pIC ₅₀ ^[h]	\leq 5	4.07
2C9 pK _i ^[i]	\leq 6	4.82
2D6 affinity category ^[j]	Low/Medium	Low
PPB90 category ^[k]	Low	Low

Table 2. *In Silico* Profiling of Physicochemical and Pharmacokinetic Properties for Compound HM. **[a]** Sets of physicochemical and pharmacokinetic parameters suggested for oral CNS-directed therapeutics (Segall et al., 2016) **[b]** Molecular weight. **[c]** Intrinsic aqueous solubility. **[d]** Calculated octanol/water partition coefficient, **[e]** Blood-Brain Barrier Penetration logarithm (Bharate et al., 2018). **[f]** Classification for human intestinal absorption. **[g]** Classification of P-glycoprotein transport. **[h]** Predicts the pIC₅₀ values for inhibition of hERG K⁺ channels. **[i]** Predicts the pK_i values for affinity with CYP2C9. **[j]** Cytochrome P450 CYP2D6 Classification. **[k]** Plasma Protein Binding Classification (90%).

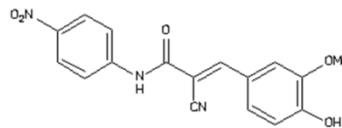
4.17 HM's Effect Could be Mimicked by a Casein Kinase 2 Inhibitor

A previous study have reported a direct interaction between HM and CK2 (Hung et al., 2009). Interestingly, other data have revealed a connection between CK2 activation and PrP^C function (Chen et al., 2008a, Meggio et al., 2000) (Negro et al., 2000) (Wang et al., 2013) (Zamponi et al., 2017), as well as an alteration of the expression pattern of CK2 subunits in the brain of experimental models of prion diseases (Chen et al., 2008b). These data suggest that HM may exert its anti-prion activity by directly acting on CK2. In order to test this possibility, we evaluated the rescuing ability of a recently identified, selective inhibitor of CK2 (ZINC01453593) by DBCA (Fig. 18a). We observed a dose-dependent rescue of mutant PrP toxicity at low micromolar concentrations (Fig. 18b). Importantly, a derivative (ZINC04175581, Fig. 18c) carrying a chemical modification that abrogates binding to CK2 showed no rescuing effects (Fig. 18d). Collectively, these data suggest that the inhibitory effects of HM on mutant PrP toxicity could be mimicked by compounds targeting CK2.

(a)

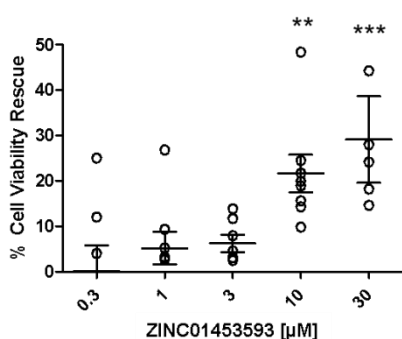


(c)



(b)

Zeocin	-	+	-	+
ZINC01453593	-	-	+	+



(d)

Zeocin	-	+	-	+
ZINC04175581	-	-	+	+

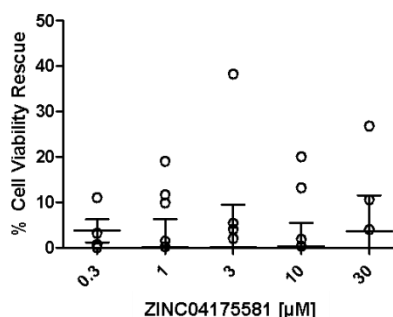


Figure 18: A CK2 inhibitor Rescues Mutant PrP Toxicity. The DBCA was employed to evaluate the ability of a specific CK2 inhibitor (chemical structure depicted in panel **a**) and a derivative (panel **c**) to suppress mutant PrP toxicity in HEK293 cells. Pictures above the graphs (panels **b** and **d**) show examples of wells after MTT assay. Bar graphs illustrate the quantification of the dose-dependent rescuing effects of each compound. Mean values were obtained from a minimum of 4 independent cell culture preparations, and expressed as percentage of cell viability rescue, using the equation described above. Statistically-significant differences (*) between compound-treated and untreated cells were estimated by One-way ANOVA, Dunnet post-hoc test (p values are indicated as ** <0.01 , *** <0.001).

4.18 Discussion

The absence of a valid treatment option for prion diseases raises the urgency of designing novel therapeutic concepts and alternative experimental strategies rather than just screening for PrP^{Sc}-lowering compounds. At this aim, the concept of altering the correct localization of PrP^C as a potential therapeutic strategy for prion diseases have been initially explored through the perturbation of the membrane environment where PrP^C is expressed. As PrP^C is delivered to lipid rafts, a variety inhibitors of cholesterol synthesis, like lovastatin and squalastatin (Bate et al., 2004), (Taraboulos et al., 1995), have been tested *in vitro* and *in vivo*. However, despite the promising results *in vitro*, none of these treatments resulted in a significant regression of the disease once tested in animal models, probably because the tolerable dosages were too low to induce a relevant reduction of PrP^C surface levels. Similarly, the alteration of membranes composition through GPI analogues, or the release of GPI-anchored proteins exerted by sulphonylurea derivatives as glimiperide (Bate et al., 2009), (Bate et al., 2010), although successful in cell models, do not appear as clinically appealing, since the non-specific action of these compounds may cause a high risk of side effects. Despite the broad diffusion of high content imaging platforms, only a few works to date have exploited the rationale of perturbing PrP^C localization to carry out screening campaigns. Here, we sought to capitalize on the rationale of removing PrP^C from the cell surface as a paradigm to identify novel chemical agents capable of counteracting prion replication and toxicity. To pursue this objective, we developed a cell-based HCS assay relying on the double evaluation of PrP^C localization both on the membrane and in the intracellular compartments, thanks to a fluorescently tagged PrP^C construct and an automated segmentation paradigm. We employed this new platform to screen two libraries of SMs focused on repurposing and on autophagy. In order to exclude false positives, as molecules inducing a global alteration of membrane dynamics and cytotoxic compounds, we filtered and validated the candidate hits with a battery of biochemical and cell imaging-based secondary assays. Upon testing the selected hits with two different models of prion and toxicity we identified HM as a lead molecule, showing specific PrP^C-re-localizing activity and potent anti-prion effects.

From a technical point standpoint our data highlighted that this screening technique could be suitable for rapidly testing several thousands of molecules in a semi-automatic fashion. Since it does not require staining procedures, the assay can be further optimized to scaled-up

formats, for example by adapting it to fully automatic robotic platforms. Given the nature of the revelation system, it is not excludable however that the assay failed to detect false negatives that could be influenced by the presence of an EGFP tag attached to PrP^C (i.e. molecules that would re-localize untagged PrP^C but not EGFP-PrP^C). Also, molecules proportionally reducing both the surface and the internal levels of EGFP-PrP^C might not alter the S/I parameter. This second issue however could be simply solved by measuring in parallel also the total fluorescence of the cells and analyzing it as a separate informative feature. In this way such platform would also be adaptable to screen for compounds globally lowering PrP^C levels. In addition, a number of false positives emerged from the primary screen, mainly related to the intrinsic auto-fluorescence of several SMs. To overcome these limits, we designed an extensive experimental workflow aimed at eliminating possible false positives through orthogonal assays and selecting the most promising candidate hits. Amongst the possible solutions, the use of a PrP construct tagged with a fluorophore emitting in the far-red spectrum seems the best strategy to overcome this issue, as we noticed that the majority of the auto-fluorescent compounds emits in the EGFP range. Another major issue observed is that even positive controls treated with Imynodin-17 showed a relatively small dynamic range of PrP^C redistribution from the cell membrane. This lack of sensitivity could be imputable to an excessive overexpression of EGFP-PrP^C in the clonal cell line used for the screening, needed for an efficient segmentation, but contrasting the efficacy of the positive controls and plausibly of the SMs tested too. A feasible compromise to solve this limitation could be to use another clonal line expressing lower levels of EGFP-PrP^C, possibly employing a more potent acquisition tool.

However, despite this apparent lack of sensitivity, the reliability of the method is largely supported by the data we obtained. In fact, the analyses re-discovered QNC, a classical anti-prion compound QNC (Barret et al., 2003), (Korth et al., 2001) and highlighted a new anti-prion compound HM, even though the number of compounds tested was relatively low.

The acridine derivative QNC was proposed for the treatment of prion diseases two decades ago (Doh-Ura et al., 2000) as it inhibits PrP^{Sc} formation in prion-infected cells, with EC50 values in the low micromolar range (Korth et al., 2001), (Ryou et al., 2003). In our hands QNC induced the re-localization of EGFP-PrP^C already at 3 μ M and tackled prion accumulation in cell cultures at comparable concentrations, in line with all the previous reports. The mechanism of action of QNC is still unknown, although NMR and SPR studies highlighted that QNC could act as a molecular chaperon by directly binding the globular

domain of human recPrP (Nakagaki et al., 2013, Kawatake et al., 2006), inducing a conformational change and thus preventing PrP^{Sc} conversion (Georgieva et al., 2006). However, QNC seems to have no effect on PrP^{Sc} propagation in cell-free conversion systems (Doh-Ura et al., 2000), (Kirby et al., 2003). Accordingly, also our SPR analyses showed that QNC weakly binds to recPrP only in the high micromolar range, making it unlikely that its high anti-prion efficiency might rely on direct interaction with PrP^C. Interestingly, in previous work from our laboratory, we observed similar properties also in CPZ, another tricyclic compound chemically similar to QNC (Stincardini et al., 2017). We showed that like QNC, CPZ binds to PrP^C only at non-pharmacologically relevant concentrations and is not able to counteract prion replication in cell-free systems, while its activity relies instead on the dynamin-dependent re-localization of PrP^C from the plasma membrane. These data collectively highlight a new possible mechanism of action of tricyclic derivatives, which would be worthy of being investigated more in detail.

Also BFA, a molecule already known to inhibit PrP^C trafficking to the cell membrane (Taraboulos et al., 1992), emerged amongst the primary hits. BFA has been initially used in cellular models to study PrP^C synthesis and membrane delivery through the ER and Golgi compartments. As a result of a lack of PrP^C membrane expression, it was shown that BFA blocks the synthesis of PrP^{Sc} (Borchelt et al., 1992), (Taraboulos et al., 1992). It is unclear though why in our hands BFA did not show such a marked effect. It is to note however that the high toxicity associated with BFA treatment in prion-infected cultures makes it difficult to entangle the specific anti-prion effect from the global cytotoxicity.

Similarly TAC, the third hit we found, has already been tested in different prion models, as one of its main targets, the Ca²⁺/calmodulin-dependent phosphatase (calcineurin), seems to be involved in the ER stress associated with PrP^{Sc} generation (Agostinho and Oliveira, 2003), (Mukherjee et al., 2010). Once tested in different mice models, TAC exerted a modest delay of the disease progression and a lower degree of neurodegeneration (Mukherjee et al., 2010), (Nakagaki et al., 2013, Shah et al., 2019). Surprisingly, in a recent report, Karapetyan and colleagues screened compounds lowering the expression of PrP^C with a FRET-based high throughput assay (PrP-FEHTA) and found that TAC significantly reduced PrP^{Sc} *in vitro*, possibly acting at a transcriptional level. However, once tested in a different *in vivo* model, also in this case TAC did not induce any extension in the lifespan of prion-infected mice (Karapetyan et al., 2013). Oddly, in our hands TAC did seem neither to alter global PrP^C levels nor to prevent prion accumulation *in vitro*.

Despite having screened a relatively small number of compounds, our results also identified HM as the most promising new candidate hit among the different molecules emerged from the screen. HM is an NP isolated from dried heartwood of *Caesalpinia Sappam* (Cooksey, 2010), never tested in prion models before. HM has been widely employed in histology for staining cell nuclei and a number of other cytoplasmic organelles as well as myelin sheaths, although its precise binding mode is still uncertain. In addition to the widely known dyeing properties, HM has extensively been used in oriental medicine to treat a variety of pathological states, from infections to anti-hypertension and inflammation, thanks to its antimicrobial, antioxidant, anticonvulsant, and anti-inflammatory properties, even though also in this case its mechanism of action is mostly unknown (Cooksey, 2010), (Dapson and Bain, 2015). In principle, such a wide reactivity with several cellular components may indicate a low effect specificity, a common feature of so-called pan-assay interference compounds (PAINS) (Baell and Walters, 2014), chemicals that non-specifically react with multiple biological targets and often appear as false positive hits in drug screenings. However, the possibility that HM may just represent a false positive hit in our screen is at least unlikely, for several reasons. First, we validated the effect of HM using a variety of orthogonal assays, from PrP^C re-localization to prion replication inhibition and suppression of mutant PrP toxicity. Moreover, PAINS often share common features, including high IC₅₀ values (high micromolar to millimolar range) and steep dose-response curves, while HM showed a consistent dose-dependent activity in all the experimental contexts at low micromolar concentrations, with similar IC₅₀ values across the different assays. Also, the *in silico* profiling we carried out revealed promising ADME values. Thus, while from a pharmaco-chemical point of view HM may belong to PAINS, it is unlikely that this molecule was just a false positive in our screen, and instead, the comprehension of its ability to redistribute PrP^C from the cell surface may reveal valuable insights into the biology of this protein. Together, these considerations suggest that although from a pharmacological standpoint HM does not immediately appear as an ideal candidate molecule, it may still be worth in the future to evaluate the therapeutic potentials of this compound in mouse models of prion diseases. Interestingly, few additional studies have tested HM *in vivo*, for example by assessing its inhibitory potentials on tumor growth or atherogenic pathways (Choi et al., 2003), (Hung et al., 2013). In particular, one study reported a significant decrease of tumor volume in a lung cancer model upon continuous diet supplementation with HM for two months, apparently in the absence of any intrinsic toxicity (Hung et al., 2013). Unfortunately, no information is available in the literature

about the ability of HM to target the CNS. Our *in silico* estimation of BBB penetration however, revealed that HM might likely permeate the BBB with an efficiency comparable to other NPs or derived drugs targeting the CNS (Bharate et al., 2018).

As a result of its pleiotropic biological action it is still challenging to understand the mechanism of action by which HM induces the re-localization of PrP^C. A previous cell-based screening of a library of natural compounds, showed that HM specifically suppresses cancer cell growth through the direct and selective inhibition of CK2 (Hung et al., 2009). The CK2 holoenzyme, a highly conserved serine/threonine kinase, is a tetramer composed of two catalytic (α or α') and two regulatory (β) subunits, generally kept in an inactive state through an atypical oligomerization mechanism (Lolli et al., 2017, Lolli et al., 2012, Lolli et al., 2014). In mammals, this enzyme is ubiquitously expressed in many different tissues, particularly enriched in the CNS, and it is involved in the control of a variety of cellular processes, including the cell cycle, apoptosis, transcriptional regulation and signal transduction (Nunez de Villavicencio-Diaz et al., 2017). In the brain, CK2 has been reported to play functions in neural development, axonal growth, synaptic transmission and plasticity (Cen et al., 2018, Chao et al., 2006) (Diaz-Nido et al., 1994), (Nunez de Villavicencio-Diaz et al., 2017, Sanchez-Ponce et al., 2011).

Interestingly, a number of previous reports described a potential connection between CK2 and prion diseases. For example, a study described an alteration of CK2 subunits in brains of experimental models of prion diseases, as well as in two individuals affected by familiar CJD and FFI (Chen et al., 2008b). Two additional studies reported the ability of CK2 to bind and phosphorylate PrP^C on serine 154 (Chen et al., 2008a), (Meggio et al., 2000), (Negro et al., 2000). As a possible effect of such interaction, PrP^C was also shown to increase the CK2-dependent phosphorylation of other physiological substrates (Meggio et al., 2000). The biological significance of this interaction has been investigated by Wang and colleagues in 2013, who proved that PrP-CK2 complexes affect microtubule dynamics and stability (Wang et al., 2013). Intriguingly, in a recent work, it has been observed that PrP overexpression induces a significant inhibition of fast axonal transport (FAT) via a CK2 mediated mechanism. Hyper-activated CK2 phosphorylates kinesin, a motor protein responsible for vesicular cargoes movement along the microtubules, causing the release of vesicular cargoes from the cytoskeleton (Zamponi et al., 2017). Collectively, these data suggest the existence of a cross-talk between PrP^C function and CK2-dependent vesicular dynamics at the cell membrane. This conclusion directly connects to our own observation regarding the ability of a novel CK2

inhibitor to suppress the toxicity of a mutant PrP in cell cultures, suggesting that further investigation of the CK2-PrP^C pathway may lead to the identification of novel pharmacological targets for prion diseases.

In summary, this work presents a unique experimental paradigm for the screening of compounds capable of altering PrP^C localization, potentially suitable for more extensive high throughput screening campaigns, allowing to test much bigger chemical libraries. Our new tool also validates the rationale of tackling prion replication and toxicity by removing PrP^C from the cell surface and, once further optimized, would be likely leading to the identification of additional molecules capable of inducing the removal of PrP^C from the cell surface.

We identified HM as a potential anti-prion compound and showed that this molecule could inhibit prion replication and mutant PrP toxicity in cells. Interestingly, molecules acting by re-localizing PrP^C from the cell surface could potentially be combined with classical anti-prion compounds directly targeting the production or stability of PrP^{Sc}. Therefore, our results lay the groundwork for the identification of novel chemical scaffolds that may synergize with existing strategies to define new combinatorial therapies for prion diseases.

CHAPTER 5. RESULTS PART II: TARGETING PRPC TOXICITY

5.1 Specific Aims and Rationale

PrP^C plays two distinct roles in prion diseases, by supporting the PrP^{Sc}-templated propagation and by mediating its neurotoxic effects. The role as toxicity-transducing receptor has also been shown in several other neurodegenerative conditions, where PrP^C binds different misfolded protein isoforms, including oligomeric assemblies of the amyloid β peptide and the protein α -synuclein, mediating a downstream neurotoxic cascade (Ferreira et al., 2017), (Lauren et al., 2009), (Resenberger et al., 2011). In the context of prion diseases it has been shown that PrP molecules carrying artificial deletions (residues 95-105, called Δ CR mutant) and disease-associated point mutations (P102L, G114V and G131V) in the CR region, induce unusual ionic currents once expressed in cells (Solomon et al., 2010), (Solomon et al., 2012). Cells expressing Δ CR PrP mutants were also shown to be hypersensitive to several cationic drugs including aminoglycosides and phleomycin analogues, which were used to establish DBCA as a tool to identify compounds capable of suppressing mutant PrP toxicity (Massignan et al., 2011). Indeed, two previous studies capitalized on an optimized and scaled-up format of the DBCA to screen large libraries of commercially available compounds and identified several SMs suppressing mutant PrP toxicity in cell cultures (Imberdis et al., 2016), (Mercer and Harris, 2019). Unfortunately, the identified molecules require further steps of chemical rearrangement to be suitable drug candidates.

5.2 Experimental Workflow

In this study, we optimized one of the compounds that emerged from DBCA-based screenings, referred to as LD24, and characterized the pharmacological properties of its improved derivatives in different experimental contexts. At this aim we developed an original synthetic scheme and carried out iterative chemical optimization cycles to generate a series of rearranged SMs (Fig. 1.1). The first set of LD24 derivatives was screened by DBCA (Fig. 1.2), then the best performing molecules were evaluated in a dose-response fashion with the same experimental paradigm (Fig. 1.3) to select the one with the lowest EC50. The selected

molecule has then been validated considering its direct binding to recombinant PrP^C with DMR, the alteration of PrP^C synthesis by Western blotting, the perturbation of PrP^C localization, using cells stably expressing an EGFP-PrP^C construct and the effect on prion propagation with the scrapie cell assay (Fig. 1.3). After the validation step the SM was then tested in a set of secondary assays, evaluating its efficacy against PrP^C- induced toxicity, by measuring the inhibition of mutant PrP currents in whole-cell patch-clamp recordings and the preservation of dendritic spines in A β -treated primary neurons (Fig. 1.4). After a second chemical rearrangement aimed at improving the pharmacokinetic properties and the efficacy (Fig 1.6), the best performing molecule was tested for its rescue of PrP^{Sc}-delivered synaptotoxicity in mouse brain slices (Fig. 1.7).

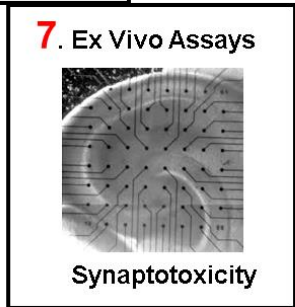
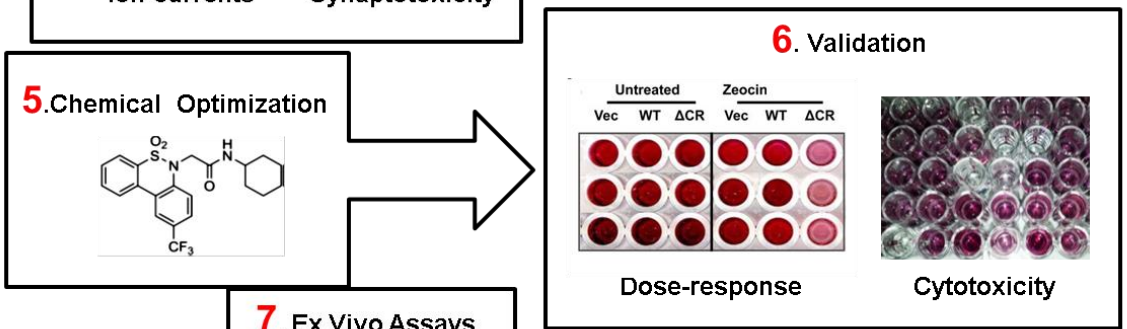
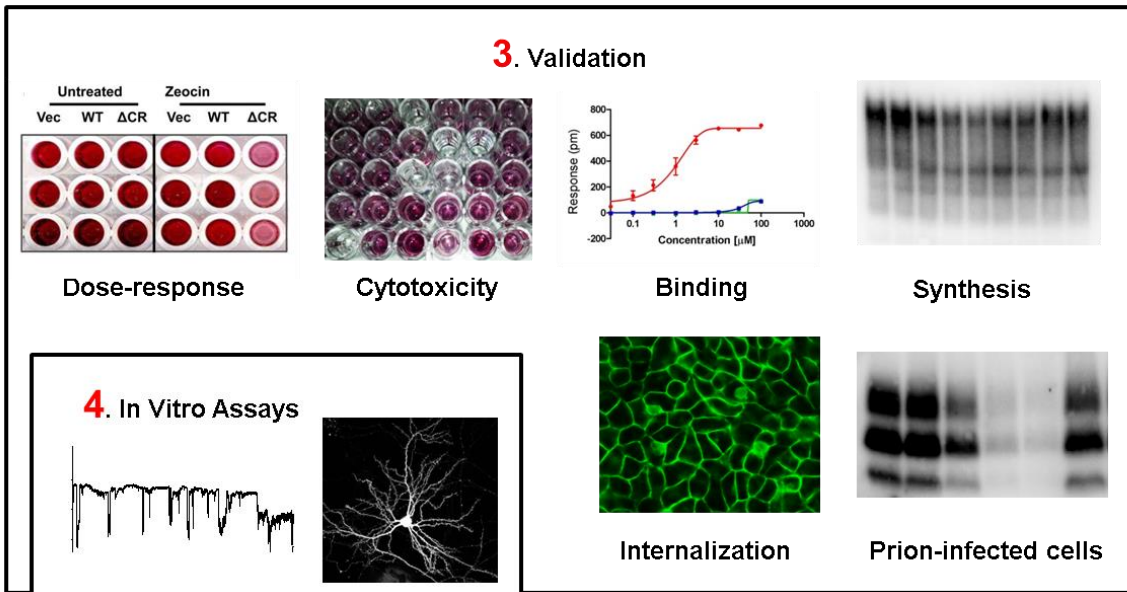
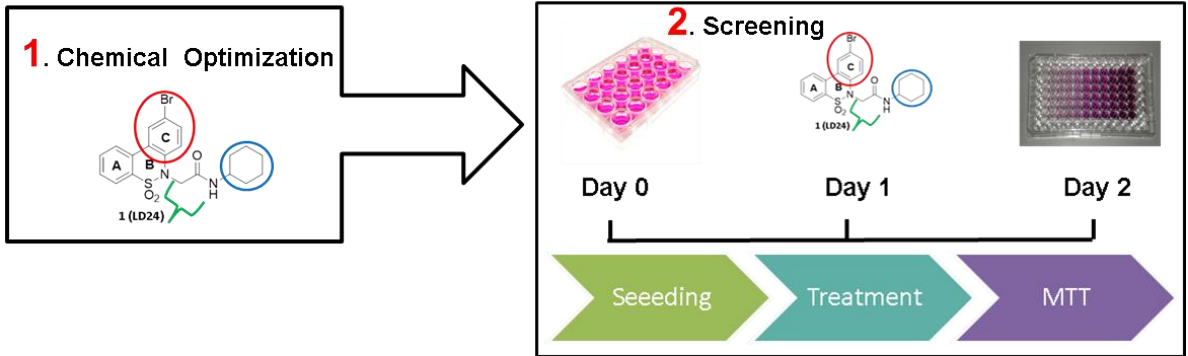


Figure 1: Workflow of the Study. 1. LD24 has been chemically optimized via substitutions in three regions. 2. The derivative compounds have then been screened with DBCA in a single concentration. 3. The best performing SMs have been studied with a series of different assays: dose-response DBCA and cytotoxicity have been performed to obtain IC₅₀ and LD₅₀ for each molecule. Then, the hit with the highest IC₅₀ has then been validated considering its binding to PrP^C, the effect on PrP^C synthesis, the internalization of PrP^C and the effect on prion accumulation in infected cells. 4. The best derivative has been tested in two *in vitro* models of prion toxicity: the rescue of the ionic currents induced by Δ CR mutant and the preservation of synapses after A β neurotoxic stimulation. 5. The candidate molecule underwent a second round of chemical optimization and 6. The derivatives have been tested again with dose-response DBCA and cytotoxicity to select the most powerful one. 7. The best performing second generation derivative has finally been tested in an *ex vivo* model of prion-induced synaptotoxicity.

5.3 Characterization of LD24

For this study we focused on LD24 [dibenzo [3,4][c,e]thiazine 5,5-dioxide] (Fig. 2a), which possesses a drug-like scaffold suitable for chemical optimization. Consistent with previous data, we confirmed that LD24 is capable of inhibiting mutant PrP toxicity by DBCA in the low micromolar range (IC₅₀ = 1.11 μ M; Fig. 2b) in almost complete absence of toxicity, as evaluated by MTT assay (lethal dose at 50%, LD₅₀ > 100 μ M; Fig. 2c). Importantly, the compound was not active against RML prions in chronically infected cells, confirming that this molecule seems to target mutant PrP-mediated toxicity but not prion replication (Fig. 2d).

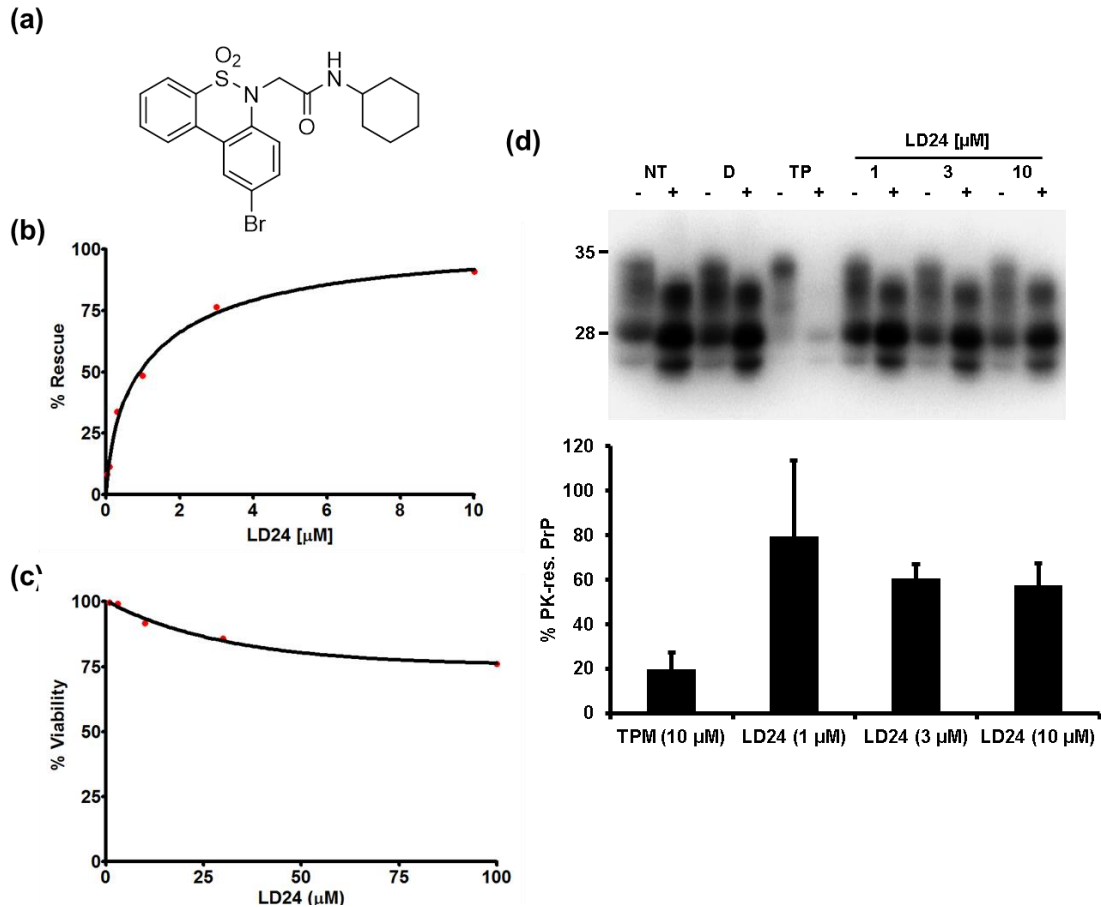


Figure 2: Characterization of LD24. (a) chemical structure of LD24. (b) DBCA % Rescue of LD24 evaluated by MTT on HEK cells treated with five serial dilutions (0.1 – 0.3 – 1 – 3 – 10 μM) of the SM and Zeocin for 48 h. Data were fitted by a 4PL non-linear regression model. (c) % Viability evaluated by MTT on HEK cells stably expressing DCR PrP treated with eight concentrations (0.03 - 0.1 – 0.3 – 1 – 3 – 10 – 30 – 100 μM) of LD24 for 48 h. Data were fitted by a 4PL non-linear regression model (d) Western blot and relative histogram of PrP signal in N2a.3 cells stably infected with RML prion strain treated with LD24 (1, 3, 10 μM), TP (10 μM) or vehicle (DMSO, volume equivalent). Samples have been incubated in absence (-) or presence (+) of PK. Histogram shows the densitometric quantification of PrP (D18 antibody) in PK-treated samples normalized on total proteins level in the respective PK-lane. N=3.

5.4 Five LD24 Derivatives Show Improved Rescuing Activity

In the first round of exploration of the LD24 chemical scaffold, we designed and synthesized 36 derivatives covering three chemical regions of the compound (Fig. 3a) with the dual goal of improving potency and acquiring structure-activity relationship (SAR) information. The medicinal chemistry optimization process was thus pursued following two different approaches by: i) looking for strictly analogues of LD24 commercially available and by selecting a small library of chemically diverse compounds representative of the whole set of available molecules from vendors, ii) planning and realizing chemical modifications uncovered by molecules available from vendors and exploiting traditional a medicinal chemistry approach. In particular, three chemical regions of LD24 were explored such as i) the C ring by inserting differently positioned substituents, ii) the N—6 amide linker by varying its nature, iii) the nature of the amide substituent by replacing the cyclohexyl moiety with different groups. The 36 derivatives obtained were then screened by DBCA at a single concentration of 1 μ M (Fig. 3b). HEK293 stably expressing PrP Δ CR construct were treated in the presence of antibiotic Zeocin and each LD24 derivative for 48 h. Cell viability was then evaluated with an MTT assay and the rescuing activity of the derivatives was calculated as the percentage over LD24 rescue. We observed that six molecules: SM228, SM229, SM231, SM336, SM337 and SM339 induced a relevant increase of rescue compared to LD24. Amongst them, we decided to select for the further steps of the study the SMs inducing at least a 20% improvement of rescuing activity, namely SM228, SM229 and SM231.

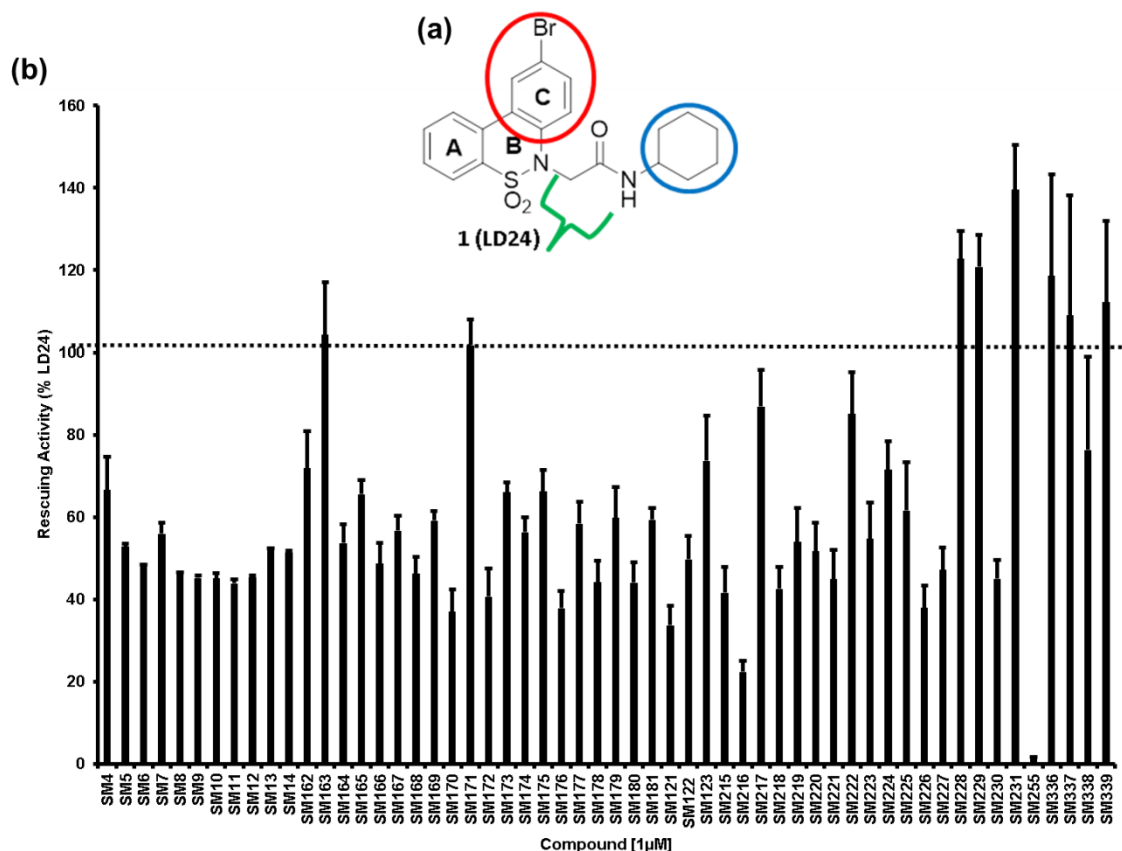


Figure 3: DBCA Screening of LD24 Derivatives. (a) Chemical structure of LD24. The optimized regions are marked in red (C ring), green (the N—6 amide linker) and blue (amide substituent). (b) Histogram showing the % Rescuing Activity over LD24 of each derivative, measured with an MTT on HEK293 Δ CR cells treated with each SM (1 μ M) or LD24 in presence of Zeocin for 48 h. Rescue for each SM was calculated using the following equation: $R = (T-Z)/(U-Z)$ (R: rescuing effect; T: cell viability in compound-treated samples; Z: cell viability in zeocin-treated samples; U: cell viability in untreated samples) and the normalized on LD24 rescue (dashed line).

5.5 Three LD24 Derivatives Showed an Improved IC50

The three potent derivatives identified in the screening, SM228, SM229 and SM231 (Fig. 4a, d, g), were then tested with the same experimental paradigm in a dose-response assay. As depicted in Figure 4, all the three molecules showed an improved activity by DBCA in the high nanomolar range (Fig. 4b, e, h). However, the SMs showed also a higher cytotoxicity when administered to HEK293 Δ CR cells as compared to the parent compound (Fig. 4c, f, i, and Fig. 2c). Given its higher efficacy in rescuing PrP-driven toxicity we decided to select SM231 for the further validation steps.

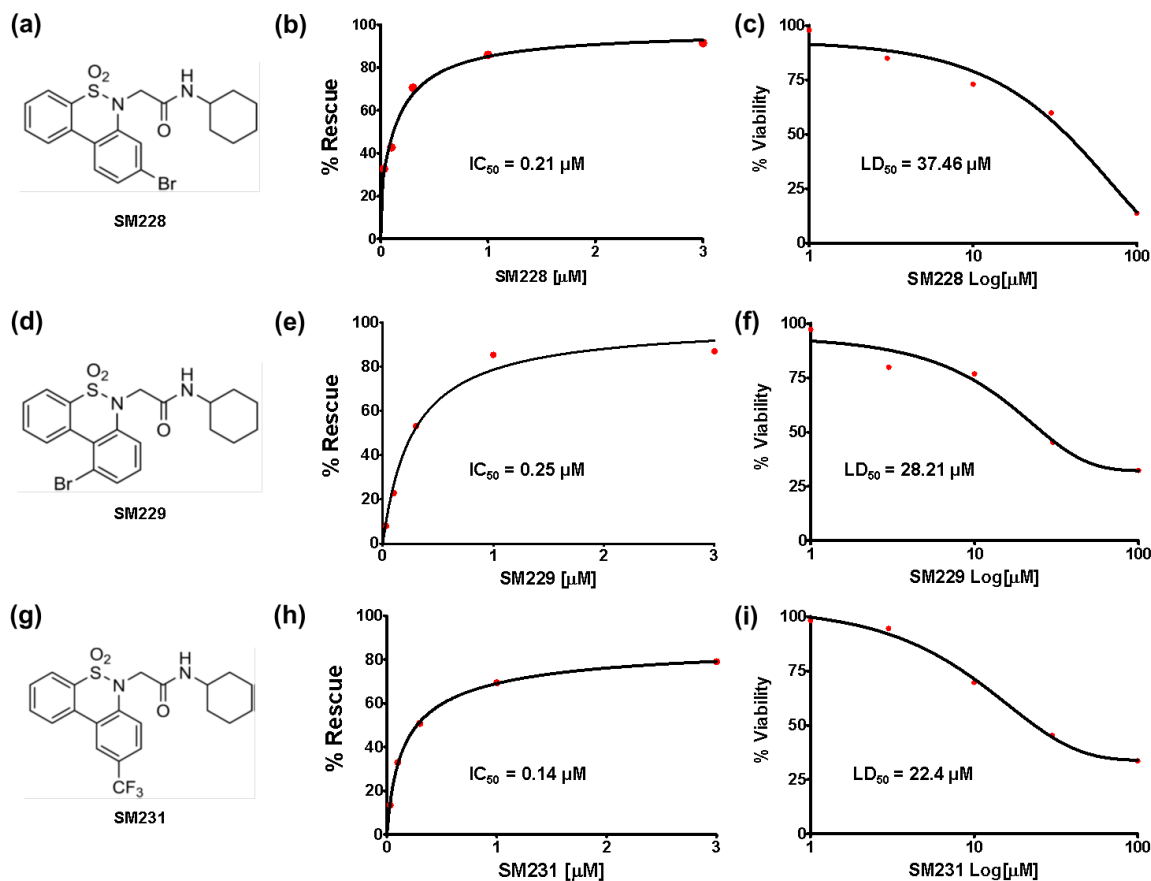


Figure 4: Dose-Response Assay of the Primary Hits. (a, d, g) Chemical structure of SM228, SM229 and SM231 respectively. (b, e, h) Graphs illustrate the IC₅₀ obtained after the quantification of the dose-dependent rescuing effect of each molecule during DBCA, measured with an MTT assay. Molecules have been administered at different concentrations (0.03 – 0.1 – 0.3 – 1 – 3 μM) in the presence of Zeocin for 48 h. Mean values are expressed as the percentage of cell viability rescue, using the following equation: $R = (T-Z)/(U-Z)$ (R: rescuing effect; T: cell viability in compound-treated samples; Z: cell viability in zeocin-treated samples; U: cell viability in untreated samples). Data were fitted by a 4PL non-linear regression model. N=4. (c, f, i) Graphs show the LD₅₀ obtained after the quantification of cell viability in HEK293 cells stably expressing ΔCR PrP upon incubation with the SMs at different concentrations (1 – 3 – 10 – 30 – 100 μM), detected by MTT assay after 48 h. Graphs show the quantification of at least 4 independent experiments. Data were normalized over vehicle (DMSO, corresponding volume) controls, and fitted by a 4PL non-linear regression model.

5.6 SM231 Does not Act by Directly Binding to PrP^C

In light of the improved ability of the newly identified compound to suppress the toxicity of mutant PrP by DBCA, we sought to test the hypothesis that this molecule act by directly targeting PrP^C. First, we evaluated the direct binding of SM231 to mouse recombinant full-length PrP^C by DMR. As controls, we used TP and CPZ (Fig. 5, blue and green lines

respectively), two compounds previously reported to show a high and low affinity for PrP^C, respectively (Massignan et al., 2016), (Stincardini et al., 2017). As shown in Figure 5 no interaction between SM231 and recPrP^C was observed (Fig. 5, red line), even at the highest concentration tested (1 mM).

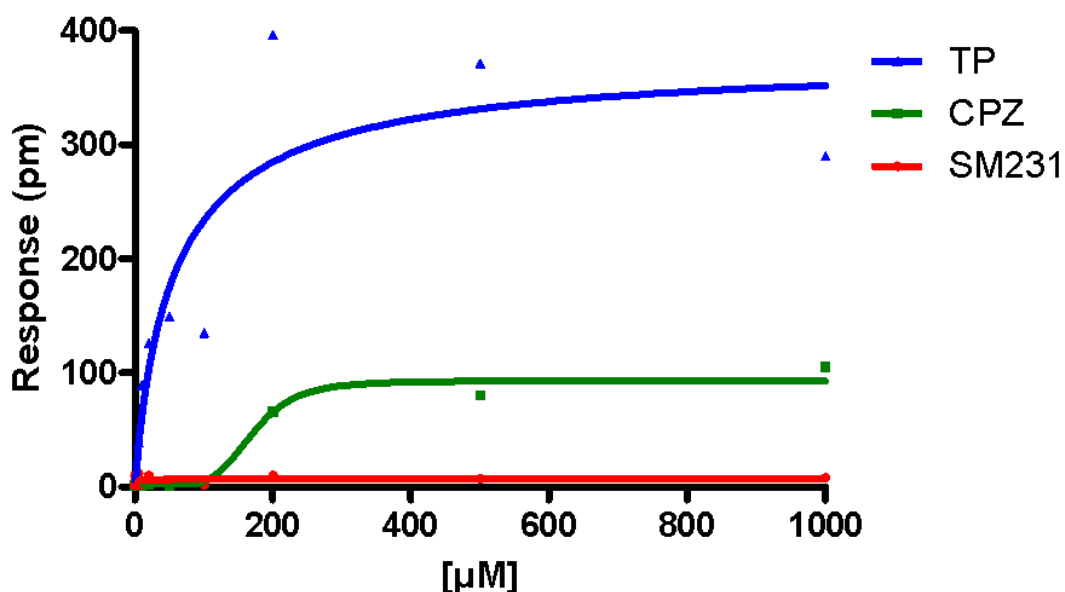


Figure 5: DMR-Based Detection of Binding to PrPC. Different concentrations of SM231, TP and CPZ were added to label-free microplate well surfaces on which full-length, human recPrP^C have previously been immobilized. Measurements were performed before (baseline) and after adding each compound. The output signal for each well was obtained by subtracting the signal of the protein-coated reference area to the signal of the uncoated area. The final response (pm) was obtained by subtracting the baseline output to the average of three final output signals. TP (blue dots) and CPZ (green dots) were used as positive controls. All signals were fitted (continuous lines) to a sigmoidal function using a 4PL non-linear regression model.

5.7 SM231 Does not Alter PrPC Expression

Next, we tested whether SM231 could act by altering PrP^C expression. HEK293 cells stably expressing WT PrP^C were treated with SM231 at different concentrations (0.03-10 μM). Total PrP^C levels were then evaluated by Western blotting in whole-cell lysates (Fig. 6a). As shown in the histogram in Figure 6b no difference in PrP^C expression was found upon treatment with SM231, suggesting that the rescue of PrP-induced toxicity might not be exerted by a reduction in its global levels.

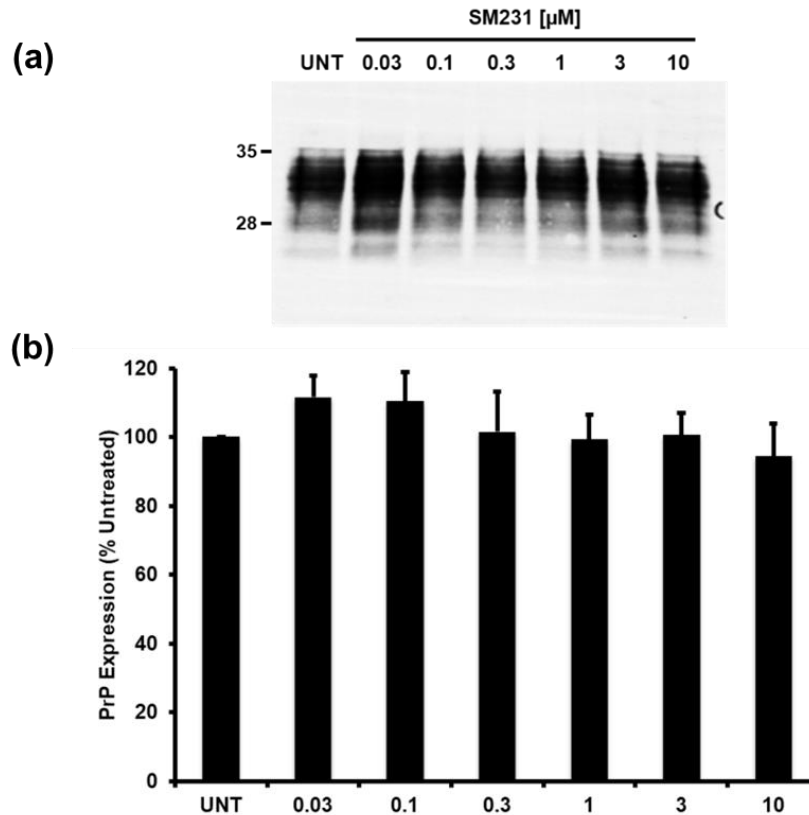


Figure 6: Evaluation of PrP^C Levels by Western Blotting. (a) Blot represents total PrP^C molecules in HEK293 cells stably expressing WT PrP and exposed to different concentrations of SM231 (as indicated), detected by probing membrane blots with an anti-PrP antibody (D18). (b) The graph shows the quantification of 3 independent cell culture preparations. Data were acquired by densitometric analysis of PrP bands, and expressed as % of PrP expression over untreated controls. Statistical differences were estimated by one-way ANOVA, Dunnet post-hoc test.

5.8 SM231 Does not Change EGFP-PrP^C Localization

Finally, we hypothesized that the compound might promote the re-localization of PrP^C from the cell surface, a mechanism of action recently described for CPZ, (Stincardini et al., 2017) and accounting for a possible reduction of Zeocin influx during DBCA. HEK293 cells stably expressing an EGFP-PrP^C were treated with different concentrations of SM231 (1-3-10 μM), CPZ (10 μM and 30 μM) or vehicle control (DMSO 0.2%), and PrP^C localization at the cell surface was monitored by Operetta plate reader (Perkin Elmer) (Fig. 7). Results showed that as expected, in the vehicle-treated cells EGFP-PrP^C has a prevalent membrane localization (Fig. 7a), forming the usual honeycomb pattern already observed (see Chapter 1). Consistently with what previously published (Stincardini et al., 2017), CPZ induced a dose-

dependent re-localization of EGFP-PrP^C from the cell surface to intracellular compartments (Fig. 7b, c). Conversely, no changes were detected in cells treated with SM231, where the pattern of localization of EGFP-PrP^C appears comparable to vehicle controls for all the concentrations tested (Fig. 7d, e and f), suggesting that the molecule does not act by reducing PrP^C membrane expression.

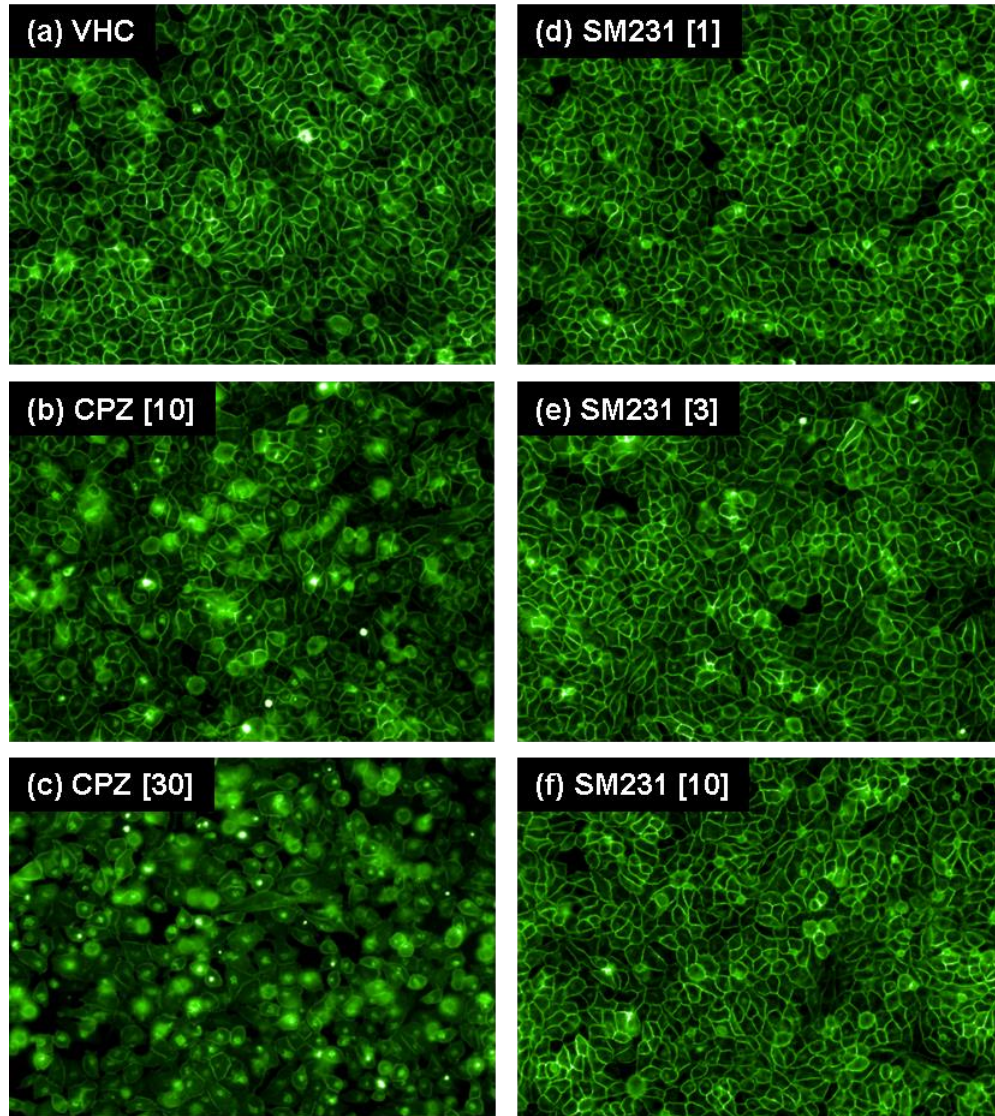


Figure 7: Re-localization of EGFP-PrP^C. Representative images show the re-localization of EGFP-PrP^C upon treatment for 24 h with (a) vehicle (VHC, DMSO 0.2%), (b, c) CPZ 10 or 30 μM and (d, f) SM231 1, 3, 10 μM respectively. Images, from three independent cell culture preparations, were acquired with Operetta Imaging System.

5.9 SM231 Fails to Suppress Prion Replication in Cells

The original study describing the identification of LD24 also reported that the molecule is ineffective against prion replication in cell cultures. Since our derivative SM231 is more active than LD24 by at least an order of magnitude, we sought to test its potential anti-prion effects in N2a cells chronically infected with two different prion strains (RML or 22L). Cells were exposed for 72 h to different concentrations of SM231 (0.03-50 μM) and PrP^{Sc} levels were evaluated by quantifying the amount of proteinase K (PK)-resistant PrP by Western blotting. TP (50 μM) or D (DMSO, volume equivalent) were used as positive or negative controls, respectively. We observed a reduction of RML prions upon exposure to SM231 only at the highest doses (30 and 50 μM , Fig. 8a, b), which were two orders of magnitude higher than those at which the compound inhibits mutant PrP toxicity. Moreover, the compound showed detectable toxicity at the same concentrations (Fig. 4f). Nearly identical results were obtained in 22L-infected N2a cells (Fig 8c, d), suggesting that SM231, like its parent compound LD24 is not able to efficiently counteract prion conversion.

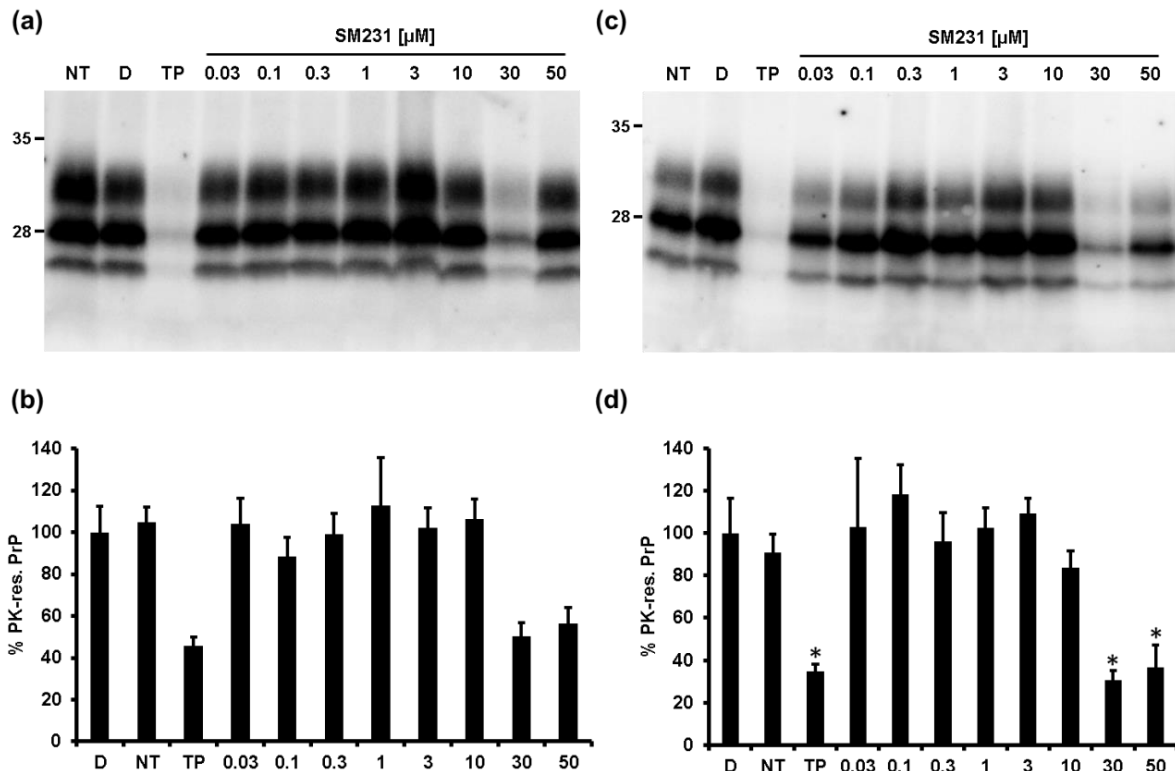


Figure 8: Test of Anti-Prion Activity in Cells Infected with 22L and RML Prion Strains. Representative blots of PK-resistant PrP molecules in N2a.3 cells chronically infected with the RML (a) or 22L (c) mouse prion strains exposed to different concentrations of SM231 (as indicated) or TP (50

μM). Signals were detected by probing membrane blots with an anti-PrP antibody (D18). **(b, d)** Graphs show the quantification of at least 4 independent cell culture preparations. Data were normalized over D (DMSO, volume equivalent) controls, and analyzed with a one-way ANOVA, Dunnet post-hoc test, p values are: $* < 0.05$.

5.10 SM231 Suppresses the Channel Activity of Mutant PrP

All the compounds previously identified by using the DBCA, including LD24, are known to inhibit cellular hypersensitivity to cationic antibiotics, but their rescuing activity of mutant PrP-induced currents has never been directly tested. In order to address this gap, we relied on patch clamping techniques. First, we aimed at recapitulating previous data and recorded whole-cell currents from HEK293 cells stably expressing either WT or ΔCR PrP molecules. Consistent with previous observations, in ΔCR PrP-expressing cells held at -80 mV we detected inward currents that spontaneously fluctuated over a time of seconds to minutes, reaching amplitudes of ~ 2000 pA (Solomon et al., 2012). As expected, these currents were completely absent in WT PrP-expressing cells (Fig. 9a, b). Next, we repeated the experiments on ΔCR PrP-expressing cells pre-incubated with SM231 (3 or $10 \mu\text{M}$) or vehicle (DMSO, volume equivalent) control. We found that the SM almost completely silenced cationic currents at both concentrations tested, which were instead unaltered in the vehicle control (Fig. 9c, d). These results demonstrated that SM231 suppresses both mutant PrP-dependent antibiotic hypersensitivity and channel activity.

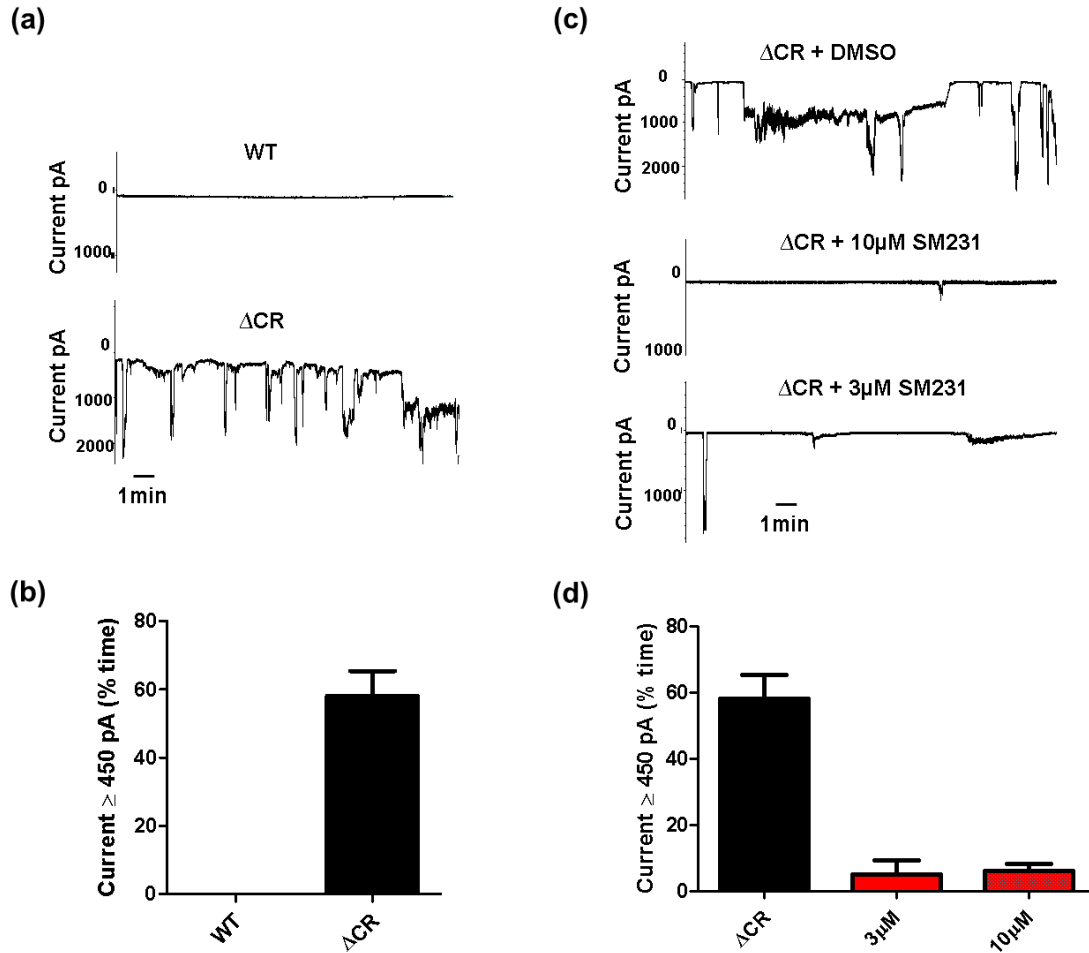


Figure 9: Measurement of the Ionic Currents by Whole-Cell Patch Clamp. (a) Representation of a 10 minutes whole-cell patch-clamp recording registered from HEK293 cells expressing either WT or Δ CR PrP, at a holding potential of -80 mV. (b) Inward currents recorded from WT or Δ CR PrP HEK293 cells were plotted as the percentage of total time the cells exhibited currents ≥ 450 pA (mean \pm S.E.M., $n \geq 5$ cells), at a holding potential of -80 mV. Statistically-significant differences (*) between WT or Δ CR were estimated by Student t-test (c) Representation of a 10 minutes whole-cell patch-clamp recording registered from HEK293 cells expressing Δ CR PrP, treated with vehicle (DMSO equal volume) or SM231 at different concentrations (3 and 10 μ M), at a holding potential of -80 mV. (d) Histogram depicts the inward currents recorded from Δ CR PrP HEK293 cells treated with vehicle (Δ CR, black column) or SM231 (3 and 10 μ M, red columns), plotted as the percentage of total time the cells exhibited currents ≥ 450 pA (mean \pm S.E.M., $n \geq 5$ cells), at a holding potential of -80 mV. Statistically-significant differences (*) were estimated by Student t-test, p values are: $* < 0.05$.

5.11 SM231 Inhibits the PrP^C-Dependent Synaptotoxicity of A β Oligomers

Recent studies identified a role for PrP^C into the toxicity of various misfolded oligomers of diseases-associated proteins, such as the amyloid β , whose accumulation underlines the cognitive decline occurring in AC (Lauren et al., 2009), (Resenberger et al., 2011). The interaction between PrP^C and A β oligomers unleashes a rapid, toxic signaling pathway involving mGluR5, the activation of the tyrosine kinase Fyn, and the phosphorylation of the NR2B subunit of NMDA receptor, ultimately producing dysregulation of receptor function, excitotoxicity and dendritic spines retraction (Um et al., 2013). In order to evaluate the effect of SM231 on A β -induced activation of Fyn, we exposed primary hippocampal neurons to A β oligomers for 20 minutes. We confirmed evaluating by Western blot the Triton-insoluble fractions, that the oligomers induce the rapid phosphorylation of the Fyn kinase (Fig. 10). Consistent with previous observations, this effect was prevented by treatment with a PrP^C-directed compound as TP (Massignan et al., 2016). Importantly, co-incubation with SM231 (3 μ M) completely abrogated A β effects, restoring Fyn phosphorylation to normal levels (Fig. 10).

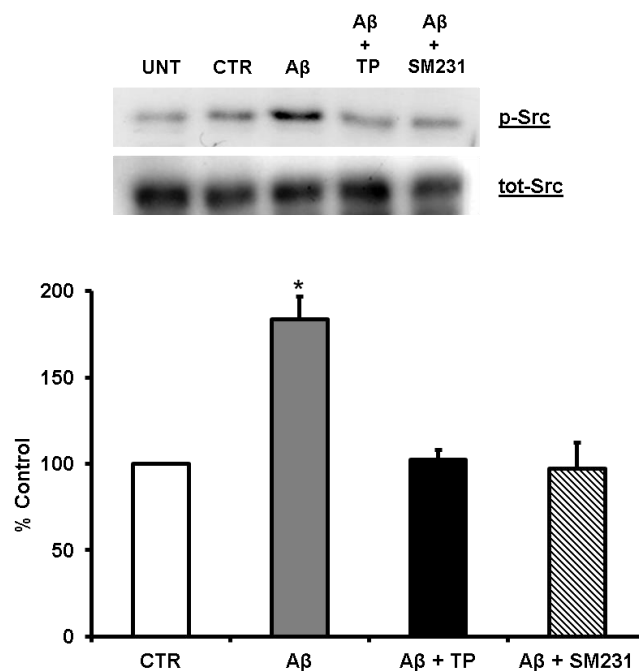


Figure 10: Evaluation of the Activation of Fyn Pathway by Western Blotting. Representative blots and relative quantification of the phosphorylation of Fyn kinase upon treatment with A β oligomers. Primary hippocampal neurons (DIV12) pre-treated for 20 minutes with vehicle (DMSO, volume

*equivalent), TP or SM231 and exposed to A β oligomers (3 μ M, monomer equivalent concentration) for 20 minutes. Triton-insoluble fractions were analyzed by immunoblot with antibodies against phospho-SFK (Tyr 416) or total Fyn. Actin was used as loading control. The picture shows an example of a Western blot for p-Fyn and Fyn. The graph reports the quantification of 3 independent experiments. Values are expressed as the percentage of vehicle (VHC)-treated cells, normalized on the intensity of the corresponding Actin bands. *Statistical significance was estimated by one-way ANOVA, Tukey post-hoc test, p values are: * <0.05 .*

Next, we directly tested the ability of SM231 to block A β oligomer-dependent synaptotoxicity. Primary hippocampal neurons were incubated for 3 hours with A β oligomers (3 μ M). Consistent with previous reports, we observed a decrease of several post-synaptic markers (GluN2A and GluN2B NMDA receptor subunits, GluA1 and GluA2 AMPA receptor subunits and PSD-95), as evaluated by Western blot of the Triton-insoluble fractions (Fig. 11). As expected, these effects were rescued by treatment with TP. Importantly, co-incubation with SM231 (10 μ M) for 20 minutes significantly rescued the levels of all the post-synaptic markers. Importantly, once incubated alone, SM231 did not induce any variation in the post-synaptic markers. The level of a control protein (Actin) was not affected by either A β oligomers or SM231. These data show that SM231 suppresses the ability of A β oligomers to subvert the function of PrP^C and activate a neurotoxic signaling pathway.

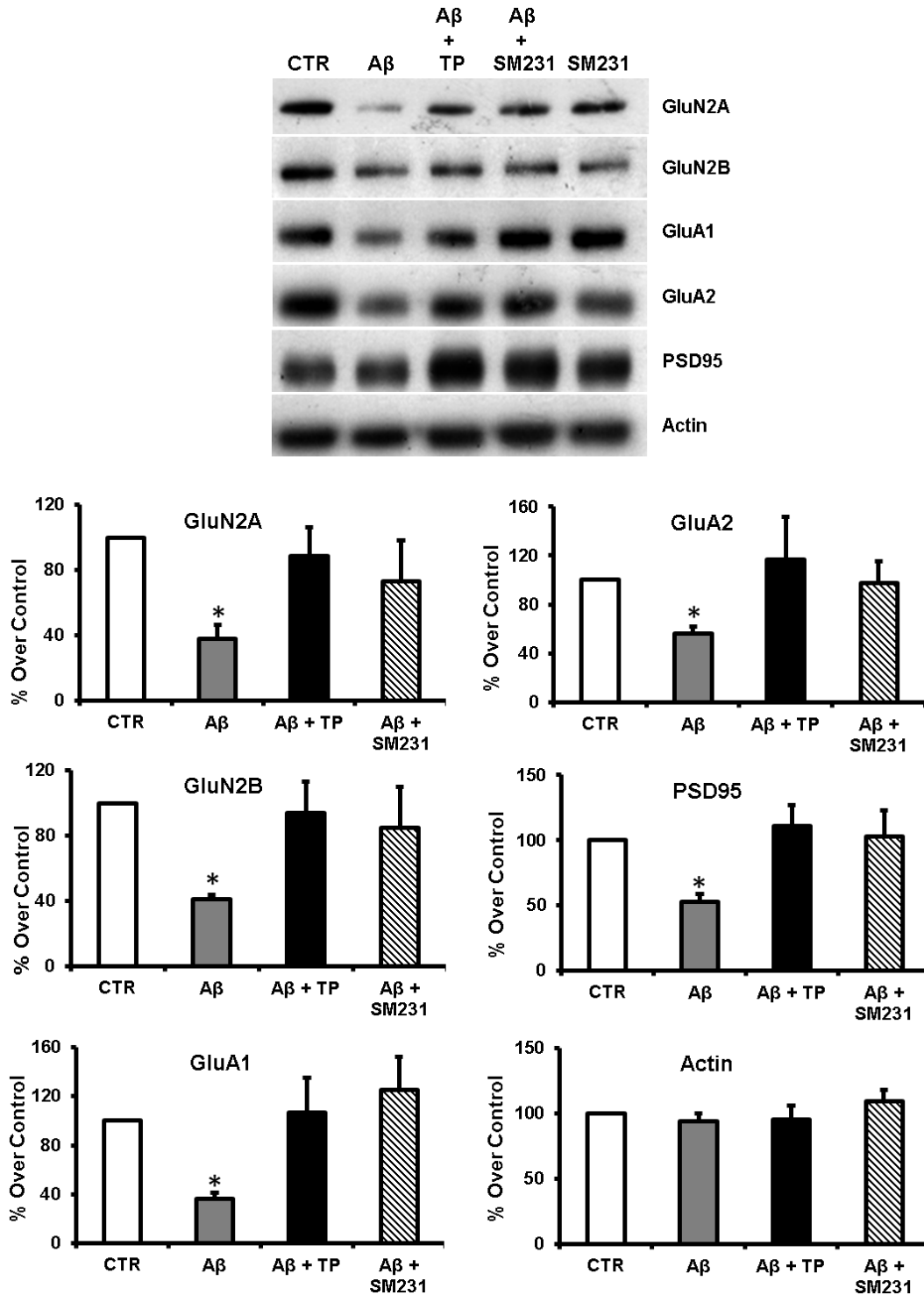


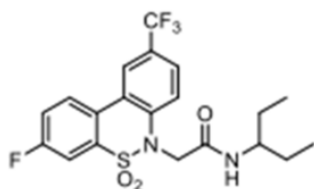
Figure 11: Evaluation of Synapse Loss by Western Blotting. Representative Western blots and relative quantifications of post-synaptic markers (*GluN2A*, *GluN2B*, *GluA1*, *GluA2*, *PSD95*) in Triton-insoluble fractions extracted from primary hippocampal neurons, pre-treated for 20 min with or without TP (10 μ M) or SM231 (10 μ M), and exposed for 3 h to A β oligomers (3 μ M) or vehicle (DMSO, volume equivalent). A β oligomers induced a loss of post-synaptic markers, which was significantly attenuated

by pre-incubation with TP or SM231. Quantification of 3 experiments is shown in the graph. Protein levels were normalized over Actin. Actin levels were not significantly affected by A β oligomer treatment. For each marker data were normalized over CTR and analyzed with one-way ANOVA, Tukey post-hoc test, p values are: * <0.05 .

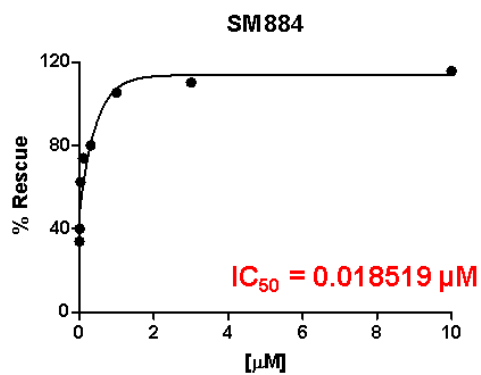
5.12 A Derivative of SM231 Shows Improved Rescuing Activity in DBCA

In light of the promising results obtained when we acutely tested SM231 on primary cultures, we sought to investigate the activity of the molecule using in a more complex model of PrP-driven neurodegeneration based on brain slices. However, in preliminary experiments (data not shown) SM231 showed low metabolic stability and poor solubility in an aqueous medium, two properties which hamper its use in brain slices. Also, the first round of chemical optimization increased the intrinsic cytotoxicity of the derivatives, as SM231 showed an LD50 roughly five times higher than LD24 (Fig. 2c and Fig. 4c). In order to overcome these issues, we carried out a further chemical optimization cycle, functionalizing positions predicted to be involved in the low metabolic stability of SM231. We obtained seven re-optimized SMs, named SM879, SM880, SM881, SM882, SM883, SM884 and SM885, which were again assayed by DBCA in a dose-response fashion. The majority of the derivatives did not exert a significant amelioration of cell viability rescue, and were therefore discarded (Fig. 12c). Only one of them, named SM884 (Fig. 12a), showed a highly improved rescuing activity as compared to SM231 with an IC50 in the low nanomolar range, suggesting that the potency of SM884 is roughly ten times higher than SM231 (Fig. 12b). For this reason, we decided to select SM884 for further prion toxicity assay.

(a)



(b)



(c)

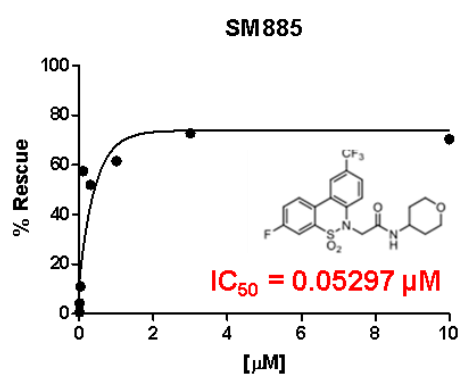
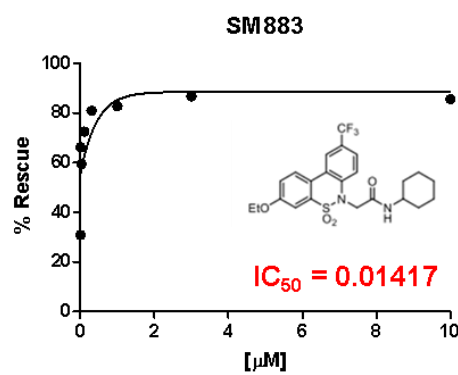
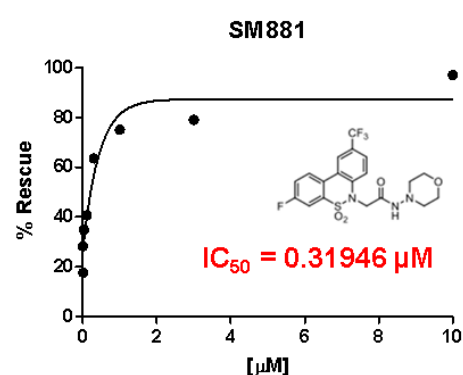
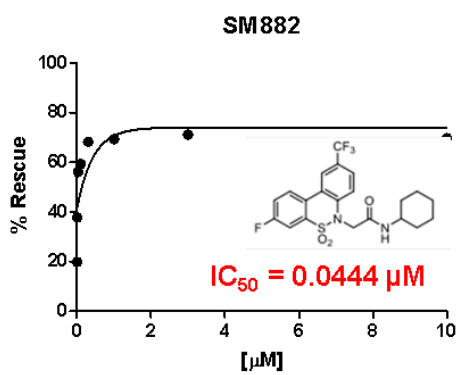
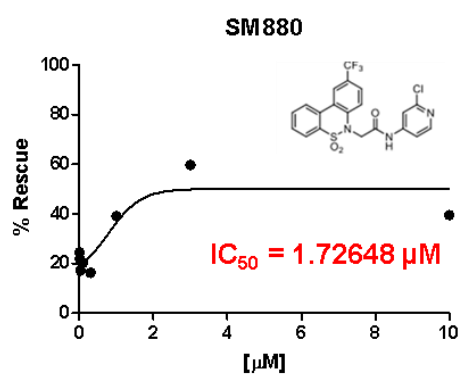
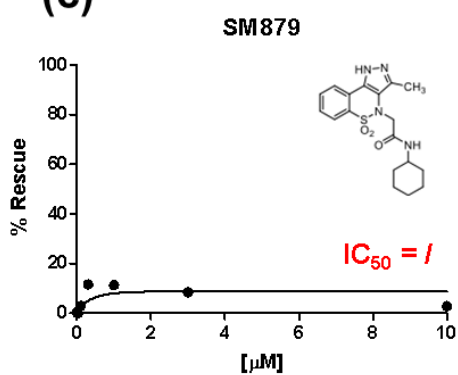
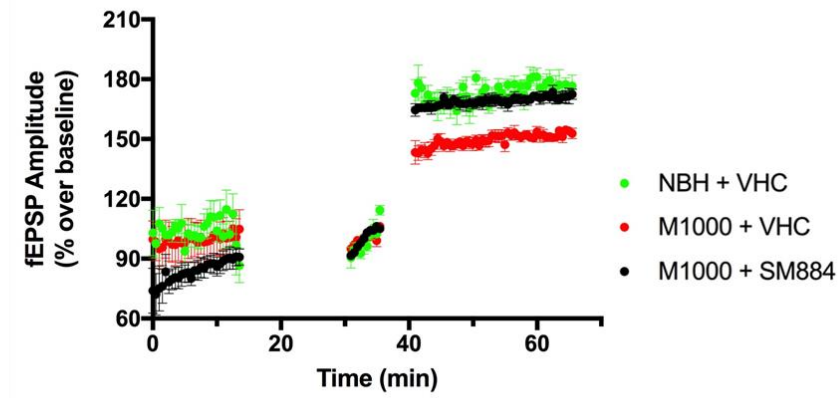


Figure 12: Evaluation of the second-generation derivatives by DBCA. (a) chemical structure of SM884. **(b, c)** Graphs illustrate the IC₅₀ obtained after the quantification of the dose-dependent rescuing effect of SM884, SM879, SM880, SM881, SM882, SM883 and SM885 measured with a DBCA after an MTT assay. SMs have been administered at different concentrations (0.003 – 0.01 – 0.03 – 0.1 – 0.3 – 1 – 3 – 10 μM) in presence of Zeocin. Mean values are expressed as the percentage of cell viability rescue, using the following equation: $R = (T-Z)/(U-Z)$ (R: rescuing effect; T: cell viability in compound-treated samples; Z: cell viability in zeocin-treated samples; U: cell viability in untreated samples). Data were fitted by a 4PL non-linear regression model. N=3,

5.13 SM884 Inhibits Acute Prion Toxicity in Brain Slices

Therefore, we tested whether SM884 is able to inhibit prion-induced toxicity a recently developed *ex vivo* model based on brain slices recording. In this assay, hippocampal CA1 region LTP has been exploited as a paradigm of prion-derived synaptotoxicity, acutely exposing mouse brain slices to prion-infected cells lysates, as recently published by Foliaki and colleagues (Foliaki et al., 2018). LTP in mouse hippocampal slices was measured with a Multi Electrode Array (MEA) system (Multi Channel Systems) stimulating the Shaffer collateral (CA3) region, while recording the response of the CA1 area. The fEPSP amplitude was recorded for a 35 minutes baseline, and LTP was induced with a tetanic stimulation and recorded for an additional 30 minutes (Fig. 13a). Prion synaptotoxicity was induced by incubating the slices for 5 minutes during the baseline with a 4% w/v lysate of MoRK13 cells chronically infected with M1000 mouse-adapted human prion strain. Lysate from mock moRK13 cells, “infected” with NBH, already reported as non-synaptotoxic (Fig. 13b, green dots, (Foliaki et al., 2018), was used as a negative control. In order to evaluate the potential rescuing activity of SM884, the molecule was continuously perfused during the whole recording. As expected, the administration of M1000 homogenate induced a consistent decrease of fEPSP amplitude compared to NBH-treated slices (Fig. 13a, red dotted recording), which resulted in a significant decrease of LTP (Fig. 13b, red dots), We found that SM884 administration at a concentration of 0.03 μM induces a significant rescue of LTP (Fig. 13b, black dots). These results were also entirely consistent with the estimated EC₅₀ of the compound in cells (0.018 μM), as evaluated by DBCA (Fig. 12b), and clearly showed that SM884 is capable of suppressing the synaptic impairment induced by prions in the low nanomolar concentration range.

(a)



(b)

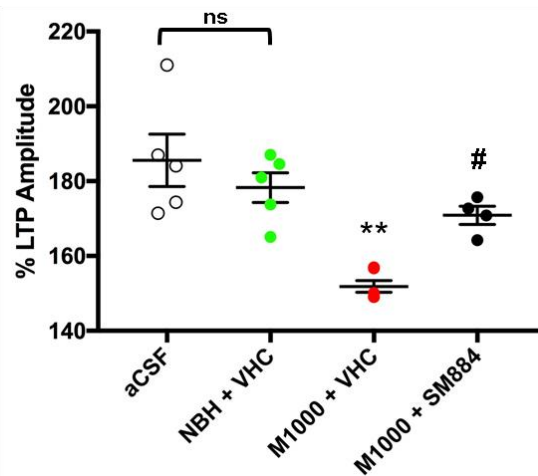


Figure 13: Evaluation of Acute Prion Toxicity with MEA. (a) Graph showing the average fEPSP amplitude recorded from hippocampal slices from 12-week old mice. Slices were superfused for 5 minutes with 4% w/v lysate of moRK13 cell line stably infected with brain homogenate from M1000 infected mice or NBH (mock-infected cell line treated with normal brain homogenate) during the baseline recording. Vehicle (DMSO, equal volume) or SM884 0.03 μ M were superfused during the entire duration of the recording. After the tetanic stimulation (3 trains, 100 Hz each) M1000-treated slices showed a consistent reduction of the fEPSP amplitude compared to NBH-treated controls. Conversely, treatment with SM884 completely prevented the fEPSP amplitude reduction induced by M1000 treatment. (b) Graph showing the % LTP amplitude calculated as the average fEPSP amplitude of the last 10 minutes of recording over the average fEPSP amplitude of the last five minutes before the tetanic stimulation. aCSF (white dots) represents the slices treated with superfusion medium only; NBH + VHC (green dots) represents the slices treated with 4% w/v NBH homogenate and superfused with vehicle alone; M1000 + VHC represents the slices treated with 4% w/v M1000 homogenate and superfused with vehicle alone while M1000+ SM884 represents the slices treated with 4% w/v NBH homogenate and superfused with SM884 0.03 μ M. LTP was analyzed with One-way ANOVA, Dunnet's post-hoc test. N=5.

5.13 Discussion

Multiple lines of evidence indicated that PrP^C is strictly involved both in prion infectivity and in prion toxicity. PrP^C sustains the propagation of PrP^{Sc} and mediates its neurotoxic effects. The role of neurotoxicity mediator has also been highlighted in other pathologies of the nervous system as AD and PD since PrP^C collects and transduces the signals of different misfolded proteins, including amyloid β and alpha-synuclein oligomers (Ferreira et al., 2017), (Lauren et al., 2009), (Resenberger et al., 2011). Previous structure-function analyses identified unusual ionic currents in cells expressing pathogenic PrP molecules carrying single point mutations or deletions in the central hydrophobic region of the protein, which were shown to be connected to the ability of PrP^C to transduce neurotoxic signals (Solomon et al., 2010), (Solomon et al., 2012). Collectively, these data support the rationale of designing compounds that directly or indirectly target PrP^C and test their therapeutic potentials in different experimental disease contexts. At this aim, the DBCA, based on the intrinsic toxicity of the artificial mutant Δ CR PrP, can recapitulate these properties and be used as an experimental paradigm capable of detecting the spontaneous toxicity of PrP mutants in cell culture (Massignan et al., 2011). Such phenotype was employed in several previous reports to study compounds active against mutant PrP toxicity (Imberdis et al., 2016), (Massignan et al., 2016), (Massignan et al., 2017).

A previous DBCA-based screening campaign identified one promising compound, LD24, reducing the cytotoxic effect of Δ CR mutant in the low micromolar range (Imberdis et al., 2016). Unfortunately, LD24 showed also a toxicity profile unsuitable for further studies. At this purpose in this work we developed an original synthetic scheme, carrying out iterative chemical optimization cycles to rearrange LD24 and generating a series of improved drug candidate derivatives. In the medicinal chemistry optimization process employed we modified three chemical regions of LD24, the C ring, the N—6 amide and the amide substituent. For each step of optimization, the newly generated compounds have been tested through DBCA to determine their EC50 as well as the LD50. The most promising compounds have then been studied in different models of prion toxicity with increasing biological complexity.

We have found that one first generation compound, SM231 and its second generation derivative SM884 potently inhibited mutant PrP currents and cytotoxicity in cell cultures, abrogated A β -induced, PrP^C-dependent, dendritic spines degeneration in primary neurons and rescued PrP^{Sc}-delivered synaptotoxicity in mouse brain slices.

From a technical standpoint, the reliability of our cyclic optimization scheme is clearly highlighted by the progressive reduction of the EC50 obtained after two steps of rearrangement. The EC50 in fact was decreased of a hundredfold, starting from an estimated concentration of 1 μM for LD24, to values in the low nanomolar range (14 nM) for SM884, as measured by DBCA.

Another advantage of our cyclic rearrangement protocol is that it allowed us to evaluate and correct in parallel also the toxicity of the derivate molecules. The first round of chemical optimization in fact increased the intrinsic cytotoxicity of the derivatives, as SM231 showed an LD50 roughly five times higher than LD24. With the second modification step we not only reduced of a tenfold the EC50, bringing it to the low nanomolar range, but we also increased the LD50 to a high micromolar value, expanding the potential therapeutic window of our candidate.

From the standpoint of SAR evaluation, our results provided several important observations about the LD4 scaffold. Chemical modifications made at the spacer region were not fruitful. Conversely, substitutions at the C ring improved potency, with the 9-CF3 derivative (SM231) being the most potent hit. Branched alkyl chains on the cyclohexyl group were not tolerated, whereas two substituted phenyl rings generated analogues with potency comparable to the reference compound. Collectively, these results provide important insights into the activity of this chemical scaffold, and directly suggest chemistry schemes to engineer even more optimized analogues

Surprisingly, none of the compounds generated showed effects against prion replication in cell cultures. The parent compound LD24 induced no relevant reduction of PrP^{Sc} in N2a cells infected with RML prion strain when tested up to 10 μM . Similarly, SM231 exerted no significant effect on scrapie propagation in both RML and 22L infected cells at the same concentrations. However, we observed a reduction in the PK resistant fraction at higher concentrations. It is unlikely though that this effect was specific, since its concentration range is completely inconsistent with the EC50 predicted by DBCA, which was roughly more than a hundred times lower (0.1 μM). It is to note that we also observed significant cytotoxicity associated with SM231 treatment at 30 and 50 μM . Thus it is difficult to entangle the anti-prion effect from a non-specific confounding factor related to the intrinsic toxicity of the molecule.

One of the major pitfalls of the chemical rearrangement - DBCA cycle is to iteratively select and improve molecules counteracting only Zeocin-induced toxicity in ΔCR expressing cells,

and thus not pharmacologically relevant. At this aim we designed several validation steps to monitor the efficacy of the compounds in other models of PrPC-induced toxicity. We observed that both SM231 and its derivative SM884 exerted significant neuroprotection in two models of neurotoxicity. In fact, in neuronal cultures treated with A β oligomers, the acute administration of SM321 efficiently inhibited the activation of Fyn pathway, preventing dendritic spines loss. Also, the administration of SM884 to brain slices tackled the inhibition of hippocampal LTP generated by the exposure to PrP^{Sc}. Importantly, the effective concentrations were consistent with those observed in the DBCA assay. These data confirm the paradigm of PrP^C as an oligomer collector, and highlight the importance of targeting PrP^C not just in the context of prion diseases but also in AD. It would be interesting to evaluate the efficacy of SM321 and SM884 in another model of PrP^C-mediated neurodegeneration, as PD, to have further confirmation of the oligomer receptor hypothesis and validate the relevance of our compounds in a broader spectrum of diseases.

A second exciting gap, worthy of being unraveled, is the mechanism of action of SM231 and SM884. For this purpose we have designed our experimental plan also including a panel of assays aimed at identifying the possible mode of action of the compound. Thanks to that, we can now exclude that our compounds inhibit PrP^C-mediated toxicity by directly acting on PrP^C. We have shown in fact that SM231 is not only incapable of binding recPrP, but also does not alter either its global levels or its membrane localization. Also, considering the latter two possible mechanisms, it is unlikely that they could represent a plausible explanation for the acute effect we observed in neural cultures and brain slices. Thus, a likely hypothesis is that our SMs act on a factor involved in the toxic cascade downstream of PrP^C. This hypothetical partner should be expressed and active either in HEK293 cells and in neural cultures/tissue. To date there is no comprehensive understanding of the pathways involved in PrP^C toxicity, as a variety of kinase cascades has been proposed. Furthermore, the mechanism by which Δ CR PrP^C promotes the passage of ions and cationic molecules is still a mystery. However, several lines of evidence clearly proved that the role of PrP^C in mediating A β oligomers toxicity relies on the interaction with mGluR5 metabotropic glutamate receptors, which in turn activate Fyn kinase cascade, promoting the phosphorylation of the NR2B subunit of NMDARs, leading to a synaptic rearrangement process (Um et al., 2012). Although the involvement of Fyn signaling has also been proposed to explain the physiological function of PrP^C (Chen et al., 2013), (Krebs et al., 2007), (Santuccione et al., 2005), its possible role in mediating the neurotoxic events triggering synapse and neural loss

in prion diseases and the involvement of mGluR5 receptor has not been proven so far, making it an appealing field of study.

In conclusion we have built here a novel paradigm to develop molecules blocking PrP^C toxicity, relying on cyclic chemical optimization steps coupled to the evaluation of the EC50 by DBCA. Thank to this approach we have found a candidate compound, SM231 and its derivative SM884, able to tackle the neurotoxic cascade mediated by PrP^C upon administration of scrapie and A β oligomers, making our SMs even more appealing drug candidates not just for prion diseases but also for many other amyloidopathies. These results altogether define new potential therapeutics against PrP^C-mediated toxicity and provide pharmacological support for the concept that prion replication and toxicity could be two distinct phenomena.

CHAPTER 6: CONCLUSIONS

Despite the unceasing efforts, all the clinical trials designed so far to test drugs tackling prion diseases led to no positive outcome. This lack of success was likely imputable to an intrinsic initial flaw. The majority of the compounds studied in the first decades after the discovery of prions were directed against PrP^{Sc} isoform and its aggregates, which were considered the only critical players for prion spreading and neurotoxicity (Barreca et al., 2018). This point of view radically changed in the last 15 years, when compelling evidence progressively uncovered the role of PrP^C isoform in disease pathology. PrP^C, in fact, is not just inert material for prion conversion, but actively mediates a variety of cytotoxic cascades not only in prion disease but also in other neurodegenerative conditions as AD and PD (Ferreira et al., 2017), (Lauren et al., 2009), (Mallucci et al., 2003), (Resenberger et al., 2011).

In an attempt to target PrP^C, in this work, I planned and conducted two different screening campaigns, by following two distinct therapeutic paradigms, either focusing on PrP^C localization or PrP^C toxicity.

In the first part, I designed an automated high-content screening platform to measure PrP^C re-localization from the cell membrane to the intracellular compartments, and I coupled it to a set of cellular and biochemical validation assays. With this new tool, I screened two repurposing-directed chemical libraries, and I found one candidate hit, HM. Treatment with HM induced substantial and specific re-localization of PrP^C, and also significantly inhibited prion replication and toxicity in different cellular assays. These results not only shed light a new anti-prion compound, never tested in prion diseases so far, but also set the basis for future, broader high-content screening campaigns, aimed at finding molecules re-localizing PrP^C. Collectively this evidence clearly outlines that the concept of altering PrP^C localization is a promising new pharmacological strategy worthy of being explored.

In the second part, I adopted a scheme of cyclic chemical rearrangement to optimize a candidate molecule, selected in a previous screening campaign (Imberdis et al., 2016), blocking the cytotoxicity of a mutant PrP^C. After each rearrangement step, I extensively validated the selected derivatives in different models of PrP^C-mediated toxicity with increasing biological complexity. I found that one molecule, SM231, and its derivative SM884, block PrP^C mediated toxicity not only in cellular and *ex vivo* models of prion disease but also in an *in vitro* model of AD in the low nanomolar range. Interestingly, even if tested at high concentrations, our molecules did not exert any relevant reduction of PrP^{Sc} conversion.

These results offer a new anti-prion compound, potentially suitable also for other neurodegenerative conditions involving PrP^C-mediated toxicity and set a solid proof of concept that it is possible to uncouple PrP^C toxicity from prion replication.

Collectively my results define new therapeutic strategies and related screening paradigms, highlighting two possible candidate chemical scaffolds which will be worthy of further investigation in the future.

ACKNOWLEDGEMENTS

I want to start by thanking my Tutor, Prof Biasini, and my Supervisor, Dr. Massignan, for the great opportunity and the constant trust they gave me. Second, but no less important, I want to thank Tania and Emiliano, who took care of me over these three years

Of course, I can't forget to mention all the people from my laboratory, with whom I shared a right amount of frustrating moments, but many other great ones too. A special thanks go particularly to Maria, Francesca, Giulia M and Giulia F.

I also want to acknowledge all the friends who made my stay here special: Caterina, Aurora, Jacopo, Marchetto, Seba, Marica, Nicola, Giorgione, Simone, Matteo (and even Ross), who have been the closest thing to a family, a quite unlikely one, but still a good one.

Not leaving the CIBIO-related world, I can't forget to mention also Peppe, Claudio, Michael, Martina, Claudia, Michela and Giovanni.

As these three years haven't just been about work, I want to express my gratefulness to all the other friends who made me survive in Trento when there wasn't much hope. The biggest thanks go especially to Francesca, and also to the other girls from V class, all my friends from Due Punti and of course my flatmates Betta, Luca and Nosiola.

Quickly moving down-under, I want to extend my gratitude to Prof. Steve Collins, whom I owe one of the most life-changing experiences I had and all the people from his laboratory. Of course, I can't forget to thank my Australian family and all my other mates from Melbourne, may we meet again.

Coming back to this hemisphere, I want to thank my friends from outside the valley, who have always been close despite the distance. Giulia, who has been looking after me since I can remember, and also Anastasia, Sara, Sem, Alain, Federico, Frank, Giorgio, Remo, Santra, Nicolò, Laretta, Laura, Chiara and Pietro.

Lastly, I want to thank my family, who always supported me in its own weird way. My auntie and my uncle, hoping to make you proud of me as you are now. My sister Lisa, who always brings me down to earth. My nephew Andrea who gave a new purpose to my work. My parents, who will always walk by my side towards the next chapter.

BIBLIOGRAPHY

- ABDULRAHMAN, B. A., ABDELAZIZ, D., THAPA, S., LU, L., JAIN, S., GILCH, S., PRONIUK, S., ZUKIWSKI, A. & SCHATZL, H. M. 2017. The celecoxib derivatives AR-12 and AR-14 induce autophagy and clear prion-infected cells from prions. *Sci Rep*, 7, 17565.
- ABSKHARON, R. N., GIACHIN, G., WOHLKONIG, A., SOROR, S. H., PARDON, E., LEGNAME, G. & STEYAERT, J. 2014. Probing the N-terminal beta-sheet conversion in the crystal structure of the human prion protein bound to a nanobody. *J Am Chem Soc*, 136, 937-44.
- ADJOU, K. T., DEMAIMAY, R., DESLYS, J. P., LASMEZAS, C. I., BERINGUE, V., DEMART, S., LAMOURY, F., SEMAN, M. & DORMONT, D. 1999. MS-8209, a water-soluble amphotericin B derivative, affects both scrapie agent replication and PrPres accumulation in Syrian hamster scrapie. *J Gen Virol*, 80 (Pt 4), 1079-85.
- ADJOU, K. T., DEMAIMAY, R., LASMEZAS, C., DESLYS, J. P., SEMAN, M. & DORMONT, D. 1995. MS-8209, a new amphotericin B derivative, provides enhanced efficacy in delaying hamster scrapie. *Antimicrob Agents Chemother*, 39, 2810-2.
- ADJOU, K. T., PRIVAT, N., DEMART, S., DESLYS, J. P., SEMAN, M., HAUW, J. J. & DORMONT, D. 2000. MS-8209, an amphotericin B analogue, delays the appearance of spongiosis, astrogliosis and PrPres accumulation in the brain of scrapie-infected hamsters. *J Comp Pathol*, 122, 3-8.
- ADLE-BIASSETTE, H., VERNEY, C., PEOC'H, K., DAUGE, M. C., RAZAVI, F., CHOUDAT, L., GRESSENS, P., BUDKA, H. & HENIN, D. 2006. Immunohistochemical expression of prion protein (PrPC) in the human forebrain during development. *J Neuropathol Exp Neurol*, 65, 698-706.
- AGOSTINHO, P. & OLIVEIRA, C. R. 2003. Involvement of calcineurin in the neurotoxic effects induced by amyloid-beta and prion peptides. *Eur J Neurosci*, 17, 1189-96.
- AGRIMI, U., NONNO, R., DELL'OMO, G., DI BARI, M. A., CONTE, M., CHIAPPINI, B., ESPOSITO, E., DI GUARDO, G., WINDL, O., VACCARI, G. & LIPP, H. P. 2008. Prion protein amino acid determinants of differential susceptibility and molecular feature of prion strains in mice and voles. *PLoS Pathog*, 4, e1000113.
- AGUIB, Y., HEISEKE, A., GILCH, S., RIEMER, C., BAIER, M., SCHATZL, H. M. & ERTMER, A. 2009. Autophagy induction by trehalose counteracts cellular prion infection. *Autophagy*, 5, 361-9.
- AGUZZI, A. & FALSIG, J. 2012. Prion propagation, toxicity and degradation. *Nat Neurosci*, 15, 936-9.
- AGUZZI, A., HEIKENWALDER, M. & POLYMERIDOU, M. 2007. Insights into prion strains and neurotoxicity. *Nat Rev Mol Cell Biol*, 8, 552-61.
- AHN, M., GHAEMMAGHAMI, S., HUANG, Y., PHUAN, P. W., MAY, B. C., GILES, K., DEARMOND, S. J. & PRUSINER, S. B. 2012. Pharmacokinetics of quinacrine efflux from mouse brain via the P-glycoprotein efflux transporter. *PLoS One*, 7, e39112.
- AIMI, T., SUZUKI, K., HOSHINO, T. & MIZUSHIMA, T. 2015. Dextran sulfate sodium inhibits amyloid-beta oligomer binding to cellular prion protein. *J Neurochem*, 134, 611-7.
- ALTMIPPEN, H. C., PROX, J., PUIG, B., KLUTH, M. A., BERNREUTHER, C., THURM, D., JORISSEN, E., PETROWITZ, B., BARTSCH, U., DE STROOPER, B., SAFTIG, P. & GLATZEL, M. 2011. Lack of a-disintegrin-and-metalloproteinase ADAM10 leads to intracellular accumulation and loss of shedding of the cellular prion protein in vivo. *Mol Neurodegener*, 6, 36.
- ALTMIPPEN, H. C., PUIG, B., DOHLER, F., THURM, D. K., FALKER, C., KRAEMANN, S. & GLATZEL, M. 2012. Proteolytic processing of the prion protein in health and disease. *Am J Neurodegener Dis*, 1, 15-31.

- AMIN, L., NGUYEN, X. T., ROLLE, I. G., D'ESTE, E., GIACHIN, G., TRAN, T. H., SERBEC, V. C., COJOC, D. & LEGNAME, G. 2016. Characterization of prion protein function by focal neurite stimulation. *J Cell Sci*, 129, 3878-3891.
- ANANTHARAM, V., KANTHASAMY, A., CHOI, C. J., MARTIN, D. P., LATCHOUMYCANDANE, C., RICHT, J. A. & KANTHASAMY, A. G. 2008. Opposing roles of prion protein in oxidative stress- and ER stress-induced apoptotic signaling. *Free Radic Biol Med*, 45, 1530-41.
- ANDREOLETTI, O., LACROUX, C., CHABERT, A., MONNEREAU, L., TABOURET, G., LANTIER, F., BERTHON, P., EYCHENNE, F., LAFOND-BENESTAD, S., ELSEN, J. M. & SCHELCHER, F. 2002. PrP(Sc) accumulation in placentas of ewes exposed to natural scrapie: influence of foetal PrP genotype and effect on ewe-to-lamb transmission. *J Gen Virol*, 83, 2607-16.
- ANTONYUK, S. V., TREVITT, C. R., STRANGE, R. W., JACKSON, G. S., SANGAR, D., BATCHELOR, M., COOPER, S., FRASER, C., JONES, S., GEORGIU, T., KHALILI-SHIRAZI, A., CLARKE, A. R., HASNAIN, S. S. & COLLINGE, J. 2009. Crystal structure of human prion protein bound to a therapeutic antibody. *Proc Natl Acad Sci U S A*, 106, 2554-8.
- ARNOLD, J. E., TIPLER, C., LASZLO, L., HOPE, J., LANDON, M. & MAYER, R. J. 1995. The abnormal isoform of the prion protein accumulates in late-endosome-like organelles in scrapie-infected mouse brain. *J Pathol*, 176, 403-11.
- ASANTE, E. A., GOWLAND, I., GRIMSHAW, A., LINEHAN, J. M., SMIDAK, M., HOUGHTON, R., OSIGUWA, O., TOMLINSON, A., JOINER, S., BRANDNER, S., WADSWORTH, J. D. & COLLINGE, J. 2009. Absence of spontaneous disease and comparative prion susceptibility of transgenic mice expressing mutant human prion proteins. *J Gen Virol*, 90, 546-58.
- ATARASHI, R., SANO, K., SATOH, K. & NISHIDA, N. 2011. Real-time quaking-induced conversion: a highly sensitive assay for prion detection. *Prion*, 5, 150-3.
- AULIC, S., MASPERONE, L., NARKIEWICZ, J., ISOPI, E., BISTAFFA, E., AMBROSETTI, E., PASTORE, B., DE CECCO, E., SCAINI, D., ZAGO, P., MODA, F., TAGLIAVINI, F. & LEGNAME, G. 2017. alpha-Synuclein Amyloids Hijack Prion Protein to Gain Cell Entry, Facilitate Cell-to-Cell Spreading and Block Prion Replication. *Sci Rep*, 7, 10050.
- BAELL, J. & WALTERS, M. A. 2014. Chemistry: Chemical con artists foil drug discovery. *Nature*, 513, 481-3.
- BAHL, J. M., HEEGAARD, N. H., FALKENHORST, G., LAURSEN, H., HOGENHAVEN, H., MOLBAK, K., JESPERGAARD, C., HOUGS, L., WALDEMAR, G., JOHANNSEN, P. & CHRISTIANSEN, M. 2009. The diagnostic efficiency of biomarkers in sporadic Creutzfeldt-Jakob disease compared to Alzheimer's disease. *Neurobiol Aging*, 30, 1834-41.
- BAKER, H. F., DUCHEN, L. W., JACOBS, J. M. & RIDLEY, R. M. 1990. Spongiform encephalopathy transmitted experimentally from Creutzfeldt-Jakob and familial Gerstmann-Straussler-Scheinker diseases. *Brain*, 113 (Pt 6), 1891-909.
- BAKER, H. F. & RIDLEY, R. M. 1996. Creutzfeldt-Jakob disease and bovine spongiform encephalopathy. Study so far provides no evidence for maternal and horizontal transmission. *BMJ*, 312, 843.
- BALDUCCI, C., BEEG, M., STRAVALACI, M., BASTONE, A., SCLIP, A., BIASINI, E., TAPPELLA, L., COLOMBO, L., MANZONI, C., BORSELLO, T., CHIESA, R., GOBBI, M., SALMONA, M. & FORLONI, G. 2010. Synthetic amyloid-beta oligomers impair long-term memory independently of cellular prion protein. *Proc Natl Acad Sci U S A*, 107, 2295-300.
- BARAL, P. K., SWAYAMPAKULA, M., ROUT, M. K., KAV, N. N., SPYRACOPOULOS, L., AGUZZI, A. & JAMES, M. N. 2014. Structural basis of prion inhibition by phenothiazine compounds. *Structure*, 22, 291-303.
- BARINGER, J. R. & PRUSINER, S. B. 1978. Experimental scrapie in mice: ultrastructural observations. *Ann Neurol*, 4, 205-11.

- BARON, T., BENCSIK, A., BIACABE, A. G., MORIGNAT, E. & BESSEN, R. A. 2007. Phenotypic similarity of transmissible mink encephalopathy in cattle and L-type bovine spongiform encephalopathy in a mouse model. *Emerg Infect Dis*, 13, 1887-94.
- BARRECA, M. L., IRACI, N., BIGGI, S., CECCHETTI, V. & BIASINI, E. 2018. Pharmacological Agents Targeting the Cellular Prion Protein. *Pathogens*, 7.
- BARRET, A., TAGLIAVINI, F., FORLONI, G., BATE, C., SALMONA, M., COLOMBO, L., DE LUIGI, A., LIMIDO, L., SUARDI, S., ROSSI, G., AUVRE, F., ADJOU, K. T., SALES, N., WILLIAMS, A., LASMEZAS, C. & DESLYS, J. P. 2003. Evaluation of quinacrine treatment for prion diseases. *J Virol*, 77, 8462-9.
- BARRIA, M. A., LEE, A., GREEN, A. J., KNIGHT, R. & HEAD, M. W. 2018. Rapid amplification of prions from variant Creutzfeldt-Jakob disease cerebrospinal fluid. *J Pathol Clin Res*, 4, 86-92.
- BARRY, A. E., KLYUBIN, I., MC DONALD, J. M., MABLY, A. J., FARRELL, M. A., SCOTT, M., WALSH, D. M. & ROWAN, M. J. 2011. Alzheimer's disease brain-derived amyloid-beta-mediated inhibition of LTP in vivo is prevented by immunotargeting cellular prion protein. *J Neurosci*, 31, 7259-63.
- BASLER, K., OESCH, B., SCOTT, M., WESTAWAY, D., WALCHLI, M., GROTH, D. F., MCKINLEY, M. P., PRUSINER, S. B. & WEISSMANN, C. 1986. Scrapie and cellular PrP isoforms are encoded by the same chromosomal gene. *Cell*, 46, 417-28.
- BATE, C., SALMONA, M., DIOMEDE, L. & WILLIAMS, A. 2004. Squalenstatin cures prion-infected neurons and protects against prion neurotoxicity. *J Biol Chem*, 279, 14983-90.
- BATE, C., TAYEBI, M., DIOMEDE, L., SALMONA, M. & WILLIAMS, A. 2009. Glimpepiride reduces the expression of PrPc, prevents PrPSc formation and protects against prion mediated neurotoxicity in cell lines. *PLoS One*, 4, e8221.
- BATE, C., TAYEBI, M. & WILLIAMS, A. 2010. A glycosylphosphatidylinositol analogue reduced prion-derived peptide mediated activation of cytoplasmic phospholipase A2, synapse degeneration and neuronal death. *Neuropharmacology*, 59, 93-9.
- BAUMANN, F., TOLNAY, M., BRABECK, C., PAHNKE, J., KLOZ, U., NIEMANN, H. H., HEIKENWALDER, M., RULICKE, T., BURKLE, A. & AGUZZI, A. 2007. Lethal recessive myelin toxicity of prion protein lacking its central domain. *EMBO J*, 26, 538-47.
- BEHRENS, A., GENOUD, N., NAUMANN, H., RULICKE, T., JANETT, F., HEPPNER, F. L., LEDERMANN, B. & AGUZZI, A. 2002. Absence of the prion protein homologue Doppel causes male sterility. *EMBO J*, 21, 3652-8.
- BENCSIK, A., DEBEER, S., PETIT, T. & BARON, T. 2009. Possible case of maternal transmission of feline spongiform encephalopathy in a captive cheetah. *PLoS One*, 4, e6929.
- BENDHEIM, P. E., BOCKMAN, J. M., MCKINLEY, M. P., KINGSBURY, D. T. & PRUSINER, S. B. 1985. Scrapie and Creutzfeldt-Jakob disease prion proteins share physical properties and antigenic determinants. *Proc Natl Acad Sci U S A*, 82, 997-1001.
- BENESTAD, S. L., AUSTBO, L., TRANULIS, M. A., ESPENES, A. & OLSAKER, I. 2012. Healthy goats naturally devoid of prion protein. *Vet Res*, 43, 87.
- BENITO-LEON, J. 2004. Combined quinacrine and chlorpromazine therapy in fatal familial insomnia. *Clin Neuropharmacol*, 27, 201-3.
- BERALDO, F. H., ARANTES, C. P., SANTOS, T. G., MACHADO, C. F., ROFFE, M., HAJJ, G. N., LEE, K. S., MAGALHAES, A. C., CAETANO, F. A., MANCINI, G. L., LOPES, M. H., AMERICO, T. A., MAGDESIAN, M. H., FERGUSON, S. S., LINDEN, R., PRADO, M. A. & MARTINS, V. R. 2011. Metabotropic glutamate receptors transduce signals for neurite outgrowth after binding of the prion protein to laminin gamma1 chain. *FASEB J*, 25, 265-79.
- BERALDO, F. H., ARANTES, C. P., SANTOS, T. G., QUEIROZ, N. G., YOUNG, K., RYLETT, R. J., MARKUS, R. P., PRADO, M. A. & MARTINS, V. R. 2010. Role of alpha7 nicotinic acetylcholine receptor in

- calcium signaling induced by prion protein interaction with stress-inducible protein 1. *J Biol Chem*, 285, 36542-50.
- BERANGER, F., CROZET, C., GOLDSBOROUGH, A. & LEHMANN, S. 2008. Trehalose impairs aggregation of PrP^{Sc} molecules and protects prion-infected cells against oxidative damage. *Biochem Biophys Res Commun*, 374, 44-8.
- BERANGER, F., MANGE, A., GOUD, B. & LEHMANN, S. 2002. Stimulation of PrP(C) retrograde transport toward the endoplasmic reticulum increases accumulation of PrP(Sc) in prion-infected cells. *J Biol Chem*, 277, 38972-7.
- BERNOULLI, C., SIEGFRIED, J., BAUMGARTNER, G., REGLI, F., RABINOWICZ, T., GAJDUSEK, D. C. & GIBBS, C. J., JR. 1977. Danger of accidental person-to-person transmission of Creutzfeldt-Jakob disease by surgery. *Lancet*, 1, 478-9.
- BERTUCHI, F. R., BOURGEON, D. M., LANDEMBERGER, M. C., MARTINS, V. R. & CERCHIARO, G. 2012. PrP^C displays an essential protective role from oxidative stress in an astrocyte cell line derived from PrP^C knockout mice. *Biochem Biophys Res Commun*, 418, 27-32.
- BESSEN, R. A., KOCISKO, D. A., RAYMOND, G. J., NANDAN, S., LANSBURY, P. T. & CAUGHEY, B. 1995. Non-genetic propagation of strain-specific properties of scrapie prion protein. *Nature*, 375, 698-700.
- BESSEN, R. A. & MARSH, R. F. 1992. Biochemical and physical properties of the prion protein from two strains of the transmissible mink encephalopathy agent. *J Virol*, 66, 2096-101.
- BHARATE, S. S., MIGNANI, S. & VISHWAKARMA, R. A. 2018. Why Are the Majority of Active Compounds in the CNS Domain Natural Products? A Critical Analysis. *J Med Chem*, 61, 10345-10374.
- BIRKETT, C. R., HENNION, R. M., BEMBRIDGE, D. A., CLARKE, M. C., CHREE, A., BRUCE, M. E. & BOSTOCK, C. J. 2001. Scrapie strains maintain biological phenotypes on propagation in a cell line in culture. *EMBO J*, 20, 3351-8.
- BISHOP, M. T., HART, P., AITCHISON, L., BAYBUTT, H. N., PLINSTON, C., THOMSON, V., TUZI, N. L., HEAD, M. W., IRONSIDE, J. W., WILL, R. G. & MANSON, J. C. 2006. Predicting susceptibility and incubation time of human-to-human transmission of vCJD. *Lancet Neurol*, 5, 393-8.
- BISHOP, M. T., WILL, R. G. & MANSON, J. C. 2010. Defining sporadic Creutzfeldt-Jakob disease strains and their transmission properties. *Proc Natl Acad Sci U S A*, 107, 12005-10.
- BOCKMAN, J. M., KINGSBURY, D. T., MCKINLEY, M. P., BENDHEIM, P. E. & PRUSINER, S. B. 1985. Creutzfeldt-Jakob disease prion proteins in human brains. *N Engl J Med*, 312, 73-8.
- BOELLAARD, J. W. & SCHLOTE, W. 1980. [Subacute spongiform encephalopathy with multiform plaque formation. "Peculiar familial-hereditary disease of CNS [spinocerebellar atrophy with dementia, plaques, and plaque-like deposits in cerebellum and cerebrum" (Gerstmann, Strausler, Scheinker)] (author's transl)]. *Acta Neuropathol*, 49, 205-12.
- BOELLAARD, J. W., SCHLOTE, W. & TATEISHI, J. 1989. Neuronal autophagy in experimental Creutzfeldt-Jakob's disease. *Acta Neuropathol*, 78, 410-8.
- BOLTON, D. C., MCKINLEY, M. P. & PRUSINER, S. B. 1982. Identification of a protein that purifies with the scrapie prion. *Science*, 218, 1309-11.
- BOLTON, D. C., MEYER, R. K. & PRUSINER, S. B. 1985. Scrapie PrP 27-30 is a sialoglycoprotein. *J Virol*, 53, 596-606.
- BONE, I., BELTON, L., WALKER, A. S. & DARBYSHIRE, J. 2008. Intraventricular pentosan polysulphate in human prion diseases: an observational study in the UK. *Eur J Neurol*, 15, 458-64.
- BONGIANNI, M., ORRU, C., GROVEMAN, B. R., SACCHETTO, L., FIORINI, M., TONOLI, G., TRIVA, G., CAPALDI, S., TESTI, S., FERRARI, S., CAGNIN, A., LADOGANA, A., POLEGGI, A., COLAIZZO, E., TIPLE, D., VAIANELLA, L., CASTRICIANO, S., MARCHIONI, D., HUGHSON, A. G., IMPERIALE, D.,

- CATTARUZZA, T., FABRIZI, G. M., POCCHIARI, M., MONACO, S., CAUGHEY, B. & ZANUSSO, G. 2017. Diagnosis of Human Prion Disease Using Real-Time Quaking-Induced Conversion Testing of Olfactory Mucosa and Cerebrospinal Fluid Samples. *JAMA Neurol*, 74, 155-162.
- BORCHELT, D. R., ROGERS, M., STAHL, N., TELLING, G. & PRUSINER, S. B. 1993. Release of the cellular prion protein from cultured cells after loss of its glycoinositol phospholipid anchor. *Glycobiology*, 3, 319-29.
- BORCHELT, D. R., SCOTT, M., TARABOULOS, A., STAHL, N. & PRUSINER, S. B. 1990. Scrapie and cellular prion proteins differ in their kinetics of synthesis and topology in cultured cells. *J Cell Biol*, 110, 743-52.
- BORCHELT, D. R., TARABOULOS, A. & PRUSINER, S. B. 1992. Evidence for synthesis of scrapie prion proteins in the endocytic pathway. *J Biol Chem*, 267, 16188-99.
- BOSQUE, P. J. 2002. Bovine spongiform encephalopathy, chronic wasting disease, scrapie, and the threat to humans from prion disease epizootics. *Curr Neurol Neurosci Rep*, 2, 488-95.
- BRANDNER, S., ISENMANN, S., RAEBER, A., FISCHER, M., SAILER, A., KOBAYASHI, Y., MARINO, S., WEISSMANN, C. & AGUZZI, A. 1996a. Normal host prion protein necessary for scrapie-induced neurotoxicity. *Nature*, 379, 339-43.
- BRANDNER, S., RAEBER, A., SAILER, A., BLATTNER, T., FISCHER, M., WEISSMANN, C. & AGUZZI, A. 1996b. Normal host prion protein (PrP^C) is required for scrapie spread within the central nervous system. *Proc Natl Acad Sci U S A*, 93, 13148-51.
- BREMER, J., BAUMANN, F., TIBERI, C., WESSIG, C., FISCHER, H., SCHWARZ, P., STEELE, A. D., TOYKA, K. V., NAVE, K. A., WEIS, J. & AGUZZI, A. 2010. Axonal prion protein is required for peripheral myelin maintenance. *Nat Neurosci*, 13, 310-8.
- BRIBIAN, A., FONTANA, X., LLORENS, F., GAVIN, R., REINA, M., GARCIA-VERDUGO, J. M., TORRES, J. M., DE CASTRO, F. & DEL RIO, J. A. 2012. Role of the cellular prion protein in oligodendrocyte precursor cell proliferation and differentiation in the developing and adult mouse CNS. *PLoS One*, 7, e33872.
- BROWN, D. & WANECK, G. L. 1992. Glycosyl-phosphatidylinositol-anchored membrane proteins. *J Am Soc Nephrol*, 3, 895-906.
- BROWN, D. R., QIN, K., HERMS, J. W., MADLUNG, A., MANSON, J., STROME, R., FRASER, P. E., KRUCK, T., VON BOHLEN, A., SCHULZ-SCHAEFFER, W., GIESE, A., WESTAWAY, D. & KRETZSCHMAR, H. 1997a. The cellular prion protein binds copper in vivo. *Nature*, 390, 684-7.
- BROWN, D. R., SCHULZ-SCHAEFFER, W. J., SCHMIDT, B. & KRETZSCHMAR, H. A. 1997b. Prion protein-deficient cells show altered response to oxidative stress due to decreased SOD-1 activity. *Exp Neurol*, 146, 104-12.
- BROWN, P., PREECE, M., BRANDEL, J. P., SATO, T., MCSHANE, L., ZERR, I., FLETCHER, A., WILL, R. G., POCCHIARI, M., CASHMAN, N. R., D'AIGNAUX, J. H., CERVENAKOVA, L., FRADKIN, J., SCHONBERGER, L. B. & COLLINS, S. J. 2000. Iatrogenic Creutzfeldt-Jakob disease at the millennium. *Neurology*, 55, 1075-81.
- BROWNING, S. R., MASON, G. L., SEWARD, T., GREEN, M., ELIASON, G. A., MATHIASON, C., MILLER, M. W., WILLIAMS, E. S., HOOVER, E. & TELLING, G. C. 2004. Transmission of prions from mule deer and elk with chronic wasting disease to transgenic mice expressing cervid PrP. *J Virol*, 78, 13345-50.
- BRUCE, M. E., MCBRIDE, P. A. & FARQUHAR, C. F. 1989. Precise targeting of the pathology of the sialoglycoprotein, PrP, and vacuolar degeneration in mouse scrapie. *Neurosci Lett*, 102, 1-6.
- BUDKA, H. 2003. Neuropathology of prion diseases. *Br Med Bull*, 66, 121-30.
- BUELER, H., AGUZZI, A., SAILER, A., GREINER, R. A., AUTENRIED, P., AGUET, M. & WEISSMANN, C. 1993. Mice devoid of PrP are resistant to scrapie. *Cell*, 73, 1339-47.

- BUELER, H., FISCHER, M., LANG, Y., BLUETHMANN, H., LIPP, H. P., DEARMOND, S. J., PRUSINER, S. B., AGUET, M. & WEISSMANN, C. 1992. Normal development and behaviour of mice lacking the neuronal cell-surface PrP protein. *Nature*, 356, 577-82.
- BUELER, H., RAEBER, A., SAILER, A., FISCHER, M., AGUZZI, A. & WEISSMANN, C. 1994. High prion and PrP^{Sc} levels but delayed onset of disease in scrapie-inoculated mice heterozygous for a disrupted PrP gene. *Mol Med*, 1, 19-30.
- BUGE, A., ESCOUROLLE, R., BRION, S., RANCUREL, G., HAUW, J. J., MEHAUT, M., GRAY, F. & GAJDUSEK, D. C. 1978. [Familial Creutzfeldt-Jakob disease. A clinical and pathological study of three cases in a family with eight affected members in three generations (author's transl)]. *Rev Neurol (Paris)*, 134, 165-81.
- BUTLER, D. A., SCOTT, M. R., BOCKMAN, J. M., BORCHELT, D. R., TARABOULOS, A., HSIAO, K. K., KINGSBURY, D. T. & PRUSINER, S. B. 1988. Scrapie-infected murine neuroblastoma cells produce protease-resistant prion proteins. *J Virol*, 62, 1558-64.
- CAETANO, F. A., LOPES, M. H., HAJJ, G. N., MACHADO, C. F., PINTO ARANTES, C., MAGALHAES, A. C., VIEIRA MDE, P., AMERICO, T. A., MASSENSINI, A. R., PRIOLA, S. A., VORBERG, I., GOMEZ, M. V., LINDEN, R., PRADO, V. F., MARTINS, V. R. & PRADO, M. A. 2008. Endocytosis of prion protein is required for ERK1/2 signaling induced by stress-inducible protein 1. *J Neurosci*, 28, 6691-702.
- CAMPEAU, J. L., WU, G., BELL, J. R., RASMUSSEN, J. & SIM, V. L. 2013. Early increase and late decrease of purkinje cell dendritic spine density in prion-infected organotypic mouse cerebellar cultures. *PLoS One*, 8, e81776.
- CANCELLOTTI, E., BRADFORD, B. M., TUZI, N. L., HICKEY, R. D., BROWN, D., BROWN, K. L., BARRON, R. M., KISIELEWSKI, D., PICCARDO, P. & MANSON, J. C. 2010. Glycosylation of PrP^C determines timing of neuroinvasion and targeting in the brain following transmissible spongiform encephalopathy infection by a peripheral route. *J Virol*, 84, 3464-75.
- CARLSON, G. A., DEARMOND, S. J., TORCHIA, M., WESTAWAY, D. & PRUSINER, S. B. 1994. Genetics of prion diseases and prion diversity in mice. *Philos Trans R Soc Lond B Biol Sci*, 343, 363-9.
- CARLSON, G. A., GOODMAN, P. A., LOVETT, M., TAYLOR, B. A., MARSHALL, S. T., PETERSON-TORCHIA, M., WESTAWAY, D. & PRUSINER, S. B. 1988. Genetics and polymorphism of the mouse prion gene complex: control of scrapie incubation time. *Mol Cell Biol*, 8, 5528-40.
- CARTONI, C., SCHININA, M. E., MARAS, B., NONNO, R., VACCARI, G., DI BARIA, M. A., CONTE, M., LIU, Q. G., LU, M., CARDONE, F., WINDL, O., POCCHIARI, M. & AGRIMI, U. 2005. Identification of the pathological prion protein allotypes in scrapie-infected heterozygous bank voles (*Clethrionomys glareolus*) by high-performance liquid chromatography-mass spectrometry. *J Chromatogr A*, 1081, 122-6.
- CARULLA, P., BRIBIAN, A., RANGEL, A., GAVIN, R., FERRER, I., CAELLES, C., DEL RIO, J. A. & LLORENS, F. 2011. Neuroprotective role of PrP^C against kainate-induced epileptic seizures and cell death depends on the modulation of JNK3 activation by GluR6/7-PSD-95 binding. *Mol Biol Cell*, 22, 3041-54.
- CASPI, S., HALIMI, M., YANAI, A., SASSON, S. B., TARABOULOS, A. & GABIZON, R. 1998. The anti-prion activity of Congo red. Putative mechanism. *J Biol Chem*, 273, 3484-9.
- CASTILLA, J., SAA, P., MORALES, R., ABID, K., MAUNDRELL, K. & SOTO, C. 2006. Protein misfolding cyclic amplification for diagnosis and prion propagation studies. *Methods Enzymol*, 412, 3-21.
- CATHALA, F., CHATELAIN, J., BROWN, P., DUMAS, M. & GAJDUSEK, D. C. 1980. Familial Creutzfeldt-Jakob disease. Autosomal dominance in 14 members over 3 generations. *J Neurol Sci*, 47, 343-51.

- CAUGHEY, B. 1991. In vitro expression and biosynthesis of prion protein. *Curr Top Microbiol Immunol*, 172, 93-107.
- CAUGHEY, B., BROWN, K., RAYMOND, G. J., KATZENSTEIN, G. E. & THRESHER, W. 1994. Binding of the protease-sensitive form of PrP (prion protein) to sulfated glycosaminoglycan and congo red [corrected]. *J Virol*, 68, 2135-41.
- CAUGHEY, B., ERNST, D. & RACE, R. E. 1993. Congo red inhibition of scrapie agent replication. *J Virol*, 67, 6270-2.
- CAUGHEY, B. & RACE, R. E. 1992. Potent inhibition of scrapie-associated PrP accumulation by congo red. *J Neurochem*, 59, 768-71.
- CAUGHEY, B., RACE, R. E., ERNST, D., BUCHMEIER, M. J. & CHESEBRO, B. 1989. Prion protein biosynthesis in scrapie-infected and uninfected neuroblastoma cells. *J Virol*, 63, 175-81.
- CAUGHEY, B. & RAYMOND, G. J. 1993. Sulfated polyanion inhibition of scrapie-associated PrP accumulation in cultured cells. *J Virol*, 67, 643-50.
- CAUGHEY, W. S., RAYMOND, L. D., HORIUCHI, M. & CAUGHEY, B. 1998. Inhibition of protease-resistant prion protein formation by porphyrins and phthalocyanines. *Proc Natl Acad Sci U S A*, 95, 12117-22.
- CEN, L. P., LIU, Y. F., NG, T. K., LUO, J. M., VAN ROOIJEN, N., ZHANG, M., PANG, C. P. & CUI, Q. 2018. Casein kinase-II inhibition promotes retinal ganglion cell survival and axonal regeneration. *Exp Eye Res*, 177, 153-159.
- CHAKRABARTI, O. & HEGDE, R. S. 2009. Functional depletion of mahogunin by cytosolically exposed prion protein contributes to neurodegeneration. *Cell*, 137, 1136-47.
- CHAO, C. C., CHIANG, C. H., MA, Y. L. & LEE, E. H. 2006. Molecular mechanism of the neurotrophic effect of GDNF on DA neurons: role of protein kinase CK2. *Neurobiol Aging*, 27, 105-18.
- CHATELAIN, J., CATHALA, F., BROWN, P., RAHARISON, S., COURT, L. & GAJDUSEK, D. C. 1981. Epidemiologic comparisons between Creutzfeldt-Jakob disease and scrapie in France during the 12-year period 1968-1979. *J Neurol Sci*, 51, 329-37.
- CHEN, J., GAO, C., SHI, Q., WANG, G., LEI, Y., SHAN, B., ZHANG, B., DONG, C., SHI, S., WANG, X., TIAN, C., HAN, J. & DONG, X. 2008a. Casein kinase II interacts with prion protein in vitro and forms complex with native prion protein in vivo. *Acta Biochim Biophys Sin (Shanghai)*, 40, 1039-47.
- CHEN, J. M., GAO, C., SHI, Q., SHAN, B., LEI, Y. J., DONG, C. F., AN, R., WANG, G. R., ZHANG, B. Y., HAN, J. & DONG, X. P. 2008b. Different expression patterns of CK2 subunits in the brains of experimental animals and patients with transmissible spongiform encephalopathies. *Arch Virol*, 153, 1013-20.
- CHEN, R. J., CHANG, W. W., LIN, Y. C., CHENG, P. L. & CHEN, Y. R. 2013. Alzheimer's amyloid-beta oligomers rescue cellular prion protein induced tau reduction via the Fyn pathway. *ACS Chem Neurosci*, 4, 1287-96.
- CHEN, S., YADAV, S. P. & SUREWICZ, W. K. 2010. Interaction between human prion protein and amyloid-beta (A β) oligomers: role OF N-terminal residues. *J Biol Chem*, 285, 26377-83.
- CHEN, S. G., TEPLow, D. B., PARCHI, P., TELLER, J. K., GAMBETTI, P. & AUTILIO-GAMBETTI, L. 1995. Truncated forms of the human prion protein in normal brain and in prion diseases. *J Biol Chem*, 270, 19173-80.
- CHESEBRO, B., RACE, B., MEADE-WHITE, K., LACASSE, R., RACE, R., KLINGEBORN, M., STRIEBEL, J., DORWARD, D., MCGOVERN, G. & JEFFREY, M. 2010. Fatal transmissible amyloid encephalopathy: a new type of prion disease associated with lack of prion protein membrane anchoring. *PLoS Pathog*, 6, e1000800.

- CHESEBRO, B., RACE, R., WEHRLY, K., NISHIO, J., BLOOM, M., LECHNER, D., BERGSTROM, S., ROBBINS, K., MAYER, L., KEITH, J. M. & ET AL. 1985. Identification of scrapie prion protein-specific mRNA in scrapie-infected and uninfected brain. *Nature*, 315, 331-3.
- CHESEBRO, B., TRIFILO, M., RACE, R., MEADE-WHITE, K., TENG, C., LACASSE, R., RAYMOND, L., FAVARA, C., BARON, G., PRIOLA, S., CAUGHEY, B., MASLIAH, E. & OLDSTONE, M. 2005. Anchorless prion protein results in infectious amyloid disease without clinical scrapie. *Science*, 308, 1435-9.
- CHIESA, R., PICCARDO, P., GHETTI, B. & HARRIS, D. A. 1998. Neurological illness in transgenic mice expressing a prion protein with an insertional mutation. *Neuron*, 21, 1339-51.
- CHITI, Z., KNUtSEN, O. M., BETMOUNI, S. & GREENE, J. R. 2006. An integrated, temporal study of the behavioural, electrophysiological and neuropathological consequences of murine prion disease. *Neurobiol Dis*, 22, 363-73.
- CHOHAN, G., PENNINGTON, C., MACKENZIE, J. M., ANDREWS, M., EVERINGTON, D., WILL, R. G., KNIGHT, R. S. & GREEN, A. J. 2010. The role of cerebrospinal fluid 14-3-3 and other proteins in the diagnosis of sporadic Creutzfeldt-Jakob disease in the UK: a 10-year review. *J Neurol Neurosurg Psychiatry*, 81, 1243-8.
- CHOI, J. H., JEONG, T. S., KIM, D. Y., KIM, Y. M., NA, H. J., NAM, K. H., LEE, S. B., KIM, H. C., OH, S. R., CHOI, Y. K., BOK, S. H. & OH, G. T. 2003. Hematein inhibits atherosclerosis by inhibition of reactive oxygen generation and NF-kappaB-dependent inflammatory mediators in hyperlipidemic mice. *J Cardiovasc Pharmacol*, 42, 287-95.
- CHRISTENSEN, H. M. & HARRIS, D. A. 2009. A deleted prion protein that is neurotoxic in vivo is localized normally in cultured cells. *J Neurochem*, 108, 44-56.
- CHUNG, E., JI, Y., SUN, Y., KASCSAK, R. J., KASCSAK, R. B., MEHTA, P. D., STRITTMATTER, S. M. & WISNIEWSKI, T. 2010. Anti-PrPC monoclonal antibody infusion as a novel treatment for cognitive deficits in an Alzheimer's disease model mouse. *BMC Neurosci*, 11, 130.
- CINGARAM, P. K., NYESTE, A., DONDAPATI, D. T., FODOR, E. & WELKER, E. 2015. Prion Protein Does Not Confer Resistance to Hippocampus-Derived Zpl Cells against the Toxic Effects of Cu²⁺, Mn²⁺, Zn²⁺ and Co²⁺ Not Supporting a General Protective Role for PrP in Transition Metal Induced Toxicity. *PLoS One*, 10, e0139219.
- CIRIC, D. & REZAEI, H. 2015. Biochemical insight into the prion protein family. *Front Cell Dev Biol*, 3, 5.
- CLARK, W. W., HOURRIGAN, J. L. & HADLOW, W. J. 1995. Encephalopathy in cattle experimentally infected with the scrapie agent. *Am J Vet Res*, 56, 606-12.
- CLARKE, M. C. & HAIG, D. A. 1970a. Evidence for the multiplication of scrapie agent in cell culture. *Nature*, 225, 100-1.
- CLARKE, M. C. & HAIG, D. A. 1970b. Multiplication of scrapie agent in cell culture. *Res Vet Sci*, 11, 500-1.
- COITINHO, A. S., FREITAS, A. R., LOPES, M. H., HAJJ, G. N., ROESLER, R., WALZ, R., ROSSATO, J. I., CAMMAROTA, M., IZQUIERDO, I., MARTINS, V. R. & BRENTANI, R. R. 2006. The interaction between prion protein and laminin modulates memory consolidation. *Eur J Neurosci*, 24, 3255-64.
- COLLINGE, J. 1999. Variant Creutzfeldt-Jakob disease. *Lancet*, 354, 317-23.
- COLLINGE, J. & CLARKE, A. R. 2007. A general model of prion strains and their pathogenicity. *Science*, 318, 930-6.
- COLLINGE, J., GORHAM, M., HUDSON, F., KENNEDY, A., KEOGH, G., PAL, S., ROSSOR, M., RUDGE, P., SIDDIQUE, D., SPYER, M., THOMAS, D., WALKER, S., WEBB, T., WROE, S. & DARBYSHIRE, J. 2009. Safety and efficacy of quinacrine in human prion disease (PRION-1 study): a patient-preference trial. *Lancet Neurol*, 8, 334-44.

- COLLINGE, J., PALMER, M. S. & DRYDEN, A. J. 1991. Genetic predisposition to iatrogenic Creutzfeldt-Jakob disease. *Lancet*, 337, 1441-2.
- COLLINGE, J., PALMER, M. S., SIDLE, K. C., GOWLAND, I., MEDORI, R., IRONSIDE, J. & LANTOS, P. 1995. Transmission of fatal familial insomnia to laboratory animals. *Lancet*, 346, 569-70.
- COLLINGE, J., WHITTINGTON, M. A., SIDLE, K. C., SMITH, C. J., PALMER, M. S., CLARKE, A. R. & JEFFERYS, J. G. 1994. Prion protein is necessary for normal synaptic function. *Nature*, 370, 295-7.
- COLLINS, S., BOYD, A., FLETCHER, A., GONZALES, M. F., MCLEAN, C. A. & MASTERS, C. L. 2000. Recent advances in the pre-mortem diagnosis of Creutzfeldt-Jakob disease. *Journal of Clinical Neuroscience*, 7, 195-202.
- COLLINS, S. J., LEWIS, V., BRAZIER, M., HILL, A. F., FLETCHER, A. & MASTERS, C. L. 2002. Quinacrine does not prolong survival in a murine Creutzfeldt-Jakob disease model. *Ann Neurol*, 52, 503-6.
- CONCHA-MARAMBIO, L., PRITZKOW, S., MODA, F., TAGLIAVINI, F., IRONSIDE, J. W., SCHULZ, P. E. & SOTO, C. 2016. Detection of prions in blood from patients with variant Creutzfeldt-Jakob disease. *Sci Transl Med*, 8, 370ra183.
- COOKSEY, C. 2010. Hematoxylin and related compounds--an annotated bibliography concerning their origin, properties, chemistry, and certain applications. *Biotech Histochem*, 85, 65-82.
- CORTES, C. J., QIN, K., COOK, J., SOLANKI, A. & MASTRIANNI, J. A. 2012. Rapamycin delays disease onset and prevents PrP plaque deposition in a mouse model of Gerstmann-Straussler-Scheinker disease. *J Neurosci*, 32, 12396-405.
- COURAGEOT, M. P., DAUDE, N., NONNO, R., PAQUET, S., DI BARI, M. A., LE DUR, A., CHAPUIS, J., HILL, A. F., AGRIMI, U., LAUDE, H. & VILETTE, D. 2008. A cell line infectible by prion strains from different species. *J Gen Virol*, 89, 341-7.
- CRAMM, M., SCHMITZ, M., KARCH, A., MITROVA, E., KUHN, F., SCHROEDER, B., RAEBER, A., VARGES, D., KIM, Y. S., SATOH, K., COLLINS, S. & ZERR, I. 2016. Stability and Reproducibility Underscore Utility of RT-QuIC for Diagnosis of Creutzfeldt-Jakob Disease. *Mol Neurobiol*, 53, 1896-1904.
- CRONIER, S., LAUDE, H. & PEYRIN, J. M. 2004. Prions can infect primary cultured neurons and astrocytes and promote neuronal cell death. *Proc Natl Acad Sci U S A*, 101, 12271-6.
- CUNNINGHAM, C., DEACON, R., WELLS, H., BOCHE, D., WATERS, S., DINIZ, C. P., SCOTT, H., RAWLINS, J. N. & PERRY, V. H. 2003. Synaptic changes characterize early behavioural signs in the ME7 model of murine prion disease. *Eur J Neurosci*, 17, 2147-55.
- DAPSON, R. W. & BAIN, C. L. 2015. Brazilwood, sappanwood, brazilin and the red dye brazilein: from textile dyeing and folk medicine to biological staining and musical instruments. *Biotech Histochem*, 90, 401-23.
- DAUDE, N., LEHMANN, S. & HARRIS, D. A. 1997. Identification of intermediate steps in the conversion of a mutant prion protein to a scrapie-like form in cultured cells. *J Biol Chem*, 272, 11604-12.
- DAVID, A. S., GRANT, R. & BALLANTYNE, J. P. 1984. Unsuccessful treatment of Creutzfeldt-Jakob disease with acyclovir. *Lancet*, 1, 512-3.
- DE CECCO, E. & LEGNAME, G. 2018. The role of the prion protein in the internalization of alpha-synuclein amyloids. *Prion*, 12, 23-27.
- DE LUIGI, A., COLOMBO, L., DIOMEDE, L., CAPOBIANCO, R., MANGIERI, M., MICCOLO, C., LIMIDO, L., FORLONI, G., TAGLIAVINI, F. & SALMONA, M. 2008. The efficacy of tetracyclines in peripheral and intracerebral prion infection. *PLoS One*, 3, e1888.
- DEARMOND, S. J., MCKINLEY, M. P., BARRY, R. A., BRAUNFELD, M. B., MCCOLLOCH, J. R. & PRUSINER, S. B. 1985. Identification of prion amyloid filaments in scrapie-infected brain. *Cell*, 41, 221-35.

- DEARMOND, S. J., MOBLEY, W. C., DEMOTT, D. L., BARRY, R. A., BECKSTEAD, J. H. & PRUSINER, S. B. 1987. Changes in the localization of brain prion proteins during scrapie infection. *Neurology*, 37, 1271-80.
- DEARMOND, S. J., SANCHEZ, H., YEHIELY, F., QIU, Y., NINCHAK-CASEY, A., DAGGETT, V., CAMERINO, A. P., CAYETANO, J., ROGERS, M., GROTH, D., TORCHIA, M., TREMBLAY, P., SCOTT, M. R., COHEN, F. E. & PRUSINER, S. B. 1997. Selective neuronal targeting in prion disease. *Neuron*, 19, 1337-48.
- DECKWERTH, T. L., ELLIOTT, J. L., KNUDSON, C. M., JOHNSON, E. M., JR., SNIDER, W. D. & KORSMEYER, S. J. 1996. BAX is required for neuronal death after trophic factor deprivation and during development. *Neuron*, 17, 401-11.
- DEMAIMAY, R., ADJOU, K. T., BERINGUE, V., DEMART, S., LASMEZAS, C. I., DESLYS, J. P., SEMAN, M. & DORMONT, D. 1997. Late treatment with polyene antibiotics can prolong the survival time of scrapie-infected animals. *J Virol*, 71, 9685-9.
- DEMAIMAY, R., HARPER, J., GORDON, H., WEAVER, D., CHESEBRO, B. & CAUGHEY, B. 1998. Structural aspects of Congo red as an inhibitor of protease-resistant prion protein formation. *J Neurochem*, 71, 2534-41.
- DI BARI, M. A., NONNO, R., CASTILLA, J., D'AGOSTINO, C., PIRISINU, L., RICCARDI, G., CONTE, M., RICHT, J., KUNKLE, R., LANGEVELD, J., VACCARI, G. & AGRIMI, U. 2013. Chronic wasting disease in bank voles: characterisation of the shortest incubation time model for prion diseases. *PLoS Pathog*, 9, e1003219.
- DIAZ-NIDO, J., MIZUNO, K., NAWA, H. & MARSHAK, D. R. 1994. Regulation of protein kinase CK2 isoform expression during rat brain development. *Cell Mol Biol Res*, 40, 581-5.
- DICKINSON, A. G. & FRASER, H. 1969. Modification of the pathogenesis of scrapie in mice by treatment of the agent. *Nature*, 222, 892-3.
- DICKINSON, A. G., MEIKLE, V. M. & FRASER, H. 1968. Identification of a gene which controls the incubation period of some strains of scrapie agent in mice. *J Comp Pathol*, 78, 293-9.
- DIRINGER, H. & EHLERS, B. 1991. Chemoprophylaxis of scrapie in mice. *J Gen Virol*, 72 (Pt 2), 457-60.
- DOH-URA, K., ISHIKAWA, K., MURAKAMI-KUBO, I., SASAKI, K., MOHRI, S., RACE, R. & IWAKI, T. 2004. Treatment of transmissible spongiform encephalopathy by intraventricular drug infusion in animal models. *J Virol*, 78, 4999-5006.
- DOH-URA, K., IWAKI, T. & CAUGHEY, B. 2000. Lysosomotropic agents and cysteine protease inhibitors inhibit scrapie-associated prion protein accumulation. *J Virol*, 74, 4894-7.
- DOLMAN, C. L. & DALY, L. L. 1982. Spino-cerebello-cerebral degeneration with amyloid plaques (Gerstmann, Straussler, Scheinker syndrome). *Can J Neurol Sci*, 9, 439-42.
- DONNE, D. G., VILES, J. H., GROTH, D., MEHLHORN, I., JAMES, T. L., COHEN, F. E., PRUSINER, S. B., WRIGHT, P. E. & DYSON, H. J. 1997. Structure of the recombinant full-length hamster prion protein PrP(29-231): the N terminus is highly flexible. *Proc Natl Acad Sci U S A*, 94, 13452-7.
- DOSSENA, S., IMERI, L., MANGIERI, M., GAROFOLI, A., FERRARI, L., SENATORE, A., RESTELLI, E., BALDUCCI, C., FIORDALISO, F., SALIO, M., BIANCHI, S., FIORITI, L., MORBIN, M., PINCHERLE, A., MARCON, G., VILLANI, F., CARLI, M., TAGLIAVINI, F., FORLONI, G. & CHIESA, R. 2008. Mutant prion protein expression causes motor and memory deficits and abnormal sleep patterns in a transgenic mouse model. *Neuron*, 60, 598-609.
- DRON, M., MOUDJOU, M., CHAPUIS, J., SALAMAT, M. K., BERNARD, J., CRONIER, S., LANGEVIN, C. & LAUDE, H. 2010. Endogenous proteolytic cleavage of disease-associated prion protein to produce C2 fragments is strongly cell- and tissue-dependent. *J Biol Chem*, 285, 10252-64.
- DUFFY, P., WOLF, J., COLLINS, G., DEVOE, A. G., STREETEN, B. & COWEN, D. 1974. Letter: Possible person-to-person transmission of Creutzfeldt-Jakob disease. *N Engl J Med*, 290, 692-3.

- DUPIEREUX, I., FALISSE-POIRRIER, N., ZORZI, W., WATT, N. T., THELLIN, O., ZORZI, D., PIERARD, O., HOOPER, N. M., HEINEN, E. & ELMOUALIJ, B. 2008. Protective effect of prion protein via the N-terminal region in mediating a protective effect on paraquat-induced oxidative injury in neuronal cells. *J Neurosci Res*, 86, 653-9.
- DURIG, J., GIESE, A., SCHULZ-SCHAEFFER, W., ROSENTHAL, C., SCHMUCKER, U., BIESCHKE, J., DUHRSEN, U. & KRETZSCHMAR, H. A. 2000. Differential constitutive and activation-dependent expression of prion protein in human peripheral blood leucocytes. *Br J Haematol*, 108, 488-95.
- EHLERS, B. & DIRINGER, H. 1984. Dextran sulphate 500 delays and prevents mouse scrapie by impairment of agent replication in spleen. *J Gen Virol*, 65 (Pt 8), 1325-30.
- EIDEN, M., HOFFMANN, C., BALKEMA-BUSCHMANN, A., MULLER, M., BAUMGARTNER, K. & GROSCHUP, M. H. 2010. Biochemical and immunohistochemical characterization of feline spongiform encephalopathy in a German captive cheetah. *J Gen Virol*, 91, 2874-83.
- ENARI, M., FLECHSIG, E. & WEISSMANN, C. 2001. Scrapie prion protein accumulation by scrapie-infected neuroblastoma cells abrogated by exposure to a prion protein antibody. *Proc Natl Acad Sci U S A*, 98, 9295-9.
- ENDO, T., GROTH, D., PRUSINER, S. B. & KOBATA, A. 1989. Diversity of oligosaccharide structures linked to asparagines of the scrapie prion protein. *Biochemistry*, 28, 8380-8.
- ERTMER, A., GILCH, S., YUN, S. W., FLECHSIG, E., KLEBL, B., STEIN-GERLACH, M., KLEIN, M. A. & SCHATZL, H. M. 2004. The tyrosine kinase inhibitor STI571 induces cellular clearance of PrPSc in prion-infected cells. *J Biol Chem*, 279, 41918-27.
- ESPINOSA, J. C., NONNO, R., DI BARI, M., AGUILAR-CALVO, P., PIRISINU, L., FERNANDEZ-BORGES, N., VANNI, I., VACCARI, G., MARIN-MORENO, A., FRASSANITO, P., LORENZO, P., AGRIMI, U. & TORRES, J. M. 2016. PrPC Governs Susceptibility to Prion Strains in Bank Vole, While Other Host Factors Modulate Strain Features. *J Virol*, 90, 10660-10669.
- FALSIG, J., JULIUS, C., MARGALITH, I., SCHWARZ, P., HEPPNER, F. L. & AGUZZI, A. 2008. A versatile prion replication assay in organotypic brain slices. *Nat Neurosci*, 11, 109-17.
- FALSIG, J., SONATI, T., HERRMANN, U. S., SABAN, D., LI, B., ARROYO, K., BALLMER, B., LIBERSKI, P. P. & AGUZZI, A. 2012. Prion pathogenesis is faithfully reproduced in cerebellar organotypic slice cultures. *PLoS Pathog*, 8, e1002985.
- FANG, C., IMBERDIS, T., GARZA, M. C., WILLE, H. & HARRIS, D. A. 2016. A Neuronal Culture System to Detect Prion Synaptotoxicity. *PLoS Pathog*, 12, e1005623.
- FANG, C., WU, B., LE, N. T. T., IMBERDIS, T., MERCER, R. C. C. & HARRIS, D. A. 2018. Prions activate a p38 MAPK synaptotoxic signaling pathway. *PLoS Pathog*, 14, e1007283.
- FERAUDET, C., MOREL, N., SIMON, S., VOLLAND, H., FROBERT, Y., CREMINON, C., VILETTE, D., LEHMANN, S. & GRASSI, J. 2005. Screening of 145 anti-PrP monoclonal antibodies for their capacity to inhibit PrPSc replication in infected cells. *J Biol Chem*, 280, 11247-58.
- FERNANDEZ-BORGES, N., DI BARI, M. A., ERANA, H., SANCHEZ-MARTIN, M., PIRISINU, L., PARRA, B., ELEZGARAI, S. R., VANNI, I., LOPEZ-MORENO, R., VACCARI, G., VENEGAS, V., CHARCO, J. M., GIL, D., HARRATHI, C., D'AGOSTINO, C., AGRIMI, U., MAYORAL, T., REQUENA, J. R., NONNO, R. & CASTILLA, J. 2018. Cofactors influence the biological properties of infectious recombinant prions. *Acta Neuropathol*, 135, 179-199.
- FERNANDEZ-FUNEZ, P., CASAS-TINTO, S., ZHANG, Y., GOMEZ-VELAZQUEZ, M., MORALES-GARZA, M. A., CEPEDA-NIETO, A. C., CASTILLA, J., SOTO, C. & RINCON-LIMAS, D. E. 2009. In vivo generation of neurotoxic prion protein: role for hsp70 in accumulation of misfolded isoforms. *PLoS Genet*, 5, e1000507.

- FERNANDEZ-FUNEZ, P., SANCHEZ-GARCIA, J. & RINCON-LIMAS, D. E. 2017. Drosophila models of prionopathies: insight into prion protein function, transmission, and neurotoxicity. *Curr Opin Genet Dev*, 44, 141-148.
- FERNANDEZ-FUNEZ, P., ZHANG, Y., CASAS-TINTO, S., XIAO, X., ZOU, W. Q. & RINCON-LIMAS, D. E. 2010. Sequence-dependent prion protein misfolding and neurotoxicity. *J Biol Chem*, 285, 36897-908.
- FERREIRA, A. P. A. & BOUCROT, E. 2018. Mechanisms of Carrier Formation during Clathrin-Independent Endocytosis. *Trends Cell Biol*, 28, 188-200.
- FERREIRA, D. G., TEMIDO-FERREIRA, M., VICENTE MIRANDA, H., BATALHA, V. L., COELHO, J. E., SZEGO, E. M., MARQUES-MORGADO, I., VAZ, S. H., RHEE, J. S., SCHMITZ, M., ZERR, I., LOPES, L. V. & OUTEIRO, T. F. 2017. alpha-synuclein interacts with PrP(C) to induce cognitive impairment through mGluR5 and NMDAR2B. *Nat Neurosci*, 20, 1569-1579.
- FERRER, I. 2002. Synaptic pathology and cell death in the cerebellum in Creutzfeldt-Jakob disease. *Cerebellum*, 1, 213-22.
- FERRER, S., CARTIER, L., LOLAS, F. & PEREZ, M. 1982. [Syndromic diversities in Creutzfeldt-Jakob disease: neurophysiological and histopathological correlates]. *Arq Neuropsiquiatr*, 40, 39-53.
- FIELD, E. J. 1968. Transmission of kuru to mice. *Lancet*, 1, 981-2.
- FISCHER, M., RULICKE, T., RAEBER, A., SAILER, A., MOSER, M., OESCH, B., BRANDNER, S., AGUZZI, A. & WEISSMANN, C. 1996. Prion protein (PrP) with amino-proximal deletions restoring susceptibility of PrP knockout mice to scrapie. *EMBO J*, 15, 1255-64.
- FLUHARTY, B. R., BIASINI, E., STRAVALACI, M., SCLIP, A., DIOMEDE, L., BALDUCCI, C., LA VITOLA, P., MESSA, M., COLOMBO, L., FORLONI, G., BORSELLO, T., GOBBI, M. & HARRIS, D. A. 2013. An N-terminal fragment of the prion protein binds to amyloid-beta oligomers and inhibits their neurotoxicity in vivo. *J Biol Chem*, 288, 7857-66.
- FOLIAKI, S. T., LEWIS, V., FINKELSTEIN, D. I., LAWSON, V., COLEMAN, H. A., SENESI, M., ISLAM, A. M. T., CHEN, F., SARROS, S., ROBERTS, B., ADLARD, P. A. & COLLINS, S. J. 2018. Prion acute synaptotoxicity is largely driven by protease-resistant PrP^{Sc} species. *PLoS Pathog*, 14, e1007214.
- FORLONI, G., IUSSICH, S., AWAN, T., COLOMBO, L., ANGERETTI, N., GIROLA, L., BERTANI, I., POLI, G., CARAMELLI, M., GRAZIA BRUZZONE, M., FARINA, L., LIMIDO, L., ROSSI, G., GIACCONE, G., IRONSIDE, J. W., BUGIANI, O., SALMONA, M. & TAGLIAVINI, F. 2002. Tetracyclines affect prion infectivity. *Proc Natl Acad Sci U S A*, 99, 10849-54.
- FORLONI, G., SALMONA, M., MARCON, G. & TAGLIAVINI, F. 2009. Tetracyclines and prion infectivity. *Infect Disord Drug Targets*, 9, 23-30.
- FORLONI, G., TETTAMANTI, M., LUCCA, U., ALBANESE, Y., QUAGLIO, E., CHIESA, R., ERBETTA, A., VILLANI, F., REDAELLI, V., TAGLIAVINI, F., ARTUSO, V. & ROITER, I. 2015. Preventive study in subjects at risk of fatal familial insomnia: Innovative approach to rare diseases. *Prion*, 9, 75-9.
- FRANCESCHINI, A., BAIARDI, S., HUGHSON, A. G., MCKENZIE, N., MODA, F., ROSSI, M., CAPELLARI, S., GREEN, A., GIACCONE, G., CAUGHEY, B. & PARCHI, P. 2017. High diagnostic value of second generation CSF RT-QuIC across the wide spectrum of CJD prions. *Sci Rep*, 7, 10655.
- FRASER, H. 2000. Phillips report and the origin of BSE. *Vet Rec*, 147, 724.
- FRASER, H. & DICKINSON, A. G. 1973. Scrapie in mice. Agent-strain differences in the distribution and intensity of grey matter vacuolation. *J Comp Pathol*, 83, 29-40.
- FRIEDMAN-LEVI, Y., MEINER, Z., CANELLO, T., FRID, K., KOVACS, G. G., BUDKA, H., AVRAHAM, D. & GABIZON, R. 2011. Fatal prion disease in a mouse model of genetic E200K Creutzfeldt-Jakob disease. *PLoS Pathog*, 7, e1002350.

- FRIGG, R., WENZEL, A., SAMARDZIJA, M., OESCH, B., WARIWODA, H., NAVARINI, A. A., SEELIGER, M. W., TANIMOTO, N., REME, C. & GRIMM, C. 2006. The prion protein is neuroprotective against retinal degeneration in vivo. *Exp Eye Res*, 83, 1350-8.
- FUHRMANN, M., MITTEREGGER, G., KRETZSCHMAR, H. & HERMS, J. 2007. Dendritic pathology in prion disease starts at the synaptic spine. *J Neurosci*, 27, 6224-33.
- FURLOW, T. W., JR., WHITLEY, R. J. & WILMES, F. J. 1982. Repeated suppression of Creutzfeldt-Jakob disease with vidarabine. *Lancet*, 2, 564-5.
- GAJDUSEK, D. C. 1977. Unconventional viruses and the origin and disappearance of kuru. *Science*, 197, 943-60.
- GAJDUSEK, D. C., GIBBS, C. J. & ALPERS, M. 1966. Experimental transmission of a Kuru-like syndrome to chimpanzees. *Nature*, 209, 794-6.
- GAJDUSEK, D. C. & GIBBS, C. J., JR. 1971. Transmission of two subacute spongiform encephalopathies of man (Kuru and Creutzfeldt-Jakob disease) to new world monkeys. *Nature*, 230, 588-91.
- GAJDUSEK, D. C., GIBBS, C. J., JR., ASHER, D. M. & DAVID, E. 1968. Transmission of experimental kuru to the spider monkey (*Ateles geoffreyi*). *Science*, 162, 693-4.
- GAJDUSEK, D. C. & ZIGAS, V. 1957. Degenerative disease of the central nervous system in New Guinea; the endemic occurrence of kuru in the native population. *N Engl J Med*, 257, 974-8.
- GAJDUSEK, D. C. & ZIGAS, V. 1959. Kuru; clinical, pathological and epidemiological study of an acute progressive degenerative disease of the central nervous system among natives of the Eastern Highlands of New Guinea. *Am J Med*, 26, 442-69.
- GAMBETTI, P., KONG, Q., ZOU, W., PARCHI, P. & CHEN, S. G. 2003a. Sporadic and familial CJD: classification and characterisation. *Br Med Bull*, 66, 213-39.
- GAMBETTI, P., PARCHI, P. & CHEN, S. G. 2003b. Hereditary Creutzfeldt-Jakob disease and fatal familial insomnia. *Clin Lab Med*, 23, 43-64.
- GANDINI, A. & BOLOGNESI, M. L. 2017. Therapeutic Approaches to Prion Diseases. *Prog Mol Biol Transl Sci*, 150, 433-453.
- GASPERINI, L., MENEGHETTI, E., LEGNAME, G. & BENETTI, F. 2016. In Absence of the Cellular Prion Protein, Alterations in Copper Metabolism and Copper-Dependent Oxidase Activity Affect Iron Distribution. *Front Neurosci*, 10, 437.
- GASPERINI, L., MENEGHETTI, E., PASTORE, B., BENETTI, F. & LEGNAME, G. 2015. Prion protein and copper cooperatively protect neurons by modulating NMDA receptor through S-nitrosylation. *Antioxid Redox Signal*, 22, 772-84.
- GEORGIEVA, D., SCHWARK, D., VON BERGEN, M., REDECKE, L., GENOV, N. & BETZEL, C. 2006. Interactions of recombinant prions with compounds of therapeutical significance. *Biochem Biophys Res Commun*, 344, 463-70.
- GESCHWIND, M. D., KUO, A. L., WONG, K. S., HAMAN, A., DEVEREUX, G., RAUDABAUGH, B. J., JOHNSON, D. Y., TORRES-CHAE, C. C., FINLEY, R., GARCIA, P., THAI, J. N., CHENG, H. Q., NEUHAUS, J. M., FORNER, S. A., DUNCAN, J. L., POSSIN, K. L., DEARMOND, S. J., PRUSINER, S. B. & MILLER, B. L. 2013. Quinacrine treatment trial for sporadic Creutzfeldt-Jakob disease. *Neurology*, 81, 2015-23.
- GHAEMMAGHAMI, S., AHN, M., LESSARD, P., GILES, K., LEGNAME, G., DEARMOND, S. J. & PRUSINER, S. B. 2009. Continuous quinacrine treatment results in the formation of drug-resistant prions. *PLoS Pathog*, 5, e1000673.
- GHETTI, B., DLOUHY, S. R., GIACCONE, G., BUGIANI, O., FRANGIONE, B., FARLOW, M. R. & TAGLIAVINI, F. 1995. Gerstmann-Straussler-Scheinker disease and the Indiana kindred. *Brain Pathol*, 5, 61-75.

- GIBBS, C. J., JR., AMYX, H. L., BACOTE, A., MASTERS, C. L. & GAJDUSEK, D. C. 1980. Oral transmission of kuru, Creutzfeldt-Jakob disease, and scrapie to nonhuman primates. *J Infect Dis*, 142, 205-8.
- GIBBS, C. J., JR. & GAJDUSEK, D. C. 1971. Transmission and characterization of the agents of spongiform virus encephalopathies: kuru, Creutzfeldt-Jakob disease, scrapie and mink encephalopathy. *Res Publ Assoc Res Nerv Ment Dis*, 49, 383-410.
- GIBBS, C. J., JR., GAJDUSEK, D. C., ASHER, D. M., ALPERS, M. P., BECK, E., DANIEL, P. M. & MATTHEWS, W. B. 1968. Creutzfeldt-Jakob disease (spongiform encephalopathy): transmission to the chimpanzee. *Science*, 161, 388-9.
- GIBSON, P. E., BELL, T. M. & FIELD, E. J. 1972. Failure of the scrapie agent to replicate in L5178Y mouse leukaemic cells. *Res Vet Sci*, 13, 95-6.
- GILCH, S., CHITTOOR, N., TAGUCHI, Y., STUART, M., JEWELL, J. E. & SCHATZL, H. M. 2011. Chronic wasting disease. *Top Curr Chem*, 305, 51-77.
- GILCH, S., KRAMMER, C. & SCHATZL, H. M. 2008. Targeting prion proteins in neurodegenerative disease. *Expert Opin Biol Ther*, 8, 923-40.
- GILES, K., OLSON, S. H. & PRUSINER, S. B. 2017. Developing Therapeutics for PrP Prion Diseases. *Cold Spring Harb Perspect Med*, 7.
- GIMBEL, D. A., NYGAARD, H. B., COFFEY, E. E., GUNTHER, E. C., LAUREN, J., GIMBEL, Z. A. & STRITTMATTER, S. M. 2010. Memory impairment in transgenic Alzheimer mice requires cellular prion protein. *J Neurosci*, 30, 6367-74.
- GIRI, R. K., YOUNG, R., PITSTICK, R., DEARMOND, S. J., PRUSINER, S. B. & CARLSON, G. A. 2006. Prion infection of mouse neurospheres. *Proc Natl Acad Sci U S A*, 103, 3875-80.
- GLATZEL, M., ABELA, E., MAISSEN, M. & AGUZZI, A. 2003. Extraneural pathologic prion protein in sporadic Creutzfeldt-Jakob disease. *N Engl J Med*, 349, 1812-20.
- GODSAVE, S. F., WILLE, H., KUJALA, P., LATAWIEC, D., DEARMOND, S. J., SERBAN, A., PRUSINER, S. B. & PETERS, P. J. 2008. Cryo-immunogold electron microscopy for prions: toward identification of a conversion site. *J Neurosci*, 28, 12489-99.
- GOLDING, M. C., LONG, C. R., CARMELL, M. A., HANNON, G. J. & WESTHUSIN, M. E. 2006. Suppression of prion protein in livestock by RNA interference. *Proc Natl Acad Sci U S A*, 103, 5285-90.
- GONATAS, N. K., TERRY, R. D. & WEISS, M. 1964. Ultrastructural studies in Jacob-Creutzfeldt disease. *Trans Am Neurol Assoc*, 89, 13-4.
- GONIOTAKI, D., LAKKARAJU, A. K. K., SHRIVASTAVA, A. N., BAKIRCI, P., SORCE, S., SENATORE, A., MARPAKWAR, R., HORNEMANN, S., GASPARINI, F., TRILLER, A. & AGUZZI, A. 2017. Inhibition of group-I metabotropic glutamate receptors protects against prion toxicity. *PLoS Pathog*, 13, e1006733.
- GOOLD, R., RABBANIAN, S., SUTTON, L., ANDRE, R., ARORA, P., MOONGA, J., CLARKE, A. R., SCHIAVO, G., JAT, P., COLLINGE, J. & TABRIZI, S. J. 2011. Rapid cell-surface prion protein conversion revealed using a novel cell system. *Nat Commun*, 2, 281.
- GOTTE, D. R., BENESTAD, S. L., LAUDE, H., ZURBRIGGEN, A., OEVERMANN, A. & SEUBERLICH, T. 2011. Atypical scrapie isolates involve a uniform prion species with a complex molecular signature. *PLoS One*, 6, e27510.
- GRANER, E., MERCADANTE, A. F., ZANATA, S. M., FORLENZA, O. V., CABRAL, A. L., VEIGA, S. S., JULIANO, M. A., ROESLER, R., WALZ, R., MINETTI, A., IZQUIERDO, I., MARTINS, V. R. & BRENTANI, R. R. 2000. Cellular prion protein binds laminin and mediates neuritogenesis. *Brain Res Mol Brain Res*, 76, 85-92.
- GRASSMANN, A., WOLF, H., HOFMANN, J., GRAHAM, J. & VORBERG, I. 2013. Cellular aspects of prion replication in vitro. *Viruses*, 5, 374-405.

- GRAY, B. C., SISOVA, Z., PERRY, V. H. & O'CONNOR, V. 2009. Selective presynaptic degeneration in the synaptopathy associated with ME7-induced hippocampal pathology. *Neurobiol Dis*, 35, 63-74.
- GROVEMAN, B. R., DOLAN, M. A., TAUBNER, L. M., KRAUS, A., WICKNER, R. B. & CAUGHEY, B. 2014. Parallel in-register intermolecular beta-sheet architectures for prion-seeded prion protein (PrP) amyloids. *J Biol Chem*, 289, 24129-42.
- GUILLOT-SESTIER, M. V., SUNYACH, C., DRUON, C., SCARZELLO, S. & CHECLER, F. 2009. The alpha-secretase-derived N-terminal product of cellular prion, N1, displays neuroprotective function in vitro and in vivo. *J Biol Chem*, 284, 35973-86.
- GUO, K., MUTTER, R., HEAL, W., REDDY, T. R., COPE, H., PRATT, S., THOMPSON, M. J. & CHEN, B. 2008. Synthesis and evaluation of a focused library of pyridine dicarbonitriles against prion disease. *Eur J Med Chem*, 43, 93-106.
- HADDON, D. J., HUGHES, M. R., ANTIGNANO, F., WESTAWAY, D., CASHMAN, N. R. & MCNAGNY, K. M. 2009. Prion protein expression and release by mast cells after activation. *J Infect Dis*, 200, 827-31.
- HADLOW, W. J., PRUSINER, S. B., KENNEDY, R. C. & RACE, R. E. 1980. Brain tissue from persons dying of Creutzfeldt-Jakob disease causes scrapie-like encephalopathy in goats. *Ann Neurol*, 8, 628-32.
- HAGIWARA, K., NAKAMURA, Y., NISHIJIMA, M. & YAMAKAWA, Y. 2007. Prevention of prion propagation by dehydrocholesterol reductase inhibitors in cultured cells and a therapeutic trial in mice. *Biol Pharm Bull*, 30, 835-8.
- HAIGH, C. L., MCGLADE, A. R. & COLLINS, S. J. 2015. MEK1 transduces the prion protein N2 fragment antioxidant effects. *Cell Mol Life Sci*, 72, 1613-29.
- HAIK, S., BRANDEL, J. P., SALOMON, D., SAZDOVITCH, V., DELASNERIE-LAUPRETRE, N., LAPLANCHE, J. L., FAUCHEUX, B. A., SOUBRIE, C., BOHER, E., BELORGEY, C., HAUW, J. J. & ALPEROVITCH, A. 2004. Compassionate use of quinacrine in Creutzfeldt-Jakob disease fails to show significant effects. *Neurology*, 63, 2413-5.
- HAIK, S., MARCON, G., MALLET, A., TETTAMANTI, M., WELARATNE, A., GIACCONE, G., AZIMI, S., PIETRINI, V., FABREGUETTES, J. R., IMPERIALE, D., CESARO, P., BUFFA, C., AUCAN, C., LUCCA, U., PECKEU, L., SUARDI, S., TRANCHANT, C., ZERR, I., HOUILLIER, C., REDAELLI, V., VESPIGNANI, H., CAMPANELLA, A., SELLAL, F., KRASNIANSKI, A., SEILHEAN, D., HEINEMANN, U., SEDEL, F., CANOVI, M., GOBBI, M., DI FEDE, G., LAPLANCHE, J. L., POCCHIARI, M., SALMONA, M., FORLONI, G., BRANDEL, J. P. & TAGLIAVINI, F. 2014. Doxycycline in Creutzfeldt-Jakob disease: a phase 2, randomised, double-blind, placebo-controlled trial. *Lancet Neurol*, 13, 150-8.
- HALDAR, S., TRIPATHI, A., QIAN, J., BESERRA, A., SUDA, S., MCELWEE, M., TURNER, J., HOPFER, U. & SINGH, N. 2015. Prion protein promotes kidney iron uptake via its ferrireductase activity. *J Biol Chem*, 290, 5512-22.
- HALLIDAY, M. & MALLUCCI, G. R. 2015. Review: Modulating the unfolded protein response to prevent neurodegeneration and enhance memory. *Neuropathol Appl Neurobiol*, 41, 414-27.
- HALLIDAY, M., RADFORD, H., ZENTS, K. A. M., MOLLOY, C., MORENO, J. A., VERITY, N. C., SMITH, E., ORTORI, C. A., BARRETT, D. A., BUSHELL, M. & MALLUCCI, G. R. 2017. Repurposed drugs targeting eIF2 α -P-mediated translational repression prevent neurodegeneration in mice. *Brain*, 140, 1768-1783.
- HANNAOUI, S., GOUGEROT, A., PRIVAT, N., LEVAVASSEUR, E., BIZAT, N., HAUW, J. J., BRANDEL, J. P. & HAIK, S. 2014. Cycline efficacy on the propagation of human prions in primary cultured neurons is strain-specific. *J Infect Dis*, 209, 1144-8.

- HARAGUCHI, T., FISHER, S., OLOFSSON, S., ENDO, T., GROTH, D., TARENTINO, A., BORCHELT, D. R., TEPLow, D., HOOD, L., BURLINGAME, A. & ET AL. 1989. Asparagine-linked glycosylation of the scrapie and cellular prion proteins. *Arch Biochem Biophys*, 274, 1-13.
- HARDING, H. P., ZENG, H., ZHANG, Y., JUNGRIES, R., CHUNG, P., PLESKEN, H., SABATINI, D. D. & RON, D. 2001. Diabetes mellitus and exocrine pancreatic dysfunction in *perk*^{-/-} mice reveals a role for translational control in secretory cell survival. *Mol Cell*, 7, 1153-63.
- HARRIS, D. A., CHIESA, R., DRISALDI, B., QUAGLIO, E., MIGHELI, A., PICCARDO, P. & GHETTI, B. 2003. A murine model of a familial prion disease. *Clin Lab Med*, 23, 175-86.
- HARRIS, D. A., HUBER, M. T., VAN DIJKEN, P., SHYNG, S. L., CHAIT, B. T. & WANG, R. 1993. Processing of a cellular prion protein: identification of N- and C-terminal cleavage sites. *Biochemistry*, 32, 1009-16.
- HARRIS, D. A. & TRUE, H. L. 2006. New insights into prion structure and toxicity. *Neuron*, 50, 353-7.
- HARRISON, P. M., KHACHANE, A. & KUMAR, M. 2010. Genomic assessment of the evolution of the prion protein gene family in vertebrates. *Genomics*, 95, 268-77.
- HARTMANN, C. A., MARTINS, V. R. & LIMA, F. R. 2013. High levels of cellular prion protein improve astrocyte development. *FEBS Lett*, 587, 238-44.
- HAVIV, Y., AVRAHAMI, D., OVADIA, H., BEN-HUR, T., GABIZON, R. & SHARON, R. 2008. Induced neuroprotection independently from PrPSc accumulation in a mouse model for prion disease treated with simvastatin. *Arch Neurol*, 65, 762-75.
- HAY, B., BARRY, R. A., LIEBERBURG, I., PRUSINER, S. B. & LINGAPPA, V. R. 1987. Biogenesis and transmembrane orientation of the cellular isoform of the scrapie prion protein [published erratum appears in *Mol Cell Biol* 1987 May;7(5):2035]. *Mol Cell Biol*, 7, 914-20.
- HEISEKE, A., AGUIB, Y., RIEMER, C., BAIER, M. & SCHATZL, H. M. 2009. Lithium induces clearance of protease resistant prion protein in prion-infected cells by induction of autophagy. *J Neurochem*, 109, 25-34.
- HEISEKE, A., AGUIB, Y. & SCHATZL, H. M. 2010. Autophagy, prion infection and their mutual interactions. *Curr Issues Mol Biol*, 12, 87-97.
- HEPPNER, F. L., MUSAHL, C., ARRIGHI, I., KLEIN, M. A., RULICKE, T., OESCH, B., ZINKERNAGEL, R. M., KALINKE, U. & AGUZZI, A. 2001. Prevention of scrapie pathogenesis by transgenic expression of anti-prion protein antibodies. *Science*, 294, 178-82.
- HERRAIZ, T., GONZALEZ, D., ANCIN-AZPILICUETA, C., ARAN, V. J. & GUILLEN, H. 2010. beta-Carboline alkaloids in *Peganum harmala* and inhibition of human monoamine oxidase (MAO). *Food Chem Toxicol*, 48, 839-45.
- HERVA, M. E., RELANO-GINES, A., VILLA, A. & TORRES, J. M. 2010. Prion infection of differentiated neurospheres. *J Neurosci Methods*, 188, 270-5.
- HETZ, C., RUSSELAKIS-CARNEIRO, M., MAUNDRELL, K., CASTILLA, J. & SOTO, C. 2003. Caspase-12 and endoplasmic reticulum stress mediate neurotoxicity of pathological prion protein. *EMBO J*, 22, 5435-45.
- HILL, A. F., ANTONIOU, M. & COLLINGE, J. 1999a. Protease-resistant prion protein produced in vitro lacks detectable infectivity. *J Gen Virol*, 80 (Pt 1), 11-4.
- HILL, A. F., BUTTERWORTH, R. J., JOINER, S., JACKSON, G., ROSSOR, M. N., THOMAS, D. J., FROSH, A., TOLLEY, N., BELL, J. E., SPENCER, M., KING, A., AL-SARRAJ, S., IRONSDALE, J. W., LANTOS, P. L. & COLLINGE, J. 1999b. Investigation of variant Creutzfeldt-Jakob disease and other human prion diseases with tonsil biopsy samples. *Lancet*, 353, 183-9.
- HILL, A. F., JOINER, S., LINEHAN, J., DESBRUSLAIS, M., LANTOS, P. L. & COLLINGE, J. 2000. Species-barrier-independent prion replication in apparently resistant species. *Proc Natl Acad Sci U S A*, 97, 10248-53.

- HOGAN, R. N., BARINGER, J. R. & PRUSINER, S. B. 1987. Scrapie infection diminishes spines and increases varicosities of dendrites in hamsters: a quantitative Golgi analysis. *J Neuropathol Exp Neurol*, 46, 461-73.
- HOPE, J., MORTON, L. J., FARQUHAR, C. F., MULTHAUP, G., BEYREUTHER, K. & KIMBERLIN, R. H. 1986. The major polypeptide of scrapie-associated fibrils (SAF) has the same size, charge distribution and N-terminal protein sequence as predicted for the normal brain protein (PrP). *EMBO J*, 5, 2591-7.
- HOPE, J., MULTHAUP, G., REEKIE, L. J., KIMBERLIN, R. H. & BEYREUTHER, K. 1988. Molecular pathology of scrapie-associated fibril protein (PrP) in mouse brain affected by the ME7 strain of scrapie. *Eur J Biochem*, 172, 271-7.
- HORNSHAW, M. P., MCDERMOTT, J. R., CANDY, J. M. & LAKEY, J. H. 1995. Copper binding to the N-terminal tandem repeat region of mammalian and avian prion protein: structural studies using synthetic peptides. *Biochem Biophys Res Commun*, 214, 993-9.
- HSIAO, K., BAKER, H. F., CROW, T. J., POULTER, M., OWEN, F., TERWILLIGER, J. D., WESTAWAY, D., OTT, J. & PRUSINER, S. B. 1989. Linkage of a prion protein missense variant to Gerstmann-Straussler syndrome. *Nature*, 338, 342-5.
- HSIAO, K., DLOUHY, S. R., FARLOW, M. R., CASS, C., DA COSTA, M., CONNEALLY, P. M., HODES, M. E., GHETTI, B. & PRUSINER, S. B. 1992. Mutant prion proteins in Gerstmann-Straussler-Scheinker disease with neurofibrillary tangles. *Nat Genet*, 1, 68-71.
- HSIAO, K. K., SCOTT, M., FOSTER, D., GROTH, D. F., DEARMOND, S. J. & PRUSINER, S. B. 1990. Spontaneous neurodegeneration in transgenic mice with mutant prion protein. *Science*, 250, 1587-90.
- HSICH, G., KENNEY, K., GIBBS, C. J., LEE, K. H. & HARRINGTON, M. G. 1996. The 14-3-3 brain protein in cerebrospinal fluid as a marker for transmissible spongiform encephalopathies. *N Engl J Med*, 335, 924-30.
- HUNG, M. S., XU, Z., CHEN, Y., SMITH, E., MAO, J. H., HSIEH, D., LIN, Y. C., YANG, C. T., JABLONS, D. M. & YOU, L. 2013. Hematein, a casein kinase II inhibitor, inhibits lung cancer tumor growth in a murine xenograft model. *Int J Oncol*, 43, 1517-22.
- HUNG, M. S., XU, Z., LIN, Y. C., MAO, J. H., YANG, C. T., CHANG, P. J., JABLONS, D. M. & YOU, L. 2009. Identification of hematein as a novel inhibitor of protein kinase CK2 from a natural product library. *BMC Cancer*, 9, 135.
- HUNTER, N. 1997. PrP genetics in sheep and the applications for scrapie and BSE. *Trends Microbiol*, 5, 331-4.
- HYEON, J. W., KIM, S. Y., LEE, S. M., LEE, J., AN, S. S., LEE, M. K. & LEE, Y. S. 2017. Anti-Prion Screening for Acridine, Dextran, and Tannic Acid using Real Time-Quaking Induced Conversion: A Comparison with PrPSc-Infected Cell Screening. *PLoS One*, 12, e0170266.
- IMBERDIS, T., HEERES, J. T., YUEH, H., FANG, C., ZHEN, J., RICH, C. B., GLICKSMAN, M., BEELER, A. B. & HARRIS, D. A. 2016. Identification of Anti-prion Compounds using a Novel Cellular Assay. *J Biol Chem*, 291, 26164-26176.
- IMRAN, M. & MAHMOOD, S. 2011. An overview of animal prion diseases. *Virology*, 8, 493.
- IRONSIDE, J. W., RITCHIE, D. L. & HEAD, M. W. 2017. Prion diseases. *Handb Clin Neurol*, 145, 393-403.
- ISHIKURA, N., CLEVER, J. L., BOUZAMONDO-BERNSTEIN, E., SAMAYOA, E., PRUSINER, S. B., HUANG, E. J. & DEARMOND, S. J. 2005. Notch-1 activation and dendritic atrophy in prion disease. *Proc Natl Acad Sci U S A*, 102, 886-91.
- IVANOVA, L., BARMADA, S., KUMMER, T. & HARRIS, D. A. 2001. Mutant prion proteins are partially retained in the endoplasmic reticulum. *J Biol Chem*, 276, 42409-21.

- IWAMARU, Y., TAKENOUCI, T., OGIHARA, K., HOSHINO, M., TAKATA, M., IMAMURA, M., TAGAWA, Y., HAYASHI-KATO, H., USHIKI-KAKU, Y., SHIMIZU, Y., OKADA, H., SHINAGAWA, M., KITANI, H. & YOKOYAMA, T. 2007. Microglial cell line established from prion protein-overexpressing mice is susceptible to various murine prion strains. *J Virol*, 81, 1524-7.
- IWASAKI, Y., MORI, K., ITO, M., AKAGI, A., MIMURO, M., KITAMOTO, T. & YOSHIDA, M. 2017. An autopsy case of Creutzfeldt-Jakob disease with a prion protein gene codon 180 mutation presenting with pathological laughing and an exaggerated startle reaction. *Neuropathology*, 37, 575-581.
- JACOB, H., PYRKOSCH, W. & STRUBE, H. 1950. [The hereditary form of Creutzfeldt-Jakob disease (the Backer family)]. *Arch Psychiatr Nervenkr Z Gesamte Neurol Psychiatr*, 184, 653-74.
- JAMES, T. L., LIU, H., ULYANOV, N. B., FARR-JONES, S., ZHANG, H., DONNE, D. G., KANEKO, K., GROTH, D., MEHLHORN, I., PRUSINER, S. B. & COHEN, F. E. 1997. Solution structure of a 142-residue recombinant prion protein corresponding to the infectious fragment of the scrapie isoform. *Proc Natl Acad Sci U S A*, 94, 10086-91.
- JEFFREY, M., FRASER, J. R., HALLIDAY, W. G., FOWLER, N., GOODSIR, C. M. & BROWN, D. A. 1995. Early unsuspected neuron and axon terminal loss in scrapie-infected mice revealed by morphometry and immunocytochemistry. *Neuropathol Appl Neurobiol*, 21, 41-9.
- JEFFREY, M. & GONZALEZ, L. 2007. Classical sheep transmissible spongiform encephalopathies: pathogenesis, pathological phenotypes and clinical disease. *Neuropathol Appl Neurobiol*, 33, 373-94.
- JEFFREY, M., MCGOVERN, G., GOODSIR, C. M., BROWN, K. L. & BRUCE, M. E. 2000. Sites of prion protein accumulation in scrapie-infected mouse spleen revealed by immuno-electron microscopy. *J Pathol*, 191, 323-32.
- JEONG, J. K., MOON, M. H., LEE, Y. J., SEOL, J. W. & PARK, S. Y. 2012. Melatonin-induced autophagy protects against human prion protein-mediated neurotoxicity. *J Pineal Res*, 53, 138-46.
- JIMENEZ-HUETE, A., LIEVENS, P. M., VIDAL, R., PICCARDO, P., GHETTI, B., TAGLIAVINI, F., FRANGIONE, B. & PRELLI, F. 1998. Endogenous proteolytic cleavage of normal and disease-associated isoforms of the human prion protein in neural and non-neural tissues. *Am J Pathol*, 153, 1561-72.
- JIMI, T., WAKAYAMA, Y., SHIBUYA, S., NAKATA, H., TOMARU, T., TAKAHASHI, Y., KOSAKA, K., ASANO, T. & KATO, K. 1992. High levels of nervous system-specific proteins in cerebrospinal fluid in patients with early stage Creutzfeldt-Jakob disease. *Clin Chim Acta*, 211, 37-46.
- JOHNSTON, A. R., FRASER, J. R., JEFFREY, M. & MACLEOD, N. 1998a. Alterations in potassium currents may trigger neurodegeneration in murine scrapie. *Exp Neurol*, 151, 326-33.
- JOHNSTON, A. R., FRASER, J. R., JEFFREY, M. & MACLEOD, N. 1998b. Synaptic plasticity in the CA1 area of the hippocampus of scrapie-infected mice. *Neurobiol Dis*, 5, 188-95.
- JONES, D. R., TAYLOR, W. A., BATE, C., DAVID, M. & TAYEBI, M. 2010. A camelid anti-PrP antibody abrogates PrP replication in prion-permissive neuroblastoma cell lines. *PLoS One*, 5, e9804.
- JOSHI-BARR, S., BETT, C., CHIANG, W. C., TREJO, M., GOEBEL, H. H., SIKORSKA, B., LIBERSKI, P., RAEBER, A., LIN, J. H., MASLIAH, E. & SIGURDSON, C. J. 2014. De novo prion aggregates trigger autophagy in skeletal muscle. *J Virol*, 88, 2071-82.
- KANAANI, J., PRUSINER, S. B., DIACOVO, J., BAEKKESKOV, S. & LEGNAME, G. 2005. Recombinant prion protein induces rapid polarization and development of synapses in embryonic rat hippocampal neurons in vitro. *J Neurochem*, 95, 1373-86.
- KANG, Y. S., ZHAO, X., LOVAAS, J., EISENBERG, E. & GREENE, L. E. 2009. Clathrin-independent internalization of normal cellular prion protein in neuroblastoma cells is associated with the Arf6 pathway. *J Cell Sci*, 122, 4062-9.

- KARAPETYAN, Y. E., SFERRAZZA, G. F., ZHOU, M., OTTENBERG, G., SPICER, T., CHASE, P., FALLAHI, M., HODDER, P., WEISSMANN, C. & LASMEZAS, C. I. 2013. Unique drug screening approach for prion diseases identifies tacrolimus and astemizole as antiprion agents. *Proc Natl Acad Sci U S A*, 110, 7044-9.
- KASCSEK, R. J., RUBENSTEIN, R. & CARP, R. I. 1991. Evidence for biological and structural diversity among scrapie strains. *Curr Top Microbiol Immunol*, 172, 139-52.
- KATZ, M. & KOPROWSKI, H. 1968. Failure to demonstrate a relationship between scrapie and production of interferon in mice. *Nature*, 219, 639-40.
- KAWATAKE, S., NISHIMURA, Y., SAKAGUCHI, S., IWAKI, T. & DOH-URA, K. 2006. Surface plasmon resonance analysis for the screening of anti-prion compounds. *Biol Pharm Bull*, 29, 927-32.
- KEMPSTER, S., BATE, C. & WILLIAMS, A. 2007. Simvastatin treatment prolongs the survival of scrapie-infected mice. *Neuroreport*, 18, 479-82.
- KHOSRAVANI, H., ZHANG, Y., TSUTSUI, S., HAMEED, S., ALTIER, C., HAMID, J., CHEN, L., VILLEMAIRE, M., ALI, Z., JIRIK, F. R. & ZAMPONI, G. W. 2008. Prion protein attenuates excitotoxicity by inhibiting NMDA receptors. *J Gen Physiol*, 131, i5.
- KIMBERLIN, R. H. & WALKER, C. 1977. Characteristics of a short incubation model of scrapie in the golden hamster. *J Gen Virol*, 34, 295-304.
- KIMBERLIN, R. H. & WALKER, C. A. 1978. Evidence that the transmission of one source of scrapie agent to hamsters involves separation of agent strains from a mixture. *J Gen Virol*, 39, 487-96.
- KIRBY, L., BIRKETT, C. R., RUDYK, H., GILBERT, I. H. & HOPE, J. 2003. In vitro cell-free conversion of bacterial recombinant PrP to PrPres as a model for conversion. *J Gen Virol*, 84, 1013-20.
- KITAMOTO, T., SHIN, R. W., DOH-URA, K., TOMOKANE, N., MIYAZONO, M., MURAMOTO, T. & TATEISHI, J. 1992. Abnormal isoform of prion proteins accumulates in the synaptic structures of the central nervous system in patients with Creutzfeldt-Jakob disease. *Am J Pathol*, 140, 1285-94.
- KITAMOTO, T., TATEISHI, J. & SATO, Y. 1988. Immunohistochemical verification of senile and kuru plaques in Creutzfeldt-Jakob disease and the allied disease. *Ann Neurol*, 24, 537-42.
- KITAMOTO, T., TATEISHI, J., TASHIMA, T., TAKESHITA, I., BARRY, R. A., DEARMOND, S. J. & PRUSINER, S. B. 1986. Amyloid plaques in Creutzfeldt-Jakob disease stain with prion protein antibodies. *Ann Neurol*, 20, 204-8.
- KLEENE, R., LOERS, G., LANGER, J., FROBERT, Y., BUCK, F. & SCHACHNER, M. 2007. Prion protein regulates glutamate-dependent lactate transport of astrocytes. *J Neurosci*, 27, 12331-40.
- KLINGENSTEIN, R., LOBER, S., KUJALA, P., GODSAVE, S., LELIVELD, S. R., GMEINER, P., PETERS, P. J. & KORTH, C. 2006. Tricyclic antidepressants, quinacrine and a novel, synthetic chimera thereof clear prions by destabilizing detergent-resistant membrane compartments. *J Neurochem*, 98, 748-59.
- KLUNK, W. E., DEBNATH, M. L., KOROS, A. M. & PETTEGREW, J. W. 1998. Chrysamine-G, a lipophilic analogue of Congo red, inhibits A beta-induced toxicity in PC12 cells. *Life Sci*, 63, 1807-14.
- KLUNK, W. E., DEBNATH, M. L. & PETTEGREW, J. W. 1994. Development of small molecule probes for the beta-amyloid protein of Alzheimer's disease. *Neurobiol Aging*, 15, 691-8.
- KOCISKO, D. A., BARON, G. S., RUBENSTEIN, R., CHEN, J., KUIZON, S. & CAUGHEY, B. 2003. New inhibitors of scrapie-associated prion protein formation in a library of 2000 drugs and natural products. *J Virol*, 77, 10288-94.
- KOCISKO, D. A., COME, J. H., PRIOLA, S. A., CHESEBRO, B., RAYMOND, G. J., LANSBURY, P. T. & CAUGHEY, B. 1994. Cell-free formation of protease-resistant prion protein. *Nature*, 370, 471-4.

- KONDRU, N., MANNE, S., GREENLEE, J., WEST GREENLEE, H., ANANTHARAM, V., HALBUR, P., KANTHASAMY, A. & KANTHASAMY, A. 2017. Integrated Organotypic Slice Cultures and RT-QuIC (OSCAR) Assay: Implications for Translational Discovery in Protein Misfolding Diseases. *Sci Rep*, 7, 43155.
- KONOLD, T., MOORE, S. J., BELLWORTHY, S. J. & SIMMONS, H. A. 2008. Evidence of scrapie transmission via milk. *BMC Vet Res*, 4, 14.
- KORTH, C., KANEKO, K. & PRUSINER, S. B. 2000. Expression of unglycosylated mutated prion protein facilitates PrP(Sc) formation in neuroblastoma cells infected with different prion strains. *J Gen Virol*, 81, 2555-63.
- KORTH, C., MAY, B. C., COHEN, F. E. & PRUSINER, S. B. 2001. Acridine and phenothiazine derivatives as pharmacotherapeutics for prion disease. *Proc Natl Acad Sci U S A*, 98, 9836-41.
- KOVACS, G. G. & BUDKA, H. 2008. Prion diseases: from protein to cell pathology. *Am J Pathol*, 172, 555-65.
- KOVANEN, J., HALTIA, M. & CANTELL, K. 1980. Failure of interferon to modify Creutzfeldt-Jakob disease. *Br Med J*, 280, 902.
- KREBS, B., WIEBELITZ, A., BALITZKI-KORTE, B., VASSALLO, N., PALUCH, S., MITTEREGGER, G., ONODERA, T., KRETZSCHMAR, H. A. & HERMS, J. 2007. Cellular prion protein modulates the intracellular calcium response to hydrogen peroxide. *J Neurochem*, 100, 358-67.
- KRETZSCHMAR, H. A., STOWRING, L. E., WESTAWAY, D., STUBBLEBINE, W. H., PRUSINER, S. B. & DEARMOND, S. J. 1986. Molecular cloning of a human prion protein cDNA. *DNA*, 5, 315-24.
- KRETZSCHMAR, H. A., TINGS, T., MADLUNG, A., GIESE, A. & HERMS, J. 2000. Function of PrP(C) as a copper-binding protein at the synapse. *Arch Virol Suppl*, 239-49.
- KUBOTA, T., HAMAZOE, Y., HASHIGUCHI, S., ISHIBASHI, D., AKASAKA, K., NISHIDA, N., KATAMINE, S., SAKAGUCHI, S., KUROKI, R., NAKASHIMA, T. & SUGIMURA, K. 2012. Direct evidence of generation and accumulation of beta-sheet-rich prion protein in scrapie-infected neuroblastoma cells with human IgG1 antibody specific for beta-form prion protein. *J Biol Chem*, 287, 14023-39.
- KUFFER, A., LAKKARAJU, A. K., MOGHA, A., PETERSEN, S. C., AIRICH, K., DOUCERAIN, C., MARPAKWAR, R., BAKIRCI, P., SENATORE, A., MONNARD, A., SCHIAVI, C., NUVOLONE, M., GROSSHANS, B., HORNEMANN, S., BASSILANA, F., MONK, K. R. & AGUZZI, A. 2016. The prion protein is an agonistic ligand of the G protein-coupled receptor Adgrg6. *Nature*, 536, 464-8.
- LANDIS, D. M., WILLIAMS, R. S. & MASTERS, C. L. 1981. Golgi and electronmicroscopic studies of spongiform encephalopathy. *Neurology*, 31, 538-49.
- LASMEZAS, C. I., DESLYS, J. P., DEMAIMAY, R., ADJOU, K. T., LAMOURY, F., DORMONT, D., ROBAIN, O., IRONSIDE, J. & HAUW, J. J. 1996. BSE transmission to macaques. *Nature*, 381, 743-4.
- LAUREN, J., GIMBEL, D. A., NYGAARD, H. B., GILBERT, J. W. & STRITTMATTER, S. M. 2009. Cellular prion protein mediates impairment of synaptic plasticity by amyloid-beta oligomers. *Nature*, 457, 1128-32.
- LAWSON, V. A., VELLA, L. J., STEWART, J. D., SHARPLES, R. A., KLEMM, H., MACHALEK, D. M., MASTERS, C. L., CAPPAL, R., COLLINS, S. J. & HILL, A. F. 2008. Mouse-adapted sporadic human Creutzfeldt-Jakob disease prions propagate in cell culture. *Int J Biochem Cell Biol*, 40, 2793-801.
- LEGNAME, G., BASKAKOV, I. V., NGUYEN, H. O., RIESNER, D., COHEN, F. E., DEARMOND, S. J. & PRUSINER, S. B. 2004. Synthetic mammalian prions. *Science*, 305, 673-6.
- LEHMANN, S. & HARRIS, D. A. 1996. Two mutant prion proteins expressed in cultured cells acquire biochemical properties reminiscent of the scrapie isoform. *Proc Natl Acad Sci U S A*, 93, 5610-4.

- LEWIS, V., HILL, A. F., HAIGH, C. L., KLUG, G. M., MASTERS, C. L., LAWSON, V. A. & COLLINS, S. J. 2009. Increased proportions of C1 truncated prion protein protect against cellular M1000 prion infection. *J Neuropathol Exp Neurol*, 68, 1125-35.
- LI, A., CHRISTENSEN, H. M., STEWART, L. R., ROTH, K. A., CHIESA, R. & HARRIS, D. A. 2007. Neonatal lethality in transgenic mice expressing prion protein with a deletion of residues 105-125. *EMBO J*, 26, 548-58.
- LIANG, J. & KONG, Q. 2012. alpha-Cleavage of cellular prion protein. *Prion*, 6, 453-60.
- LIAO, Y. C., LEBO, R. V., CLAWSON, G. A. & SMUCKLER, E. A. 1986. Human prion protein cDNA: molecular cloning, chromosomal mapping, and biological implications. *Science*, 233, 364-7.
- LIBERSKI, P. P. 1990. Ultrastructural neuropathologic features of bovine spongiform encephalopathy. *J Am Vet Med Assoc*, 196, 1682.
- LIBERSKI, P. P., BROWN, D. R., SIKORSKA, B., CAUGHEY, B. & BROWN, P. 2008. Cell death and autophagy in prion diseases (transmissible spongiform encephalopathies). *Folia Neuropathol*, 46, 1-25.
- LIBERSKI, P. P., GAJDUSEK, D. C. & BROWN, P. 2002. How do neurons degenerate in prion diseases or transmissible spongiform encephalopathies (TSEs): neuronal autophagy revisited. *Acta Neurobiol Exp (Wars)*, 62, 141-7.
- LIBERSKI, P. P., SIKORSKA, B., BRATOSIEWICZ-WASIK, J., GAJDUSEK, D. C. & BROWN, P. 2004. Neuronal cell death in transmissible spongiform encephalopathies (prion diseases) revisited: from apoptosis to autophagy. *Int J Biochem Cell Biol*, 36, 2473-90.
- LIMA, F. R., ARANTES, C. P., MURAS, A. G., NOMIZO, R., BRENTANI, R. R. & MARTINS, V. R. 2007. Cellular prion protein expression in astrocytes modulates neuronal survival and differentiation. *J Neurochem*, 103, 2164-76.
- LINDEN, R., MARTINS, V. R., PRADO, M. A., CAMMAROTA, M., IZQUIERDO, I. & BRENTANI, R. R. 2008. Physiology of the prion protein. *Physiol Rev*, 88, 673-728.
- LIPTON, S. A., CHOI, Y. B., PAN, Z. H., LEI, S. Z., CHEN, H. S., SUCHER, N. J., LOSCALZO, J., SINGEL, D. J. & STAMLER, J. S. 1993. A redox-based mechanism for the neuroprotective and neurodestructive effects of nitric oxide and related nitroso-compounds. *Nature*, 364, 626-32.
- LIU, H., FARR-JONES, S., ULYANOV, N. B., LLINAS, M., MARQUSEE, S., GROTH, D., COHEN, F. E., PRUSINER, S. B. & JAMES, T. L. 1999. Solution structure of Syrian hamster prion protein rPrP(90-231). *Biochemistry*, 38, 5362-77.
- LLORENS, F., CARULLA, P., VILLA, A., TORRES, J. M., FORTES, P., FERRER, I. & DEL RIO, J. A. 2013. PrP(C) regulates epidermal growth factor receptor function and cell shape dynamics in Neuro2a cells. *J Neurochem*, 127, 124-38.
- LOLLI, G., NARESSI, D., SARNO, S. & BATTISTUTTA, R. 2017. Characterization of the oligomeric states of the CK2 alpha2beta2 holoenzyme in solution. *Biochem J*, 474, 2405-2416.
- LOLLI, G., PINNA, L. A. & BATTISTUTTA, R. 2012. Structural determinants of protein kinase CK2 regulation by autoinhibitory polymerization. *ACS Chem Biol*, 7, 1158-63.
- LOLLI, G., RANCHIO, A. & BATTISTUTTA, R. 2014. Active form of the protein kinase CK2 alpha2beta2 holoenzyme is a strong complex with symmetric architecture. *ACS Chem Biol*, 9, 366-71.
- LOPES, M. H., HAJJ, G. N., MURAS, A. G., MANCINI, G. L., CASTRO, R. M., RIBEIRO, K. C., BRENTANI, R. R., LINDEN, R. & MARTINS, V. R. 2005. Interaction of cellular prion and stress-inducible protein 1 promotes neuritogenesis and neuroprotection by distinct signaling pathways. *J Neurosci*, 25, 11330-9.
- LORENZ, H., WINDL, O. & KRETZSCHMAR, H. A. 2002. Cellular phenotyping of secretory and nuclear prion proteins associated with inherited prion diseases. *J Biol Chem*, 277, 8508-16.

- LOUBET, D., DAKOWSKI, C., PIETRI, M., PRADINES, E., BERNARD, S., CALLEBERT, J., ARDILA-OSORIO, H., MOUILLET-RICHARD, S., LAUNAY, J. M., KELLERMANN, O. & SCHNEIDER, B. 2012. Neuritogenesis: the prion protein controls beta1 integrin signaling activity. *FASEB J*, 26, 678-90.
- LUGARESI, E., MEDORI, R., MONTAGNA, P., BARUZZI, A., CORTELLI, P., LUGARESI, A., TINUPER, P., ZUCCONI, M. & GAMBETTI, P. 1986. Fatal familial insomnia and dysautonomia with selective degeneration of thalamic nuclei. *N Engl J Med*, 315, 997-1003.
- LUK, C., JONES, S., THOMAS, C., FOX, N. C., MOK, T. H., MEAD, S., COLLINGE, J. & JACKSON, G. S. 2016. Diagnosing Sporadic Creutzfeldt-Jakob Disease by the Detection of Abnormal Prion Protein in Patient Urine. *JAMA Neurol*, 73, 1454-1460.
- MAGALHAES, A. C., SILVA, J. A., LEE, K. S., MARTINS, V. R., PRADO, V. F., FERGUSON, S. S., GOMEZ, M. V., BRENTANI, R. R. & PRADO, M. A. 2002. Endocytic intermediates involved with the intracellular trafficking of a fluorescent cellular prion protein. *J Biol Chem*, 277, 33311-8.
- MAKRINO, E., COLLINGE, J. & ANTONIOU, M. 2002. Genomic characterization of the human prion protein (PrP) gene locus. *Mamm Genome*, 13, 696-703.
- MALLUCCI, G., DICKINSON, A., LINEHAN, J., KLOHN, P. C., BRANDNER, S. & COLLINGE, J. 2003. Depleting neuronal PrP in prion infection prevents disease and reverses spongiosis. *Science*, 302, 871-4.
- MALLUCCI, G. R., RATTE, S., ASANTE, E. A., LINEHAN, J., GOWLAND, I., JEFFERYS, J. G. & COLLINGE, J. 2002. Post-natal knockout of prion protein alters hippocampal CA1 properties, but does not result in neurodegeneration. *EMBO J*, 21, 202-10.
- MALLUCCI, G. R., WHITE, M. D., FARMER, M., DICKINSON, A., KHATUN, H., POWELL, A. D., BRANDNER, S., JEFFERYS, J. G. & COLLINGE, J. 2007. Targeting cellular prion protein reverses early cognitive deficits and neurophysiological dysfunction in prion-infected mice. *Neuron*, 53, 325-35.
- MANGE, A., BERANGER, F., PEOC'H, K., ONODERA, T., FROBERT, Y. & LEHMANN, S. 2004. Alpha- and beta- cleavages of the amino-terminus of the cellular prion protein. *Biol Cell*, 96, 125-32.
- MANSON, J. C., CLARKE, A. R., HOOPER, M. L., AITCHISON, L., MCCONNELL, I. & HOPE, J. 1994. 129/Ola mice carrying a null mutation in PrP that abolishes mRNA production are developmentally normal. *Mol Neurobiol*, 8, 121-7.
- MANSON, J. C., JAMIESON, E., BAYBUTT, H., TUZI, N. L., BARRON, R., MCCONNELL, I., SOMERVILLE, R., IRONSIDE, J., WILL, R., SY, M. S., MELTON, D. W., HOPE, J. & BOSTOCK, C. 1999. A single amino acid alteration (101L) introduced into murine PrP dramatically alters incubation time of transmissible spongiform encephalopathy. *EMBO J*, 18, 6855-64.
- MARELLA, M., LEHMANN, S., GRASSI, J. & CHABRY, J. 2002. Filipin prevents pathological prion protein accumulation by reducing endocytosis and inducing cellular PrP release. *J Biol Chem*, 277, 25457-64.
- MARIJANOVIC, Z., CAPUTO, A., CAMPANA, V. & ZURZOLO, C. 2009. Identification of an intracellular site of prion conversion. *PLoS Pathog*, 5, e1000426.
- MASSIGNAN, T., BIASINI, E. & HARRIS, D. A. 2011. A Drug-Based Cellular Assay (DBCA) for studying cytotoxic and cytoprotective activities of the prion protein: A practical guide. *Methods*, 53, 214-9.
- MASSIGNAN, T., CIMINI, S., STINCARDINI, C., CEROVIC, M., VANNI, I., ELEZGARAI, S. R., MORENO, J., STRAVALACI, M., NEGRO, A., SANGIOVANNI, V., RESTELLI, E., RICCARDI, G., GOBBI, M., CASTILLA, J., BORSELLO, T., NONNO, R. & BIASINI, E. 2016. A cationic tetrapyrrole inhibits toxic activities of the cellular prion protein. *Sci Rep*, 6, 23180.

- MASSIGNAN, T., SANGIOVANNI, V., BIGGI, S., STINCARDINI, C., ELEZGARAI, S. R., MAIETTA, G., ANDREEV, I. A., RATMANOVA, N. K., BELOV, D. S., LUKYANENKO, E. R., BELOV, G. M., BARRECA, M. L., ALTIERI, A., KURKIN, A. V. & BIASINI, E. 2017. A Small-Molecule Inhibitor of Prion Replication and Mutant Prion Protein Toxicity. *ChemMedChem*, 12, 1286-1292.
- MASSIGNAN, T., STEWART, R. S., BIASINI, E., SOLOMON, I. H., BONETTO, V., CHIESA, R. & HARRIS, D. A. 2010. A novel, drug-based, cellular assay for the activity of neurotoxic mutants of the prion protein. *J Biol Chem*, 285, 7752-65.
- MASTERS, C. L., GAJDUSEK, D. C. & GIBBS, C. J., JR. 1981. Creutzfeldt-Jakob disease virus isolations from the Gerstmann-Straussler syndrome with an analysis of the various forms of amyloid plaque deposition in the virus-induced spongiform encephalopathies. *Brain*, 104, 559-88.
- MASULLO, C., MACCHI, G., XI, Y. G. & POCCHIARI, M. 1992. Failure to ameliorate Creutzfeldt-Jakob disease with amphotericin B therapy. *J Infect Dis*, 165, 784-5.
- MATAMOROS-ANGLES, A., GAYOSSO, L. M., RICHAUD-PATIN, Y., DI DOMENICO, A., VERGARA, C., HERVERA, A., SOUSA, A., FERNANDEZ-BORGES, N., CONSIGLIO, A., GAVIN, R., LOPEZ DE MATORANA, R., FERRER, I., LOPEZ DE MUNAIN, A., RAYA, A., CASTILLA, J., SANCHEZ-PERNAUTE, R. & DEL RIO, J. A. 2018. iPS Cell Cultures from a Gerstmann-Straussler-Scheinker Patient with the Y218N PRNP Mutation Recapitulate tau Pathology. *Mol Neurobiol*, 55, 3033-3048.
- MATHEWS, J. D. 1968. A transmission model for kuru. *Proc Aust Assoc Neurol*, 5, 325-9.
- MATHEWS, J. D., GLASSE, R. & LINDENBAUM, S. 1968. Kuru and cannibalism. *Lancet*, 2, 449-52.
- MATHIASON, C. K., POWERS, J. G., DAHMES, S. J., OSBORN, D. A., MILLER, K. V., WARREN, R. J., MASON, G. L., HAYS, S. A., HAYES-KLUG, J., SEELIG, D. M., WILD, M. A., WOLFE, L. L., SPRAKER, T. R., MILLER, M. W., SIGURDSON, C. J., TELLING, G. C. & HOOVER, E. A. 2006. Infectious prions in the saliva and blood of deer with chronic wasting disease. *Science*, 314, 133-6.
- MAYOR, S. & RIEZMAN, H. 2004. Sorting GPI-anchored proteins. *Nat Rev Mol Cell Biol*, 5, 110-20.
- MCDONALD, A. J. & MILLHAUSER, G. L. 2014. PrP overdrive: does inhibition of alpha-cleavage contribute to PrP(C) toxicity and prion disease? *Prion*, 8.
- MCGUIRE, L. I., PEDEN, A. H., ORRU, C. D., WILHAM, J. M., APPLEFORD, N. E., MALLINSON, G., ANDREWS, M., HEAD, M. W., CAUGHEY, B., WILL, R. G., KNIGHT, R. S. & GREEN, A. J. 2012. Real time quaking-induced conversion analysis of cerebrospinal fluid in sporadic Creutzfeldt-Jakob disease. *Ann Neurol*, 72, 278-85.
- MCKINLEY, M. P., TARABOULOS, A., KENAGA, L., SERBAN, D., STIEBER, A., DEARMOND, S. J., PRUSINER, S. B. & GONATAS, N. 1991. Ultrastructural localization of scrapie prion proteins in cytoplasmic vesicles of infected cultured cells. *Lab Invest*, 65, 622-30.
- MCMAHON, H. E., MANGE, A., NISHIDA, N., CREMINON, C., CASANOVA, D. & LEHMANN, S. 2001. Cleavage of the amino terminus of the prion protein by reactive oxygen species. *J Biol Chem*, 276, 2286-91.
- MCNALLY, K. L., WARD, A. E. & PRIOLA, S. A. 2009. Cells expressing anchorless prion protein are resistant to scrapie infection. *J Virol*, 83, 4469-75.
- MEDORI, R. & TRITSCHLER, H. J. 1993. Prion protein gene analysis in three kindreds with fatal familial insomnia (FFI): codon 178 mutation and codon 129 polymorphism. *Am J Hum Genet*, 53, 822-7.
- MEDORI, R., TRITSCHLER, H. J., LEBLANC, A., VILLARE, F., MANETTO, V., CHEN, H. Y., XUE, R., LEAL, S., MONTAGNA, P., CORTELLI, P. & ET AL. 1992. Fatal familial insomnia, a prion disease with a mutation at codon 178 of the prion protein gene. *N Engl J Med*, 326, 444-9.
- MEGGIO, F., NEGRO, A., SARNO, S., RUZZENE, M., BERTOLI, A., SORGATO, M. C. & PINNA, L. A. 2000. Bovine prion protein as a modulator of protein kinase CK2. *Biochem J*, 352 Pt 1, 191-6.

- MENEGHETTI, E., GASPERINI, L., VIRGILIO, T., MODA, F., TAGLIAVINI, F., BENETTI, F. & LEGNAME, G. 2019. Prions Strongly Reduce NMDA Receptor S-Nitrosylation Levels at Pre-symptomatic and Terminal Stages of Prion Diseases. *Mol Neurobiol*, 56, 6035-6045.
- MERCER, R. C. & HARRIS, D. A. 2019. Identification of anti-prion drugs and targets using toxicity-based assays. *Curr Opin Pharmacol*, 44, 20-27.
- MEYER, R. K., MCKINLEY, M. P., BOWMAN, K. A., BRAUNFELD, M. B., BARRY, R. A. & PRUSINER, S. B. 1986. Separation and properties of cellular and scrapie prion proteins. *Proc Natl Acad Sci U S A*, 83, 2310-4.
- MIELE, G., JEFFREY, M., TURNBULL, D., MANSON, J. & CLINTON, M. 2002. Ablation of cellular prion protein expression affects mitochondrial numbers and morphology. *Biochem Biophys Res Commun*, 291, 372-7.
- MILHAVET, O., MANGE, A., CASANOVA, D. & LEHMANN, S. 2000. Effect of Congo red on wild-type and mutated prion proteins in cultured cells. *J Neurochem*, 74, 222-30.
- MILLSON, G. C., HUNTER, G. D. & KIMBERLIN, R. H. 1971. An experimental examination of the scrapie agent in cell membrane mixtures. II. The association of scrapie activity with membrane fractions. *J Comp Pathol*, 81, 255-65.
- MODA, F., GAMBETTI, P., NOTARI, S., CONCHA-MARAMBIO, L., CATANIA, M., PARK, K. W., MADERNA, E., SUARDI, S., HAIK, S., BRANDEL, J. P., IRONSIDE, J., KNIGHT, R., TAGLIAVINI, F. & SOTO, C. 2014. Prions in the urine of patients with variant Creutzfeldt-Jakob disease. *N Engl J Med*, 371, 530-9.
- MOK, S. W., THELEN, K. M., RIEMER, C., BAMME, T., GULTNER, S., LUTJOHANN, D. & BAIER, M. 2006. Simvastatin prolongs survival times in prion infections of the central nervous system. *Biochem Biophys Res Commun*, 348, 697-702.
- MOORE, R. C., MASTRANGELO, P., BOUZAMONDO, E., HEINRICH, C., LEGNAME, G., PRUSINER, S. B., HOOD, L., WESTAWAY, D., DEARMOND, S. J. & TREMBLAY, P. 2001. Doppel-induced cerebellar degeneration in transgenic mice. *Proc Natl Acad Sci U S A*, 98, 15288-93.
- MOORE, R. C., REDHEAD, N. J., SELFRIDGE, J., HOPE, J., MANSON, J. C. & MELTON, D. W. 1995. Double replacement gene targeting for the production of a series of mouse strains with different prion protein gene alterations. *Biotechnology (N Y)*, 13, 999-1004.
- MORENO, J. A., HALLIDAY, M., MOLLOY, C., RADFORD, H., VERITY, N., AXTEN, J. M., ORTORI, C. A., WILLIS, A. E., FISCHER, P. M., BARRETT, D. A. & MALLUCCI, G. R. 2013. Oral treatment targeting the unfolded protein response prevents neurodegeneration and clinical disease in prion-infected mice. *Sci Transl Med*, 5, 206ra138.
- MORENO, J. A., RADFORD, H., PERETTI, D., STEINERT, J. R., VERITY, N., MARTIN, M. G., HALLIDAY, M., MORGAN, J., DINSDALE, D., ORTORI, C. A., BARRETT, D. A., TSAYTLER, P., BERTOLOTTI, A., WILLIS, A. E., BUSHELL, M. & MALLUCCI, G. R. 2012. Sustained translational repression by eIF2alpha-P mediates prion neurodegeneration. *Nature*, 485, 507-11.
- MOSER, M., COLELLO, R. J., POTT, U. & OESCH, B. 1995. Developmental expression of the prion protein gene in glial cells. *Neuron*, 14, 509-17.
- MUKHERJEE, A., MORALES-SCHEIHING, D., GONZALEZ-ROMERO, D., GREEN, K., TAGLIALATELA, G. & SOTO, C. 2010. Calcineurin inhibition at the clinical phase of prion disease reduces neurodegeneration, improves behavioral alterations and increases animal survival. *PLoS Pathog*, 6, e1001138.
- MURALI, A., MAUE, R. A. & DOLPH, P. J. 2014. Reversible symptoms and clearance of mutant prion protein in an inducible model of a genetic prion disease in *Drosophila melanogaster*. *Neurobiol Dis*, 67, 71-8.

- NAKAGAKI, T., SATOH, K., ISHIBASHI, D., FUSE, T., SANO, K., KAMATARI, Y. O., KUWATA, K., SHIGEMATSU, K., IWAMARU, Y., TAKENOUCI, T., KITANI, H., NISHIDA, N. & ATARASHI, R. 2013. FK506 reduces abnormal prion protein through the activation of autolysosomal degradation and prolongs survival in prion-infected mice. *Autophagy*, 9, 1386-94.
- NAKAGAWA, T., ZHU, H., MORISHIMA, N., LI, E., XU, J., YANKNER, B. A. & YUAN, J. 2000. Caspase-12 mediates endoplasmic-reticulum-specific apoptosis and cytotoxicity by amyloid-beta. *Nature*, 403, 98-103.
- NAZOR, K. E., KUHN, F., SEWARD, T., GREEN, M., ZWALD, D., PURRO, M., SCHMID, J., BIFFIGER, K., POWER, A. M., OESCH, B., RAEHER, A. J. & TELLING, G. C. 2005. Immunodetection of disease-associated mutant PrP, which accelerates disease in GSS transgenic mice. *EMBO J*, 24, 2472-80.
- NEGRO, A., MEGGIO, F., BERTOLI, A., BATTISTUTTA, R., SORGATO, M. C. & PINNA, L. A. 2000. Susceptibility of the prion protein to enzymic phosphorylation. *Biochem Biophys Res Commun*, 271, 337-41.
- NERI, G., FIGA-TALAMANCA, L., DI BATTISTA, G. C. & LO RUSSO, F. 1984. [Amantadine in Creutzfeldt-Jakob disease. Review of the literature and case contribution]. *Riv Neurobiol*, 30, 47-56.
- NEWMAN, P. K. 1984. Acyclovir in Creutzfeldt-Jakob disease. *Lancet*, 1, 793.
- NGUYEN, X. T. A., TRAN, T. H., COJOC, D. & LEGNAME, G. 2019. Copper Binding Regulates Cellular Prion Protein Function. *Mol Neurobiol*, 56, 6121-6133.
- NICOLL, A. J. & COLLINGE, J. 2009. Preventing prion pathogenicity by targeting the cellular prion protein. *Infect Disord Drug Targets*, 9, 48-57.
- NICOLL, A. J., TREVITT, C. R., TATTUM, M. H., RISSE, E., QUARTERMAN, E., IBARRA, A. A., WRIGHT, C., JACKSON, G. S., SESSIONS, R. B., FARROW, M., WALTHO, J. P., CLARKE, A. R. & COLLINGE, J. 2010. Pharmacological chaperone for the structured domain of human prion protein. *Proc Natl Acad Sci U S A*, 107, 17610-5.
- NIEZNAWSKA, H., BANDYSZEWSKA, M., SUREWICZ, K., ZAJKOWSKI, T., SUREWICZ, W. K. & NIEZNAWSKI, K. 2018. Identification of prion protein-derived peptides of potential use in Alzheimer's disease therapy. *Biochim Biophys Acta Mol Basis Dis*, 1864, 2143-2153.
- NISHIMURA, T., SAKUDO, A., HASHIYAMA, Y., YACHI, A., SAEKI, K., MATSUMOTO, Y., OGAWA, M., SAKAGUCHI, S., ITOHARA, S. & ONODERA, T. 2007. Serum withdrawal-induced apoptosis in Zrch1 prion protein (PrP) gene-deficient neuronal cell line is suppressed by PrP, independent of Doppel. *Microbiol Immunol*, 51, 457-66.
- NOBLE, G. P. & SUPATTAPONE, S. 2015. Dissociation of recombinant prion autocatalysis from infectivity. *Prion*, 9, 405-11.
- NOH, K., LEE, H., CHOI, T. Y., JOO, Y., KIM, S. J., KIM, H., KIM, J. Y., JAHNG, J. W., LEE, S., CHOI, S. Y. & LEE, S. J. 2019. Negr1 controls adult hippocampal neurogenesis and affective behaviors. *Mol Psychiatry*, 24, 1189-1205.
- NONNO, R., DI BARI, M. A., CARDONE, F., VACCARI, G., FAZZI, P., DELL'OMO, G., CARTONI, C., INGROSSO, L., BOYLE, A., GALENO, R., SBRICCOLI, M., LIPP, H. P., BRUCE, M., POCCHIARI, M. & AGRIMI, U. 2006. Efficient transmission and characterization of Creutzfeldt-Jakob disease strains in bank voles. *PLoS Pathog*, 2, e12.
- NOVAKOFSKI, J., BREWER, M. S., MATEUS-PINILLA, N., KILLEFER, J. & MCCUSKER, R. H. 2005. Prion biology relevant to bovine spongiform encephalopathy. *J Anim Sci*, 83, 1455-76.
- NUNEZ DE VILLAVICENCIO-DIAZ, T., RABALSKI, A. J. & LITCHFIELD, D. W. 2017. Protein Kinase CK2: Intricate Relationships within Regulatory Cellular Networks. *Pharmaceuticals (Basel)*, 10.

- NUSSBAUM, R. E., HENDERSON, W. M., PATTISON, I. H., ELCOCK, N. V. & DAVIES, D. C. 1975. The establishment of sheep flocks of predictable susceptibility to experimental scrapie. *Res Vet Sci*, 18, 49-58.
- NUVOLONE, M., HERMANN, M., SORCE, S., RUSSO, G., TIBERI, C., SCHWARZ, P., MINIKEL, E., SANOUDOU, D., PELCZAR, P. & AGUZZI, A. 2016. Strictly co-isogenic C57BL/6J-Prnp^{-/-} mice: A rigorous resource for prion science. *J Exp Med*, 213, 313-27.
- OESCH, B., WESTAWAY, D., WALCHLI, M., MCKINLEY, M. P., KENT, S. B., AEBERSOLD, R., BARRY, R. A., TEMPST, P., TEFLOW, D. B., HOOD, L. E. & ET AL. 1985. A cellular gene encodes scrapie PrP²⁷⁻³⁰ protein. *Cell*, 40, 735-46.
- OH, J. M., SHIN, H. Y., PARK, S. J., KIM, B. H., CHOI, J. K., CHOI, E. K., CARP, R. I. & KIM, Y. S. 2008. The involvement of cellular prion protein in the autophagy pathway in neuronal cells. *Mol Cell Neurosci*, 39, 238-47.
- ORCI, L., TAGAYA, M., AMHERDT, M., PERRELET, A., DONALDSON, J. G., LIPPINCOTT-SCHWARTZ, J., KLAUSNER, R. D. & ROTHMAN, J. E. 1991. Brefeldin A, a drug that blocks secretion, prevents the assembly of non-clathrin-coated buds on Golgi cisternae. *Cell*, 64, 1183-95.
- ORRU, C. D., BONGIANNI, M., TONOLI, G., FERRARI, S., HUGHSON, A. G., GROVEMAN, B. R., FIORINI, M., POCCHIARI, M., MONACO, S., CAUGHEY, B. & ZANUSSO, G. 2014. A test for Creutzfeldt-Jakob disease using nasal brushings. *N Engl J Med*, 371, 519-29.
- ORRU, C. D., HUGHSON, A. G., GROVEMAN, B. R., CAMPBELL, K. J., ANSON, K. J., MANCA, M., KRAUS, A. & CAUGHEY, B. 2016. Factors That Improve RT-QuIC Detection of Prion Seeding Activity. *Viruses*, 8.
- ORRU, C. D., WILHAM, J. M., RAYMOND, L. D., KUHN, F., SCHROEDER, B., RAEBER, A. J. & CAUGHEY, B. 2011. Prion disease blood test using immunoprecipitation and improved quaking-induced conversion. *MBio*, 2, e00078-11.
- ORSI, A., FIORITI, L., CHIESA, R. & SITIA, R. 2006. Conditions of endoplasmic reticulum stress favor the accumulation of cytosolic prion protein. *J Biol Chem*, 281, 30431-8.
- OTTO, M., CEPEK, L., RATZKA, P., DOEHLINGER, S., BOEKHOFF, I., WILTFANG, J., IRLE, E., PERGANDE, G., ELLERS-LENZ, B., WINDL, O., KRETZSCHMAR, H. A., POSER, S. & PRANGE, H. 2004. Efficacy of flupirtine on cognitive function in patients with CJD: A double-blind study. *Neurology*, 62, 714-8.
- OWEN, F., POULTER, M., LOFTHOUSE, R., COLLINGE, J., CROW, T. J., RISBY, D., BAKER, H. F., RIDLEY, R. M., HSIAO, K. & PRUSINER, S. B. 1989. Insertion in prion protein gene in familial Creutzfeldt-Jakob disease. *Lancet*, 1, 51-2.
- OWEN, J. P., REES, H. C., MADDISON, B. C., TERRY, L. A., THORNE, L., JACKMAN, R., WHITELAM, G. C. & GOUGH, K. C. 2007. Molecular profiling of ovine prion diseases by using thermolysin-resistant PrP^{Sc} and endogenous C2 PrP fragments. *J Virol*, 81, 10532-9.
- PAISLEY, D., BANKS, S., SELFRIDGE, J., MCLENNAN, N. F., RITCHIE, A. M., MCEWAN, C., IRVINE, D. S., SAUNDERS, P. T., MANSON, J. C. & MELTON, D. W. 2004. Male infertility and DNA damage in Doppel knockout and prion protein/Doppel double-knockout mice. *Am J Pathol*, 164, 2279-88.
- PAN, K. M., BALDWIN, M., NGUYEN, J., GASSET, M., SERBAN, A., GROTH, D., MEHLHORN, I., HUANG, Z., FLETTERICK, R. J., COHEN, F. E. & ET AL. 1993. Conversion of alpha-helices into beta-sheets features in the formation of the scrapie prion proteins. *Proc Natl Acad Sci U S A*, 90, 10962-6.
- PANKIEWICZ, J., PRELLI, F., SY, M. S., KASCSAK, R. J., KASCSAK, R. B., SPINNER, D. S., CARP, R. I., MEEKER, H. C., SADOWSKI, M. & WISNIEWSKI, T. 2006. Clearance and prevention of prion infection in cell culture by anti-PrP antibodies. *Eur J Neurosci*, 23, 2635-47.

- PARCHI, P., CASTELLANI, R., CAPELLARI, S., GHETTI, B., YOUNG, K., CHEN, S. G., FARLOW, M., DICKSON, D. W., SIMA, A. A., TROJANOWSKI, J. Q., PETERSEN, R. B. & GAMBETTI, P. 1996. Molecular basis of phenotypic variability in sporadic Creutzfeldt-Jakob disease. *Ann Neurol*, 39, 767-78.
- PARCHI, P., GIESE, A., CAPELLARI, S., BROWN, P., SCHULZ-SCHAEFFER, W., WINDL, O., ZERR, I., BUDKA, H., KOPP, N., PICCARDO, P., POSER, S., ROJANI, A., STREICHEMBERGER, N., JULIEN, J., VITAL, C., GHETTI, B., GAMBETTI, P. & KRETZSCHMAR, H. 1999. Classification of sporadic Creutzfeldt-Jakob disease based on molecular and phenotypic analysis of 300 subjects. *Ann Neurol*, 46, 224-33.
- PARRY, H. B. 1979. Elimination of natural scrapie in sheep by sire genotype selection. *Nature*, 277, 127-9.
- PATTISON, I. H. 1965. Scrapie in the welsh mountain breed of sheep and its experimental transmission to goats. *Vet Rec*, 77, 1388-90.
- PATTISON, I. H., HOARE, M. N., JEBBETT, J. N. & WATSON, W. A. 1972. Spread of scrapie to sheep and goats by oral dosing with foetal membranes from scrapie-affected sheep. *Vet Rec*, 90, 465-8.
- PATTISON, I. H. & JONES, K. M. 1967. The possible nature of the transmissible agent of scrapie. *Vet Rec*, 80, 2-9.
- PEDERSEN, N. S. & SMITH, E. 2002. Prion diseases: epidemiology in man. *APMIS*, 110, 14-22.
- PERALTA, O. A. & EYESTONE, W. H. 2009. Quantitative and qualitative analysis of cellular prion protein (PrP(C)) expression in bovine somatic tissues. *Prion*, 3, 161-70.
- PERETZ, D., WILLIAMSON, R. A., KANEKO, K., VERGARA, J., LECLERC, E., SCHMITT-ULMS, G., MEHLHORN, I. R., LEGNAME, G., WORMALD, M. R., RUDD, P. M., DWEK, R. A., BURTON, D. R. & PRUSINER, S. B. 2001. Antibodies inhibit prion propagation and clear cell cultures of prion infectivity. *Nature*, 412, 739-43.
- PEROVIC, S., SCHRODER, H. C., PERGANDE, G., USHIJIMA, H. & MULLER, W. E. 1997. Effect of flupirtine on Bcl-2 and glutathione level in neuronal cells treated in vitro with the prion protein fragment (PrP106-126). *Exp Neurol*, 147, 518-24.
- PERRIER, V., SOLASSOL, J., CROZET, C., FROBERT, Y., MOURTON-GILLES, C., GRASSI, J. & LEHMANN, S. 2004. Anti-PrP antibodies block PrPSc replication in prion-infected cell cultures by accelerating PrPC degradation. *J Neurochem*, 89, 454-63.
- PETERS, P. J., MIRONOV, A., JR., PERETZ, D., VAN DONSELAAR, E., LECLERC, E., ERPEL, S., DEARMOND, S. J., BURTON, D. R., WILLIAMSON, R. A., VEY, M. & PRUSINER, S. B. 2003. Trafficking of prion proteins through a caveolae-mediated endosomal pathway. *J Cell Biol*, 162, 703-17.
- PETSCH, B., MULLER-SCHIFFMANN, A., LEHLE, A., ZIRDUM, E., PRIKULIS, I., KUHN, F., RAEBER, A. J., IRONSIDE, J. W., KORTH, C. & STITZ, L. 2011. Biological effects and use of PrPSc- and PrP-specific antibodies generated by immunization with purified full-length native mouse prions. *J Virol*, 85, 4538-46.
- PFEIFER, A., EIGENBROD, S., AL-KHADRA, S., HOFMANN, A., MITTEREGGER, G., MOSER, M., BERTSCH, U. & KRETZSCHMAR, H. 2006. Lentivector-mediated RNAi efficiently suppresses prion protein and prolongs survival of scrapie-infected mice. *J Clin Invest*, 116, 3204-10.
- PLUMMER, P. J. 1946. Scrapie-A Disease of Sheep: A Review of the literature. *Can J Comp Med Vet Sci*, 10, 49-54.
- POCCHIARI, M., CASACCIA, P. & LADOGANA, A. 1989. Amphotericin B: a novel class of antiscrapie drugs. *J Infect Dis*, 160, 795-802.
- POCCHIARI, M., SCHMITTINGER, S. & MASULLO, C. 1987. Amphotericin B delays the incubation period of scrapie in intracerebrally inoculated hamsters. *J Gen Virol*, 68 (Pt 1), 219-23.

- POLI, G., MARTINO, P. A., VILLA, S., CARCASSOLA, G., GIANNINO, M. L., DALL'ARA, P., POLLERA, C., IUSSICH, S., TRANQUILLO, V. M., BAREGGI, S., MANTEGAZZA, P. & PONTI, W. 2004. Evaluation of anti-prion activity of congo red and its derivatives in experimentally infected hamsters. *Arzneimittelforschung*, 54, 406-15.
- POLI, G., PONTI, W., CARCASSOLA, G., CECILIANI, F., COLOMBO, L., DALL'ARA, P., GERVASONI, M., GIANNINO, M. L., MARTINO, P. A., POLLERA, C., VILLA, S. & SALMONA, M. 2003. In vitro evaluation of the anti-prionic activity of newly synthesized congo red derivatives. *Arzneimittelforschung*, 53, 875-88.
- POLYMENIDOU, M., TRUSHEIM, H., STALLMACH, L., MOOS, R., JULIUS, C., MIELE, G., LENZ-BAUER, C. & AGUZZI, A. 2008. Canine MDCK cell lines are refractory to infection with human and mouse prions. *Vaccine*, 26, 2601-14.
- POWELL-JACKSON, J., WELLER, R. O., KENNEDY, P., PREECE, M. A., WHITCOMBE, E. M. & NEWSOM-DAVIS, J. 1985. Creutzfeldt-Jakob disease after administration of human growth hormone. *Lancet*, 2, 244-6.
- PREMZL, M., GREASY, J. E., JERMIIN, L. S., SIMONIC, T. & MARSHALL GRAVES, J. A. 2004. Evolution of vertebrate genes related to prion and Shadoo proteins--clues from comparative genomic analysis. *Mol Biol Evol*, 21, 2210-31.
- PREMZL, M., SANGIORGIO, L., STRUMBO, B., MARSHALL GRAVES, J. A., SIMONIC, T. & GREASY, J. E. 2003. Shadoo, a new protein highly conserved from fish to mammals and with similarity to prion protein. *Gene*, 314, 89-102.
- PRIOLA, S. A. & CHESEBRO, B. 1998. Abnormal properties of prion protein with insertional mutations in different cell types. *J Biol Chem*, 273, 11980-5.
- PRIOLA, S. A. & LAWSON, V. A. 2001. Glycosylation influences cross-species formation of protease-resistant prion protein. *EMBO J*, 20, 6692-9.
- PRIOLA, S. A., RAINES, A. & CAUGHEY, W. 2003. Prophylactic and therapeutic effects of phthalocyanine tetrasulfonate in scrapie-infected mice. *J Infect Dis*, 188, 699-705.
- PRIOLA, S. A., RAINES, A. & CAUGHEY, W. S. 2000. Porphyrin and phthalocyanine antiscrapie compounds. *Science*, 287, 1503-6.
- PRUSINER, S. B. 1989. Creutzfeldt-Jakob disease and scrapie prions. *Alzheimer Dis Assoc Disord*, 3, 52-78.
- PRUSINER, S. B. 1991. Molecular biology of prion diseases. *Science*, 252, 1515-22.
- PRUSINER, S. B., BOLTON, D. C., GROTH, D. F., BOWMAN, K. A., COCHRAN, S. P. & MCKINLEY, M. P. 1982. Further purification and characterization of scrapie prions. *Biochemistry*, 21, 6942-50.
- PRUSINER, S. B., GROTH, D. F., BILDSTEIN, C., MASIARZ, F. R., MCKINLEY, M. P. & COCHRAN, S. P. 1980. Electrophoretic properties of the scrapie agent in agarose gels. *Proc Natl Acad Sci U S A*, 77, 2984-8.
- PRUSINER, S. B., GROTH, D. F., BOLTON, D. C., KENT, S. B. & HOOD, L. E. 1984. Purification and structural studies of a major scrapie prion protein. *Cell*, 38, 127-34.
- PRUSINER, S. B., HADLOW, W. J., GARFIN, D. E., COCHRAN, S. P., BARINGER, J. R., RACE, R. E. & EKLUND, C. M. 1978. Partial purification and evidence for multiple molecular forms of the scrapie agent. *Biochemistry*, 17, 4993-9.
- PRUSINER, S. B., MCKINLEY, M. P., GROTH, D. F., BOWMAN, K. A., MOCK, N. I., COCHRAN, S. P. & MASIARZ, F. R. 1981. Scrapie agent contains a hydrophobic protein. *Proc Natl Acad Sci U S A*, 78, 6675-9.
- PRUSINER, S. B., SCOTT, M., FOSTER, D., PAN, K. M., GROTH, D., MIRENDA, C., TORCHIA, M., YANG, S. L., SERBAN, D., CARLSON, G. A. & ET AL. 1990. Transgenic studies implicate interactions between homologous PrP isoforms in scrapie prion replication. *Cell*, 63, 673-86.

- PRUSINER, S. B., SCOTT, M. R., DEARMOND, S. J. & COHEN, F. E. 1998. Prion protein biology. *Cell*, 93, 337-48.
- PUIG, B., ALTMIEPPEN, H. C., THURM, D., GEISSEN, M., CONRAD, C., BRAULKE, T. & GLATZEL, M. 2011. N-glycans and glycosylphosphatidylinositol-anchor act on polarized sorting of mouse PrP(C) in Madin-Darby canine kidney cells. *PLoS One*, 6, e24624.
- RACHIDI, W., VILETTE, D., GUIRAUD, P., ARLOTTO, M., RIONDEL, J., LAUDE, H., LEHMANN, S. & FAVIER, A. 2003. Expression of prion protein increases cellular copper binding and antioxidant enzyme activities but not copper delivery. *J Biol Chem*, 278, 9064-72.
- RAEBER, A. J., MURAMOTO, T., KORNBURG, T. B. & PRUSINER, S. B. 1995. Expression and targeting of Syrian hamster prion protein induced by heat shock in transgenic *Drosophila melanogaster*. *Mech Dev*, 51, 317-27.
- RAMASAMY, I., LAW, M., COLLINS, S. & BROOKE, F. 2003. Organ distribution of prion proteins in variant Creutzfeldt-Jakob disease. *Lancet Infect Dis*, 3, 214-22.
- RAYMOND, G. J., BOSSERS, A., RAYMOND, L. D., O'ROURKE, K. I., MCHOLLAND, L. E., BRYANT, P. K., 3RD, MILLER, M. W., WILLIAMS, E. S., SMITS, M. & CAUGHEY, B. 2000. Evidence of a molecular barrier limiting susceptibility of humans, cattle and sheep to chronic wasting disease. *EMBO J*, 19, 4425-30.
- RAYMOND, G. J., HOPE, J., KOCISKO, D. A., PRIOLA, S. A., RAYMOND, L. D., BOSSERS, A., IRONSIDE, J., WILL, R. G., CHEN, S. G., PETERSEN, R. B., GAMBETTI, P., RUBENSTEIN, R., SMITS, M. A., LANSBURY, P. T., JR. & CAUGHEY, B. 1997. Molecular assessment of the potential transmissibilities of BSE and scrapie to humans. *Nature*, 388, 285-8.
- RAYMOND, G. J., ZHAO, H. T., RACE, B., RAYMOND, L. D., WILLIAMS, K., SWAYZE, E. E., GRAFFAM, S., LE, J., CARON, T., STATHOPOULOS, J., O'KEEFE, R., LUBKE, L. L., REIDENBACH, A. G., KRAUS, A., SCHREIBER, S. L., MAZUR, C., CABIN, D. E., CARROLL, J. B., MINIKEL, E. V., KORDASIEWICZ, H., CAUGHEY, B. & VALLABH, S. M. 2019. Antisense oligonucleotides extend survival of prion-infected mice. *JCI Insight*, 5.
- REQUENA, J. R. & WILLE, H. 2014. The structure of the infectious prion protein: experimental data and molecular models. *Prion*, 8, 60-6.
- RESENBERGER, U. K., HARMEIER, A., WOERNER, A. C., GOODMAN, J. L., MULLER, V., KRISHNAN, R., VABULAS, R. M., KRETZSCHMAR, H. A., LINDQUIST, S., HARTL, F. U., MULTHAUP, G., WINKLHOFER, K. F. & TATZELT, J. 2011. The cellular prion protein mediates neurotoxic signalling of beta-sheet-rich conformers independent of prion replication. *EMBO J*, 30, 2057-70.
- RICHT, J. A., KASINATHAN, P., HAMIR, A. N., CASTILLA, J., SATHIYASEELAN, T., VARGAS, F., SATHIYASEELAN, J., WU, H., MATSUSHITA, H., KOSTER, J., KATO, S., ISHIDA, I., SOTO, C., ROBL, J. M. & KUROIWA, Y. 2007. Production of cattle lacking prion protein. *Nat Biotechnol*, 25, 132-8.
- RIEK, R., HORNE-MANN, S., WIDER, G., GLOCKSHUBER, R. & WUTHRICH, K. 1997. NMR characterization of the full-length recombinant murine prion protein, mPrP(23-231). *FEBS Lett*, 413, 282-8.
- RIGOLI, M., SPAGNOLLI, G., FACCIOLI, P., REQUENA, J. R. & BIASINI, E. 2019. Ok Google, how could I design therapeutics against prion diseases? *Curr Opin Pharmacol*, 44, 39-45.
- ROBAKIS, N. K., DEVINE-GAGE, E. A., JENKINS, E. C., KASCSAK, R. J., BROWN, W. T., KRAWCZUN, M. S. & SILVERMAN, W. P. 1986. Localization of a human gene homologous to the PrP gene on the p arm of chromosome 20 and detection of PrP-related antigens in normal human brain. *Biochem Biophys Res Commun*, 140, 758-65.

- ROGERS, M., YEHIELY, F., SCOTT, M. & PRUSINER, S. B. 1993. Conversion of truncated and elongated prion proteins into the scrapie isoform in cultured cells. *Proc Natl Acad Sci U S A*, 90, 3182-6.
- ROSSI, D., COZZIO, A., FLECHSIG, E., KLEIN, M. A., RULICKE, T., AGUZZI, A. & WEISSMANN, C. 2001. Onset of ataxia and Purkinje cell loss in PrP null mice inversely correlated with Dpl level in brain. *EMBO J*, 20, 694-702.
- ROUCOU, X., GAINS, M. & LEBLANC, A. C. 2004. Neuroprotective functions of prion protein. *J Neurosci Res*, 75, 153-61.
- RUBINSZTEIN, D. C., DIFIGLIA, M., HEINTZ, N., NIXON, R. A., QIN, Z. H., RAVIKUMAR, B., STEFANIS, L. & TOLKOVSKY, A. 2005. Autophagy and its possible roles in nervous system diseases, damage and repair. *Autophagy*, 1, 11-22.
- RUDYK, H., KNAGGS, M. H., VASILJEVIC, S., HOPE, J., BIRKETT, C. & GILBERT, I. H. 2003. Synthesis and evaluation of analogues of Congo red as potential compounds against transmissible spongiform encephalopathies. *Eur J Med Chem*, 38, 567-79.
- RYOU, C., LEGNAME, G., PERETZ, D., CRAIG, J. C., BALDWIN, M. A. & PRUSINER, S. B. 2003. Differential inhibition of prion propagation by enantiomers of quinacrine. *Lab Invest*, 83, 837-43.
- SABORIO, G. P., PERMANNE, B. & SOTO, C. 2001. Sensitive detection of pathological prion protein by cyclic amplification of protein misfolding. *Nature*, 411, 810-3.
- SAKAGUCHI, S., KATAMINE, S., NISHIDA, N., MORIUCHI, R., SHIGEMATSU, K., SUGIMOTO, T., NAKATANI, A., KATAOKA, Y., HOUTANI, T., SHIRABE, S., OKADA, H., HASEGAWA, S., MIYAMOTO, T. & NODA, T. 1996. Loss of cerebellar Purkinje cells in aged mice homozygous for a disrupted PrP gene. *Nature*, 380, 528-31.
- SALAMAT, M. K., DRON, M., CHAPUIS, J., LANGEVIN, C. & LAUDE, H. 2011. Prion propagation in cells expressing PrP glycosylation mutants. *J Virol*, 85, 3077-85.
- SALAZAR, S. V. & STRITTMATTER, S. M. 2017. Cellular prion protein as a receptor for amyloid-beta oligomers in Alzheimer's disease. *Biochem Biophys Res Commun*, 483, 1143-1147.
- SALES, N., HASSIG, R., RODOLFO, K., DI GIAMBERARDINO, L., TRAFFORT, E., RUAT, M., FRETIER, P. & MOYA, K. L. 2002. Developmental expression of the cellular prion protein in elongating axons. *Eur J Neurosci*, 15, 1163-77.
- SANCHEZ-PONCE, D., MUNOZ, A. & GARRIDO, J. J. 2011. Casein kinase 2 and microtubules control axon initial segment formation. *Mol Cell Neurosci*, 46, 222-34.
- SANDBERG, M. K., AL-DOUJAILY, H., SHARPS, B., CLARKE, A. R. & COLLINGE, J. 2011. Prion propagation and toxicity in vivo occur in two distinct mechanistic phases. *Nature*, 470, 540-2.
- SANO, K., SATOH, K., ATARASHI, R., TAKASHIMA, H., IWASAKI, Y., YOSHIDA, M., SANJO, N., MURAI, H., MIZUSAWA, H., SCHMITZ, M., ZERR, I., KIM, Y. S. & NISHIDA, N. 2013. Early detection of abnormal prion protein in genetic human prion diseases now possible using real-time QUIC assay. *PLoS One*, 8, e54915.
- SANTUCCIONE, A., SYTNYK, V., LESHCHYNS'KA, I. & SCHACHNER, M. 2005. Prion protein recruits its neuronal receptor NCAM to lipid rafts to activate p59fyn and to enhance neurite outgrowth. *J Cell Biol*, 169, 341-54.
- SARNATARO, D., CAPUTO, A., CASANOVA, P., PURI, C., PALADINO, S., TIVODAR, S. S., CAMPANA, V., TACCHETTI, C. & ZURZOLO, C. 2009. Lipid rafts and clathrin cooperate in the internalization of PrP in epithelial FRT cells. *PLoS One*, 4, e5829.
- SCHMITT-ULMS, G., LEGNAME, G., BALDWIN, M. A., BALL, H. L., BRADON, N., BOSQUE, P. J., CROSSIN, K. L., EDELMAN, G. M., DEARMOND, S. J., COHEN, F. E. & PRUSINER, S. B. 2001. Binding of neural cell adhesion molecules (N-CAMs) to the cellular prion protein. *J Mol Biol*, 314, 1209-25.

- SCHMITZ, M., CRAMM, M., LLORENS, F., CANDELISE, N., MULLER-CRAMM, D., VARGES, D., SCHULZ-SCHAEFFER, W. J., ZAFAR, S. & ZERR, I. 2016. Application of an in vitro-amplification assay as a novel pre-screening test for compounds inhibiting the aggregation of prion protein scrapie. *Sci Rep*, 6, 28711.
- SCHMITZ, M., ZAFAR, S., SILVA, C. J. & ZERR, I. 2014. Behavioral abnormalities in prion protein knockout mice and the potential relevance of PrP(C) for the cytoskeleton. *Prion*, 8, 381-6.
- SCOTT-MCKEAN, J. J., SUREWICZ, K., CHOI, J. K., RUFFIN, V. A., SALAMEH, A. I., NIEZNANSKI, K., COSTA, A. C. S. & SUREWICZ, W. K. 2016. Soluble prion protein and its N-terminal fragment prevent impairment of synaptic plasticity by Aβ oligomers: Implications for novel therapeutic strategy in Alzheimer's disease. *Neurobiol Dis*, 91, 124-131.
- SCOTT, M., FOSTER, D., MIRENDA, C., SERBAN, D., COUFAL, F., WALCHLI, M., TORCHIA, M., GROTH, D., CARLSON, G., DEARMOND, S. J., WESTAWAY, D. & PRUSINER, S. B. 1989. Transgenic mice expressing hamster prion protein produce species-specific scrapie infectivity and amyloid plaques. *Cell*, 59, 847-57.
- SEGALL, M. D., YUSOF, I. & CHAMPNESS, E. J. 2016. Avoiding Missed Opportunities by Analyzing the Sensitivity of Our Decisions. *J Med Chem*, 59, 4267-77.
- SENATORE, A., COLLEONI, S., VERDERIO, C., RESTELLI, E., MORINI, R., CONDLIFFE, S. B., BERTANI, I., MANTOVANI, S., CANOVI, M., MICOTTI, E., FORLONI, G., DOLPHIN, A. C., MATTEOLI, M., GOBBI, M. & CHIESA, R. 2012. Mutant PrP suppresses glutamatergic neurotransmission in cerebellar granule neurons by impairing membrane delivery of VGCC α(2)δ-1 Subunit. *Neuron*, 74, 300-13.
- SHAH, S. Z. A., ZHAO, D., TAGLIALATELA, G., HUSSAIN, T., DONG, H., SABIR, N., MANGI, M. H., WU, W., LAI, M., ZHANG, X., DUAN, Y., WANG, L., ZHOU, X. & YANG, L. 2019. Combinatory FK506 and Minocycline Treatment Alleviates Prion-Induced Neurodegenerative Events via Caspase-Mediated MAPK-NRF2 Pathway. *Int J Mol Sci*, 20.
- SHAKED, Y., HIJAZI, N. & GABIZON, R. 2002. Doppel and PrP(C) do not share the same membrane microenvironment. *FEBS Lett*, 530, 85-8.
- SHMERLING, D., HEGYI, I., FISCHER, M., BLATTLER, T., BRANDNER, S., GOTZ, J., RULICKE, T., FLECHSIG, E., COZZIO, A., VON MERING, C., HANGARTNER, C., AGUZZI, A. & WEISSMANN, C. 1998. Expression of amino-terminally truncated PrP in the mouse leading to ataxia and specific cerebellar lesions. *Cell*, 93, 203-14.
- SHYNG, S. L., HEUSER, J. E. & HARRIS, D. A. 1994. A glycolipid-anchored prion protein is endocytosed via clathrin-coated pits. *J Cell Biol*, 125, 1239-50.
- SHYNG, S. L., HUBER, M. T. & HARRIS, D. A. 1993. A prion protein cycles between the cell surface and an endocytic compartment in cultured neuroblastoma cells. *J Biol Chem*, 268, 15922-8.
- SHYNG, S. L., MOULDER, K. L., LESKO, A. & HARRIS, D. A. 1995. The N-terminal domain of a glycolipid-anchored prion protein is essential for its endocytosis via clathrin-coated pits. *J Biol Chem*, 270, 14793-800.
- SHYU, W. C., CHEN, C. P., SAEKI, K., KUBOSAKI, A., MATSUMOTO, Y., ONODERA, T., DING, D. C., CHIANG, M. F., LEE, Y. J., LIN, S. Z. & LI, H. 2005. Hypoglycemia enhances the expression of prion protein and heat-shock protein 70 in a mouse neuroblastoma cell line. *J Neurosci Res*, 80, 887-94.
- SIGURDSON, C. J. & MILLER, M. W. 2003. Other animal prion diseases. *Br Med Bull*, 66, 199-212.
- SILBER, B. M., GEVER, J. R., RAO, S., LI, Z., RENSLO, A. R., WIDJAJA, K., WONG, C., GILES, K., FREYMAN, Y., ELEPANO, M., IRWIN, J. J., JACOBSON, M. P. & PRUSINER, S. B. 2014. Novel compounds lowering the cellular isoform of the human prion protein in cultured human cells. *Bioorg Med Chem*, 22, 1960-72.

- SINGH, A., ISAAC, A. O., LUO, X., MOHAN, M. L., COHEN, M. L., CHEN, F., KONG, Q., BARTZ, J. & SINGH, N. 2009a. Abnormal brain iron homeostasis in human and animal prion disorders. *PLoS Pathog*, 5, e1000336.
- SINGH, A., MOHAN, M. L., ISAAC, A. O., LUO, X., PETRAK, J., VYORAL, D. & SINGH, N. 2009b. Prion protein modulates cellular iron uptake: a novel function with implications for prion disease pathogenesis. *PLoS One*, 4, e4468.
- SISO, S., PUIG, B., VAREA, R., VIDAL, E., ACIN, C., PRINZ, M., MONTRASIO, F., BADIOLA, J., AGUZZI, A., PUMAROLA, M. & FERRER, I. 2002. Abnormal synaptic protein expression and cell death in murine scrapie. *Acta Neuropathol*, 103, 615-26.
- SOLFOROSI, L., CRIADO, J. R., MCGAVERN, D. B., WIRZ, S., SANCHEZ-ALAVEZ, M., SUGAMA, S., DEGIORGIO, L. A., VOLPE, B. T., WISEMAN, E., ABALOS, G., MASLIAH, E., GILDEN, D., OLDSTONE, M. B., CONTI, B. & WILLIAMSON, R. A. 2004. Cross-linking cellular prion protein triggers neuronal apoptosis in vivo. *Science*, 303, 1514-6.
- SOLOMON, I. H., BIASINI, E. & HARRIS, D. A. 2012. Ion channels induced by the prion protein: mediators of neurotoxicity. *Prion*, 6, 40-5.
- SOLOMON, I. H., KHATRI, N., BIASINI, E., MASSIGNAN, T., HUETTNER, J. E. & HARRIS, D. A. 2011. An N-terminal polybasic domain and cell surface localization are required for mutant prion protein toxicity. *J Biol Chem*, 286, 14724-36.
- SOLOMON, I. H., SCHEPKER, J. A. & HARRIS, D. A. 2010. Prion neurotoxicity: insights from prion protein mutants. *Curr Issues Mol Biol*, 12, 51-61.
- SONATI, T., REIMANN, R. R., FALSIG, J., BARAL, P. K., O'CONNOR, T., HORNEMANN, S., YAGANOGLU, S., LI, B., HERRMANN, U. S., WIELAND, B., SWAYAMPAKULA, M., RAHMAN, M. H., DAS, D., KAV, N., RIEK, R., LIBERSKI, P. P., JAMES, M. N. & AGUZZI, A. 2013. The toxicity of antiprion antibodies is mediated by the flexible tail of the prion protein. *Nature*, 501, 102-6.
- SPAGNOLLI, G., RIGOLI, M., ORIOLI, S., SEVILLANO, A. M., FACCIOLI, P., WILLE, H., BIASINI, E. & REQUENA, J. R. 2019. Full atomistic model of prion structure and conversion. *PLoS Pathog*, 15, e1007864.
- SPARKES, R. S., SIMON, M., COHN, V. H., FOURNIER, R. E., LEM, J., KLISAK, I., HEINZMANN, C., BLATT, C., LUCERO, M., MOHANDAS, T. & ET AL. 1986. Assignment of the human and mouse prion protein genes to homologous chromosomes. *Proc Natl Acad Sci U S A*, 83, 7358-62.
- SPRAKER, T. R., MILLER, M. W., WILLIAMS, E. S., GETZY, D. M., ADRIAN, W. J., SCHOONVELD, G. G., SPOWART, R. A., O'ROURKE, K. I., MILLER, J. M. & MERZ, P. A. 1997. Spongiform encephalopathy in free-ranging mule deer (*Odocoileus hemionus*), white-tailed deer (*Odocoileus virginianus*) and Rocky Mountain elk (*Cervus elaphus nelsoni*) in northcentral Colorado. *J Wildl Dis*, 33, 1-6.
- SPUDICH, A., FRIGG, R., KILIC, E., KILIC, U., OESCH, B., RAEBER, A., BASSETTI, C. L. & HERMANN, D. M. 2005. Aggravation of ischemic brain injury by prion protein deficiency: role of ERK-1/-2 and STAT-1. *Neurobiol Dis*, 20, 442-9.
- STAHL, N., BALDWIN, M. A., HECKER, R., PAN, K. M., BURLINGAME, A. L. & PRUSINER, S. B. 1992. Glycosylinositol phospholipid anchors of the scrapie and cellular prion proteins contain sialic acid. *Biochemistry*, 31, 5043-53.
- STAHL, N., BALDWIN, M. A., TEPLow, D. B., HOOD, L., GIBSON, B. W., BURLINGAME, A. L. & PRUSINER, S. B. 1993. Structural studies of the scrapie prion protein using mass spectrometry and amino acid sequencing. *Biochemistry*, 32, 1991-2002.
- STAHL, N., BORCHELT, D. R., HSIAO, K. & PRUSINER, S. B. 1987. Scrapie prion protein contains a phosphatidylinositol glycolipid. *Cell*, 51, 229-40.

- STEINHOFF, B. J., RACKER, S., HERRENDORF, G., POSER, S., GROSCHE, S., ZERR, I., KRETZSCHMAR, H. & WEBER, T. 1996. Accuracy and reliability of periodic sharp wave complexes in Creutzfeldt-Jakob disease. *Arch Neurol*, 53, 162-6.
- STENGEL, E. & WILSON, W. E. 1946. Jakob-Creutzfeldt disease. *J Ment Sci*, 92, 370-8.
- STEWART, R. S., DRISALDI, B. & HARRIS, D. A. 2001. A transmembrane form of the prion protein contains an uncleaved signal peptide and is retained in the endoplasmic Reticulum. *Mol Biol Cell*, 12, 881-9.
- STEWART, R. S. & HARRIS, D. A. 2005. A transmembrane form of the prion protein is localized in the Golgi apparatus of neurons. *J Biol Chem*, 280, 15855-64.
- STIMSON, E., HOPE, J., CHONG, A. & BURLINGAME, A. L. 1999. Site-specific characterization of the N-linked glycans of murine prion protein by high-performance liquid chromatography/electrospray mass spectrometry and exoglycosidase digestions. *Biochemistry*, 38, 4885-95.
- STINCARDINI, C., MASSIGNAN, T., BIGGI, S., ELEZGARAI, S. R., SANGIOVANNI, V., VANNI, I., PANCHER, M., ADAMI, V., MORENO, J., STRAVALACI, M., MAIETTA, G., GOBBI, M., NEGRO, A., REQUENA, J. R., CASTILLA, J., NONNO, R. & BIASINI, E. 2017. An antipsychotic drug exerts anti-prion effects by altering the localization of the cellular prion protein. *PLoS One*, 12, e0182589.
- STOHR, J., ELFRINK, K., WEINMANN, N., WILLE, H., WILLBOLD, D., BIRKMANN, E. & RIESNER, D. 2011. In vitro conversion and seeded fibrillization of posttranslationally modified prion protein. *Biol Chem*, 392, 415-21.
- SUPATTAPONE, S., BOSQUE, P., MURAMOTO, T., WILLE, H., AAGAARD, C., PERETZ, D., NGUYEN, H. O., HEINRICH, C., TORCHIA, M., SAFAR, J., COHEN, F. E., DEARMOND, S. J., PRUSINER, S. B. & SCOTT, M. 1999. Prion protein of 106 residues creates an artificial transmission barrier for prion replication in transgenic mice. *Cell*, 96, 869-78.
- TAGLIAVINI, F., MCARTHUR, R. A., CANCIANI, B., GIACCONE, G., PORRO, M., BUGIANI, M., LIEVENS, P. M., BUGIANI, O., PERI, E., DALL'ARA, P., ROCCHI, M., POLI, G., FORLONI, G., BANDIERA, T., VARASI, M., SUARATO, A., CASSUTTI, P., CERVINI, M. A., LANSEN, J., SALMONA, M. & POST, C. 1997. Effectiveness of anthracycline against experimental prion disease in Syrian hamsters. *Science*, 276, 1119-22.
- TAGLIAVINI, F., PRELLI, F., PORRO, M., SALMONA, M., BUGIANI, O. & FRANGIONE, B. 1992. A soluble form of prion protein in human cerebrospinal fluid: implications for prion-related encephalopathies. *Biochem Biophys Res Commun*, 184, 1398-404.
- TAMGUNEY, G., GILES, K., BOUZAMONDO-BERNSTEIN, E., BOSQUE, P. J., MILLER, M. W., SAFAR, J., DEARMOND, S. J. & PRUSINER, S. B. 2006. Transmission of elk and deer prions to transgenic mice. *J Virol*, 80, 9104-14.
- TARABOULOS, A., RAEHER, A. J., BORCHELT, D. R., SERBAN, D. & PRUSINER, S. B. 1992. Synthesis and trafficking of prion proteins in cultured cells. *Mol Biol Cell*, 3, 851-63.
- TARABOULOS, A., ROGERS, M., BORCHELT, D. R., MCKINLEY, M. P., SCOTT, M., SERBAN, D. & PRUSINER, S. B. 1990. Acquisition of protease resistance by prion proteins in scrapie-infected cells does not require asparagine-linked glycosylation. *Proc Natl Acad Sci U S A*, 87, 8262-6.
- TARABOULOS, A., SCOTT, M., SEMENOV, A., AVRAHAM, D., LASZLO, L. & PRUSINER, S. B. 1995. Cholesterol depletion and modification of COOH-terminal targeting sequence of the prion protein inhibit formation of the scrapie isoform. *J Cell Biol*, 129, 121-32.
- TATEISHI, J., BROWN, P., KITAMOTO, T., HOQUE, Z. M., ROOS, R., WOLLMAN, R., CERVENAKOVA, L. & GAJDUSEK, D. C. 1995. First experimental transmission of fatal familial insomnia. *Nature*, 376, 434-5.

- TATEISHI, J., KITAMOTO, T., DOH-URA, K., SAKAKI, Y., STEINMETZ, G., TRANCHANT, C., WARTER, J. M. & HELDT, N. 1990. Immunochemical, molecular genetic, and transmission studies on a case of Gerstmann-Straussler-Scheinker syndrome. *Neurology*, 40, 1578-81.
- TATEISHI, J., KITAMOTO, T., HASHIGUCHI, H. & SHII, H. 1988. Gerstmann-Straussler-Scheinker disease: immunohistological and experimental studies. *Ann Neurol*, 24, 35-40.
- TATEISHI, J., KITAMOTO, T., HOQUE, M. Z. & FURUKAWA, H. 1996. Experimental transmission of Creutzfeldt-Jakob disease and related diseases to rodents. *Neurology*, 46, 532-7.
- TATZELT, J., PRUSINER, S. B. & WELCH, W. J. 1996. Chemical chaperones interfere with the formation of scrapie prion protein. *EMBO J*, 15, 6363-73.
- TAYLOR, D. R. & HOOPER, N. M. 2006. The prion protein and lipid rafts. *Mol Membr Biol*, 23, 89-99.
- TAYLOR, D. R., PARKIN, E. T., COCKLIN, S. L., AULT, J. R., ASHCROFT, A. E., TURNER, A. J. & HOOPER, N. M. 2009. Role of ADAMs in the ectodomain shedding and conformational conversion of the prion protein. *J Biol Chem*, 284, 22590-600.
- TAYLOR, D. R., WATT, N. T., PERERA, W. S. & HOOPER, N. M. 2005. Assigning functions to distinct regions of the N-terminus of the prion protein that are involved in its copper-stimulated, clathrin-dependent endocytosis. *J Cell Sci*, 118, 5141-53.
- TELLING, G. C., HAGA, T., TORCHIA, M., TREMBLAY, P., DEARMOND, S. J. & PRUSINER, S. B. 1996. Interactions between wild-type and mutant prion proteins modulate neurodegeneration in transgenic mice. *Genes Dev*, 10, 1736-50.
- TELLING, G. C., SCOTT, M., MASTRIANNI, J., GABIZON, R., TORCHIA, M., COHEN, F. E., DEARMOND, S. J. & PRUSINER, S. B. 1995. Prion propagation in mice expressing human and chimeric PrP transgenes implicates the interaction of cellular PrP with another protein. *Cell*, 83, 79-90.
- TERZANO, M. G., MONTANARI, E., CALZETTI, S., MANCIA, D. & LECHI, A. 1983. The effect of amantadine on arousal and EEG patterns in Creutzfeldt-Jakob disease. *Arch Neurol*, 40, 555-9.
- THACKRAY, A. M., ANDREOLETTI, O. & BUJDOSO, R. 2016. Bioassay of prion-infected blood plasma in PrP transgenic *Drosophila*. *Biochem J*, 473, 4399-4412.
- THACKRAY, A. M., ANDREOLETTI, O. & BUJDOSO, R. 2018. Mammalian prion propagation in PrP transgenic *Drosophila*. *Brain*, 141, 2700-2710.
- THACKRAY, A. M., MUHAMMAD, F., ZHANG, C., DENYER, M., SPIROPOULOS, J., CROWTHER, D. C. & BUJDOSO, R. 2012. Prion-induced toxicity in PrP transgenic *Drosophila*. *Exp Mol Pathol*, 92, 194-201.
- THELLUNG, S., SCOTI, B., CORSARO, A., VILLA, V., NIZZARI, M., GAGLIANI, M. C., PORCILE, C., RUSSO, C., PAGANO, A., TACCHETTI, C., CORTESE, K. & FLORIO, T. 2018. Pharmacological activation of autophagy favors the clearing of intracellular aggregates of misfolded prion protein peptide to prevent neuronal death. *Cell Death Dis*, 9, 166.
- TOBLER, I., GAUS, S. E., DEBOER, T., ACHERMANN, P., FISCHER, M., RULICKE, T., MOSER, M., OESCH, B., MCBRIDE, P. A. & MANSON, J. C. 1996. Altered circadian activity rhythms and sleep in mice devoid of prion protein. *Nature*, 380, 639-42.
- TODD, N. V., MORROW, J., DOH-URA, K., DEALLER, S., O'HARE, S., FARLING, P., DUDDY, M. & RAINOV, N. G. 2005. Cerebroventricular infusion of pentosan polysulphate in human variant Creutzfeldt-Jakob disease. *J Infect*, 50, 394-6.
- TORRES, M., CASTILLO, K., ARMISEN, R., STUTZIN, A., SOTO, C. & HETZ, C. 2010. Prion protein misfolding affects calcium homeostasis and sensitizes cells to endoplasmic reticulum stress. *PLoS One*, 5, e15658.
- TOUIL, F., PRATT, S., MUTTER, R. & CHEN, B. 2006. Screening a library of potential prion therapeutics against cellular prion proteins and insights into their mode of biological activities by surface plasmon resonance. *J Pharm Biomed Anal*, 40, 822-32.

- TRANULIS, M. A., ESPENES, A., COMINCINI, S., SKRETTING, G. & HARBITZ, I. 2001. The PrP-like protein Doppel gene in sheep and cattle: cDNA sequence and expression. *Mamm Genome*, 12, 376-9.
- TURK, E., TEPLow, D. B., HOOD, L. E. & PRUSINER, S. B. 1988. Purification and properties of the cellular and scrapie hamster prion proteins. *Eur J Biochem*, 176, 21-30.
- TURNBAUGH, J. A., UNTERBERGER, U., SAA, P., MASSIGNAN, T., FLUHARTY, B. R., BOWMAN, F. P., MILLER, M. B., SUPATTAPONE, S., BIASINI, E. & HARRIS, D. A. 2012. The N-terminal, polybasic region of PrP(C) dictates the efficiency of prion propagation by binding to PrP(Sc). *J Neurosci*, 32, 8817-30.
- UM, J. W., KAUFMAN, A. C., KOSTYLEV, M., HEISS, J. K., STAGI, M., TAKAHASHI, H., KERRISK, M. E., VORTMEYER, A., WISNIEWSKI, T., KOLESKE, A. J., GUNTHER, E. C., NYGAARD, H. B. & STRITTMATTER, S. M. 2013. Metabotropic glutamate receptor 5 is a coreceptor for Alzheimer abeta oligomer bound to cellular prion protein. *Neuron*, 79, 887-902.
- UM, J. W., NYGAARD, H. B., HEISS, J. K., KOSTYLEV, M. A., STAGI, M., VORTMEYER, A., WISNIEWSKI, T., GUNTHER, E. C. & STRITTMATTER, S. M. 2012. Alzheimer amyloid-beta oligomer bound to postsynaptic prion protein activates Fyn to impair neurons. *Nat Neurosci*, 15, 1227-35.
- UM, J. W. & STRITTMATTER, S. M. 2013. Amyloid-beta induced signaling by cellular prion protein and Fyn kinase in Alzheimer disease. *Prion*, 7, 37-41.
- UNTERBERGER, U., HOFTBERGER, R., GELPI, E., FLICKER, H., BUDKA, H. & VOIGTLANDER, T. 2006. Endoplasmic reticulum stress features are prominent in Alzheimer disease but not in prion diseases in vivo. *J Neuropathol Exp Neurol*, 65, 348-57.
- VASSALLO, N., HERMS, J., BEHRENS, C., KREBS, B., SAEKI, K., ONODERA, T., WINDL, O. & KRETZSCHMAR, H. A. 2005. Activation of phosphatidylinositol 3-kinase by cellular prion protein and its role in cell survival. *Biochem Biophys Res Commun*, 332, 75-82.
- VAZQUEZ-FERNANDEZ, E., ALONSO, J., PASTRANA, M. A., RAMOS, A., STITZ, L., VIDAL, E., DYNIN, I., PETSCH, B., SILVA, C. J. & REQUENA, J. R. 2012. Structural organization of mammalian prions as probed by limited proteolysis. *PLoS One*, 7, e50111.
- VAZQUEZ-FERNANDEZ, E., YOUNG, H. S., REQUENA, J. R. & WILLE, H. 2017. The Structure of Mammalian Prions and Their Aggregates. *Int Rev Cell Mol Biol*, 329, 277-301.
- VELLA, L. J., SHARPLES, R. A., LAWSON, V. A., MASTERS, C. L., CAPPAL, R. & HILL, A. F. 2007. Packaging of prions into exosomes is associated with a novel pathway of PrP processing. *J Pathol*, 211, 582-90.
- VEY, M., PILKUHN, S., WILLE, H., NIXON, R., DEARMOND, S. J., SMART, E. J., ANDERSON, R. G., TARABOULOS, A. & PRUSINER, S. B. 1996. Subcellular colocalization of the cellular and scrapie prion proteins in caveolae-like membranous domains. *Proc Natl Acad Sci U S A*, 93, 14945-9.
- VILES, J. H., COHEN, F. E., PRUSINER, S. B., GOODIN, D. B., WRIGHT, P. E. & DYSON, H. J. 1999. Copper binding to the prion protein: structural implications of four identical cooperative binding sites. *Proc Natl Acad Sci U S A*, 96, 2042-7.
- VILETTE, D., ANDREOLETTI, O., ARCHER, F., MADELAINE, M. F., VILOTTE, J. L., LEHMANN, S. & LAUDE, H. 2001. Ex vivo propagation of infectious sheep scrapie agent in heterologous epithelial cells expressing ovine prion protein. *Proc Natl Acad Sci U S A*, 98, 4055-9.
- VINCENT, B., PAITEL, E., FROBERT, Y., LEHMANN, S., GRASSI, J. & CHECLER, F. 2000. Phorbol ester-regulated cleavage of normal prion protein in HEK293 human cells and murine neurons. *J Biol Chem*, 275, 35612-6.
- VINCENT, B., PAITEL, E., SAFTIG, P., FROBERT, Y., HARTMANN, D., DE STROOPER, B., GRASSI, J., LOPEZ-PEREZ, E. & CHECLER, F. 2001. The disintegrins ADAM10 and TACE contribute to the constitutive and phorbol ester-regulated normal cleavage of the cellular prion protein. *J Biol Chem*, 276, 37743-6.

- VOGTHERR, M., GRIMME, S., ELSHORST, B., JACOBS, D. M., FIEBIG, K., GRIESINGER, C. & ZAHN, R. 2003. Antimalarial drug quinacrine binds to C-terminal helix of cellular prion protein. *J Med Chem*, 46, 3563-4.
- VORBERG, I. & CHIESA, R. 2019. Experimental models to study prion disease pathogenesis and identify potential therapeutic compounds. *Curr Opin Pharmacol*, 44, 28-38.
- VORBERG, I., RAINES, A., STORY, B. & PRIOLA, S. A. 2004. Susceptibility of common fibroblast cell lines to transmissible spongiform encephalopathy agents. *J Infect Dis*, 189, 431-9.
- WADSWORTH, J. D., JOINER, S., LINEHAN, J. M., BALKEMA-BUSCHMANN, A., SPIROPOULOS, J., SIMMONS, M. M., GRIFFITHS, P. C., GROSCHUP, M. H., HOPE, J., BRANDNER, S., ASANTE, E. A. & COLLINGE, J. 2013. Atypical scrapie prions from sheep and lack of disease in transgenic mice overexpressing human prion protein. *Emerg Infect Dis*, 19, 1731-9.
- WANG, L. H., ROTHBERG, K. G. & ANDERSON, R. G. 1993. Mis-assembly of clathrin lattices on endosomes reveals a regulatory switch for coated pit formation. *J Cell Biol*, 123, 1107-17.
- WANG, Z. Y., SHI, Q., WANG, S. B., TIAN, C., XU, Y., GUO, Y., CHEN, C., ZHANG, J. & DONG, X. P. 2013. Co-expressions of casein kinase 2 (CK2) subunits restore the down-regulation of tubulin levels and disruption of microtubule structures caused by PrP mutants. *J Mol Neurosci*, 50, 14-22.
- WATT, N. T., ROUTLEDGE, M. N., WILD, C. P. & HOOPER, N. M. 2007. Cellular prion protein protects against reactive-oxygen-species-induced DNA damage. *Free Radic Biol Med*, 43, 959-67.
- WATT, N. T., TAYLOR, D. R., GILLOTT, A., THOMAS, D. A., PERERA, W. S. & HOOPER, N. M. 2005. Reactive oxygen species-mediated beta-cleavage of the prion protein in the cellular response to oxidative stress. *J Biol Chem*, 280, 35914-21.
- WATTS, J. C., BOURKAS, M. E. C. & ARSHAD, H. 2018. The function of the cellular prion protein in health and disease. *Acta Neuropathol*, 135, 159-178.
- WATTS, J. C., GILES, K., PATEL, S., OEHLER, A., DEARMOND, S. J. & PRUSINER, S. B. 2014. Evidence that bank vole PrP is a universal acceptor for prions. *PLoS Pathog*, 10, e1003990.
- WATTS, J. C., GILES, K., STOHR, J., OEHLER, A., BHARDWAJ, S., GRILLO, S. K., PATEL, S., DEARMOND, S. J. & PRUSINER, S. B. 2012. Spontaneous generation of rapidly transmissible prions in transgenic mice expressing wild-type bank vole prion protein. *Proc Natl Acad Sci U S A*, 109, 3498-503.
- WATTS, J. C. & PRUSINER, S. B. 2014. Mouse models for studying the formation and propagation of prions. *J Biol Chem*, 289, 19841-9.
- WATTS, J. C. & WESTAWAY, D. 2007. The prion protein family: diversity, rivalry, and dysfunction. *Biochim Biophys Acta*, 1772, 654-72.
- WEISE, J., CROME, O., SANDAU, R., SCHULZ-SCHAEFFER, W., BAHR, M. & ZERR, I. 2004. Upregulation of cellular prion protein (PrP^c) after focal cerebral ischemia and influence of lesion severity. *Neurosci Lett*, 372, 146-50.
- WEISE, J., SANDAU, R., SCHWARTING, S., CROME, O., WREDE, A., SCHULZ-SCHAEFFER, W., ZERR, I. & BAHR, M. 2006. Deletion of cellular prion protein results in reduced Akt activation, enhanced postischemic caspase-3 activation, and exacerbation of ischemic brain injury. *Stroke*, 37, 1296-300.
- WESTAWAY, D., DEARMOND, S. J., CAYETANO-CANLAS, J., GROTH, D., FOSTER, D., YANG, S. L., TORCHIA, M., CARLSON, G. A. & PRUSINER, S. B. 1994. Degeneration of skeletal muscle, peripheral nerves, and the central nervous system in transgenic mice overexpressing wild-type prion proteins. *Cell*, 76, 117-29.
- WESTERGARD, L., TURNBAUGH, J. A. & HARRIS, D. A. 2011. A naturally occurring C-terminal fragment of the prion protein (PrP) delays disease and acts as a dominant-negative inhibitor of PrP^{Sc} formation. *J Biol Chem*, 286, 44234-42.

- WHITE, M. D., FARMER, M., MIRABILE, I., BRANDNER, S., COLLINGE, J. & MALLUCCI, G. R. 2008. Single treatment with RNAi against prion protein rescues early neuronal dysfunction and prolongs survival in mice with prion disease. *Proc Natl Acad Sci U S A*, 105, 10238-43.
- WIERSMA, V. I., VAN HECKE, W., SCHEPER, W., VAN OSCH, M. A., HERMSEN, W. J., ROZEMULLER, A. J. & HOOZEMANS, J. J. 2016. Activation of the unfolded protein response and granulovacuolar degeneration are not common features of human prion pathology. *Acta Neuropathol Commun*, 4, 113.
- WILESMITH, J. W. 1988. Bovine spongiform encephalopathy. *Vet Rec*, 122, 614.
- WILESMITH, J. W., RYAN, J. B., HUESTON, W. D. & HOINVILLE, L. J. 1992. Bovine spongiform encephalopathy: epidemiological features 1985 to 1990. *Vet Rec*, 130, 90-4.
- WILHAM, J. M., ORRU, C. D., BESSEN, R. A., ATARASHI, R., SANO, K., RACE, B., MEADE-WHITE, K. D., TAUBNER, L. M., TIMMES, A. & CAUGHEY, B. 2010. Rapid end-point quantitation of prion seeding activity with sensitivity comparable to bioassays. *PLoS Pathog*, 6, e1001217.
- WILL, R. G., IRONSIDE, J. W., ZEIDLER, M., COUSENS, S. N., ESTIBEIRO, K., ALPEROVITCH, A., POSER, S., POCCHIARI, M., HOFMAN, A. & SMITH, P. G. 1996. A new variant of Creutzfeldt-Jakob disease in the UK. *Lancet*, 347, 921-5.
- WILLE, H., MICHELITSCH, M. D., GUENEBAUT, V., SUPATTAPONE, S., SERBAN, A., COHEN, F. E., AGARD, D. A. & PRUSINER, S. B. 2002. Structural studies of the scrapie prion protein by electron crystallography. *Proc Natl Acad Sci U S A*, 99, 3563-8.
- WILLIAMS, E. S. & YOUNG, S. 1980. Chronic wasting disease of captive mule deer: a spongiform encephalopathy. *J Wildl Dis*, 16, 89-98.
- WINDL, O., BUCHHOLZ, M., NEUBAUER, A., SCHULZ-SCHAEFFER, W., GROSCHUP, M., WALTER, S., ARENDT, S., NEUMANN, M., VOSS, A. K. & KRETZSCHMAR, H. A. 2005. Breaking an absolute species barrier: transgenic mice expressing the mink PrP gene are susceptible to transmissible mink encephalopathy. *J Virol*, 79, 14971-5.
- WINKLHOFER, K. F., HESKE, J., HELLER, U., REINTJES, A., MURANYI, W., MOAREFI, I. & TATZELT, J. 2003. Determinants of the in vivo folding of the prion protein. A bipartite function of helix 1 in folding and aggregation. *J Biol Chem*, 278, 14961-70.
- WOLF, H., HOSSINGER, A., FEHLINGER, A., BUTTNER, S., SIM, V., MCKENZIE, D. & VORBERG, I. M. 2015. Deposition pattern and subcellular distribution of disease-associated prion protein in cerebellar organotypic slice cultures infected with scrapie. *Front Neurosci*, 9, 410.
- WONGSRIKEAO, P., SUTOU, S., KUNISHI, M., DONG, Y. J., BAI, X. & OTOI, T. 2011. Combination of the somatic cell nuclear transfer method and RNAi technology for the production of a prion gene-knockdown calf using plasmid vectors harboring the U6 or tRNA promoter. *Prion*, 5, 39-46.
- XU, K. & ZHU, X. P. 2012. Endoplasmic reticulum stress and prion diseases. *Rev Neurosci*, 23, 79-84.
- YADAVALLI, R., GUTTMANN, R. P., SEWARD, T., CENTERS, A. P., WILLIAMSON, R. A. & TELLING, G. C. 2004. Calpain-dependent endoproteolytic cleavage of PrP^{Sc} modulates scrapie prion propagation. *J Biol Chem*, 279, 21948-56.
- YAMASAKI, T., SUZUKI, A., HASEBE, R. & HORIUCHI, M. 2014. Comparison of the anti-prion mechanism of four different anti-prion compounds, anti-PrP monoclonal antibody 44B1, pentosan polysulfate, chlorpromazine, and U18666A, in prion-infected mouse neuroblastoma cells. *PLoS One*, 9, e106516.
- YANG, W., COOK, J., RASSBACH, B., LEMUS, A., DEARMOND, S. J. & MASTRIANNI, J. A. 2009. A New Transgenic Mouse Model of Gerstmann-Straussler-Scheinker Syndrome Caused by the A117V Mutation of PRNP. *J Neurosci*, 29, 10072-80.

- YI, C. W., WANG, L. Q., HUANG, J. J., PAN, K., CHEN, J. & LIANG, Y. 2018. Glycosylation Significantly Inhibits the Aggregation of Human Prion Protein and Decreases Its Cytotoxicity. *Sci Rep*, 8, 12603.
- YIM, Y. I., PARK, B. C., YADAVALLI, R., ZHAO, X., EISENBERG, E. & GREENE, L. E. 2015. The multivesicular body is the major internal site of prion conversion. *J Cell Sci*, 128, 1434-43.
- YOKOYAMA, T., KIMURA, K. M., USHIKI, Y., YAMADA, S., MOROOKA, A., NAKASHIBA, T., SASSA, T. & ITOHARA, S. 2001. In vivo conversion of cellular prion protein to pathogenic isoforms, as monitored by conformation-specific antibodies. *J Biol Chem*, 276, 11265-71.
- YOU, H., TSUTSUI, S., HAMEED, S., KANNANAYAKAL, T. J., CHEN, L., XIA, P., ENGBERS, J. D., LIPTON, S. A., STYS, P. K. & ZAMPONI, G. W. 2012. Abeta neurotoxicity depends on interactions between copper ions, prion protein, and N-methyl-D-aspartate receptors. *Proc Natl Acad Sci U S A*, 109, 1737-42.
- YU, G., CHEN, J., XU, Y., ZHU, C., YU, H., LIU, S., SHA, H., CHEN, J., XU, X., WU, Y., ZHANG, A., MA, J. & CHENG, G. 2009. Generation of goats lacking prion protein. *Mol Reprod Dev*, 76, 3.
- YU, G., CHEN, J., YU, H., LIU, S., CHEN, J., XU, X., SHA, H., ZHANG, X., WU, G., XU, S. & CHENG, G. 2006. Functional disruption of the prion protein gene in cloned goats. *J Gen Virol*, 87, 1019-27.
- YUN, S. W., ERTMER, A., FLECHSIG, E., GILCH, S., RIEDERER, P., GERLACH, M., SCHATZL, H. M. & KLEIN, M. A. 2007. The tyrosine kinase inhibitor imatinib mesylate delays prion neuroinvasion by inhibiting prion propagation in the periphery. *J Neurovirol*, 13, 328-37.
- ZAMPONI, E., BURATTI, F., CATALDI, G., CAICEDO, H. H., SONG, Y., JUNGBAUER, L. M., LADU, M. J., BISBAL, M., LORENZO, A., MA, J., HELGUERA, P. R., MORFINI, G. A., BRADY, S. T. & PIGINO, G. F. 2017. Prion protein inhibits fast axonal transport through a mechanism involving casein kinase 2. *PLoS One*, 12, e0188340.
- ZERR, I. 2009. Therapeutic trials in human transmissible spongiform encephalopathies: recent advances and problems to address. *Infect Disord Drug Targets*, 9, 92-9.

APPENDIX

Constructs and Antibodies

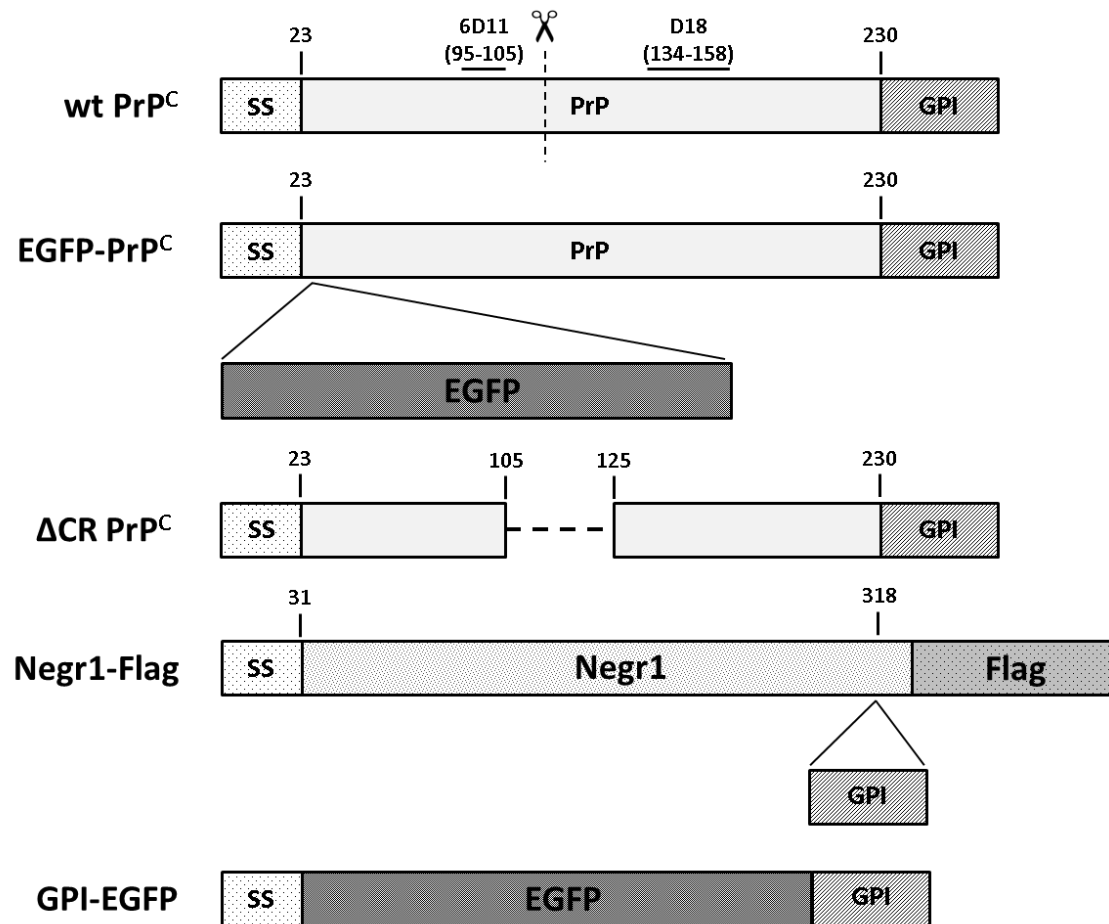


Figure S1 Schematic of constructs. *The picture illustrates the different constructs employed in the study.*

The Non-Validated Hits

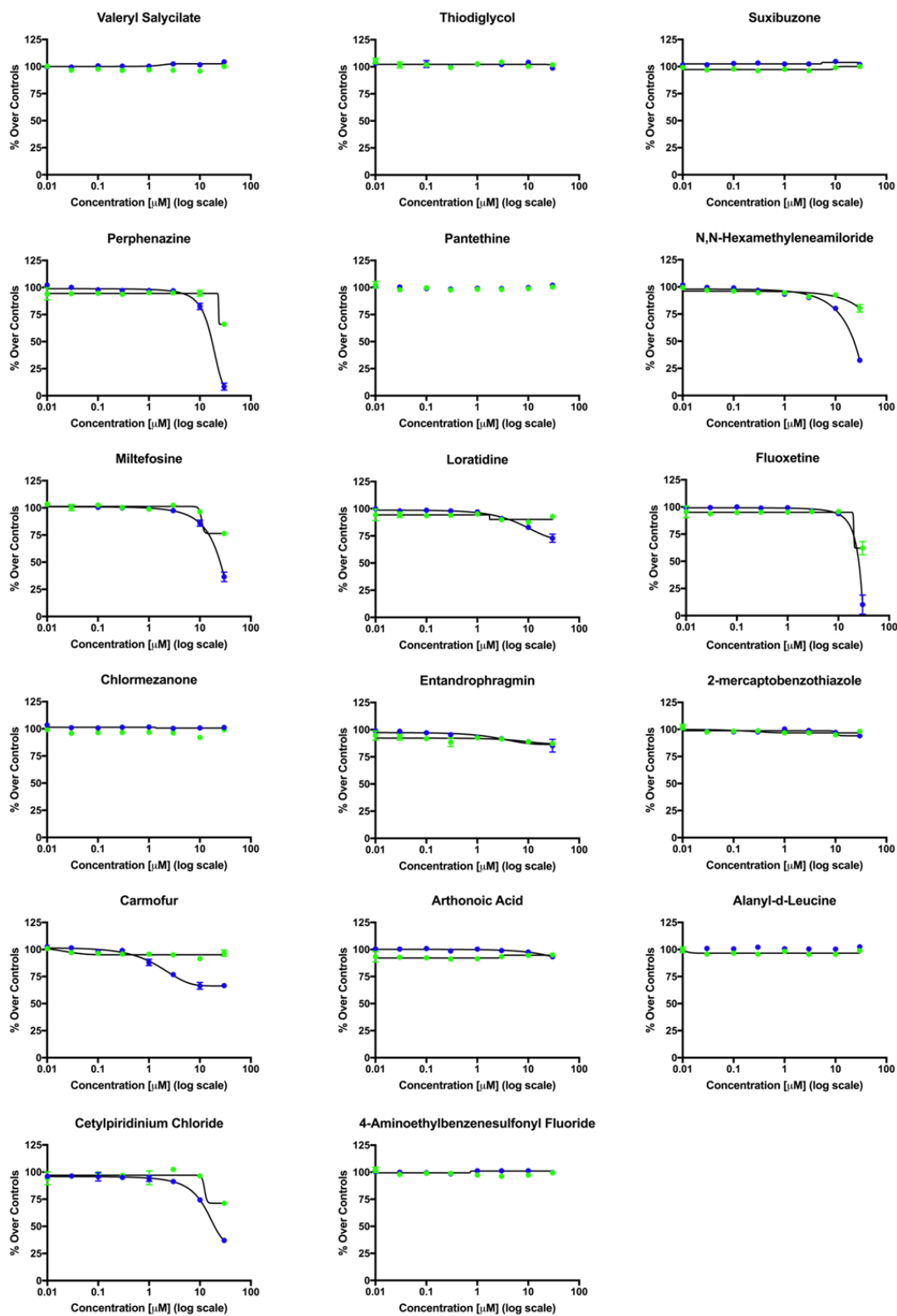


Figure S2 Dose-Response Assays for non-Validated Molecules. Graphs depict the quantification of EGFP-PrP^C re-localization (green dots) or cytotoxicity (blue dots) upon compound treatments, both acquired with Operetta Imaging System and quantified with the Harmony software. Data from three independent experiments were fitted by using the 4PL non-linear regression model. Statistical analyses were as follow: Valeryl Salicylate, % Surface/Internal EGFP-PrP^C not fitted, % Cells R²=0.94; Thiodiglycol, %Surface/Internal EGFP-PrP^C not fitted, % Cells R²=0.21; Suxibuzone, % Surface/Internal EGFP-PrP^C R²=0.42, % Cells R²=0.18; Perphenazine, % Surface/Internal EGFP-PrP^C R²=0.99, % Cells R²=0.96; Pantethine, % Surface/Internal EGFP-PrP^C not fitted, % Cells not fitted; N,N-Hexamethyleneamiloride, % Surface/Internal EGFP-PrP^C R²=0.83, % Cells R²=0.99; Miltefosine, % Surface/Internal EGFP-PrP^C R²=0.95, % Cells R²=0.99; Loratidine, % Surface/Internal EGFP-PrP^C R²=0.48, % Cells R²=0.98; Fluoxetine, % Surface/Internal EGFP-PrP^C R²=0.96, % Cells R²=0.99; Entandrophragmin, % Surface/Internal EGFP-PrP^C R²=0.37, % Cells R²=0.81; Chlormezanone, % Surface/Internal EGFP-PrP^C not fitted, %Cells R²=0.14; 2-Mercaptobenzothiazole, % Surface/Internal EGFP-PrP^C R²=0.35, % Cells R²=0.47; Carmofur, % Surface/Internal EGFP-PrP^C R²=0.53, % Cells R²=0.98; Arthoic Acid, % Surface/Internal EGFP-PrP^C R²=0.34, % Cells R²=0.81; Alanyl-d-Leucine, %Surface/Internal EGFP-PrP^C R²=0.31, % Cells not fitted; Cetylpyridinium Chloride, %Surface/Internal EGFP-PrP^C R²=0.87, % Cells R²=0.99; 4-AminoethylbenzenesulfonylFluoride, % Surface/Internal EGFP-PrP^C not fitted, % Cells R²=0.84.

Structure of LD24 Derivatives

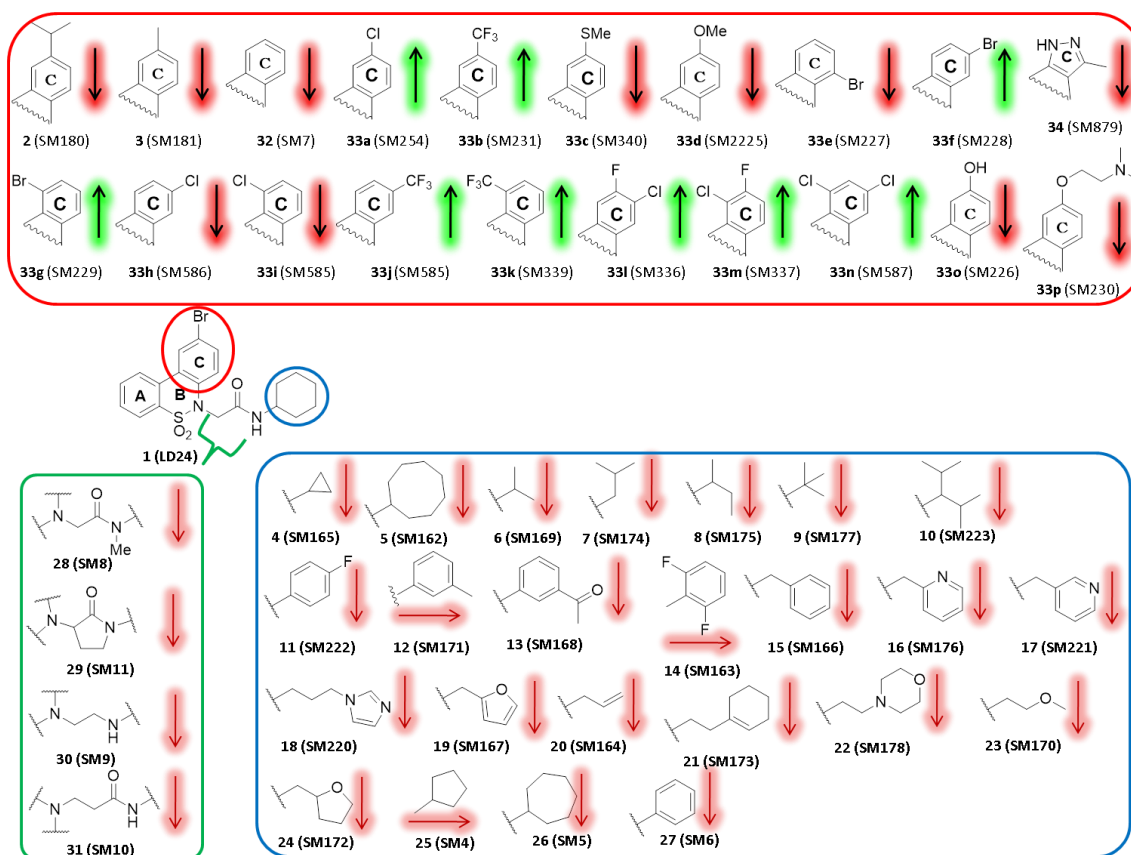
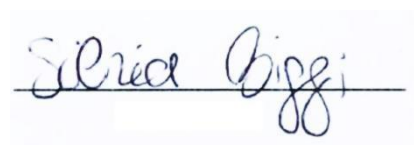


Figure S3 Representation of the Chemical Structure of LD24 Derivatives. Compounds are divided according to the different region that has been modified into three groups. Arrows represent the rescuing activity of each compound compared to LD24 as measured by DBCA.

Declaration,

I, Silvia Biggi, confirm that this is my own work and the use of other material from other sources has been properly and fully acknowledged.

Signature

A handwritten signature in black ink on a light blue background. The signature reads "Silvia Biggi" in a cursive script, written over a horizontal line.